



UNIVERSITAT DE  
BARCELONA

# Magnetic resonance imaging, cognition, and sex differences in Parkinson's disease with REM sleep behavior disorder

Javier Oltra González



Aquesta tesi doctoral està subjecta a la llicència **Reconeixement- NoComercial – SenseObraDerivada 4.0. Espanya de Creative Commons.**

Esta tesis doctoral está sujeta a la licencia **Reconocimiento - NoComercial – SinObraDerivada 4.0. España de Creative Commons.**

This doctoral thesis is licensed under the **Creative Commons Attribution-NonCommercial-NoDerivs 4.0. Spain License.**

# **Magnetic resonance imaging, cognition and sex differences in Parkinson's disease with REM sleep behavior disorder**

Javier Oltra González



**Universitat de Barcelona  
October 2022**



UNIVERSITAT DE  
BARCELONA

**Magnetic resonance imaging, cognition, and sex  
differences in Parkinson's disease with REM sleep  
behavior disorder**

Thesis presented by

Javier Oltra González

to obtain the degree of doctor from the Universitat de Barcelona  
with the requirements of the international PhD diploma

Supervised by

Dra. Carme Junquè Plaja and Dra. Bàrbara Segura Fàbregas

Programa de Doctorat en Medicina i Recerca Translacional

Facultat de Medicina i Ciències de la Salut

Universitat de Barcelona

October 2022



Barcelona, October 4th, 2022

Dr. Carme Junqué Plaja and Dr. Bàrbara Segura Fàbregas, professors at the Universitat de Barcelona,

Certify that they have guided and supervised the doctoral thesis entitled “Magnetic resonance imaging, cognition, and sex differences in Parkinson’s disease with REM sleep behavior disorder,” presented by Javier Oltra González. Doctoral thesis deposited on September 6th, authorized for its deposit by the Comissió Acadèmica del Programa de Doctorat en Medicina i Recerca Translacional on September 9th, and for its defense by the Comissió de Doctorat de la Facultat de Medicina i Ciències de la Salut on September 28th. They hereby assert that this thesis fulfills the requirements to present his defense to be awarded the title of doctor.

Signatures

Carme Junqué Plaja

Bàrbara Segura Fàbregas



## **Funding**

This thesis has been undertaken at the CJNeurolab, Grup de Neuropsicologia, Institut de Neurociències de la Universitat de Barcelona (Unitat d'Excel·lència María de Maeztu) and Institut d'Investigacions Biomèdiques August Pi i Sunyer (IDIBAPS).

The present work has been financially supported by a 2018 fellowship from the Ministerio de Ciencia, Innovación y Universidades de España (PRE2018-086675) co-financed by the European Social Fund (ERDF), associated to the project *Fenotipos cognitivos en la enfermedad de Parkinson mediante la identificación de patrones de neuroimagen multimodal* (PSI2017-86930-P), financed by the Ministerio de Economía, Industria y Competitividad de España and co-financed by the Agencia Estatal de Investigación (AEI) and the ERDF.

## Acknowledgments

A les meves directores de tesi, les doctores Carme Junqué i Bàrbara Segura, per ser guia, suport i consell al llarg d'aquests tres anys. Ha sigut un honor.

Aquesta tesi mai hauria sigut possible sense la resta de persones amb les quals he compartit el dia a dia del laboratori. A la resta de companyes del CJNeuroLab, a l'Anna Campabadal per la seva acollida i la feina mà a mà, a la Carme Uribe pels seus bons consells i la seva capacitat d'ensenyament, a la Gemma per tot el suport i la seva calma, i també a la Jèssica per tot el que estigui per venir, et desitjo el millor amb la teva tesi. Als membres del BBSLab, la Cristina, el David, la Ivet, el Kílian, el Pablo, el Ruben i la Lídia Mulet. Als membres del PENlab, la Lucia, la Maria Sunyol, el Saül, i en especial a la Marina per la seva simpatia i motivació, i per saber transmetre'ls.

Menció a part per a l'Anna Inguanzo, la Lídia Vaqué i la María Cabello, per la nostra amistat. Gràcies a les tres, entre altres moltes coses, per Milà, per les converses, les birres o el vi blanc. Sempre estaré agraït a tu, Anna, per la teva acollida i els bons records a Estocolm.

Gràcies als neuròlegs de l'Hospital Clínic de Barcelona, al Dr. Yaroslau Compta, a la Dra. María José Martí i al Dr. Francesc Valldeoriola per la seva dedicació. Especialment, voldria agrair al Dr. Alex Iranzo pels seus comentaris i observacions en relació amb la població d'estudi. A Mònica Serradell, per la seva estreta col·laboració. Moltes gràcies també a les tècniques del Centre de Diagnòstic per la Imatge, en especial a la Gema i la Vero.

Muchas gracias al doctor Dani Ferreira, por hacerme sentir uno más en los meses de estancia, por tu cercanía y por haberme transmitido tu pasión



por la investigación. Thanks, doctor Eric Westman, for your hospitality. To Greta, I am so grateful for your help and consideration. Thanks to the other people from the Karolinska Institutet for making my stay satisfactory.

Querría también agradecer el apoyo a los amigos que llevan todos estos años junto a mí en la distancia. Especialmente a Alejandro, Alberto (además de por ayudarme a vestir de roble esta tesis), Félix, Javi y María. Igualmente me gustaría agradecer a todos aquellos que me han acogido en Barcelona desde mi llegada. A Laura, Maria, Marina, Nira, Pablo y Tanit. También a todos los demás, amigos y colegas, en Asturias, Cantabria, Catalunya y otros rincones.

Agradecer a mis padres y mi hermana el apoyo y soporte en todos estos años. En especial, desde que planteé que quería dedicarme a la investigación, hace ya casi diez años, hasta el día de hoy. Gracias por estar presentes en cada momento.

Estos dos últimos años no hubieran sido lo mismo sin caminar a tu lado, Gina. Gracias por el apoyo en el día a día, tu cariño, comprensión e inmensa empatía. Por seguir caminando y haciendo camino juntos.

Moltes gràcies als voluntaris dels estudis, sense ells la recerca no seria possible.

Por último, me gustaría recordar a aquellos que ya no están. A la yaya Virgina, al tete Domi y al Jan. Siempre estaréis presentes en mi recuerdo.

# Index

<b>Glossary of abbreviations</b>	10
<b>List of publications</b>	13
<b>Resum en català</b>	14
<b>Abstract</b>	21
<b>Chapter 1 Introduction</b>	27
1. REM sleep behavior disorder: an overview	29
2. RBD and Parkinson's disease	34
2.1. RBD as a prodromal stage of Parkinson's disease	34
2.2. RBD in Parkinson's disease	39
2.2.1. Neuropathology of Parkinson's disease with RBD	40
2.2.2. Cognition in Parkinson's disease with RBD	44
2.2.3. Genetics of Parkinson's disease with RBD	47
2.2.4. Brain imaging in Parkinson's disease with RBD	47
2.2.5. Brain correlates in PD with RBD	84
3. Sex and gender in Parkinson's disease	88
<b>Chapter 2 Hypotheses and objectives</b>	95
Hypotheses	96
Objectives	97
<b>Chapter 3 Materials and methods</b>	99
1. Study samples	101
1.1. <i>de novo</i> Parkinson's disease sample	101

1.2. Parkinson's disease sample	105
2. Magnetic resonance imaging preprocessing	108
2.1. Structural MRI: cortical thickness and volumetry	108
2.2. Functional MRI: preprocessing	110
3. Statistical analyses	111
3.1. Demographic, clinical and neuropsychological measures	111
3.2. Structural MRI measures	111
3.3. Characterization of brain functional connectivity	113
<b>Chapter 4 Results</b>	117
Study 1	119
Study 2	139
Study 3	159
Study 4	175
<b>Chapter 5 General discussion</b>	195
<b>Chapter 6 Conclusions</b>	209
<b>References</b>	213

## Glossary of abbreviations

**AFNI:** Analysis of Functional NeuroImage

**ALFF:** amplitude of low-frequency fluctuation

**ANCOVA:** analysis of covariance

**ANOVA:** analyses of variance

**BCT:** Brain Connectivity Toolbox

**BFRT:** Benton Facial Recognition Test

**BNT:** Boston Naming Test

**BOLD:** blood-oxygen-level-dependent

**BVFD:** Benton Visual Form Discrimination

**CSF:** cerebrospinal fluid

**CNS:** central nervous system

**CTh:** cortical thickness

**DAT:** dopamine transporter

**DBM:** deformation-based morphometry

**dFNC:** dynamic functional network connectivity

**DLB:** dementia with Lewy bodies

**DTI:** diffusion tensor imaging

**EEG:** electroencephalogram

**EMG:** electromyographic

**EPI:** echo-planar imaging

**ESS:** Epworth Sleepiness Scale

**eTIV:** estimated total intracranial volume

**FA:** fractional anisotropy

**FLAIR:** fluid-attenuated inversion recovery

**fMRI:** functional magnetic resonance imaging

**FWHM:** full width half maximum

**GBA:** glucocerebrosidase

**GDS-15:** 15-item Geriatric Depression Scale

**GM:** gray matter

**HC:** healthy controls

**HVLT-R:** Hopkins Verbal Learning Test-Revised

**H&Y scale:** Hoehn and Yahr

**ICA-AROMA:** Independent Component Analysis based strategy for Automatic Removal of Motion Artifacts

**ICSD:** The International Classification of Sleep Disorders

**iRBD:** idiopathic/isolated RBD

**JLO:** Benton Judgment of Line Orientation Test

**L-DOPA:** levodopa

**LEED:** L-DOPA equivalent daily dose

**LNS:** Letter-Number Sequencing

**LRK2:** leucine-rich repeat kinase 2

**MAPT:** microtubule-associated protein tau

**MCI:** mild cognitive impairment

**MD:** mean diffusivity

**MDS-UPDRS:** Movement Disorder Society Unified PD Rating Scale

**MoCA:** Montreal Cognitive Assessment

**MPRAGE:** magnetization prepared rapid gradient echo

**MRI:** magnetic resonance imaging

**MSA:** multiple system atrophy

**MSQ:** Mayo Clinic Sleep Questionnaire

**Multidiscip.:** Multidisciplinary

**NREM:** no REM

**QA:** quantified anisotropy

**PD:** Parkinson's disease

**PET:** positron emission tomography

**PIGD:** postural instability and gait disorder

**PNS:** peripheral nervous system

**PPMI:** Parkinson's Progression Markers Initiative

**pRBD:** probable RBD

**PSG:** polysomnography

**RAVLT:** Rey Auditory Verbal Learning Test

**REM:** rapid eye movement

**RBD:** REM sleep behavior disorder

**RBD-I:** Innsbruck RBD Inventory

**RBDSQ:** RBD Screening Questionnaire

**RWA:** REM sleep without atonia

**SDMT:** Symbol Digits Modalities Test

**SNCA:** synuclein alpha

**SCOPA-AUT:** Scales for Outcomes in Parkinson's Disease - Autonomic Dysfunction

**SOC:** alpha-Synuclein Origin site and Connectome

**SPECT:** single-photon emission computerized tomography

**TE:** echo time

**TFNBS:** threshold-free network-based statistics

**T:** Tesla

**TMEM175:** transmembrane protein 175

**TMT:** Trail Making Test

**TR:** repetition time

**UPSIT:** University of Pennsylvania Smell Identification Test

**VBM:** voxel-based morphometry

**VMAT2:** vesicular monoamine transporter type 2

**WM:** white matter

## List of publications

Doctoral thesis presented in the compendium of articles format. The thesis consists of six specific objectives (see *Chapter 2. Hypotheses and objectives*) and includes four different published peer-reviewed papers:

**Oltra J**, Uribe C, Segura B, Campabadal A, Inguanzo A, Monté-Rubio GC, Pardo J, Martí MJ, Compta Y, Valldeoriola F, Junque C, Iranzo, A. Brain atrophy pattern in *de novo* Parkinson's disease with probable RBD associated with cognitive impairment. *npj Parkinson's Disease*. 2022; 8: 2 doi:10.1038/s41531-022-00326-7.

**JCR IF (2021): 9.304, Q1 (Neurosciences). Objectives: 1 and 2.**

**Oltra J**, Campabadal A, Segura B, Uribe C, Martí MJ, Compta Y, Valldeoriola F, Bargallo N, Iranzo A, Junque C. Disrupted functional connectivity in PD with probable RBD and its cognitive correlates. *Scientific Reports*. 2021; 11: 24351. doi:10.1038/s41598-021-03751-5.

**JCR IF (2021): 4.996, Q2 (Multidiscip. Sciences). Objectives: 3 and 4.**

**Oltra J**, Uribe C, Campabadal A, Inguanzo A, Monté-Rubio GC, Martí MJ, Compta Y, Valldeoriola F, Iranzo, A, Junque C, Segura B. Sex differences in brain and cognition in *de novo* Parkinson's disease. *Frontiers in Aging Neuroscience*. 2022; 13: 791532. doi: 10.3389/fnagi.2021.791532.

**JCR IF (2021): 5.702, Q1 (Neurosciences). Objectives: 5 and 6.**

**Oltra J**, Segura B, Uribe C, Monté-Rubio GC, Campabadal A, Inguanzo A, Pardo J, Martí MJ, Compta Y, Valldeoriola F, Iranzo, A, Junque C. Sex differences in brain atrophy and cognitive impairment in Parkinson's disease patients with and without probable rapid eye movement sleep behavior disorder. *Journal of Neurology*. 2022; 269: 1591–1599. doi:10.1007/s00415-021-10728-x.

**JCR IF (2021): 6.682, Q1 (Clinical Neurology). Objectives: 5 and 6.**

## **Resum en català**

### **Ressonància magnètica, cognició i diferències entre sexes en la malaltia de Parkinson amb trastorn de conducta del son REM**

#### **Introducció**

La tesi doctoral se centra en l'estudi de la malaltia de Parkinson (MP) amb trastorn de conducta del son REM (TCR) com a subtipus clínic de la MP. En recerca translacional, la caracterització de subtipus és un dels principals objectius en l'estudi de les malalties neurodegeneratives. Així mateix, s'espera en el futur que la identificació de subtipus tingui un paper important en les estratègies de prevenció, diagnòstic i tractament en l'àmbit de la medicina de precisió. En aquest context, la MP amb TCR apareix com a un subtipus clínic greu que prèviament s'ha associat amb pitjors característiques clíniques, cognitives, d'atròfia cerebral i pronòstic més desfavorable. Malgrat els estudis previs de ressonància magnètica (RM), la connectivitat funcional del cervell mai ha estat explorada en aquest subtipus clínic i l'evidència pel que fa als correlats cerebrals del seu deteriorament cognitiu és encara molt escassa.

D'altra banda, la influència del sexe en les malalties neurodegeneratives és un aspecte rellevant que no ha estat degudament atès fins fa poc. Les principals troballes prèvies mostren un perfil de deteriorament cognitiu i de neurodegeneració més greu en pacients homes amb MP. L'estudi de l'efecte del sexe en diferents estadis de la malaltia, particularment en etapes inicials, i més en concret en aquells subtipus més greus, com ara la MP amb TCR, podria suposar un avanç en el coneixement de l'impacte d'aquesta variable. En un futur, aquest tipus de troballes podrien afavorir



la implementació d'estratègies més acurades de diagnòstic i tractament individualitzat.

## **Hipòtesis**

Les principals hipòtesis d'aquesta tesi són :

1. Els pacients amb MP amb probable TCR presentaran característiques diferencials en mesures de RM estructural i funcional respecte als pacients sense TCR. El major deteriorament cognitiu estarà associat a les alteracions cerebrals regionals més marcades en la MP amb probable TCR.
2. S'identificaran diferències entre sexes en cognició i atrofia regional en pacients amb MP *de novo*. S'espera trobar major afectació en homes. Les diferències entre sexes en MP *de novo* seran més extenses en el grup de MP amb probable TCR en comparació amb el grup sense TCR.

## **Objectius**

Els principals objectius d'aquesta tesi són:

1. Caracteritzar estructuralment i funcionalment mitjançant anàlisis d'imatges de RM la MP amb probable TCR i correlacionar les seves característiques amb el deteriorament cognitiu.
2. Explorar les diferències entre sexes en cognició i mesures de RM estructural en MP *de novo* i en MP *de novo* amb probable TCR.

## Mètodes

Aquesta tesi doctoral es presenta com a un compendi de quatre articles, els quals responen als objectius anteriorment esmentats.

Els estudis es van dur a terme tot emprant dues mostres diferents. La primera d'elles, corresponent als *estudis 1, 3 i 4*, incloïa 205 pacients amb MP *de novo* (recentment diagnosticats i sense medicació) i 69 controls sans (CS) del consorci *Parkinson's Progression Markers Initiative (PPMI)*. La segona mostra, corresponent a l'*estudi 2*, va consistir en 59 pacients amb MP, amb més durada de la malaltia i majoritàriament medicats, de la Unitat de Parkinson i Trastorns del Moviment (Hospital Clínic de Barcelona, Barcelona, Catalunya) i 30 CS procedents de l'Institut Català de l'Envel·liment (Universitat Autònoma de Barcelona, Barcelona, Catalunya) i de familiars o amics dels pacients.

En els *estudis 1, 3 i 4*, es van obtenir mesures estructurals de gruix cortical i volumetria a partir d'adquisicions d'imatges de RM potenciades en T1, i es van analitzar amb el programari *FreeSurfer*. En l'*estudi 2*, es van extreure mesures locals i globals per l'estudi quantitatiu de grafs a partir d'adquisicions d'imatges de RM funcional en estat de repòs tot emprant el programari *Brain Connectivity Toolbox*. A més a més, en l'*estudi 2*, la connectivitat funcional del cervell es va caracteritzar amb l'ús de la tècnica *threshold-free network-based statistics*.

En els *estudis 1 i 2*, el grup de MP amb probable TCR es va comparar amb el grup sense TCR i els CS en mesures cognitives i de RM. Altrament, per a posar en relació les característiques cerebrals i el deteriorament cognitiu en el grup de MP amb probable TCR es van aplicar models de regressió lineal múltiple (*estudi 1*) i anàlisis de correlacions (*estudi 2*). En els *estudis 3 i 4*, es van explorar les diferències entre sexes en mesures

clíniques, cognitives i estructurals de RM en la mostra de MP *de novo* sencera (*estudi 3*) i en la mateixa mostra dividida en els grups de MP amb probable TCR i sense TCR (*estudi 4*).

## **Resultats**

A les anàlisis estructurals de RM en els pacients amb MP *de novo* es va trobar una reducció del tàlem esquerre en el grup de MP amb probable TCR en comparació amb el grup sense TCR. A més a més, es van trobar reduccions en el grup de MP amb probable TCR en els volums d'estructures límbiques i també de l'estriat en comparació amb els CS. Els pacients amb MP sense TCR només tenien decrements a l'amígdala dreta (*estudi 1*). Les mesures d'atròfia global van mostrar que els pacients amb MP amb probable TCR en comparació amb els CS tenien reduccions de la substància grisa cortical i subcortical, amb el corresponent augment del volum del sistema ventricular. A més a més, l'anàlisi regional del gruix cortical va mostrar un aprimament a la circumvolució superior temporal dreta en el grup de MP amb probable TCR en comparació amb els CS.

Les anàlisis de RM funcional van palesar que el grup de MP amb probable TCR en comparació amb el grup sense TCR tenia una connectivitat alterada entre dues subregions del cíngol dret i del precúneus esquerre, i també una alteració de la integritat de la xarxa cerebral (*estudi 2*). Altrament, el grup de MP amb probable TCR va mostrar una alteració de la connectivitat funcional global en comparació amb el grup de CS, tant de les connexions cortico-corticals com de les cortico-subcorticals.

Pel que fa a la cognició, en MP *de novo*, el grup amb probable TCR va mostrar deteriorament respecte al grup sense TCR en la fluïdesa verbal i la funció visuoespacial (*estudi 1*). A més a més, vam trobar associacions significatives en el grup de MP amb probable TCR entre el deteriorament

cognitiu i les reduccions de substància grisa, principalment de regions subcorticals. En la mostra de MP més avançada, el grup amb probable TCR va mostrar deteriorament en velocitat de processament i inhibició en comparació amb el grup sense TCR (*estudi 2*). El deteriorament de la velocitat de processament, la memòria verbal i la funció visuoespacial es va relacionar amb l'alteració de la connectivitat funcional en el grup de MP amb probable TCR.

L'anàlisi de la influència del sexe en el deteriorament cognitiu, en MP *de novo*, va mostrar que els pacients homes tenien major afectació en cognició general, fluïdesa verbal, velocitat de processament i memòria verbal (*estudi 3*). Altrament, les pacients dones tenien un pitjor rendiment que els pacients homes en funció visuoespacial. Amb la mostra dividida segons presència de TCR, al grup de MP amb probable TCR els pacients homes tenien una major afectació en cognició general, fluïdesa verbal i velocitat de processament (*estudi 4*).

Pel que fa a les diferències sexuals en l'atròfia cerebral en MP *de novo*, els pacients homes mostraven reduccions de volum en comparació a les pacients dones en els volums totals de substància grisa cortical i subcortical, en el tàlem, el caudat, el putamen, el pà·lid, l'hipocamp i el tronc cerebral (*estudi 3*). En la mateixa direcció, els pacients homes tenien reduccions regionals del gruix cortical a les àrees postcentral esquerra i precentral dreta en comparació amb les pacients dones. En el grup de MP amb probable TCR, els pacients homes en comparació amb les pacients dones mostraven major atròfia en les mesures globals de substància grisa cortical i subcortical, i també en la volumetria dels nuclis caudat i pà·lid i del tronc cerebral (*estudi 4*). Les diferències entre sexes en mesures d'atròfia i alteracions neuropsicològiques en el grup de MP sense TCR anaven en la mateixa direcció (major afectació en homes), però eren

menys extenses. Es va observar només un pitjor rendiment en fluïdesa verbal i menor volum del tronc cerebral.

## **Conclusions**

Hem identificat característiques cerebrals que assenyalen una atròfia a la substància grisa subcortical (a regions talàmiques, límbiques i de l'estriat) en la MP amb probable TCR en fases inicials de la malaltia (*estudi 1*). La reducció del tàlem és la principal diferència entre els dos grups de pacients.

El perfil cognitiu distintiu de la MP amb probable TCR es caracteritza en les fases inicials de la malaltia per un deteriorament incrementat en fluïdesa verbal i funció visuoespacial en comparació amb el grup sense TCR (*estudi 1*). L'atròfia de la substància grisa subcortical s'associa al deteriorament cognitiu en la MP amb probable TCR (*estudi 1*). En pacients amb MP més avançada es troba un deteriorament incrementat en velocitat de processament mental i funció inhibidòria en el grup amb probable TCR (*estudi 2*).

Els pacients amb probable TCR mostren un decrement de la connectivitat funcional amb implicació cortico-cortical i cortico-subcortical (*estudi 2*). La característica diferencial entre els dos grups de MP és la reducció de la connectivitat posterior cortico-cortical, així com l'alteració de l'eficiència global de la xarxa cerebral.

La reducció de la connectivitat funcional es relaciona amb el deteriorament visuoespacial, i l'alteració de l'eficiència de la xarxa cerebral es relaciona amb el deteriorament de la velocitat de processament i de l'aprenentatge verbal en la MP amb probable TCR en estadis més avançats (*estudi 2*). Així doncs, la connectivitat funcional

alterada explica part del deteriorament cognitiu dels pacients amb MP amb probable TCR.

Pel que fa al paper diferencial del sexe en el procés degeneratiu, hem trobat que els homes amb MP *de novo* mostren un aprimament del gruix cortical en regions frontoparietals i reduccions de volums d'estructures subcorticals en comparació amb les dones (*estudi 3*). Les diferències són més extenses en el grup de MP amb probable TCR (*estudi 4*). En la mateixa línia, les dades cognitives mostren que els homes amb MP *de novo* tenen un deteriorament cognitiu incrementat en comparació amb les dones, el qual inclou deteriorament en cognició general, fluïdesa verbal, velocitat mental de processament i memòria verbal (*estudi 3*). A més a més, el pitjor rendiment cognitiu en els homes respecte a les dones és més extens en el grup de MP amb probable TCR (*estudi 4*). Podem concloure per tant, que l'efecte del sexe en el cervell i la cognició s'evidencia en MP *de novo*, i no s'explica per l'edat per si mateixa. Altrament, la presència de TCR és un factor que contribueix a les diferències entre sexes en la MP.

En resum, la present tesi doctoral significa un progrés en la caracterització de la MP amb TCR com a un subtipus clínic de la MP. Per primera vegada, vam descriure en aquest grup de pacients les bases fonamentalment subcorticals del seu deteriorament cognitiu (*estudi 1*), així com l'alteració de la connectivitat funcional global del cervell mitjançant *network-based statistics* i la seva associació amb el rendiment cognitiu (*estudi 2*). Una altra aportació potencialment rellevant va ser el fet de trobar diferències entre sexes en mesures estructurals de RM i de cognició, les quals indiquen una major vulnerabilitat dels homes en la MP que es fa molt més palesa en aquest subtipus (*estudis 3 i 4*).

## **Abstract**

### **Magnetic resonance imaging, cognition, and sex differences in Parkinson's disease with REM sleep behavior disorder**

#### **Introduction**

This doctoral thesis is centered on Parkinson's disease (PD) with rapid eye movement sleep behavior disorder (RBD) as a clinical subtype. Characterizing subtypes is one of the main ongoing objectives of translational research on neurodegenerative diseases. Therefore, subtyping is expected to play a relevant role in future precision medicine prevention, diagnosis, and treatment approaches. In this context, PD with RBD appears as a severe clinical subtype previously associated with worse clinical, cognitive, and neurodegenerative outcomes. However, the whole-brain functional connectivity of this clinical subtype has never been explored, and evidence about the brain correlates of its cognitive impairment is still scarce.

The influence of sex in neurodegenerative diseases has been overlooked by previous research. Prior findings point to severe cognitive impairment and neurodegenerative profile in male PD patients. Besides, the study of the effect of sex at different stages of the disease, particularly in an early phase and on the eventual severe clinical subtypes, such as PD with RBD, could enhance the current understanding of the impact of this variable in PD. This knowledge might lead to more appropriate diagnostic strategies and specific therapeutic options in the future.

## Hypotheses

The main hypotheses of this thesis are:

1. PD-pRBD will be characterized by specific structural and functional MRI brain features associated with cognitive impairment.
2. There will be identified sex differences in cognition and structural MRI brain features in *de novo* PD, with worse cognitive profile and pattern of neurodegeneration in males than females. The sex differences among *de novo* PD patients will be more extended in the PD-pRBD group compared with the PD without probable RBD (PD-non pRBD) group.

## Objectives

The main objectives of this thesis are:

1. To characterize structural and functional magnetic resonance imaging (MRI) brain substrates in PD with probable RBD (PD-pRBD) and their correlates with cognitive impairment.
2. To explore sex differences in cognition and structural MRI brain features in *de novo* PD and *de novo* PD-pRBD.

## Methods

This doctoral thesis is presented as a compendium of four articles performed to achieve the mentioned objectives.

Studies comprised two different samples. The first one, used in *studies 1, 3, and 4*, was a sample of 205 *de novo* PD patients (newly diagnosed and drug-naïve) and 69 healthy controls (HC) from the Parkinson's Progression Markers Initiative (PPMI). The second sample, examined in *study 2*, consisted of 59 PD patients with more disease duration and



mostly medicated recruited from the Unitat de Parkinson i Trastorns del Moviment (Hospital Clínic de Barcelona, Barcelona, Catalunya) and 30 HC recruited from the Institut Català de l'Envel·liment (Universitat Autònoma de Barcelona, Barcelona, Catalunya) and patients' relatives. Different clinical and cognitive measures were collected for both samples.

In *studies 1, 3, and 4*, cortical thickness and volumetric measures were obtained from T1-weighted acquisitions using *FreeSurfer*. In *study 2*, local and global graph metrics were obtained from resting-state functional MRI acquisitions with *Brain Connectivity Toolbox*, and whole-brain functional connectivity was characterized using threshold-free network-based statistics.

In *studies 1 and 2*, the PD-pRBD group was compared with PD-non pRBD and HC groups in cognitive and MRI measures. Additionally, to relate brain characteristics and cognitive impairment of the PD-pRBD group, multiple linear regression models (*study 1*) and correlation analyses (*study 2*) were used. In *studies 3 and 4*, sex differences were explored in clinical, cognitive and structural MRI measures in the *de novo* PD sample and divided the sample into PD-pRBD and PD-non pRBD, respectively.

## Results

Structural MRI analyses revealed, in *de novo* PD, a left thalamic reduction in PD-pRBD compared with PD-non pRBD and reductions in limbic and striatal subcortical volumes compared with HC. Decrements in PD-non pRBD compared with HC were limited to the right amygdala (*study 1*). Moreover, cortical thickness analysis reported thinning in the right superior temporal gyrus in PD-pRBD compared with HC. Regarding global atrophy measures, reduced total cortical and subcortical GM volumes and enhanced ventricular system volume were found in PD-pRBD compared

with HC. Reductions were limited to total cortical GM volume in PD-non pRBD compared with HC.

Functional MRI analyses in more advanced PD showed that the PD-pRBD group had an altered connection between two subregions from the right cingulate and left precuneus and abnormal network integrity compared with the PD-non pRBD one (*study 2*). Besides, the PD-pRBD group showed altered whole-brain connectivity involving cortico-cortical and cortico-subcortical connections when compared with the HC group. On the other hand, the functional connectivity in the PD-non pRBD group seemed preserved.

Regarding cognitive outcomes, in *de novo* PD patients, the PD-pRBD group showed verbal fluency and visuospatial impairment compared with the PD-non pRBD group (*study 1*). In addition, we found significant associations in PD-pRBD between cognitive impairment and gray matter volume decrements, mainly subcortical ones. In the sample of more advanced PD patients, the PD-pRBD group showed mental processing speed and inhibition impairment compared with the PD-non pRBD group (*study 2*). Further, mental processing speed, verbal memory, and visuospatial impairment significantly correlated with altered functional connectivity in PD-pRBD (*study 2*).

Concerning sex differences in cognition, in *de novo* PD, males showed general cognition, verbal fluency, mental processing speed, and verbal memory impairment compared with females (*study 3*). On the other hand, females had worse performance than males in visuospatial functions. In the *de novo* PD sample divided, in PD-pRBD, males had general cognition, verbal fluency, and mental processing speed impairment compared with females (*study 4*).

As regards structural MRI measures, in *de novo* PD, males showed volume decrements compared with females in total cortical and subcortical GM; and in the thalamus, caudate, putamen, pallidum, hippocampus, and brainstem (*study 3*). Moreover, males showed thinning in the left post-central and right precentral areas compared with females. In PD-pRBD, males had volume decrements compared with females in total cortical and subcortical GM; and caudate, pallidum, and brainstem (*study 4*). In PD-non pRBD, the sex differences followed the same direction but were less widespread: females outperformed males in verbal fluency, and males had decreased brainstem volume compared with females.

## **Conclusions**

We identified structural brain characteristics that point towards early GM subcortical atrophy (involving thalamic, limbic, and striatal regions) and temporocortical atrophy in PD-pRBD (*study 1*). The smaller thalamic volume is the main characteristic that differentiates PD-pRBD from PD-non pRBD.

The distinctive cognitive profile of PD-pRBD is characterized, in *de novo* PD, by an increased impairment in verbal fluency and visuospatial function compared with PD-non-pRBD (*study 1*). The subcortical GM atrophy is associated with cognitive impairment in *de novo* PD-pRBD (*study 1*). In PD-pRBD patients with more advanced disease, the cognitive profile is characterized by an increased impairment in mental processing speed and inhibitory function (*study 2*).

The PD-pRBD patients show decreased functional connectivity involving cortico-cortical and cortico-subcortical connections in more advanced PD (*study 2*). The differential characteristics of PD-pRBD from PD-non

pRBD are the reduced posterior cortico-cortical connectivity and the network efficiency alteration.

The reduced connectivity strength correlates with visuospatial impairment in more advanced PD-pRBD. Further, the network efficiency alteration correlates with mental processing speed and verbal learning impairment (*study 2*). Therefore, altered functional connectivity is also associated with cognitive impairment in PD-pRBD patients.

Regarding sex differences, *de novo* PD males show cortical thinning in frontoparietal regions and smaller volume in several subcortical regions compared with *de novo* PD females (*study 3*), more extended in PD-pRBD than PD-non pRBD (*study 4*). Cognitive data show that *de novo* PD males have increased neuropsychological impairment than *de novo* PD females, including general cognition, verbal fluency, mental processing speed, and verbal memory impairment (*study 3*). Notable, cognitive impairment in males compared with females is more extended in *de novo* PD-pRBD than in PD-non pRBD (*study 4*). Then, the sex effect on brain and cognition is already evident in *de novo* PD, not explained by age per se. Furthermore, the presence of RBD is a contributing factor to sex differences in PD.

In summary, the present doctoral thesis has progressed in characterizing PD with RBD as a clinical PD subtype. For the first time, we described in this group of patients the subcortical basis of cognitive impairment (*study 1*), the functional connectivity disruption using whole-brain network-based statistics, and its association with cognitive performance (*study 2*). As a novelty, we found sex differences in structural brain features and cognition, which indicate a more marked male vulnerability in this PD clinical subtype (*studies 3 and 4*).

# Chapter 1

---

## Introduction

The world population is aging; according to estimations, the population over 65 years old will rise from 10% in 2022 to 16% in 2050 (1). Besides, age is one of the main risk factors for neurodegeneration. Thus, the prevalence of neurodegenerative diseases will increase in the near future. In this context, aging is one of the biggest challenges in clinical settings and translational research. For this purpose, the development and implementation of disease biomarkers are fundamental. Two major research fields are early detection and disease subtyping, which allow distinguishing patterns with different associated features. Moreover, there has been a growing interest in the impact of sex and gender on neurodegeneration. Disease subtyping and the effect of sex are relevant in the context of precision medicine for prevention, diagnosis, and treatment approaches in the upcoming years.

Rapid eye movement (REM) sleep behavior disorder (RBD) is one of the main prodromal symptoms of neurodegenerative diseases, mainly Parkinson's disease (PD) and other synucleinopathies. In addition, RBD allows characterizing a clinical subtype of PD associated with worse clinical, cognitive, and brain atrophy features. The focus of this dissertation is PD with RBD and the impact of sex on this clinical subtype. The Introduction is organized into three main sections to cover these aspects. The first section is an overview of RBD, from its diagnosis to its cerebral basis. In the second section, I will review the relation between RBD and PD, beginning with its role as a prodromal symptom and ending with PD with RBD as a clinical subtype. In the last section, I will introduce the role of sex and gender in PD.

## **1. REM sleep behavior disorder: an overview**

Rapid eye movement sleep behavior disorder is a parasomnia characterized by dream enactment and loss of REM atonia, described for the first time by Schenck et al. in 1986 (2) and recognized as a diagnostic category in 1990 in *The International Classification of Sleep Disorders, First Edition (ICSD-1)* (3). The patients with RBD show REM sleep without atonia (RWA), which enables the displaying of motor actions presumably related to the dream content. Furthermore, the dream content in these patients is frequently unpleasant; situations in which, for example, the person is being attacked or persecuted, arguing with someone, or falling off a cliff (4,5). Thus, the associated enacting usually is characterized by violent behaviors (4). Although non-violent elaborated behaviors, even pleasant, have been reported (6). The complexity of the motor behaviors ranges from simple (such as switching or jerking) to complex movements (such as talking, punching, or jumping from the bed) (2). These behaviors in RBD are associated with the causation of injuries by patients to themselves or bed partners (4,7). Moreover, RBD has been related to worse quality of life (8).

Concerning the diagnosis, the cardinal features of RBD are the presence of RWA and dream-enacting behaviors. The RWA is the hallmark of RBD diagnosis. Further, dream-enacting behaviors are associated with excessive electromyographic (EMG) activity during REM sleep. These characteristics of REM sleep are tested in patients through a polysomnography (PSG) study. The main set of diagnostic criteria for RBD comes from *The International Classification of Sleep Disorders, Third Edition (ICSD-3)* (9), which are complemented by the PSG characteristics described in the *American Academy of Sleep Medicine Manual for the Scoring of Sleep and Associated Events, Version 2.6* (10).

For more detail about the diagnostic criteria, see **Panel A**.

**Panel A. RBD Diagnostic**

***The International Classification of Sleep Disorders, Third Edition (ICSD-3)***

RBD Diagnostic criteria: A-D must be met

- A. Repeated episodes of sleep-related vocalization and/or complex motor behaviors.
- B. These behaviors are documented by polysomnography to occur during REM sleep or, based on clinical history of dream enactment, are presumed to occur during REM sleep.
- C. Polysomnographic recording demonstrates RWA.
- D. The disturbance is not better explained by another sleep disorder, mental disorder, medication or substance abuse.

***American Academy of Sleep Medicine Manual for the Scoring of Sleep and Associated Events, Version 2.6***

Scoring polysomnographic features of RBD: RBD is characterized by either or both of the following:

- A. Sustained muscle activity (tonic activity) in REM sleep:  
An epoch of REM sleep with at least 50% of the duration of the epoch having a chin EMG amplitude greater than minimum amplitude than in no REM sleep (NREM).
- B. Excessive transient muscle activity (phasic activity) in REM sleep:  
In a 30s epoch of REM sleep divided into 10 sequential 3s mini-epochs, at least five (50%) of the mini-epochs contain bursts of transient muscle activity. In RBD, excessive transient muscle activity bursts are 0.1–5.0s in duration and at least 4 times as high in amplitude as the background EMG activity.

Clinicians and researchers use validated questionnaires to screen RBD when a PSG study for RBD diagnosis is not available. According to the cut-offs of these RBD questionnaires, the patients or participants with significant RBD symptomatology receive the denomination of “probable RBD” (pRBD), in contrast to a PSG-based RBD diagnosis. Other promising methods for RBD screening are being developed, such as a wrist home-screening actigraphy tools (II).



At this point and before continuing, it is relevant to differentiate other terminology, apart from RBD and pRBD. Other basic terms in this context are “idiopathic RBD” and “isolated RBD” (iRBD); they refer to cases of RBD without a primary cause known (called “secondary RBD”). Nowadays, the term “isolated RBD” is preferred (12) because these patients eventually convert to overt an alpha-synucleinopathy (13,14), and related positive biomarkers (15) and neurodegeneration are already present (16). Concerning PD, the term PD-RBD corresponds to those patients with a PSG-based diagnosis of RBD, and PD-pRBD corresponds to those patients categorized using questionnaires (as complementary, PD-non RBD and PD-non pRBD are used). In this thesis, “PD with RBD” will be used as a general term when referring broadly to this population and when referring to results from PD samples with and without a PSG-based classification.

The most recent meta-analysis on the epidemiological aspects of iRBD reports that its prevalence is 0.68%, and pRBD prevalence is 5.65% (17). Isolated RBD is usually diagnosed in individuals older than 50 years (18,19). Although iRBD is considered a predominantly male condition, the sex ratio in iRBD varies depending on the type of study. Thus, Schenck et al. in 1993 reported a close to 9:1 male-to-female ratio, and subsequent clinical cohorts have also reported male predominance (5,19–21). However, a recent general population-based study did not show differences in iRBD prevalence between males and females (22). Considering this discrepancy between clinical and population-based samples, RBD underdiagnosis in females seems possible. In this regard, some authors have suggested that RBD is underrecognized in females because they have less dream-enacting (23) and less aggressive behaviors (24), which could lead to less likelihood of seeking medical attention.

The hypothesized pathophysiology of RBD proposes an alteration of the brain circuitry involved in the regulation of muscle tone during the REM phase. In the system involved in REM sleep atonia, different nuclei from the subcoeruleus/pre-coeruleus complex play a key role (25). During REM sleep, these nuclei have excitatory projections to the inhibitory ventromedial medulla. The nucleus of the spinal cord has inhibitory projections to spinal motor neurons. These chained events result in a reduction of the skeletal muscle tone through temporary paralysis. REM sleep behavior disorder appears when the mentioned circuitry is impaired and presents a chemical imbalance. The disequilibrium could occur in one of the two steps: in the excitatory glutamatergic projection, from the subcoeruleus/pre-coeruleus complex to the ventromedial medulla; or in the inhibitory GABA/Glycinergic projection, from the ventromedial medulla to spinal motor neurons. However, RWA is only one of the components of RBD, which is also characterized by the presence during the REM phase of vivid dreams and increased EMG activity associated with complex movements and dream enactment (25,26). In this regard, the suspected pathophysiology and dysfunction extension in RBD involves other neural circuits and neurotransmitters explored using neuroimaging techniques (27). For example, the "cortical hypothesis" proposes that the lack of inhibition of the spinal motor neurons allows the complex movements planned in the motor cortex to arise from the limbic dream-related inputs (26). **Figure 1** summarizes the main brain regions and neurotransmitters involved in normal REM sleep and RBD.

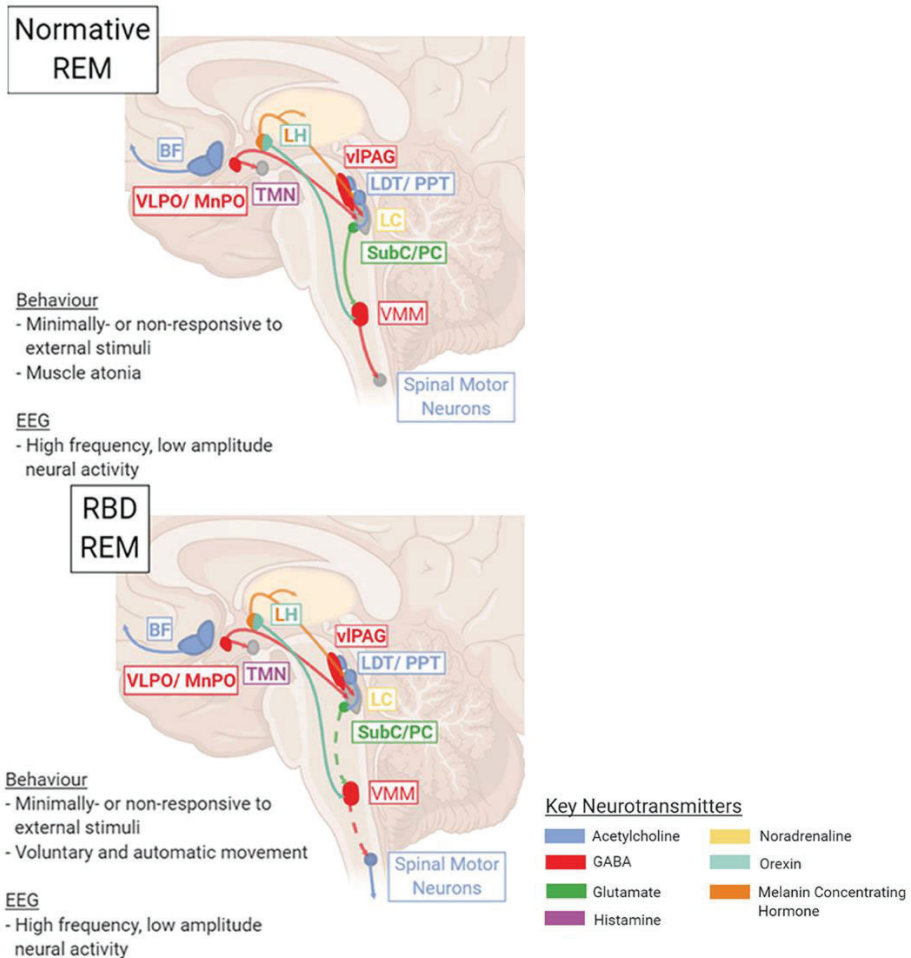


**Figure 1.** Key brain regions and neurotransmitters involved in regulation and maintenance of the REM sleep stage under healthy normative or pathological RBD conditions. In RBD, dysfunction within the SubC→VMM→Spinal Motor Neuron pathway results in a lack of REM atonia (depicted with dotted line). Abbreviations: BF, basal forebrain; LC, locus coeruleus; LDT/PPT, laterodorsal tegmentum/pedunculopontine tegmentum; LH, lateral hypothalamus; SubC/PC, subcoeruleus/pre-locus coeruleus; TMN, tuberomammillary nucleus; vIPAG, ventrolateral periaqueductal gray; VLPO/MnPO, ventrolateral preoptic nucleus/median preoptic nucleus; VMM, ventromedial medulla. Adapted from “Key brain regions and neurotransmitters involved in regulation and maintenance of the REM sleep stage under healthy normative or pathological RBD conditions” by Roguski et al. (25) licensed under CC BY-ND 4.0.

## **2. RBD and Parkinson's disease**

This section will review RBD in the context of PD, with a brief overview of RBD as a prodromal stage and its presence in neurodegenerative diseases.

### **2.1. RBD as a prodromal stage of Parkinson's disease**

Historically, the first description of iRBD as a precursor of subsequent parkinsonism was reported by Schenck et al. in 1986, the same group which introduced the term RBD (2). They observed in iRBD patients a phenoconversion of 38% to overt parkinsonism after a mean interval of 3.7 years (28). In the following update, 81% of the pool of patients initially diagnosed as iRBD developed an overt parkinsonism or dementia after a mean interval of 14.2 years, of which 50% converted to PD (29). A recent meta-analysis including 46 studies concluded that the risk for developing a neurodegenerative disease after iRBD diagnosis is 33.5% after five years and reaches 96.6% at 14 years, of which 43% converted to PD (13). Similarly, the largest international multicenter study, with a whole sample of 1,280 iRBD patients and 24 participant centers, found that 28% of patients converted to a neurodegenerative disease after a mean interval of 4.6 years, of which 56.5% developed overt parkinsonism (14). In the same study, the authors reported an overall phenoconversion rate of 6.25% per year and a risk of conversion of 73.5% after 12 years.

Thus, iRBD is associated with the further development of neurodegenerative diseases, specifically synucleopathies. De Natale et al. revised the existing literature and collected the main predictors of the progression of iRBD towards synucleopathies based on the previous evidence (30). Some of these predictors distinguish between conversion to PD or other synucleopathies, namely multiple system atrophy (MSA)

or dementia with Lewy Bodies (DLB). Therefore, progression of motor symptoms is faster in PD converters; hyposmia is associated with PD and DLB but not MSA conversion; electroencephalogram (EEG) slowing in temporal and occipital lobes, as well as alterations in the PD-related metabolic pattern are associated with PD conversion. **Table 1** summarizes the main risk factors of conversion from iRBD to an overt neurodegenerative disease; in detail in De Natale et al., 2022 (30).

**Table 1.** List of the most important predictors of progression of isolated RBD towards synucleinopathy

<b>Biomarker</b>	<b>Effect</b>
<b><i>Clinical</i></b>	
UPDRS-III	Early appearance of speech and voice alterations, followed by bradykinesia, rigidity, and rest tremor. Faster progression in PD converters
Quantitative autonomic scales scores	Urinary symptoms scores more severe in MSA converters, decline in systolic blood pressure more pronounced in DLB converters
Heart Rate Variability	Decreased in iRBD patients. Conflicting results on its predictive value
Cognitive dysfunction	Alterations in attention, executive function, and verbal memory associated with faster conversion in iRBD. DLB converters show more pronounced cognitive alterations at baseline and faster progression
Hyposmia	Associated with higher risk of phenoconversion in iRBD to DLB and PD, but not MSA
Visual dysfunction	Abnormal color vision associated with increased risk of phenoconversion. Faster progression in DLB converters
<b><i>Genetic</i></b>	
<i>GBA</i> gene variants	Higher rate of <i>GBA</i> variants in iRBD patients with higher rate of phenoconversion. Risk influenced by the severity of the mutation
<i>TMEM175</i> gene mutations	The p.Q65P variant associated with increased rate of phenoconversion to a synucleinopathy

SNCA gene CpG hypomethylation	Associated with increased risk of progression of iRBD symptoms and phenoconversion
<b>Neurophysiological</b>	
RSWA	Percentage of RSWA at baseline is a predictor of future phenoconversion. Tonic RSWA associated with higher risk of future conversion to parkinsonism, phasic RSWA associated with risk of future phenoconversion to dementia
Isolated RSWA	Conflicting results on its predicting role of future phenoconversion
EEG abnormalities	Higher $\delta$ and $\theta$ power in the cortex and higher slow-to-fast power ratio in converters. Diffuse slowing of electrical activity associated with DLB; EEG slowing in temporal and occipital lobes associated with PD
Cyclic Alternating Pattern	CAP rate reduction in future converters to a neurodegenerative disease
<b>Fluid</b>	
p-tau/total tau ratio in CSF	Reduced ratio in iRBD associated with phenoconversion at five years
<b>Imaging</b>	
Presynaptic striatal dopamine terminals [ <sup>123</sup> I]FP-CIT-SPECT and [ <sup>99m</sup> Tc]TRODAT-1-SPECT	Progressive loss of presynaptic dopamine terminals in the striatum associated with high risk of short-term conversion
Glucose metabolism [ <sup>99m</sup> Tc]ECD-SPECT and [ <sup>18</sup> F]FDG-PET	Increased hippocampal perfusion in iRBD who phenoconvert at three years. Alterations in the PD-related metabolic pattern associated with phenoconversion in iRBD
Structural MRI	Cortical thinning in frontal, parietal, and occipital cortices associated with phenoconversion in iRBD

Abbreviations: CSF, Cerebrospinal fluid; DLB, Dementia with Lewy bodies; EEG, Electroencephalogram; *GBA*, glucocerebrosidase; MRI, Magnetic resonance imaging; MSA, Multiple system atrophy; PD, Parkinson's disease; PET, Positron emission tomography; RBD, REM Sleep behavior disorder; RSWA, REM sleep without atonia; SNCA, Synuclein; SPECT, Single photon emission computerized tomography; *TMEM175*, Transmembrane protein 175; UPDRS, Unified Parkinson's disease rating scale. Adapted from "List of the most important predictors of progression of isolated RBD towards synucleinopathy" by De Natale et al. (30) licensed under CC BY-ND 4.0.

Another important issue is the trajectory of motor and non-motor symptoms from iRBD to different synucleopathies. Fereshtehnejad et al. described these trajectories of symptoms in a sample of PD and DLB converters (31). The results showed that the first symptom to appear is olfactory loss (20 years before phenoconversion); followed by color perception impairment, constipation, and erectile dysfunction (10-16 years before phenoconversion); then slight urinary dysfunction and subtle cognitive decline (7-9 years before phenoconversion); mild alteration of handwriting, turning in bed, walking, salivation, speech, and facial expression (7-11 years before phenoconversion); motor examination abnormalities (5-7 years before phenoconversion) with motor phenotypes appearing first bradykinesia, and then rigidity and tremor (5-6, 3, and 2 years before phenoconversion respectively). **Figure 2** shows the model of progression from iRBD to PD.

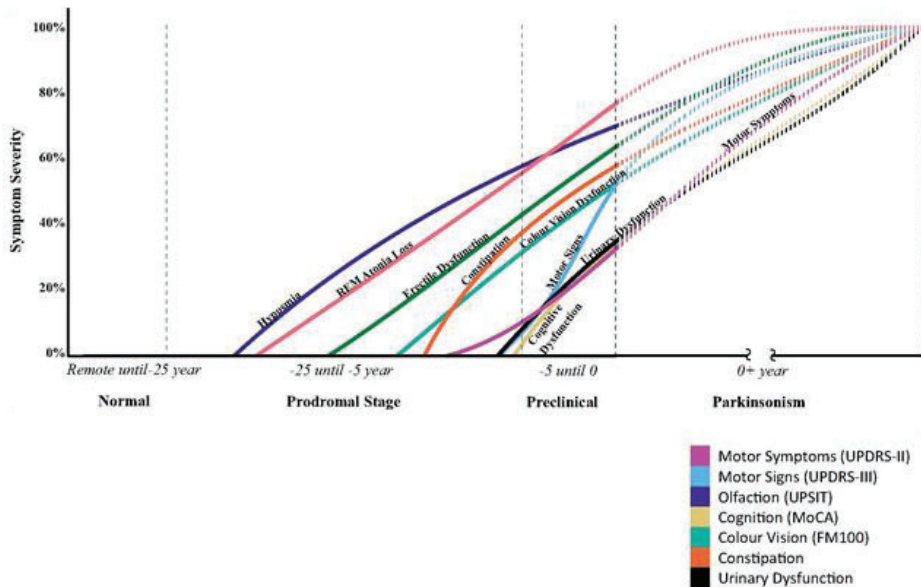


**Figure 2.** Schematic model for progression of motor and non-motor manifestations throughout the prodromal, phenoconversion and advanced stages of patients with idiopathic RBD converting to Parkinson’s disease. This schematic illustrates the approximate trajectories of the major motor and non-motor manifestations as patients progress from normal, through idiopathic RBD, to advanced Parkinson’s disease. This is based on control data, patients with idiopathic RBD tracked through time, and patients with advanced Parkinson’s disease who also have RBD. The predicted progressions after phenoconversion were dotted due to the uncertainty of real symptomatic severity without the influence of dopaminergic treatment. Olfaction is generally the first manifestation to become abnormal and reaches near maximum loss at the time of phenoconversion. The authors scaled down both cognitive and color vision dysfunction slopes by half to avoid the bias driven by DLB subjects (the estimated maximum symptoms were based on Parkinson’s disease–RBD subjects without dementia at baseline). Autonomic features are similarly present early, and approximate 50–70% maximal values at phenoconversion. REM atonic loss and color vision loss have patterns similar to autonomic loss. By contrast, motor and cognitive abnormalities start relatively late, and are at only 20–30% maximal values at the time of phenoconversion. Adapted from “Combined progression trajectory of motor and non-motor manifestations from prodromal stages to phenoconversion based on actual measurements” by Fereshtehnejad et al. (31) licensed under RightsLink.



## 2.2. RBD in Parkinson's disease

There is controversy about the prevalence of RBD in PD, considering different factors such as the use of different diagnostic procedures. The two most recent meta-analyses reported a pooled RBD prevalence of 23.6% and 42.3 % in PD (32,33). The second meta-analysis also explored the risk factors for RBD in PD and reported older age and longer disease duration as the main ones (33).

Other studies suggest that the prevalence of RBD in PD may be even higher due to the lack of screening of symptoms throughout the disease using PSG. An important aspect is that RBD is commonly not evaluated along the disease course by PSG. Notwithstanding, clinicians assess RBD symptomatology in PD using questionnaires or clinical interviews. In this context, Baumann-Vogel et al. in 2020 studied the prevalence of RBD in a sample of 540 PD patients in a sleep laboratory using PSG (34). In the University Hospital Zurich, 90% of the patients with neurodegenerative disease from the Department of Neurology underwent PSG. The rationale for this protocol is the high presence of RBD in these diseases and its clinical importance. The total prevalence of RBD in PD was 77% which contrasts with the lower prevalence reported by previous original studies and meta-analyses. Moreover, the prevalence increased with age, reaching around 90% in the group of PD patients between 75 and 89 years old.

Concerning the clinical aspects associated with RBD and PD, the evidence collected in a 2017 meta-analysis points to a strong relation with male sex, older age, longer disease duration, higher disease stage using the *Hoehn and Yahr scale (H&Y scale)*, and more motor symptomatology measured by means of the *Movement Disorder Society Unified PD Rating Scale (MDS-UPDRS) Part III* (35). Regarding the higher prevalence of RBD

in PD males, it also has been reported in iRBD (5,22). The relevance of sex in PD and RBD will be discussed in deep in the last section of the Introduction (*Section 3. Sex and gender in Parkinson's disease*). Furthermore, longitudinal studies have shown faster progression in PD-pRBD patients, specifically in motor symptomatology measured using the *MDS-UPDRS Part III* score (36), and also in those PD-pRBD patients classified as postural instability and gait dysfunction (PIGD) motor phenotype (37).

REM sleep behavior disorder in PD has been associated with worse cognitive impairment and brain abnormalities. The cognitive and neuroimaging studies will be presented in further subsections (*Subsection 2.2.2. Cognition in Parkinson's disease with RBD* and *Subsection 2.2.4. Brain imaging in Parkinson's disease with RBD*, respectively).

### **2.2.1. Neuropathology of Parkinson's disease with RBD**

So far, only one post-mortem neuropathological study has explored PD with RBD symptomatology and revealed that PD-pRBD patients had a significant increased alpha-synuclein deposition in 9 of 10 explored regions compared with PD-non pRBD: olfactory bulb, anterior medulla, anterior/mid-pons, amygdala, anterior cingulate gyrus, transentorhinal cortex, middle temporal gyrus, and inferior parietal lobule (38). In addition, a recent study showed that RBD symptomatology is associated with decreased cerebrospinal fluid (CSF) alpha-synuclein, specifically aggressive dreams (39).

## **RBD in the Braak model of Parkinson's disease staging**

The Braak staging is a model which characterizes the disease progression in PD in terms of the alpha-synuclein pathology spreading. The model establishes six stages based on the topographical and temporal properties of the alpha-synuclein spreading. In this context, the alpha-synuclein pathology initiates from the brainstem and olfactory regions and then spreads to the anteromedial temporal mesocortex and, in the later stages, to the neocortex (40). Concurrently, Braak et al. proposed the dual-hit hypothesis, in which the neurodegeneration process has its origin in a neurotropic pathogen that enters primary to the brain via nasal with anterograde propagation to the temporal lobe and secondary via gastric due to swallowing of nasal secretions in saliva (41,42). **Figure 3** represents the Braak stages in PD schematically. According to the literature, the RBD starts in the first Braak stages, probably in stage 2, with the degeneration of some pontine (e.g., sublaterodorsal nucleus) and brainstem structures (e.g., pre-coeruleus and magnocellular reticular formation) involved in the REM sleep circuitry (43).

In that regard, a recent study performed by Knudsen et al. showed an equivalent dysfunction in iRBD patients compared with PD patients, involving pathological findings in the sympathetic and parasympathetic nerves. Nonetheless, in contrast to PD patients, the majority of iRBD patients show unaltered dopaminergic innervation (27). The authors proposed that these findings support the hypothesis of the propagation of the alpha-synuclein from the peripheral autonomic nerves to the brainstem before the involvement of the dopaminergic system, which corresponds to the first Braak stages.

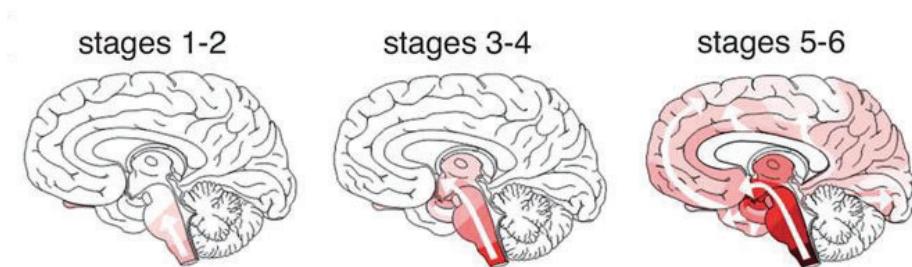


**Figure 3.** Six stages of idiopathic Parkinson's disease. The proposed regional distribution pattern of the lesions is depicted using degrees of shading for each stage. (a) Stages 1–2 are characterized by Lewy pathology in the dorsal IX/X motor nucleus, olfactory bulb, and/or intermediate reticular zone of the medulla, in the caudal raphe nuclei, gigantocellular reticular nucleus, and coeruleus-subcoeruleus complex. Stages 3–4: expansion into the midbrain, particularly the substantia nigra, pars compacta, paranigral nucleus, amygdala, basal forebrain nuclei, hypothalamus, thalamus, transentorhinal region, entorhinal region, and second sector of the Ammon's horn. Stages 5–6: thalamus expansion into the ectorhinal region (ec), insular cortex, high order sensory association areas of the neocortex and prefrontal neocortex, first order sensory association areas of the neocortex and premotor areas. Adapted from “Six stages of idiopathic Parkinson's disease” by Del Tredici et al. (44) licensed under CC BY-ND 4.0.

More recently, Borghammer et al. analyzed neuropathological evidence and proposed that not all PD patients follow a pattern of alpha-synuclein spreading from the peripheral nervous system (PNS) to the central nervous system (CNS) via retrograde vagal transport (45). This statement is based on the fact that a fraction of PD patients does not show pathology in the dorsal motor nucleus of the vagus nerve. The authors hypothesized the existence of a PNS-first and a CNS-first subtype. Thus, the PNS-first is associated with iRBD during the prodromal phase and is characterized by autonomic PNS damage before the involvement of the dopaminergic system. On the other hand, the CNS-first often is not associated with iRBD during the prodromal phase and is characterized by nigrostriatal dopaminergic dysfunction before the involvement of the autonomic PNS.

In a subsequent theoretical development, Borghammer proposed the alpha-Synuclein Origin site and Connectome (SOC) Model (46). Following the SOC Model, in the brain-first subtype (equivalent term to CNS-first), the pathology appears unilaterally, frequently in the amygdala, and as the alpha-synuclein propagation depends on connection strength, a unilateral focus of pathology will disseminate more to the ipsilateral hemisphere. Alternatively, in the body first subtype (equivalent term to PNS-first), the propagation of the alpha-synuclein follows an ascendant pattern from the vagus nerve to the bilateral dorsal motor nucleus of the vagus nerve due to the overlapping parasympathetic innervation of the gut. In consequence, the body-first patients have more symmetrical alpha-synuclein spreading, dopaminergic degeneration, and motor impairment than the brain-first patients. Further, the body-first patients at diagnosis have more alpha-synuclein burden, which leads to a faster disease progression and cognitive decline.

Of interest, following the hypothesis of two different patterns of propagation, Pyatigorskaya et al. tested the association of RBD in PD with brainstem-to-cortex and cortex-to-brainstem propagation models using a multimodal neuroimaging approach (47). They included data from key regional volumes: mean diffusivity (MD), axial diffusivity, radial diffusivity, and signal of neuromelanin-sensitive magnetic resonance imaging (MRI). The results suggested that the PD-RBD patients fit with a brainstem-to-cortex model and that PD-non RBD patients fit with a cortex-to-brainstem model, which agrees with the body-first and brain-first subtypes, respectively.

In this context, iRBD as a prodromal phase could be located in the first stages of PD, according to the Braak model. However, the beginning of

the RBD can occur in later stages of the disease, after PD diagnosis. Considering the onset of RBD, three different main PD groups could be hypothesized: 1) a group of PD with RBD patients who have iRBD as a prodromal phase of the disease; 2) a PD with RBD group with a PD diagnosis and a later development of concomitant RBD; 3) a group of PD patients who do not develop RBD. Thus, when talking about PD with RBD is relevant to consider that it might not be a homogeneous category. The neuropathology of these groups could follow different alpha-synuclein spreading patterns. The first group might have a disease progression closer to the Braak stages with its equivalent in the body-first subtype of the SOC Model. Notwithstanding, other patterns of propagation of the alpha-synucleinopathy potentially lead to a concurrent RBD at a certain point, such as the brain-first subtype.

### **2.2.2. Cognition in Parkinson's disease with RBD**

This subsection includes an overview of the cognitive profile of those PD patients with RBD compared with those without RBD. Furthermore, it covers the findings of studies focused on the prevalence of mild cognitive impairment (MCI), dementia, and cognitive progression in this PD clinical subtype.

Several cross-sectional studies have analyzed the neuropsychological profile of those PD patients with RBD, either in PD-RBD or PD-pRBD patients. Thus, in 2021 Mao et al. performed a meta-analysis including a whole pool of 39 studies, of which 18 analyzed PD-RBD patients and 21 analyzed PD-pRBD patients (48). The authors classified the different cognitive outcomes into seven main cognitive domains: global cognitive function, memory, executive function, language, processing speed/complex attention/working memory, visuospatial/constructional ability,

and psychomotor ability. The results showed that the PD-RBD patients have worse performance than PD-non RBD patients in the following cognitive domains and subdomains: global cognitive function, long-term verbal recall, long-term verbal recognition, generativity, inhibition, shifting, language, and visuospatial/constructional ability. Comparatively, the PD-pRBD patients have worse performance than PD-non pRBD patients in global cognitive function and shifting. The domains and subdomains altered in both groups, PD-RBD and PD-pRBD, are shown in Figure 4.

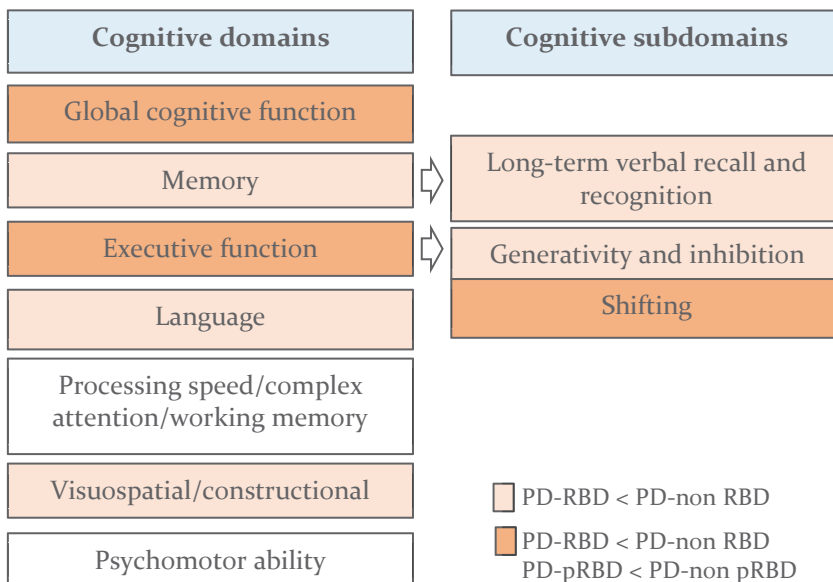


**Figure 4.** Cognitive domains and subdomains altered in PD with RBD in comparison with PD without RBD. Based on results from the meta-analysis performed by Mao et al., 2021 (48). Cognitive domains impaired in PD-RBD and PD-pRBD in dark orange; cognitive domains impaired solely in PD-RBD in light orange. Abbreviations: PD-pRBD, Parkinson’s disease with probable RBD; PD-RBD, Parkinson’s disease with RBD; PD-non pRBD, Parkinson’s disease without probable RBD; PD-non RBD, Parkinson’s disease without RBD; RBD, REM sleep behavior disorder.

In addition, some studies have shown a higher prevalence of MCI (49), a higher prevalence of dementia (50), and worse cognitive progression in general cognition (51,52), processing speed (51), verbal (51), and working memory (53). These findings are collected in detail in **Table 2**.

**Table 2.** Studies focused on mild cognitive impairment, dementia, and cognitive progression in Parkinson’s disease with RBD

Topic	Reference	Sample	Study findings
MCI prevalence	Jozwiak et al., 2017 (49)	53 PD-RBD 40 PD-non RBD	PD-RBD = 66% PD-non RBD = 23%
Dementia development	Postuma et al., 2012 (50)	27 PD-RBD 15 PD-non RBD	PD-RBD = 48% PD-non RBD = 0% (4-year f/u)
Cognitive progression	Chahine et al., 2016 <sup>a</sup> (51)	108 PD-pRBD 315 PD-non pRBD	Greater annual rate of decline in <i>MoCA</i> , <i>SDMT</i> and <i>HVLT-R</i> delayed recall in PD-pRBD (3-year f/u)
	Forbes et al., 2021 <sup>a</sup> (52)	149 PD-pRBD 274 PD-non pRBD	Faster decline in <i>MoCA</i> (6-year f/u)
	Van Patten et al., 2022 (53)	25 PD-pRBD 40 PD-non pRBD	Greater decline in attention/working memory (16-47-month f/u)

<sup>a</sup> Data from *de novo* Parkinson’s disease patients (at baseline) and their follow-ups from the Parkinson’s Progression Markers Initiative (PPMI) database. Abbreviations: f/u, follow-up; *HVLT-R*, *Hopkins Verbal Learning Test-Revised*; MCI, mild cognitive impairment; *MoCA*, *Montreal Cognitive Assessment*; PD-pRBD, Parkinson’s disease with probable RBD; PD-RBD, Parkinson’s disease with RBD; PD-non pRBD, Parkinson’s disease without probable RBD; PD-non RBD, Parkinson’s disease without RBD; RBD, REM sleep behavior disorder; REM, rapid eye movement; *SDMT*, *Symbol Digits Modalities Test*.

To sum up, PD patients with RBD have a more severe cognitive profile, with worse performance in global cognition, as well as in memory, executive, language, and visuospatial/constructional functions. Furthermore, this group of patients has shown a higher prevalence of MCI and dementia, as well as worse cognitive progression.



### 2.2.3. Genetics of Parkinson's disease with RBD

Genetic studies centered on PD with RBD are still scarce, and no studies have been performed on PD-RBD with a diagnosis based on PSG. In this context, the presence of PD-pRBD has been associated with rs3756063 (54) and rs10005233 (55) risk variants located in the 5' region of the alpha-synuclein (*SNCA*) gene (54,55), but risk variants in the 3' region of *SNCA* (54,55) and the microtubule-associated protein tau (*MAPT*) variant (54) showed no association with PD-pRBD.

Some evidence points to genetic coincidences between iRBD and PD. In this sense, iRBD has been associated with glucocerebrosidase (*GBA*) risk variants (56), leucine-rich repeat kinase 2 (*LRRK2*) protective haplotype (57), transmembrane protein 175 (*TMEM175*) variants (58), and an *SNCA* risk variant (55). However, there is no significant association between iRBD and the presence of *LRRK2* risk variants (59) and *MAPT* haplotypes (60). Remarkably, the absence of *LRRK2* risk variants in iRBD (59) matches with the fact that *LRRK2* PD carrier patients are a benign subtype (61,62).

### 2.2.4. Brain imaging in Parkinson's disease with RBD

Neuroimaging methods are one of the main approaches used to study different brain characteristics in neurodegenerative diseases. There is a growing interest in characterizing brain structure and function in PD with RBD as a relevant clinical subtype of PD. This subsection presents an overview of the previous literature on the topic. We perform a systematic revision of structural, functional, and metabolic studies. We synthesize the main findings at the end of this subsection in Tables 3 to 5.

## Gray matter characterization

Gray matter (GM) atrophy in PD with RBD has been quantified by the following approaches: voxel-based morphometry (VBM), deformation-based morphometry (DBM), vertex-based shape analysis, cortical thickness (CTh), and subcortical volumetry.

The first two studies focused on the characterization of GM in PD with RBD failed to achieve corrected statistical significance in the comparison between PD with and without RBD (63,64). Ford et al. in 2013 performed VBM analysis in a sample of 124 PD patients classified as PD-pRBD or PD-non pRBD (63) using the first item of the *Mayo Clinic Sleep Questionnaire (MSQ)* (65). They found GM reductions in the PD-pRBD group compared with the PD-non pRBD group in the parietal and temporal lobes. However, the results did not remain significant after correcting for multiple comparisons. Similarly, García-Lorenzo et al. used a VBM approach in a smaller sample, including 36 PD patients classified using PSG, and did not find significant differences between PD groups (64).

In a subsequent study in 2014, Salsone et al. performed a VBM analysis in a sample of 22 PD patients classified according to PSG (66). The results showed a significant volume reduction in the right thalamus in PD-RBD patients compared with PD-non RBD ones, corroborated using subcortical volumetry. The authors highlighted the association between thalamus atrophy and the development of RBD. The thalamic atrophy may be associated with two main factors: the accumulation of alpha-synuclein and the decrement of noradrenergic input from the locus coeruleus complex due to its impairment.

In 2016, another VBM study found volume decrements in the left hippocampus and cingulate gyrus in the PD-RBD group compared with

the PD-non RBD group, using a sample of 38 PD patients also classified through PSG (67). The authors emphasized the value of these regions in the characterization of PD-RBD since they have a relevant role in sleep regulation and are part of the default mode network.

The same year Boucetta et al. published the first multicenter study on the topic, with a large *de novo* PD sample from the Parkinson's Progression Markers Initiative (PPMI) (68). It included a pool of 309 PD patients, and DBM analyses were performed. The classification in groups depending on the RBD symptomatology was performed according to the *RBD Screening Questionnaire (RBDSQ)* (69). The results showed a volume decrement in the pontomesencephalic tegmentum in PD-pRBD compared with PD-non pRBD. Decrements in PD-pRBD were also reported in cortical (lingual gyrus) and other subcortical regions (hypothalamus, thalamus, putamen, claustrum, and amygdala). On the other hand, there were volume decrements in PD-non pRBD compared with PD-pRBD in cortical regions (right rectus and orbitofrontal gyri, bilateral olfactory trigone, medial prefrontal cortex, superior frontal gyrus, inferior frontal gyrus, midcingulate gyrus, and superior temporal gyrus). Besides, the atrophy pattern was more widespread in PD-pRBD compared with the HC group. The authors pointed up the pontomesencephalic tegmentum involvement, which takes part in the control of muscle atonia during REM sleep. In addition, they brought out that the widespread pattern of atrophy is coherent with the severe clinical profile of this subgroup of patients. Moreover, some of these regional decrements potentially contribute to sleep dysregulation, for instance, the basal ganglia.

In 2019, Kamps et al. performed a new VBM study using a *de novo* PD sample from the PPMI (70). They analyzed a whole group of 167 PD patients. The authors reported a significant decrement in the right

putamen in PD-pRBD compared with the PD-non pRBD group, consistent with previous evidence in PD-pRBD (68). They underlined that the atrophy of the putamen might be associated with a more marked degeneration of the dopaminergic nigrostriatal pathway in this clinical subtype.

In 2019 Rahayel et al. (71) explored a group of 30 PD patients classified using PSG with different techniques centered on structural GM characteristics. The applied approaches were VBM, DBM, subcortical volumetry, and, for the first time in this type of population, CTh and shape analysis. The results showed that the PD-RBD compared with the PD-non RBD patients had cortical thinning in the right inferior and superior temporal gyri, volume decrements in the left lingual gyrus and the bilateral putamen, as well as surface contraction in the bilateral putamen (Figure 4). The findings that involved the putamen are in line with the previous evidence (68,69). Thus, the impairment of the nigrostriatal pathway was hypothesized as a potential factor involved in these results. Further, the PD-RBD group had a widespread pattern of atrophy compared with the PD-non RBD when comparing both groups with HC. The authors suggested that the presence of RBD in PD patients reflected a more advanced stage of the disease concurrent with severe atrophy.

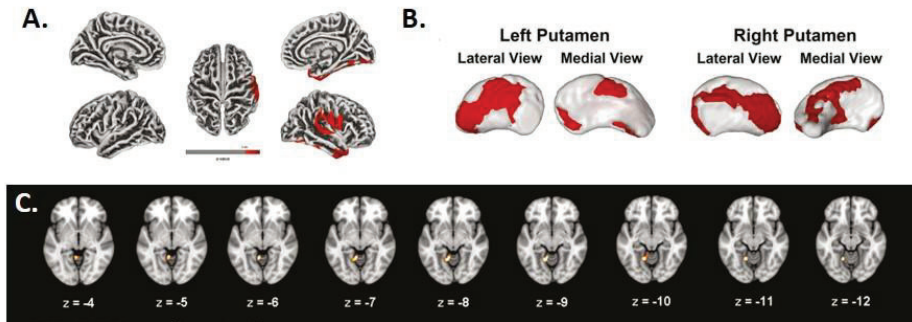


**Figure 4.** A. Cortical thinning in PD-RBD, the red cluster is showing thinning in right perisylvian areas and temporal cortex extending to fusiform cortex. B. Shape abnormalities in PD-RBD, red cluster is showing atrophy in bilateral putamen. C. Reduced GM volume in PD-RBD in left lingual, left cerebellum, and bilateral putamen using voxel-based morphometry (VBM). Adapted from “Results of surface-based cortical thickness analysis”, “Results of vertex-based subcortical shape analysis”, and “Results of volume abnormalities using voxel-based and deformation-based morphometry” by Rahayel et al. (71) licensed under RightsLink.

In 2021, Jiang et al. performed VBM analyses in a pool of 50 PD patients classified by PSG (72). They found volume decrements in PD-RBD compared with PD-non RBD in the right superior occipital gyrus and an increment in the cerebellar vermis IV/V.

Recently, Yoon et al. carried out the first longitudinal work on this topic through CTh and subcortical volumetric analysis (73). They analyzed a sample of 78 PD patients from the PPMI, with data at the *de novo* stage in the baseline and with a two-year follow-up. They found that at the *de novo* PD stage, the PD-pRBD group had cortical thinning in the bilateral inferior temporal cortex compared with PD-non pRBD (Figure 5). Regarding time effect, the PD-pRBD had cortical thinning in the left insula compared with PD-non pRBD (Figure 5), in addition to significant volume decrements in the left caudate, pallidum, and amygdala.

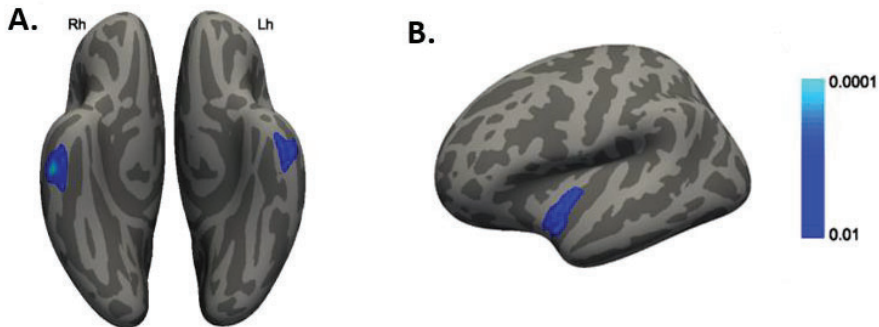


**Figure 5.** A. Cortical thinning in PD-RBD at baseline, the blue cluster is showing thinning in the bilateral inferior temporal. B. Cortical thickness group by time effect. The blue cluster is showing thinning in the left insula in PD-pRBD. Adapted from “Cross-sectional cortical thickness differences” and “Longitudinal changes in cortical thickness” by Yoon et al. (73) licensed under CC BY-ND 4.0.

In summary, structural MRI studies exploring gray matter measures report atrophy in PD patients with RBD in cortical temporal regions and basal ganglia, mainly in the putamen, and limbic regions, especially in the thalamus and the amygdala. The putamen and thalamus atrophy are possibly associated with an impairment of the dopaminergic nigrostriatal pathway. Over and above, the basal ganglia degeneration could contribute significantly to sleep dysregulation in these patients.

### **White matter characterization**

The most common technique used to measure white matter (WM) integrity is diffusion tensor imaging (DTI). The two mainly used measures are fractional anisotropy (FA), which reflects the directionality of molecular displacement, and MD, which reflects the average magnitude of molecular displacement (74).

Only a few studies have analyzed microstructural WM changes associated with PD with RBD. The first work exploring FA and MD measures in PD-

pRBD using whole-brain DTI analysis in a sample of 124 PD patients did not find significant differences between groups after correction for multiple comparisons (63). The uncorrected results included significant FA decrements in PD-pRBD compared with PD-non pRBD in the left inferior longitudinal, right corticospinal tract, and right inferior fronto-occipital and longitudinal fasciculi.

García-Lorenzo et al. found decreased FA in PD-RBD compared with HC in a sample of 36 PD patients classified using PSG (64). They did not find significant differences between PD groups or between PD-non RBD and HC. The significant cluster included the locus coeruleus complex, so the authors highlighted its involvement in REM sleep atonia and the possible implication of its structural degeneration in RBD.

A subsequent report by Lim et al. analyzed a group consisting of 38 PD classified utilizing PSG (67). The authors reported a general pattern of decrements in FA in both groups compared with HC, more widespread in PD-RBD, including anterior thalamic radiations, forceps minors, posterior visual streams, fornix, right olfactory regions, internal capsules, left external capsule, and anterior temporal lobe (**Figure 6.1**). Further, they found similar MD increments in PD-RBD and PD-non RBD compared with HC, without differences between PD groups (**Figure 6.2**).

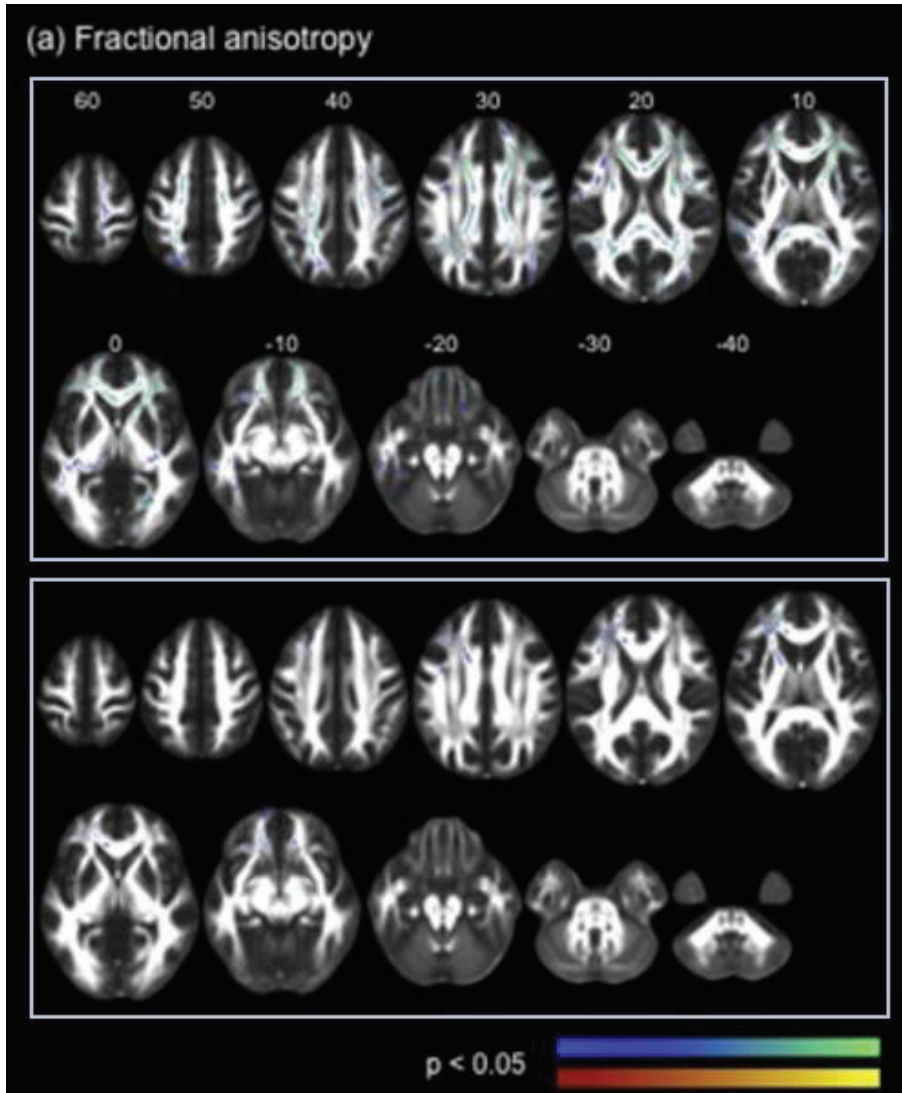


**Figure 6.1.** (a) Fractional anisotropy changes. The upper panel illustrates FA reductions in PD without RBD, and the lower panel in PD with RBD compared to healthy controls. No differences between PD without RBD and PD with RBD were found. Adapted from Lim et al. (67) licensed under RightsLink.



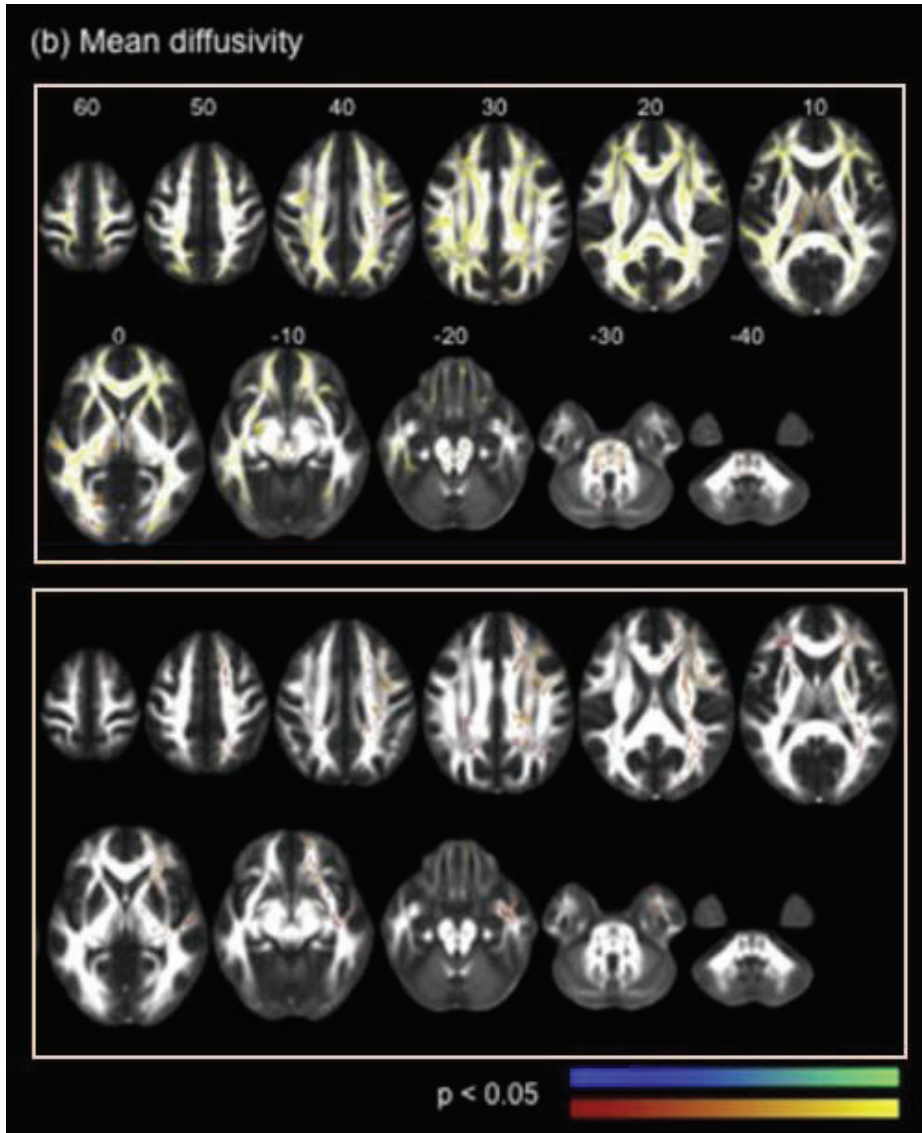


**Figure 6.2.** (b) Mean diffusivity (MD) changes. The upper panel illustrates MD increments in PD without RBD, and the lower panel in PD with RBD compared to healthy controls. Adapted from Lim et al. (67) licensed under RightsLink.

In a 2017 study, Ansari et al. analyzed a sample of 44 *de novo* PD patients from the PPMI (75). They used quantified anisotropy (QA) measurement instead of FA; this measure computed anisotropy for each fiber tract. In contrast, FA is shared by different fiber tracts within a voxel. The results showed decreased QA in PD-pRBD compared with PD-non pRBD in bilateral cingulum pathways, inferior fronto-occipital fasciculi, corticospinal tracts, middle cerebellar peduncles, and genu, body, and splenium of the corpus callosum.

In conclusion, the current findings do not support a clear pattern of atrophy according to WM abnormalities associated with PD with RBD. More research is needed to clarify the differences between PD patients with and without RBD in WM integrity measures. Specifically, approaches that analyze the circuits involved in REM sleep.

### **Neuromelanin abnormalities**

Another common neuroimaging technique used in neurodegeneration characterization, specifically in PD, is the neuromelanin-sensitive MRI. This approach allows the researchers to explore neuromelanin: a black pigment located in relevant areas in PD, such as substantia nigra pars compacta and locus coeruleus. Using neuromelanin-sensitive MRI, two studies have reported significantly less signal intensity in the coeruleus/subcoeruleus complex in PD-RBD compared with PD-non RBD (64,76) in cohorts of 36 (64) and 32 PD patients (76) classified by means of PSG. Although, in another study performed on a sample of 37 *de novo* PD patients classified using PSG, the differences in signal intensity in the coeruleus did not reach the established statistical significance (77).

## Structural connectivity

A couple of studies have investigated correlation matrices of GM volumes using graph theory approaches. First, Guo et al. in 2018 implemented structural correlation network analyses using cortical, subcortical, and cerebellar regions in a sample of 161 PD patients from the PPMI database (78). The authors found differences in nodal properties between PD groups. The PD-pRBD group showed enhanced nodal measures compared with PD-non pRBD in frontotemporal, occipital and limbic regions, as well as decreased nodal measures in the cerebellum. The authors identified relevant hubs in the limbic system and the frontal and temporal lobe, namely nodes in which there are an increased number of edges. Moreover, the PD-pRBD group involved additional hubs in limbic regions. The researchers highlighted the role of the limbic system in the reorganization of local properties and the remapping of the hubs distribution as a potential marker of the pathophysiology of PD with RBD.

Last, in 2019 Kamps et al. analyzed a sample from the PPMI database, with 167 *de novo* PD patients classified as PD-pRBD or PD-non pRBD (70). The approach consisted of seed correlation analyses based on the hippocampus, thalamus, and putamen. The analyses did not find any significant difference.

The most recent study was performed by Chen et al. and analyzed structural connectivity using a graph theory approach. The authors studied differences in global and nodal topological properties based on the estimated number of fibers obtained from DTI (79). They analyzed a pool of 171 *de novo* PD patients from the PPMI. The results showed that the PD-pRBD group, compared with the PD-non pRBD group, had less global efficiency and increased shortest path length. When analyzing nodal measures, the PD-pRBD group, compared with the PD-non pRBD

group, showed increased nodal efficiency in the right insula and left middle frontal gyrus and decreased nodal efficiency in the left temporal pole.

To sum up, there are very few studies on structural connectivity in PD with RBD. Promising methods explore not only GM volume matrices but also matrices derived from DTI measures (79), such previously in PD patients with MCI (80).

### **Functional MRI characterization**

Functional magnetic resonance imaging (fMRI) allows exploring the pattern of temporal dependence and coactivation from different brain regions. In fMRI, the core signal captured is blood-oxygen-level-dependent (BOLD). The deoxyhemoglobin changes in the brain due to blood flow and oxygenation shape the BOLD signal and reflect the neuronal activity through the neurovascular coupling mechanism (81). One of the most common approaches in the field is the exploration of the resting-state fMRI, which captures spontaneous neural activity (82). Some studies have used resting-state fMRI to characterize functional connectivity in PD with RBD; we will revise the existing literature in this point.

The first study exploring PD with RBD employing an fMRI approach was performed by Li et al. (83). The authors applied amplitude of low-frequency fluctuation (ALFF) analysis in a sample of 34 PD patients classified using PSG. The ALFF analyzes the intensity of regional spontaneous brain activity (84). The results showed reduced ALFF in the PD-RBD group in the right precentral gyrus, middle frontal gyrus, insula, and bilateral putamen compared with the PD-non RBD group. The authors highlighted that probably the functional alteration in the motor

cortex contributes to the pathophysiology of PD with RBD, as RBD components imply not only a midbrain impairment.

In a subsequent study, Gallea et al. performed network analyses focused on the locomotor, arousal, and basal ganglia-thalamic control networks in a sample of 52 PD patients classified using PSG (85). They reported reduced functional connectivity in PD-RBD compared with PD-non RBD in the arousal network involving the pedunculopontine nucleus and ventral posterior anterior cingulate cortex. Moreover, they explored the effect of having impaired postural control in addition to RBD. The results showed reduced functional connectivity in PD-RBD with impaired postural control between the pedunculopontine nucleus and the supplementary motor area, pre-supplementary motor area, and dentate nucleus (locomotor network); and between the pedunculopontine nucleus and medial prefrontal cortex (arousal network). The authors hypothesized that two territories of the pedunculopontine nucleus neurons could contribute respectively to the arousal and locomotor networks. Thus, the impairment of these territories and their overlapped regions could contribute differentially to the onset of RBD (arousal network) and postural control impairment (locomotor network) in PD patients. They found that functional connectivity of the pedunculopontine nucleus as part of the locomotor network correlated with the functional connectivity of this region as part of the arousal network in the PD with RBD groups. Therefore, they concluded that the functional alteration of the pedunculopontine nucleus links the RBD with postural control impairment in PD.

Li et al. carried out a study using a graph analysis approach with a sample of 92 PD patients from the PPMI classified using the *RBDSQ* (86). The PD-pRBD group had reduced betweenness centrality in the right

dorsolateral superior frontal gyrus, increased betweenness centrality in the left insula, and increased nodal efficiency in the bilateral thalamus compared with PD-non pRBD. They suggested that the decreased betweenness centrality in the dorsolateral superior frontal gyrus may be associated with cognitive impairment in PD with RBD, as it is part of the frontoparietal network. A possible explanation for this frontal functional abnormality may be associated with GM volume loss in this specific region. The authors interpreted the increased nodal efficiency in the thalamus, and betweenness centrality in the left insula, as compensatory mechanisms considering volume decreases in these regions in PD with RBD. Furthermore, they pointed to the potential incremented alpha-synuclein depositions in the thalamus as another relevant factor.

Another study used dynamic functional network connectivity (dFNC) to analyze a sample of 126 PD patients classified through the *RBDSQ* (87). Of note, the dFNC is an approach focused on the time-varying associations among different brain regions organized in differentiated functional networks (88,89). They reported weaker positive coupling in PD-pRBD than PD-non pRBD between the visual network and default mode network, between the default mode network and basal ganglia network, and within-network coupling in the default mode network. The authors proposed that the results showed a loss of brain dynamic, characteristic of PD with RBD.

More recently, Jiang et al. used a seed-to-whole brain approach to analyze a sample of 50 PD patients classified using *PSG* (72). In the analyses, they used as seed regions the right superior occipital gyrus and the cerebellar vermis IV/V, based on previous VBM findings. The results showed reduced functional connectivity between the right superior occipital gyrus and left fusiform gyrus, calcarine sulcus, and superior parietal gyrus

in PD-RBD. The authors suggested that this functional alteration is directly linked with the structural alteration in the PD-RBD group.

In summary, there is a limited number of fMRI studies centered on PD with RBD. The diversity of methodological approaches and the regional distribution of the results do not allow the definition of a clear pattern of functional alteration in this group of patients. Nevertheless, the reviewed studies support the existence of functional abnormalities associated with PD patients with RBD, and the most consistent finding throughout the literature resembles the altered connectivity of frontal regions.

### **Metabolic and chemical neurotransmission characterization**

Several studies have used positron emission tomography (PET) to analyze cerebral glucose metabolism in PD with RBD and the binding of some neurotransmitters, mainly dopamine.

Regarding cerebral glucose metabolism, Arnaldi et al. used [<sup>18</sup>F]FDG-PET analysis in a sample of 38 *de novo* PD patients classified through the *MSQ* (90). The results showed a reduced metabolism in PD-pRBD compared with PD-non pRBD in parieto-occipital regions, middle-temporal and angular gyri in the more affected hemisphere, which was defined as the contralateral one to the body side with motor symptoms prevalence. Additionally, the PD-pRBD group showed increased metabolism in the anterior cingulate cortex and precentral gyrus in the more affected hemisphere compared with the PD-non pRBD group.

In a subsequent study using an [<sup>18</sup>F]FDG-PET approach, Yoon et al. analyzed a group of 21 *de novo* PD-pRBD classified according to the *RBDSQ* (91). They established a PD-pRBD metabolism pattern after comparing it with an HC group. The PD-pRBD metabolism pattern

involved decreased metabolism in bilateral occipital and posterior parietal regions; and increases in the bilateral primary and supplementary motor areas, premotor cortex, thalamus, putamen, globus pallidus, rostral and orbital parts of the superior frontal gyrus, cerebellum, pons, and parahippocampal gyrus. Besides, the PD-pRBD patients had a reduced binding compared with a group of iRBD patients in the bilateral posterior putamen, anterior putamen, and caudate. To test that this pattern was characteristic of the PD-pRBD group, they analyzed its similarity to the metabolism of iRBD and PD-RBD patients. The results showed that the iRBD group metabolism had a low correlation with the PD-pRBD metabolism pattern, taking the PD-pRBD group as a reference. Besides, the PD-RBD group showed a high correlation with the PD-pRBD metabolism pattern, taking the HC group as a reference.

Shin et al. analyzed through [<sup>18</sup>F]FDG-PET a group of 25 *de novo* PD-pRBD patients classified using the *RBDSQ* (92). They described a PD-pRBD metabolism pattern after its comparison with an HC group. The PD-pRBD metabolism pattern included decreases in the right middle occipital gyrus, precuneus, superior temporal gyrus and insula, and the bilateral lingual gyrus; and increases in bilateral premotor and precentral areas, middle frontal gyrus and putamen, and right hippocampus. The metabolism of the PD-pRBD patients correlated and showed a widespread overlapping with the pattern of metabolism of a treated PD group. This metabolism pattern of treated PD involved decrements of metabolism in bilateral lateral occipital, inferior parietal, and precuneus regions; and increments in the bilateral supplementary motor area, hippocampus, putamen, thalamus, and cerebellum.

In summary, the findings point to distinct cerebral glucose metabolism in PD with RBD, including decrements in parietal and occipital regions



and increments in frontal areas, specifically in the precentral gyrus. Although, these findings must be cautiously interpreted since some studies did not include PD without RBD patients.

Another group of studies analyzed dopamine binding in PD with RBD using PET approaches. First, Kotagal et al. used an [<sup>11</sup>C]DTBZ-PET approach to explore the vesicular monoamine transporter (VMAT2) binding (93). They analyzed a whole sample of 80 PD patients classified using the *MSQ*. The analyses did not find statistically significant binding differences between PD-pRBD and PD-non pRBD.

Similarly, in a recent study Valli et al. analyzed with an [<sup>11</sup>C]DTBZ-PET approach a group of 30 PD patients classified using the *MSQ* (94). They also failed to find significant differences between PD-pRBD and PD-non pRBD groups. The results showed reduced binding in bilateral caudate, associative, motor and ventral striatum, and external and internal globus pallidus in PD-pRBD compared with HC. However, the same differences were found in PD-non pRBD compared with HC, plus the subthalamus and substantia nigra.

Other studies applied an [<sup>18</sup>F]FP-CIT-PET approach to examine the striatal dopamine transporter (DAT) binding. Besides, Chung et al. analyzed with this technique a sample of 97 PD patients classified according to the *RBDSQ* (95). The results showed a reduced binding in PD-pRBD compared with PD-non pRBD in the putamen of the less affected hemisphere.

Further, Yoon et al. performed [<sup>18</sup>F]FP-CIT-PET analyses in the above-cite study to compare the *de novo* PD-pRBD and iRBD groups (91). The results showed reduced binding in the bilateral posterior and anterior putamen, and caudate in PD-pRBD.

Similar to the previous studies, Lee et al. used [<sup>18</sup>F]FP-CIT-PET to compare a group of 30 PD-pRBD patients classified through the *RBDSQ* with an iRBD group (96). They found that the PD-pRBD group had a reduced binding in bilateral caudate, anterior and posterior putamen, and substantia nigra compared with the iRBD group.

In a subsequent study, Horsager et al. used an [<sup>18</sup>F]DOPA-PET approach to analyze dopamine binding in the putamen in a sample of 37 *de novo* PD patients classified by means of PSG (77). They did not find differences between PD-RBD and PD-non RBD, and both groups showed a significant binding reduction in the putamen compared with an iRBD group.

Valli et al. tried to characterize the extra-striatal dopamine binding within the mesocortical and mesolimbic pathways through an [<sup>11</sup>C]FLB-457-PET approach (97) in the previously described sample of 30 PD patients classified using the *MSQ* (94). The regions of interest included prefrontal, temporal, and limbic areas. The results showed that PD-pRBD and PD-non pRBD groups, compared with the control group, had reduced dopamine D2 receptor availability in the parahippocampal, superior, lateral, and inferior temporal cortices regions. The unique difference between PD groups was that the PD-pRBD group showed a steep decline in D2 availability in the left uncus parahippocampus associated with the disease staging (see *Subsection 2.2.5. Brain correlates in PD with RBD* and **Table 6**).

Briefly, the PD with RBD group shows a reduced dopamine binding in basal ganglia compared with iRBD patients. Regarding the comparison between PD groups, several single-photon emission computerized tomography (SPECT) studies have described results consistent with those found with a PET approach, including reductions of dopamine binding in

the basal ganglia in PD with RBD. We will review SPECT studies at the end of this point. Interestingly, studies focused on VMAT2 binding did not allow for differentiation of PD with and without RBD; Valli et al. discussed widely possible explanations elsewhere (94).

Noradrenaline binding has been analyzed in PD-RBD in two studies using an [<sup>11</sup>C]MeNER-PET approach (76,98). Both studies used the same cohort of 30 PD patients classified using PSG. In the first study, the authors found reduced binding in the bilateral thalamus, hypothalamus, red nucleus, locus coeruleus, median, and dorsal raphe in PD-RBD compared with PD-non RBD (76). In the second, the results showed that the PD-RBD group had a reduced binding in the bilateral primary sensorimotor cortex compared with HC, while the PD-non RBD did not (98).

It has been studied the putative implication of other neurotransmitters. Kotagal et al., in the study cited above, analyzed acetylcholine and serotonin binding using [<sup>11</sup>C]PMP-PET and [<sup>11</sup>C]DASB-PET approaches, respectively (93). The results showed a reduced [<sup>11</sup>C]PMP binding in bilateral neocortical, thalamic, and limbic cortical regions in PD-pRBD compared with PD-non pRBD. On the other hand, they did not find significant differences in [<sup>11</sup>C]DASB binding.

Thus, the PET literature exploring other neurotransmitter systems apart from the dopaminergic is still scarce. This effort could help to characterize PD with RBD, as these systems could play a relevant role in its distinct clinical and cognitive profile.

Using SPECT, several studies have tried to elucidate the characteristics of dopamine uptake in PD patients with RBD, specifically in the basal ganglia. For more detail about the sample size and the classification method (PSG or questionnaire) used in SPECT studies, see **Table 5**.

The results in *de novo* PD have shown reduced specific binding ratios in the caudate in PD-pRBD compared with PD-non pRBD, with cross-sectional (90,99,100) and longitudinal (100,101) approaches. Similar findings have been described in cross-sectional studies that compared PD-RBD and PD-non RBD groups classified by PSG (102). Moreover, reduced uptake has been observed in PD-RBD in comparison with iRBD patients (102).

Similarly, some cross-sectional studies in *de novo* PD have reported binding reductions in the putamen in PD-pRBD compared with PD-non pRBD (90,100) and iRBD (99); as well as in the comparison between PD-RBD and PD-non RBD (102). Comparably, results in the same direction have been found in more advanced patients in PD-RBD compared with iRBD (103). Longitudinally, a significant binding reduction in the putamen has been reported in PD-pRBD compared with PD-non pRBD (101).

Otherwise, some SPECT studies have failed to find differences between PD with RBD and without RBD in striatal dopamine binding (66,104).

The main findings point to a reduced dopamine uptake in basal ganglia in PD patients with RBD compared with PD patients without RBD. This binding reduction has been interpreted mainly as an increased alteration of the nigrostriatal dopaminergic pathway. Besides, the dysfunction of this circuitry is potentially related to the development of a more severe clinical profile characterized by motor symptoms and cognitive impairment.

**Table 3. Studies of structural MRI in Parkinson's disease with RBD**

Reference	Sample	Demogr.	Class.	Analysis	Contrast	Brain regions
<i>GM characterization</i>						
Boucetta et al., 2016 <sup>a</sup> (68)	69 PD-pRBD <sup>c</sup>	60.93±9.16; 6.29±6.62 m	<i>RBDSQ</i>	DBM	PD-pRBD<PD-non pRBD	↓ volume L medullary reticular formation and supramarginal gyrus; R anterior cingulate; bilateral pontomesencephalic tegmentum, basilar part of the pons, deep cerebellar nuclei, cerebral peduncle, hypothalamus, thalamus, putamen, claustrum, internal capsule, amygdala, lingual gyrus, and superior and inferior longitudinal fasciculi
	240 PD-non pRBD <sup>c</sup>	61.62±9.84; 6.85±6.66 m			PD-pRBD>PD-non pRBD	↑ volume R rectus and orbitofrontal gyri; bilateral olfactory trigone, medial prefrontal, superior frontal gyrus, inferior frontal gyrus, mid-cingulate gyrus, and superior temporal gyrus
	138 HC	59.92±10.83			PD-pRBD<HC	↓ volume L medullary reticular formation, supramarginal gyrus and anterior cingulate; R fusiform gyrus; bilateral pontomesencephalic tegmentum, deep cerebellar nuclei, substantia nigra, hypothalamus, thalamus, putamen, claustrum, amygdala, hippocampus, lingual and orbitofrontal gyri

					PD-pRBD>HC	↑ volume R rectus and superior frontal gyri; bilateral olfactory trigone, medial prefrontal, inferior frontal and midcingulate gyri
Ford et al., 2013 (63)	46 PD-pRBD 78 PD-non pRBD	66.4±9.9; 6.5±5.1 m 65.8±10.9; 6.0±4.4 m	MSQ	VBM	n.s.	
García-Lorenzo et al., 2013 (64)	24 PD-RBD 12 PD-non RBD 19 HC	62.4±8.4; 9.6±3.8 y 56.3±11.5; 9.7±4.5 y 60.2±8.3	PSG	VBM	n.s.	
Jiang et al., 2021 (72)	24 PD-RBD 26 PD-non RBD 26 HC	66.04±5.73; 6.79±3.58 y 62.96±7.41; 5.69±2.88 y 62.73±6.33	PSG	VBM	PD-RBD<PD-non RBD PD-RBD>PD-non RBD PD-RBD<HC	↓ volume R SOG ↑ volume cerebellar vermis IV/V ↓ volume L amygdala and middle cingulate gyrus; R SOG, angular, insula and cerebellum lobe VI; bilateral caudate and putamen
Kamps et al., 2019 <sup>a</sup> (70)	40 PD-pRBD <sup>C</sup> 127 PD-non pRBD <sup>C</sup>	61.1±10.72; 6.22±7.69 m 61.08±9.32; 5.56±6.92 m	RBDSQ	VBM	PD-pRBD<PD-non pRBD PD-pRBD<HC	↓ volume R putamen ↓ volume R putamen
Lim et al., 2016 (67)	24 PD-RBD 14 PD-non RBD 25 HC	69.8±6.4; 6.2±2.9 y 69.7±7.2; 4.4±3.7 y 68.5±6.6	PSG	VBM	PD-RBD<PD-non RBD PD-RBD>PD-non RBD PD-RBD<HC	↓ volume L hippocampus, cingulate gyrus ↑ volume L cuneus; R lingual gyrus ↓ volume L precuneus, cuneus, cingulate, medial frontal gyrus, postcentral gyrus; bilateral inferior parietal

Rahayel et al., 2019 (71)	15 PD-RBD	66.7±7.6; 3.9±2.9 y	PSG	CTh VBM DBM Shape analysis SB vol	PD-RBD<PD-non RBD	Cortical thinning in R perisylvian areas and inferior temporal extending to fusiform ↓ volume L lingual gyrus and cerebellum; bilateral putamen ↓ Surface bilateral putamen Cortical thinning widespread in bilateral frontal, cingulate, temporal, parietal, and occipital regions ↓ volume widespread in bilateral basal ganglia, thalamus, hippocampus, cerebellum and frontal, temporal, parietal, and occipital regions ↓ Surface L hippocampus; R accumbens, bilateral putamen, and pallidum
	15 PD-non RBD	63.1±8.9; 3.7±2.6 y			PD-RBD<HC	
	41 HC	63.3±8.1				
Salsone et al., 2014 (66)	11 PD-RBD	66.6±7.4; 4.72±4.07 y	PSG	VBM SB vol	PD-RBD<PD-non RBD	↓ volume bilateral thalamus ↓ volume bilateral thalamus
	11 PD-non RBD	66.9±7.9; 4.36±4.2 y			PD-RBD<HC	
	18 HC	65.1±7.8				
Yoon et al., 2021 <sup>a, b</sup> (73)	18 PD-pRBD <sup>c</sup>	64.9±7.9; 3.0±8.5 m	RBDSQ	CTh SB vol	Baseline: PD-pRBD<PD-non pRBD	Cortical thinning in bilateral inferior temporal Cortical thinning in L inferior temporal, superior temporal, insula, precuneus, lateral occipital, caudal middle frontal and posterior cingulate; bilateral precentral and superior parietal
	60 PD-non pRBD <sup>c</sup>	62.3±7.2; 4.1±7.2 m			Effect time: PD-pRBD	

							↓ volume L amygdala and pallidum; R accumbens; bilateral caudate, hippocampus, putamen, and thalamus Cortical thinning in L insula ↓ volume L caudate, pallidum and amygdala
<b>WM characterization</b>							
Ansari et al., 2017 <sup>a</sup> (75)	23 PD-pRBD <sup>C</sup> 31 PD-non pRBD <sup>C</sup>	59.43±10.97; 7.95±8.76 m 60.64±8.65; 7.32±8.19 m	<i>RBDSQ</i>	DTI	PD-pRBD<PD-non pRBD		↓ QA bilateral cingulum pathways, genu, body and splenium of the corpus callosum, inferior fronto-occipital fasciculi, corticospinal tracts, and middle cerebellar peduncles
Ford et al., 2013 (63)	46 PD-pRBD 78 PD-non pRBD	66.4±9.9; 6.5±5.1 m 65.8±10.9; 6.0±4.4 m	<i>MSQ</i>	DTI	n.s.		
García-Lorenzo et al., 2013 (64)	24 PD-RBD 12 PD-non RBD 19 HC	62.4±8.4; 9.6±3.8 y 56.3±11.5; 9.7±4.5 y 60.2±8.3	<i>PSG</i>	DTI	PD-RBD>HC		↑ FA L tegmentum of the midbrain and rostral pons ↑ ADC R pontine tegmentum of the midbrain (cerebral peduncles and substantia nigra)
Lim et al., 2016 (67)	24 PD-RBD 14 PD-non RBD 25 HC	69.8±6.4; 6.2±2.9 y 69.7±7.2; 4.4±3.7 y 68.5±6.6	<i>PSG</i>	DTI	PD-RBD<HC PD-RBD>HC		↓ FA bilateral frontal areas ↑ MD bilateral widespread



<b>Neuromelanin abnormalities</b>						
García-Lorenzo et al., 2013 (64)	24 PD-RBD	62.4±8.4; 9.6±3.8 y	PSG	NM-MRI	PD-RBD<PD-non RBD	↓ signal intensity coeruleus/subcoeruleus complex ↓ signal intensity coeruleus/subcoeruleus complex
	12 PD-non RBD	56.3±11.5; 9.7±4.5 y			PD-RBD<HC	
	19 HC	60.2±8.3				
Horsager et al., 2020 (77)	13 PD-RBD <sup>c</sup>	72.6±5.3; 7 [2-7] m	PSG	NM-MRI	n.s.	
	24 PD-non RBD <sup>c</sup>	62.3±7.8; 2.5 [1-8.5]m				
Sommerauer et al., 2018 (76)	16 PD-RBD	67.7±9.3; 7.6±4.6 y	PSG	NM-MRI	PD-RBD<PD-non RBD	↓ coeruleus-to-pons intensity ratio ↓ coeruleus-to-pons intensity ratio
	14 PD-non RBD	65.4±9.0; 5.0±3.6 y			PD-RBD<HC	
	12 HC	67.3±6.3				
<b>Structural connectivity</b>						
Chen et al., 2022 <sup>a</sup> (79)	74 PD-pRBD <sup>c</sup>	62.6±9.7; n.a.	RBDSQ	SCN w/ FN (90 AAL ROIs) <sup>d</sup>	PD-pRBD<PD-non pRBD	↓ global efficiency ↓ nodal efficiency in L temporal pole ↑ shortest path length ↑ nodal efficiency in R insula and L middle frontal gyrus ↓ global efficiency ↓ nodal efficiency in L temporal pole ↑ shortest path length ↑ nodal efficiency widely mainly in neocortical and paralimbic regions
	97 PD-non pRBD <sup>c</sup>	61.1±9.3; n.a.			PD-pRBD>PD-non pRBD	
	73 HC	60.2±10.1			PD-pRBD<HC PD-pRBD>HC	
Guo et al., 2018 <sup>a</sup> (78)	51 PD-pRBD	61.9±9.5; n.a.	RBDSQ	SCN w/ GM vol (116 AAL ROIs) <sup>d†</sup>	PD-pRBD<PD-non pRBD	↓ Local efficiency in several cerebellar regions and L pallidum
	140 PD-non pRBD	60.5±9.7; n.a.				
	76 HC	60.3±10.6				

	<ul style="list-style-type: none"> <li>⇓ Clustering coefficient in several cerebellar regions and L pallidum</li> <li>⇓ Betweenness in L superior temporal</li> <li>⇓ Degree in L cerebellum 4_5 and cuneus, vermis 7</li> </ul>
PD-pRBD>PD-non pRBD	<ul style="list-style-type: none"> <li>↑ Local efficiency in L pars triangularis, Rolandic operculum, calcarine and superior temporal; R inferior orbitofrontal and cerebellum 3; bilateral cuneus</li> <li>↑ Clustering coefficient in L pars triangularis, Rolandic operculum, calcarine and superior temporal; R inferior orbitofrontal, cerebellum 3 and anterior cingulate; bilateral cuneus</li> <li>↑ Betweenness in L hippocampus and pallidum; R cerebellum Crus2 and 10; bilateral cerebellum 7b</li> <li>↑ Degree in L inferior temporal; R amygdala, hippocampus, and middle temporal pole</li> </ul>
PD-pRBD<HC	<ul style="list-style-type: none"> <li>⇓ Local efficiency in several cerebellar regions</li> <li>⇓ Clustering coefficient in several cerebellar regions</li> <li>⇓ Betweenness in L cerebellum crus1 and fusiform</li> <li>⇓ Degree in L cerebellum crus I, crus II and 3;</li> </ul>

---

						PD-pRBD>HC	R pars triangularis and superior orbitofrontal ↑ Local efficiency in L fusiform, superior temporal and cuneus; R superior orbitofrontal, angular and caudate ↑ Clustering coefficient in L fusiform, superior temporal and cuneus; R superior orbitofrontal, angular and caudate ↑ Betweenness in L rectus ↑ Degree in L olfactory and temporal inferior
Kamps et al., 2019 <sup>a</sup> (70)	40 PD-pRBD <sup>c</sup>	61.1±10.72; 6.22±7.69 m	<i>RBDSQ</i>	SCA w/ GM vol <sup>e</sup>	n.s.		
	127 PD-non pRBD <sup>c</sup>	61.08±9.32; 5.56±6.92 m					
	68 HC	59.41±10.76					

Only those contrasts involving PD-RBD or PD-pRBD groups are included. Demographics are presented as age; disease duration (in y±SD, m±SD, or m[minimum-maximum]).

Abbreviations: *AAL*, *Automated Anatomical Labeling atlas*; ADC, apparent diffusion coefficient; CTh, cortical thickness; Class., classification method; DBM, deformed-based morphometry; Demogr., demographics; FA, fractional anisotropy; FN, number of fibers; GM, gray matter; HC, healthy controls; L, left; m, months; MD, mean diffusivity; MRI, magnetic resonance imaging; *MSQ*, *Mayo Sleep Questionnaire*; n.a., not available; NM-MRI, neuromelanin-sensitive MRI; n.s., not significant; PD-non pRBD, Parkinson's disease without probable RBD; PD-non RBD, Parkinson's disease without RBD; PD-pRBD, Parkinson's disease with probable RBD; PD-RBD, Parkinson's disease with RBD; PSG, polysomnography; QA, quantitative anisotropy; R, right; RBD, REM sleep behavior disorder; *RBDSQ*, *RBD Screening Questionnaire*; REM, rapid eye movement; ROIs, regions of interest; SB vol, subcortical volumetry; SCA, structural covariance analysis; SCN, structural correlation network; SOG, superior occipital gyrus; VBM, voxel-based morphometry; vol, volumetry; w/, with; y, years.

<sup>a</sup> All participants were extracted from the PPMI data (<https://www.ppmi-info.org/>).

<sup>b</sup> Longitudinal study.

<sup>c</sup> Parkinson's disease patients classified as *de novo* PD (at baseline for longitudinal studies).

<sup>d</sup> 68 cortical and 12 subcortical regions from the AAL atlas, <sup>dt</sup> including also 26 cerebellar regions.

<sup>e</sup> Bilateral hippocampus, thalamus, and putamen as seed regions.

**Table 4. Studies of functional MRI in Parkinson's disease with RBD**

Reference	Sample	Demogr.	Class.	Analysis	Contrast	Brain regions
Gallea et al., 2017 (85)	22 PD-RBD	62.4±6.4; 8.7±3.7 y	PSG	Locom., arousal and basal ganglia-thalamic ctrl. network analyses	PD-RBD<PD-non RBD	↓ FC between bilateral PPN and ventral posterior ACC (arousal network)
	16 PD-RBD PI+	61.9±9.4; 9.0±2.7 y			PD-RBD PI+<PD-non RBD	↓ FC between bilateral PPN and SMA proper, pre-SMA, and DN (locom. network); between bilateral PPN and MPFC and ventral posterior ACC (arousal network)
	14 PD-non RBD	57.9±8.8; 8.6±4.2 y			PD-RBD PI+<PD-RBD	↓ FC between bilateral PPN and SMA proper, pre-SMA, and DN (locom. network); between bilateral PPN and MPFC (arousal network)
	25 HC	59.8±8.0			PD-RBD<HC	↓ FC between bilateral PPN and ventral posterior ACC (arousal network); between bilateral SN and VA thalamus, SN and posterior putamen (basal ganglia-thalamic ctrl. network)
					PD-RBD PI+<HC	↓ FC between bilateral PPN and SMA proper, pre-SMA, and DN (locom. network); between bilateral PPN and MPFC and ventral posterior ACC (arousal network); between bilateral SN and VA thalamus SN and posterior putamen (basal ganglia-thalamic ctrl. network)

Gan et al., 2021 (87)	45 PD-pRBD	64.4±8.5;	RBDSQ	dfNC analysis	PD-pRBD>PD-non pRBD	<p>↑ fractional windows and mean dwell time in state IV (involved correlations between VIS and DMN, BG and DMN, and positive within-network coupling of DMN)</p> <p>↓ fractional windows and mean dwell time in state III (involved correlations between VIS and DMN, BG and DMN; and positive within-network coupling of SMN)</p>	
	81 PD-non pRBD	7.0±5.75 y			60.9±9.0;		PD-pRBD<HC
	37 HC	5.0±4.0 y					
Jiang et al., 2021 (72)	24 PD-RBD	66.04±5.7;	PSG	Seed-to-whole brain (R SOG and cerebel. vermis IV/V)	PD-RBD<PD-non RBD	<p>↓ FC between R SOG and L fusiform gyrus, calcarine sulcus, and superior parietal gyrus</p> <p>↓ FC between R SOG and L fusiform gyrus</p> <p>↑ FC between R SOG and L cerebel. crus II</p>	
	26 PD-non RBD	6.79±3.5 y			62.96±7.4;		PD-RBD<HC
	26 HC	5.69±2.88 y			62.73±6.33		PD-RBD>HC
Li et al., 2017 (83)	18 PD-RBD	63.9±8.2;	PSG	ALFF	PD-RBD<PD-non RBD	<p>↓ ALFF R precentral gyrus, middle frontal gyrus, and insula; bilateral putamen</p> <p>↓ ALFF R precentral and middle frontal gyri; bilateral caudate and putamen</p> <p>↑ ALFF L superior frontal gyrus</p>	
	16 PD-non RBD	5.3±4.0 y			62.8±6.6;		PD-RBD<HC
	19 HC	4.0±4.3 y			62.7±8.1		PD-RBD>HC
Li et al., 2020 <sup>a</sup> (86)	30 PD-pRBD	61.87±9.57;	RBDSQ	FN analysis	PD-pRBD<PD-non pRBD	<p>↓ BC R dorsolateral superior frontal gyrus</p> <p>↑ BC L insula</p> <p>↑ NE bilateral thalamus</p> <p>↓ NE L inferior occipital gyrus</p>	
	62 PD-non pRBD	n.a.			61.32±10.39;		PD-pRBD>PD-non pRBD
	20 HC	n.a.			64.00±9.45		PD-pRBD<HC

	↓ LE R superior parietal gyrus ↓ CC R middle frontal gyrus and superior parietal gyrus ↓ DC bilateral inferior occipital gyrus ↑ NE L olfactory and hippocampus; R posterior cingulum; bilateral thalamus ↑ DC L olfactory, hippocampus, caudate and thalamus; R posterior cingulum ↑ BC L olfactory and inferior parietal gyrus
PD-pRBD>HC	

Only those contrasts involving PD-RBD or PD-pRBD groups are included. Demographics are presented as age; disease duration in  $y \pm SD$ .

Abbreviations: ACC, anterior cingulate cortices; ALFF, amplitude of low-frequency fluctuations; BC, betweenness centrality; BG, basal ganglia network; CC, clustering coefficient; cerebel., cerebellar; Class., classification method; ctrl., control; DC, degree centrality; Demogr., demographic; dFNC, dynamic functional network connectivity; DMN, default mode network; DN, dentate nucleus; FC, functional connectivity; FN, functional network; HC, healthy controls; L, left; LE, local efficiency; locom., locomotor; MPFC, medial prefrontal cortices; MRI, magnetic resonance imaging; n.a., not available; NE, nodal efficiency; PD-non pRBD, Parkinson's disease without probable RBD; PD-non RBD, Parkinson's disease without RBD; PD-pRBD, Parkinson's disease with probable RBD; PD-RBD, Parkinson's disease with RBD; PI, postural instability; PPN, pedunculopontine nucleus; PSG, polysomnography; R, right; RBD, REM sleep behavior disorder; *RBDSQ*, *RBD Screening Questionnaire*; REM, rapid eye movement; SMA, supplementary motor area; SN, substantia nigra; SMN, sensorimotor network; SOG, superior occipital gyrus; VA, ventral anterior; VIS, visual network; y, years.

<sup>a</sup> All participants were extracted from the PPMI data (<https://www.ppmi-info.org/>).

**Table 5. Studies of PET and SPECT in Parkinson's disease with RBD**

Reference	Sample	Demogr.	Class.	Analysis	Contrast	Brain regions
<i>PET</i>						
Andersen et al., 2020 (98)	16 PD-RBD	67.7±9.3; 7.6±4.6 y	PSG	<sup>[11C]</sup> MeNER-PET	PD-RBD<HC	↓ binding in bilateral primary sensorimotor
	14 PD-non RBD	65.4±9.0; 5.0±3.6 y				
	17 iRBD	66.0±8.0; n.a.				
Arnaldi et al., 2016 (90)	25 HC	67.0±8.0	MSQ	<sup>[18F]</sup> FDG-PET	PD-pRBD<PD-non pRBD	↓ binding in MAH parieto-occipital regions, middle-temporal and angular gyri
	24 PD-pRBD <sup>C</sup>	72.8±6.2; n.a.				
	14 PD-non pRBD <sup>C</sup>	70.6±7.1; n.a.			PD-pRBD>PD-non pRBD	↑ binding in MAH anterior cingulate and precentral gyrus
	49 HC	67.8±11.6				
Chung et al., 2017 (95)	39 PD-pRBD	69.3±7.8; 5.2±1.6 y	RBDSQ	<sup>[18F]</sup> FP-CIT-PET	PD-pRBD<PD-non pRBD	↓ binding in LAH putamen
	58 PD-non pRBD	67.5±11.1; 4.9±1.5 y				
Horsager et al., 2020 (77)	13 PD-RBD <sup>C</sup>	72.6±5.3; 7[2-7] m	PSG	<sup>[18F]</sup> DOPA-PET	PD-pRBD<iRBD	↓ binding in MAH putamen
	24 PD-non RBD <sup>C</sup>	62.3±7.8; 2.5[1-8.5] m				

	22 iRBD	68.6±8.6; 7.1±5.2 y					
Kotagal et al., 2012 (93)	27 PD-pRBD	63.4±6.7; 6.4±3.7 y	MSQ	[ <sup>11</sup> C]PMP-PET	PD-pRBD<PD-non pRBD	↓ [ <sup>11</sup> C]PMP binding in bilateral neocortical, thalamic and limbic cortical regions	
	53 PD-non pRBD	65.3±7.1; 5.8±4.0 y		[ <sup>11</sup> C]DTBZ-PET			
Lee et al., 2019 (96)	30 PD-pRBD <sup>C</sup>	69.2±7.0; 1.1±0.5 y	RBDSQ PSG	[ <sup>11</sup> C]DASB-PET	PD-pRBD<iRBD	↓ binding in bilateral caudate, anterior and posterior putamen, and substantia nigra	
	30 iRBD	70.5±5.9; 4.3±3.0 y		[ <sup>18</sup> F]FP-CIT-PET			
	19 HC	70.1±4.8			PD-pRBD<HC	↓ binding in bilateral caudate, anterior and posterior putamen, and substantia nigra	
Shin et al., 2021 (92)	25 PD-pRBD <sup>C</sup>	68.4±8.6; 1.0±1.1 y	RBDSQ PSG	[ <sup>18</sup> F]FDG-PET	PD-pRBD<HC	↓ metabolism in R middle occipital gyrus, precuneus, superior temporal gyrus, and insula; bilateral lingual gyrus (PD-pRBD metabolism pattern)	
	21 treated PD	70.7±4.9; 3.8±2.3 y					
	44 iRBD; 14 iRBD for validation	69.6±5.5; 4.2±2.9 y				PD-pRBD>HC	↑ metabolism in R hippocampus; bilateral premotor, precentral, middle frontal gyrus, and putamen (PD-pRBD metabolism pattern)
							↑ PD-pRBD metabolism pattern ↑ treated PD metabolism pattern



						(↓ metabolism in lateral occipital, inferior parietal, and precuneus; ↑ metabolism in supplementary motor area, hippocampus, putamen, thalamus, and cerebellum)
Sommerauer et al., 2018 (76)	16 PD-RBD 14 PD-non RBD 12 HC	67.7±9.3; 7.6±4.6 y 65.4±9.0; 5.0±3.6 y 67.3±6.3	PSG	[ <sup>11</sup> C]MeNER-PET	PD-RBD<PD-non RBD  PD-RBD<HC	↓ binding in bilateral thalamus, hypothalamus, red nucleus, locus coeruleus, dorsal and medial raphe ↓ binding in bilateral thalamus, hypothalamus, red nucleus, locus coeruleus, dorsal and medial raphe
Valli et al., 2021 <sup>d</sup> (97)	15 PD-pRBD 15 PD-non pRBD 15 HC	68.1±6.48; 6.76±3.67 y 70.7±5.67; 7.20 ± 4.49 y 67.1±5.14	MSQ	[ <sup>11</sup> C]FLB-457-PET	PD-pRBD<HC	↓ binding in bilateral uncus parahippocampus, superior temporal, lateral temporal, and inferior temporal
Valli et al., 2021 <sup>d</sup> (94)	15 PD-pRBD 15 PD-non pRBD 15 HC	68.1±6.48; 6.76±3.67 y 70.7±5.67; 7.20 ± 4.49 y 67.1±5.14	MSQ	[ <sup>11</sup> C]DTBZ-PET	PD-pRBD<HC	↓ binding in bilateral caudate, associative striatum, motor striatum, ventral striatum, external and internal globus pallidus

Yoon et al., 2019 (91)	21 PD-pRBD <sup>c</sup>	69.2±7.8; 0.8±0.8 y	PSG	[ <sup>18</sup> F]FDG-PET	PD-pRBD<iRBD	↓ [ <sup>18</sup> F]FP-CIT binding in bilateral posterior putamen, anterior putamen and caudate ↓ [ <sup>18</sup> F]FP-CIT binding in bilateral posterior putamen, anterior putamen and caudate ↓ [ <sup>18</sup> F]FDG metabolism in bilateral occipital and posterior parietal (PD-pRBD metabolism pattern) ↑ [ <sup>18</sup> F]FDG metabolism in bilateral primary and supplementary motor areas, premotor, thalamus, putamen, globus pallidus, rostral and orbital parts of the superior frontal, cerebellum, pons, and parahippocampal gyrus (PD-pRBD metabolism pattern) ↑ PD-pRBD metabolism pattern ↑ iRBD metabolism pattern
	11 PD-RBD (validation)	69.2±5.9; 4.0±1.5 y	RBDSQ	[ <sup>18</sup> F]FP-CIT-PET	PD-pRBD<HC	
	28 iRBD	69.8±5.6; 4.4±3.9 y				
	24 HC	69.5±4.3			PD-pRBD>HC	

							(↓ metabolism in bilateral occipital and posterior parietal; ↑ metabolism bilateral supplementary motor area, putamen, and parahippocampal gyrus) ↑ PD-pRBD metabolism pattern ↑ PD-pRBD metabolism pattern
					PD-pRBD>iRBD		
					PD-RBD>HC		
<b>SPECT</b>							
Arnaldi et al., 2015 <sup>e</sup> (99)	24 PD-pRBD <sup>C</sup>	69.4±6.0; n.a.	PSG MSQ	[ <sup>123</sup> I]FP-CIT-SPECT	PD-pRBD<PD-non pRBD		↓ binding in bilateral caudate
	16 PD-non pRBD <sup>C</sup>	67.2±7.2; n.a.			PD-pRBD<iRBD		↓ binding in bilateral putamen
	12 iRBD	66.4±7.5; 52.0±44.6 m					
Arnaldi et al., 2016 <sup>e</sup> (90)	24 PD-pRBD <sup>C</sup>	72.8±6.2; n.a.	MSQ	[ <sup>123</sup> I]FP-CIT-SPECT	PD-pRBD<PD-non pRBD		↓ binding in bilateral caudate and putamen
	14 PD-non pRBD <sup>C</sup>	70.6±7.1; n.a.					
Cao et al., 2020 <sup>a, b</sup> (100)	98 PD-pRBD <sup>C</sup>	61.5±10.1 7.2±7.4	RBDSQ	[ <sup>123</sup> I]FP-CIT-SPECT	Baseline: PD-pRBD<PD-non pRBD		↓ binding in LAH caudate and putamen
	135 PD-non pRBD <sup>C</sup>	61.2±9.5; 6.7±6.9 m			1-year follow-up: PD-pRBD<PD-non pRBD		↓ binding in bilateral caudate and putamen
					2-year follow-up: PD-pRBD<PD-non pRBD		↓ binding in bilateral caudate and putamen
					4-year follow-up: PD-pRBD<PD-non pRBD		↓ binding in bilateral caudate and putamen
					Group by time: PD-pRBD<PD-non pRBD		↓ binding in bilateral caudate

Kim et al., 2020 <sup>a, b</sup> (101)	157 PD-pRBD <sup>c</sup>	61.90±9.69; 6.63±6.56 m	<i>RBDSQ</i>	<sup>[123I]</sup> FP-CIT-SPECT	Group by time, 4-year follow-up: PD-pRBD<PD-non pRBD	↓ binding in MAH caudate, putamen and striatum; bilateral caudate
	259 PD-non pRBD <sup>c</sup>	61.50±9.76; 6.73±6.60 m				
Mašková et al., 2020 (102)	11 PD-RBD <sup>c</sup>	56.3±12.4; n.a.	PSG	<sup>[123I]</sup> FP-CIT-SPECT	PD-RBD<PD-non RBD  PD-RBD<iRBD	↓ binding in MAH caudate ↓ binding in MAH caudate and putamen
	33 PD-non RBD <sup>c</sup>	(PD as a whole)				
	61 iRBD	66.4±8.1; 0.69±0.99 y				
Pagano et al., 2018 <sup>a</sup> (104)	158 PD-pRBD <sup>c</sup>	61.8±9.68; 6.53±6.54 m	<i>RBDSQ</i>	<sup>[123I]</sup> FP-CIT-SPECT	n.s.	
	263 PD-non pRBD <sup>c</sup>	61.47±9.78; 6.71±6.59 m				
Salsone et al., 2014 (66)	11 PD-RBD	66.6±7.4; 4.72±4.07 y	PSG	DAT-SPECT	n.s.	
	11 PD-non RBD	66.9±7.9; 4.36 ± 4.2 y				
	18 HC	65.1±7.8				
Zoetmulder et al., 2016 (103)	10 PD-RBD	66.60±3.44; 7.89±5.93 y	PSG	<sup>[123I]</sup> FP-CIT-SPECT	PD-RBD<iRBD  PD-RBD<HC	↓ binding in MAH putamen ↓ binding in MAH putamen
	10 PD-non RBD	66.80±8.72; 5.00±5.08 y				
	10 iRBD	61.20±9.27; 5.75±5.12 y				
	10 HC	56.20±8.28				

Only those contrasts involving PD-RBD or PD-pRBD groups are included. Demographics are presented as age; disease duration (in y±SD, m±SD, or m[minimum-maximum]). See abbreviations and annotations on the next page.

Abbreviations: Class., classification method; Demogr., demographics; HC, healthy controls; iRBD, isolated RBD; LAH, less affected hemisphere; MAH, most affected hemisphere; *MSQ*, *Mayo Sleep Questionnaire*; n.a., not available; PD-non pRBD, Parkinson's disease without probable RBD; PD-non RBD, Parkinson's disease without RBD; PD-pRBD, Parkinson's disease with probable RBD; PD-RBD, Parkinson's disease with RBD; PET, positron emission tomography; PSG, polysomnography; R, right; RBD, REM sleep behavior disorder; *RBDSQ*, *RBD Screening Questionnaire*; REM, rapid eye movement; SPECT, single-photon emission computerized tomography; y, years.

<sup>a</sup> All participants were extracted from the PPMI data (<https://www.ppmi-info.org/>).

<sup>b</sup> Longitudinal study.

<sup>c</sup> Parkinson's disease patients classified as *de novo* PD (at baseline for longitudinal studies).

<sup>d</sup> Both studies used the same sample.

<sup>e</sup> Samples partially overlapped.

### 2.2.5. Brain correlates in PD with RBD

This subsection includes an overview of the brain correlates of clinical and cognitive outcomes in PD with RBD reported in the previously revised studies, summarized in **Tables 6 and 7**, respectively.

#### **Brain correlates of clinical features**

Some studies have found neural correlates with sleep features. Regarding the percentage of REM sleep with atonia, it has been associated with lower signal intensity in the coeruleus/subcoeruleus complex using neuromelanin-sensitive MRI (64). Concerning incremented muscle activity during the tonic phase of REM sleep has been associated with incremented GM volume in the cerebellar vermis IV/V (72) and reduced noradrenaline binding in the locus coeruleus analyzed using [<sup>11</sup>C]-MeNER-PET (76). Likewise, the reduced noradrenaline binding in the locus coeruleus has been correlated with incremented muscle activity during the phasic phase of REM sleep (76). Moreover, incremented muscle activity during the NREM sleep stage has been associated with reduced dopamine binding in the putamen through [<sup>123</sup>I]-FP-CIT-SPECT (103). Last, RBD symptomatology measured using the *RBDSQ* has been positively associated with nodal efficiency of the right insula and the left middle frontal gyrus obtained using a graph theory approach from DTI (79).

As regards motor symptomatology, a higher *MDS-UPDRS Part III* score has been associated with reduced dopamine binding in the putamen using [<sup>18</sup>F]-FP-CIT-PET (95) and with decremented volume in the superior occipital gyrus (72).

The disease staging measured with the *H&Y scale* has been associated negatively with extra-striatal dopamine binding in the left uncus parahippocampus (97).

### **Brain correlates of cognitive impairment**

Impairment in general cognition has been associated longitudinally with volume decrement in the left caudate (73). Regarding specific domains, worse performance in verbal memory has been associated with volume decrements in the superior occipital gyrus (72) and longitudinally with cortical thinning in the left insula (73). Impairment in language has shown a positive correlation with volume decrements in the superior occipital gyrus (72). Mental processing speed alteration has been associated with longitudinal cortical thinning in the left insula (73). Last, executive and visuospatial/visuoperceptual impairments have been associated with decreased functional connectivity between the right superior occipital and left superior parietal gyri (72).

**Table 6. Brain correlates of clinical outcomes in Parkinson’s disease with RBD**

Reference	REM sleep without atonia	Tonic REM sleep motor activity	Phasic REM sleep motor activity	NREM sleep motor activity	RBD symptoms	Motor symptoms	PD staging
Chung et al., 2017 (95)						↓ [ <sup>18</sup> F]FP-CIT binding in LAH putamen	
García-Lorenzo et al., 2013 (64)	↓ signal intensity coeruleus/subcoeruleus complex						
Jiang et al., 2021 (72)		↑ cerebellar vermis IV/V volume				↓ superior occipital gyrus volume	
Chen et al., 2022 (79)					↑ Nodal efficiency in L middle frontal gyrus and R insula		
Sommerauer et al., 2018 (76)		↓ [ <sup>11</sup> C]-MeNER binding in locus coeruleus	↓ [ <sup>11</sup> C]-MeNER binding in locus coeruleus				
Valli et al., 2021 (97)							↓ [ <sup>11</sup> C]FLB-457 binding in L uncus parahippocampus
Zoetmulder et al., 2016 (103)					↓ [ <sup>123</sup> I]-FP-CIT binding in the putamen		

Only those results from correlations involving PD-RBD or PD-pRBD groups alone are included.

Abbreviations: L, left; LAH, less affected hemisphere; PD-pRBD, Parkinson’s disease with probable RBD; PD-RBD, Parkinson’s disease with RBD; R, right; RBD, REM sleep behavior disorder; REM, rapid eye movement.



**Table 7. Brain correlates of cognitive outcomes in Parkinson's disease with RBD**

Reference	General cognition	Memory	Language	Processing speed	Executive	VS/VP
Jiang et al., 2021 (72)		↑ superior occipital gyrus volume	↑ superior occipital gyrus volume		↑ FC R superior occipital gyrus-L superior parietal gyrus	↑ FC R superior occipital gyrus-L superior parietal gyrus
Yoon et al., 2021 (73)	↓ Longitudinal volume decrement in L caudate	↓ Longitudinal cortical thinning in L insula		↓ Longitudinal cortical thinning in L insula		

Only those results from correlations involving PD-RBD or PD-pRBD groups alone are included.

Abbreviations: L, left; PD-pRBD, Parkinson's disease with probable RBD; PD-RBD, Parkinson's disease with RBD; R, right; RBD, REM sleep behavior disorder; REM, rapid eye movement; VS/VP, visuospatial/visuo-perceptual.

### 3. Sex and gender in Parkinson's disease

There has been a growing interest in the influence of sex and gender on neurodegenerative diseases. Both variables are central to precision medicine approaches, expected to play a relevant role in the prevention, diagnosis, and treatment of neurodegenerative diseases in the upcoming years (105,106). We will review epidemiological, clinical, cognitive, and neuroimaging findings on sex differences in PD. Lastly, the mechanisms involved in sex differences in PD will be introduced.

Early population-based studies showed that males have a two-fold higher incidence of PD than females (107). The male predominance was supported by subsequent meta-analyses exploring the PD prevalence (108,109). In this context, the most recent meta-analysis showed a 1.50 male-to-female ratio for prevalence and incidence of PD (110). Likewise, iRBD prevalence is higher in males than females, as mentioned in a previous section (*Section 1. REM sleep behavior disorder: an overview*). Nevertheless, a recent general population-based study did not show differences between sexes in iRBD prevalence (22). The inconsistency of the results could be influenced by an underdiagnosis of iRBD in females because of less conspicuous symptomatology (23,24), which leads to a lower probability of seeking medical care. Of our interest, PD with RBD has been associated with male sex, according to a recent meta-analysis focused on profiling this clinical subtype (35). This result should be interpreted with caution because the same RBD underdiagnosis phenomenon could affect the PD population (111).

As regards the neuropathology of the disease, evidence from post-mortem examination is still needed. So far, only one study has reported between-sex

differences in alpha-synuclein levels in plasma, with lower concentrations in males than females (112).

Regarding clinical aspects of the PD that differ between sexes, in a recent review, Cerri et al. described sex profiles according to the existing literature (113): a female PD prototype characterized by postural tremor, frequent falls, dysphagia, gastrointestinal dysfunction, pain, and visuospatial impairment; and a male PD prototype characterized by freezing of gait, camptocormia, drooling, executive function impairment, and MCI. Nonetheless, there is controversy because of conflicting results, for example, regarding motor symptoms. Early studies found an association of female sex in PD with postural tremor (114,115) and dyskinesia (116). Nevertheless, two recent studies analyzed data from the PPMI and related male sex in PD with motor impairment. The first study reported more motor symptomatology and postural tremor in PD males (117). The second study performed longitudinal analyses and found a higher decline in motor experiences of daily living and a higher decline in motor symptomatology assessed in the ON medication state (118).

Sex differences in cognition in PD have been explored in several studies. Curtis et al. performed a meta-analysis to test differences between PD males and PD females in different cognitive domains. They found a significant sex effect in the executive domain based on the results of 22 previous studies; and concluded that PD males show more cognitive impairment in this domain than PD females (119). Furthermore, a recent longitudinal study performed on a sample of 5946 PD patients with a median follow-up of 3.1 years reported that PD males had a higher risk of developing cognitive impairment than PD females (120). In this context, other studies reported that the male sex predicted cognitive decline measured through the *Mini-Mental State Examination (MMSE)* analyzing a pool of 1350 PD patients (121); and that the male sex was

associated with progression to MCI and dementia by analyzing data from 418 PD patients (122). Thus, the evidence points to more cognitive impairment and worse prognosis in PD males. However, in a recent study using a sample of 392 PD patients, Bakeberg et al. found that longitudinally PD males and PD females showed different trajectories depending on the cognitive domain (123). In this study, baseline results showed that PD males had a worse performance in global cognition, verbal memory, and verbal fluency tasks than PD females. Nonetheless, in longitudinal analyses, the PD males showed a greater cognitive decline in global cognition and language than PD females; and PD females showed a greater cognitive decline in attention/orientation, memory, and visuospatial tasks than PD males. On the contrary, another study analyzed a sample of 423 patients from the PPMI and did not find longitudinal differences between sexes in cognitive trajectories (118).

In a recent review, Salminen et al. highlighted that despite the sex differences in clinical presentation in PD reported in the literature, neuroimaging research on the topic is still scarce, and only a few studies have explored sex differences (124). Yadav et al. explored sex differences in CTh using a sample of 43 PD males and 21 PD females (125). They found that the PD males had thinning in several frontal, parietal and occipital regions compared to PD females. Moreover, they performed a structural connectivity analysis based on mean CTh measures using a graph theory approach. The authors found that PD males, compared with PD females, showed lower connection strengths, lower clustering coefficients, and altered network hubs. In a subsequent study, Tremblay et al. analyzed a sample of 149 *de novo* PD males and 89 *de novo* PD females from the PPMI using DBM, CTh, and structural connectivity analysis based on DTI (126). The DBM results showed that *de novo* PD males had volume decrements compared with *de novo* PD females in 10 cortical regions (including the bilateral

frontal lobe, left insular lobe, right postcentral gyrus, left inferior temporal and cingulate gyrus), and left thalamus. Although, *de novo* PD females had volume decrements compared with *de novo* PD males in 6 cortical regions (including the left frontal lobe, right parietal lobe, left insular gyrus, and right occipital cortex) (Figure 7). Meanwhile, the CTh analysis did not show significant differences. Regarding the structural connectivity analysis, the authors found that *de novo* PD males, compared with *de novo* PD females, had disruptions in measures of local efficiency in several regions, including the basal ganglia, hippocampus, amygdala, and thalamus. Altogether, the current evidence points to severe atrophy in PD males compared with PD females from the early stages of the disease.

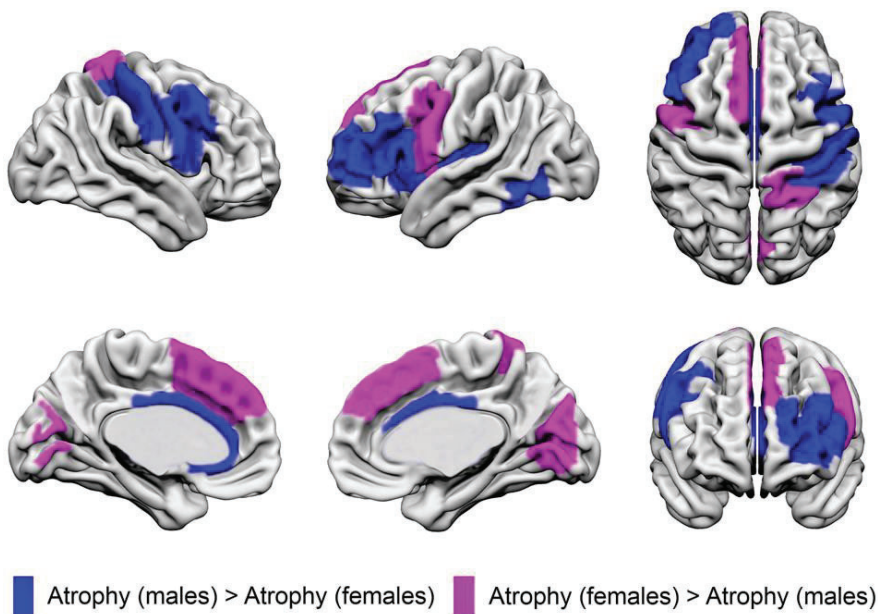


**Figure 7.** Sex differences in regional brain deformation in Parkinson’s disease. Cortical regions showing significant sex differences in DBM W-Score after FDR corrections ( $P_{\text{FDR}}\text{-value} < 0.05$ ) overlaid on the brain mesh ICBM152 template for visualization. In blue, greater atrophy in males compared to females; in pink: greater atrophy in females. Adapted from “Sex differences in regional brain deformation in Parkinson’s disease” by Tremblay et al. (126) licensed under RightsLink.

Characterization of sex differences in PD in neurotransmission has been implemented using SPECT approaches focused on the dopaminergic systems. In a seminal study, Haxxama et al. explored a sample of 157 PD males and 96 PD females and found that PD females had a higher [<sup>123</sup>I]FP-CIT striatal binding than PD males (114). Recently, Boccallini et al. applied an [<sup>123</sup>I]FP-CIT-SPECT approach in a sample of 189 *de novo* PD males and 97 *de novo* PD females from the PPMI database (127). First, the authors classified PD patients as a mild motor, intermediate, or diffuse-malignant clinical subtype. In the mild motor and intermediate subtypes, *de novo* PD males had lower binding in the putamen and showed a widespread alteration of the connectivity of the nigrostriatal dopaminergic pathway than *de novo* PD females. Both lower binding and connectivity were associated with motor impairment in *de novo* PD males in these subtypes. In the diffuse-malignant subtype, *de novo* PD males had lower binding in the putamen and more severe motor impairment than *de novo* PD females. On the other hand, *de novo* PD females had lower binding in regions of the mesolimbic dopaminergic pathway and showed a more widespread connectivity alteration in this pathway than *de novo* PD males. Moreover, anxiety in *de novo* PD females was associated with a reduced binding in the amygdala.

Different mechanisms implicated in sex differences in PD have been proposed and studied, from animal models to clinical populations. Reviewing the literature, Cerri et al. pointed to three levels in which sex impacts PD pathophysiology: dopaminergic neurodegeneration, neuroinflammation, and oxidative stress (113). In this context, the effect of sex hormones appears as a factor with transversal influence, specifically estrogens, with a potential neuroprotective role based on epidemiological evidence (128). Preclinical research has shown a connection between estrogens and antiapoptotic and

antioxidant effects (129), as well as inhibition of alpha-synuclein fibril stabilization and aggregation (130). Other studies have shown that a higher total lifetime estrogen exposure might be associated with a decreased risk of PD in females (131–134). Nevertheless, other studies have not supported this relation between estrogen exposure and PD (129,135–139).

Other relevant aspects not covered in this section are the risk and protective factors for PD and their differential sex effect, from environmental to psychical health. For example, higher levels of total and low-density cholesterol lipoprotein have been associated with a lower likelihood of developing PD in males but not in females (140). Another relevant point is the need for a gender perspective in PD, considering not only the biological aspects but also those that emerge from the gender role of the patient in a specific cultural context. From this perspective, Subramanian et al. comprehensively reviewed the needs of women with PD (128). For example, the delay suffered by women with PD in receiving a medical diagnosis and referral to a movement disorder specialist (141,142). These differences in health care may be influenced by a tendency to less reporting and emphasis on annoying symptoms by women during medical consults and because of the medical bias due to the higher PD prevalence in males (142). Both sex and gender, as well as their mutual influence, are relevant for precision medicine approaches.





## Chapter 2

---

### Hypotheses and objectives

## Hypotheses

### Main hypotheses:

1. PD-pRBD will be characterized by specific structural and functional MRI brain features associated with cognitive impairment.
2. There will be identified sex differences in cognition and structural MRI brain features in *de novo* PD, with worse cognitive profile and pattern of neurodegeneration in males than females. The sex differences among *de novo* PD patients will be more extended in the PD-pRBD group compared with the PD-non pRBD group.

### Specific hypotheses:

1. The *de novo* PD-pRBD group will show cortical and subcortical atrophy compared with *de novo* PD-non pRBD, which is expected to be similar to that previously described in PD with RBD.
2. The *de novo* PD-pRBD group will present structural neural correlates for cognitive impairment.
3. The PD-pRBD group will show reduced functional connectivity compared with PD-non pRBD.
4. The PD-pRBD group will present functional connectivity brain correlates for cognitive impairment.
5. The male sex will be associated with more cognitive impairment in *de novo* PD; the impairment will be more severe in *de novo* PD-pRBD than in *de novo* PD-non pRBD.
6. The male sex will be associated with reduced cortical and subcortical structures in *de novo* PD, more pronounced in *de novo* PD-pRBD than in *de novo* PD-non pRBD.

## Objectives

### Main objectives:

The main aim of the present doctoral thesis is to characterize the cognitive impairment and structural and functional MRI brain features of PD with RBD, as well as to explore the impact of sex differences in cognition and structural MRI measures in PD and PD with RBD.

The main objectives of this thesis are:

1. To characterize structural and functional MRI brain substrates in PD-pRBD and their correlates with cognitive impairment.
2. To explore sex differences in cognition and structural MRI brain features in *de novo* PD and *de novo* PD-pRBD.

### Specific objectives:

1. To characterize cortical and subcortical MRI brain substrates in *de novo* PD-pRBD.
2. To study cognitive impairment in *de novo* PD-pRBD and its correlation with cortical and subcortical structural MRI brain features.
3. To characterize whole-brain resting-state functional MRI connectivity in PD-pRBD.
4. To relate cognitive impairment in PD-pRBD with whole-brain resting-state functional MRI connectivity features.
5. To study sex differences in cognition in *de novo* PD and *de novo* PD-pRBD.
6. To explore the impact of sex differences in MRI brain atrophy in *de novo* PD and *de novo* PD-pRBD.



# Chapter 3

---

## Materials and methods

The studies which be part of this doctoral thesis used two different samples of Parkinson's disease (PD) patients and healthy controls (HC). **Studies 1, 3, and 4** used a multicentric sample of newly diagnosed drug naïve PD patients from the Parkinson's Progression Markers Initiative (PPMI, <https://www.ppmi-info.org/>) (143). **Study 2** used a sample of PD patients with longer disease duration and mostly medicated. These samples will be named respectively “*de novo* PD sample” and “PD sample” in this chapter.

### **Study 1**

**Oltra J**, Uribe C, Segura B, Campabadal A, Inguanzo A, Monté-Rubio GC, Pardo J, Martí MJ, Compta Y, Valldeoriola F, Junque C, Iranzo, A. Brain atrophy pattern in *de novo* Parkinson's disease with probable RBD associated with cognitive impairment. *npj Parkinson's Disease*. 2022; 8: 2 doi:10.1038/s41531-022-00326-7.

### **Study 2**

**Oltra J**, Campabadal A, Segura B, Uribe C, Martí MJ, Compta Y, Valldeoriola F, Bargallo N, Iranzo A, Junque C. Disrupted functional connectivity in PD with probable RBD and its cognitive correlates. *Scientific Reports*. 2021; 11: 24351. doi:10.1038/s41598-021-03751-5.

### **Study 3**

**Oltra J**, Uribe C, Campabadal A, Inguanzo A, Monté-Rubio GC, Martí MJ, Compta Y, Valldeoriola F, Iranzo, A, Junque C, Segura B. Sex differences in brain and cognition in *de novo* Parkinson's disease. *Frontiers in Aging Neuroscience*. 2022; 13: 791532. doi: 10.3389/fnagi.2021.791532.

### **Study 4**

**Oltra J**, Segura B, Uribe C, Monté-Rubio GC, Campabadal A, Inguanzo A, Pardo J, Martí MJ, Compta Y, Valldeoriola F, Iranzo, A, Junque C. Sex differences in brain atrophy and cognitive impairment in Parkinson's disease patients with and without probable rapid eye movement sleep behavior disorder. *Journal of Neurology*. 2022; 269: 1591–1599. doi:10.1007/s00415-021-10728-x.

# 1. Study samples

This section covers the main characteristics of the samples used in the above-mentioned studies.

## 1.1. *de novo* Parkinson's disease sample

### Participants

Magnetic Resonance imaging scans clinical and neuropsychological data were obtained from the PPMI databases. The available PPMI sample at the baseline included 311 PD patients and 137 HC. At this stage, the patients were included before any levodopa (L-DOPA) intake. All the participants provided written informed consent. Each one of the centers from the PPMI received approval from an ethical standards committee. Moreover, the central Institutional Review Board was provided by WCG IRB (tracking number: 20200597), and the study is registered at ClinicalTrials.gov (ID: NCT04477785). Inclusion criteria were: (i) recent diagnosis of PD with asymmetric resting tremor or asymmetric bradykinesia, or two from among bradykinesia, resting tremor, and rigidity; (ii) absence of PD treatment; (iii) neuroimaging evidence of significant dopamine transporter deficit consistent with a clinical diagnosis of PD, and excluding conditions that can mimic PD, such as drug-induced and vascular parkinsonism or essential tremor; (iv) T1-weighted images available (for PD and HC groups); and (v) age older than 50 and younger than 85 years old (for PD and HC groups).

The exclusion criteria for both groups were: (i) diagnosis of dementia; (ii) significant psychiatric, neurologic, or systemic comorbidity; (iii) a first-degree family member with PD; and (iv) presence of MRI motion artifacts, field distortions, intensity inhomogeneities, or detectable structural brain lesions.

The final sample in our studies included 205 *de novo* PD patients and 69 HC (Figure 8). As part of the selection process, the raw MRI acquisitions were checked. At that point, 3 PD patients and 6 HC were excluded due to motion-corrupted images. Second, *FreeSurfer* preprocessing was conducted. After quality control and fixing errors of CTh preprocessing, 94 PD patients and 56 HC were kept out. Lastly, medical conditions and medications were checked in the databases. This step implies a double-check within the inclusion criteria applied by the PPMI. It allowed confirming that any participant with relevant comorbidities entered into the subsequent analyses. Thus, 9 PD patients and 6 HC were discarded. The reasons for exclusion of these PD patients were: Two due to neurological comorbidity, 6 to psychiatric comorbidity, and 1 to cardiovascular comorbidity. In the HC group: Four participants were excluded due to pRBD according to the *RBDSQ* (69); 1 to neurological comorbidity; 1 to cardiovascular comorbidity.

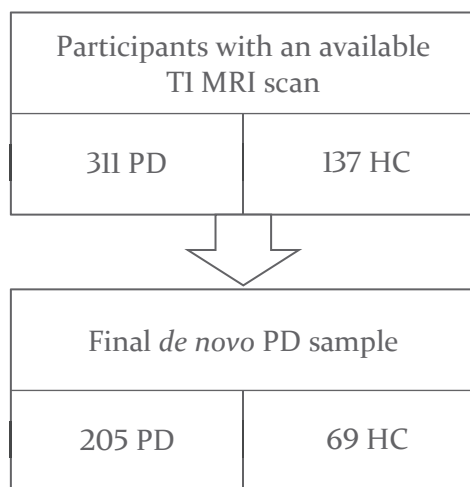


**Figure 8.** *de novo* PD sample from the PPMI.



## Probable RBD classification

REM sleep behavior disorder symptomatology was assessed with the *RBDSQ* (69). The *RBDSQ* is a patient self-administered questionnaire that covers the main RBD features. This instrument consisted of 10 items with a maximum score of 13 points and a 5-points cut-off for pRBD categorization (**Panel B**). After applying the cut-off, the *de novo* PD patients of the sample were divided into two groups, resulting in 79 PD with pRBD (PD-pRBD) and 126 PD without pRBD (PD-non pRBD) patients. These resulting groups were used in *studies 1 and 3*.

### Panel B. *RBDSQ* Screening Questionnaire (*RBDSQ*) items

1. I sometimes have very vivid dreams.
2. My dreams frequently have an aggressive or action-packed content.
3. The dream contents mostly match my nocturnal behavior.
4. I know that my arms or legs move when I sleep.
5. It thereby happened that I (almost) hurt my bed partner or myself.
6. I have or had the following phenomena during my dreams:
  - 6.1. speaking, shouting, swearing, laughing loudly
  - 6.2. sudden limb movements, "fights"
  - 6.3. gestures, complex movements, that are useless during sleep, e.g., to wave, to salute, to frighten mosquitoes, falls off the bed
  - 6.4. things that fell down around the bed, e.g., bedside lamp, book, glasses
7. It happens that my movements awake me.
8. After awakening I mostly remember the content of my dreams well.
9. My sleep is frequently disturbed.
10. I have/had a disease of the nervous system (e.g., stroke, head trauma, parkinsonism, RLS, narcolepsy, depression, epilepsy, inflammatory disease of the brain), which?

## Clinical and neuropsychological assessments

Parkinson's disease symptoms were evaluated using the *MDS-UPDRS*, particularly the *MDS-UPDRS Part III* was used for motor symptoms assessment (144). The disease severity was examined through the *H&Y scale* (145,146).

Depressive symptoms were assessed using the *15-item Geriatric Depression Scale (GDS-15)* (147), the olfactory function by means of the *University of Pennsylvania Smell Identification Test (UPSIT)* (148), the autonomic symptoms using the *Scales for Outcomes in Parkinson's Disease - Autonomic Dysfunction (SCOPA-AUT)* (149), and the excessive daytime sleepiness using the *Epworth Sleepiness Scale (ESS)* (150).

All participants underwent a comprehensive neuropsychological assessment, including the *Montreal Cognitive Assessment (MoCA)* for global cognition (151); the 15-item version of the *Benton Judgment of Line Orientation Test (JLO)* for visuospatial function (152); the phonemic fluency (letter 'f' in 1 minute) and semantic fluency (animals, vegetables and fruits in 1 minute each category) for executive function; the total learning recall, delayed recall and recognition from the *Hopkins Verbal Learning Test-Revised (HVLTR)* for memory (153); and the *Symbol Digit Modalities Test (SMDT)* (154,155) and the *Letter-Number Sequencing (LNS)* (156) for attention and working memory. The raw scores were z-scored, taking the HC group as reference. Supplementary, in *study 3*, the z-scores calculation was followed by extraction of the age, sex, and education effects through linear regression models taking the HC group as reference, resulting in adjusted z-scores.

### **Magnetic resonance imaging acquisition**

Three-dimensional T1-weighted scans were acquired at different centers on 1.5 or 3 Tesla (T) scanners using a Magnetization Prepared Rapid Gradient Echo (MPRAGE) sequence acquired in the sagittal plane. As detailed in the MRI technical operations manual of the PPMI (available at: <https://www.ppmi-info.org/study-design/research-documents-and-sops>), the acquisition parameters for all centers were: slice thickness = 1-1.5 mm; inter-slice gap = 0

mm; voxel size = 1x1x1.2 mm; matrix = 256 x 256 x 170-200. All the other parameters, including repetition time (TR) and echo time (TE), followed the manufacturer's recommendations.

## **1.2. Parkinson's disease sample**

### **Participants**

The sample consisted of 71 PD patients recruited from the Unitat de Parkinson i Trastorns del Moviment (Hospital Clínic de Barcelona, Barcelona, Catalunya) and 69 HC recruited from the Institut Català de l'Envel·liment (Universitat Autònoma de Barcelona, Barcelona, Catalunya) and patients' relatives. The study had the approval of the Ethics Committee of the Universitat de Barcelona (IRB00003099) and the Hospital Clínic de Barcelona (HCB/2014/0224). The procedures were fully explained to the participants. Subsequently, written consent was provided.

Inclusion criteria for PD patients were: (i) diagnostic criteria for PD attaining UK PD Society Brain Bank (157); and (ii) no surgical treatment with deep-brain stimulation.

Exclusion criteria were: (i) MCI for HC; (ii) PD age of onset less than 40 years; (iii) age less than 50 years; (iv) severe comorbidity due to psychiatric or neurological conditions; (v) score below 25 obtained in the *MMSE* for HC (158); (vi) claustrophobia; (vii) pathological MRI findings apart from mild white matter hyperintensities in the fluid-attenuated inversion recovery (FLAIR) sequence; (viii) MRI artifacts; (ix) absence of resting-state fMRI acquisition; (x) fMRI head motion parameter of mean interframe head motion at  $\geq 0.3$  mm translation or  $0.3^\circ$  rotation; (xi) fMRI head motion parameter of maximum interframe head motion at  $\geq 1$  mm translation or  $1^\circ$  rotation; (xii) no response

to the *Innsbruck RBD Inventory (RBD-I)* (159); (xiii) pRBD condition based on the *RBD-I* for HC.

After applying the criteria, 59 PD patients and 30 HC were selected. Thus, 12 PD patients and 39 HC were excluded. The reasons for the exclusion of PD patients were: Two for young-onset, 1 for age < 50 years, 1 for vascular parkinsonism lookalike condition, 1 for claustrophobia, 2 for the absence of fMRI, 5 for no response to the *RBD-I*. The causes for the exclusion of HC were: Four for age < 50 years, 3 for psychiatric comorbidity, 8 for MCI condition, 1 for *MMSE* score below 25, 2 for MRI artifact, 3 for fMRI head motion parameters, 5 for no response to the *RBD-I*, 13 for pRBD category.

### **Probable RBD classification**

The RBD symptoms were assessed using the *RBD-I* (159) in the PD sample. It is a 5-item self-administered questionnaire that scored the presence and frequency of the RBD symptoms (**Panel C**). The patients can be classified as pRBD with a 0.25-points cut-off after applying the calculation formula of the number of positive symptoms divided by the number of answered questions. According to the cut-off, the PD patients were classified into two groups: Twenty-seven PD-pRBD and 32 PD-non pRBD patients.

#### **Panel C. *Innsbruck RBD Inventory (RBD-I)* items**

1. Do you dream of violent or aggressive situations (e.g., to have to defend yourself)?
2. Do you scream, insult, or curse during your sleep? (Note: this does not include normal sleep talking.)
3. Do you move out of your sleep and occasionally perform “flailing” or more extensive movements?
4. Have you ever injured or nearly injured yourself or your bed partner while you were sleeping?
5. Are the above-described movements out of your sleep occasionally or always in line with the content of your dreams? (items 2, 3, 4)

## **Clinical and neuropsychological assessments**

Motor symptoms were assessed with the *MDS-UPDRS Part III* (144), disease severity with the *H&Y scale* (145,146), and olfactory function using the *UPSIT* (148).

The majority of the PD patients (almost 95%) were taking different combinations of antiparkinsonian drugs. For standardization, the L-DOPA equivalent daily dose (LEDD) was calculated (160).

All the participants underwent a comprehensive neuropsychological assessment at the Hospital Clínic de Barcelona (Barcelona, Catalunya), which included: *MMSE* for global cognition (158); *Benton Visual Form Discrimination (BVF)* (161), the 15-item version of the *JLO* (152), and *Benton Facial Recognition Test (BFRT)* (162) for visuospatial and visuoperceptual functions; total learning recall, delayed recall, and recognition from the *Rey Auditory Verbal Learning Test (RAVLT)* for memory (163); phonemic fluency (letter 'p' in 1 minute) and semantic fluency (animals in 1 minute) for executive functions (163); *Digit Span Forward and Backward* (156), *Stroop Color and Word Test* (164), *SDMT* (154,155), and *Trail Making Test part A and B (TMT)* (163) for attention and working memory; and *Boston Naming Test (BNT)* (165) for language.

## **Magnetic resonance imaging acquisition**

The MRI acquisitions were collected at the Centre de Diagnòstic per la Imatge (CDI, Hospital Clínic de Barcelona, Barcelona, Catalunya) using a 3T scanner (MAGNETOM Trio, Siemens, Germany). The scanning protocol included a high-resolution 3-dimensional T1-weighted sequence acquired in the sagittal plane using a MPRAGE sequence (TR = 2300 ms, TE = 2.98 ms, inversion time = 900 ms, 240 slices, field-of-view = 256 mm; voxel size = 1x1x1

mm); an axial FLAIR sequence (repetition time = 9000 ms, echo time = 96 ms); and a resting-state 10-min-long functional gradient-echo echo-planar imaging (EPI) sequence (240 T2\* weighted images, TR = 2.5 s, TE = 28 ms, flip angle = 80°, slice thickness = 3 mm, field-of-view = 240 mm). The participants received the following main instructions: keep their eyes closed, do not fall asleep, and do not think about anything in particular.

## 2. Magnetic resonance imaging preprocessing

This section covers an overview of the structural MRI and fMRI preprocessing methods, highlighting the procedures in common between studies.

### 2.1. Structural MRI: cortical thickness and volumetry

The following techniques were used in the studies which analyzed the *de novo* PD sample.

Cortical thickness (CTh) and MRI volumetry were estimated using the automated stream and the segmentation tools of *FreeSurfer version 6.0* (available at: <https://surfer.nmr.mgh.harvard.edu/>). Following this pipeline, the main procedures to obtain CTh measures included: removal of non-brain data, intensity normalization (166), tessellation of the GM/WM boundary, automated topology correction (167,168), identification of tissue borders (169–171), and finally calculation (171). The smoothing of the CTh maps was fixed at full width half maximum (FWHM) of 15 mm of a circularly symmetric Gaussian kernel across the surface. For MRI volumetry, automated segmentation was applied using the *Automatic Subcortical Segmentation Atlas (Aseg Atlas)* (171).

In the second step, the outputs of the preprocessing stream followed a quality control by visual inspection to check the accuracy of the registration, skull

stripping, segmentation, and cortical surface reconstruction. Preprocessing errors were fixed by automated and manual interventions, following standard procedures. If appropriate corrections were not possible, the participants were discarded.

After quality control, we obtained CTh maps, volumetric data including deep GM structures volumes (thalami, caudate nuclei, putamen nuclei, pallidum nuclei, hippocampi, amygdalae, accumbens nuclei), estimated total intracranial (eTIV), total cortical GM, and total subcortical GM volumes.

The deep GM volumes were bilateralized:

$$\frac{\textit{left volume} + \textit{right volume}}{2}$$

Volume ratios expressed in percentages were calculated:

$$\frac{\textit{volume}}{\textit{eITV}} \times 100$$

Additionally, we obtained the estimation of the global average thickness as follows (left and right hemispheres expressed as *lh* and *rh*, respectively):

$$\frac{(\textit{lh thickness} \times \textit{lh surface area}) + (\textit{rh thickness} \times \textit{rh surface area})}{\textit{lh surface area} + \textit{rh surface area}}$$

*Study 3* included adjusted z-scores of global and deep GM volumes. The adjusted z-scores were computed by extracting age, sex, and education effects using linear regression models with the HC group as reference.

## 2.2. Functional MRI: preprocessing

This technique was used in the performed study that analyzed the PD sample.

Main preprocessing of the fMRI scans used *Analysis of Functional NeuroImage* (AFNI, available at: <https://afni.nimh.nih.gov/>) tools and included: discarding the first five volumes to allow magnetization stabilization, despiking, motion correction, grand-mean scaling, linear detrending, and temporal filtering (maintaining frequencies above 0.01 Hz).

As mentioned above, exclusion criteria were applied considering head motion parameters, an exclusion cut-off for mean interframe head motion at  $\geq 0.3$  mm translation or  $0.3^\circ$  rotation; and for maximum interframe head motion at  $\geq 1$  mm translation or  $1^\circ$  rotation.

Moreover, the Independent Component Analysis based strategy for Automatic Removal of Motion Artifacts (ICA-AROMA) was used to correct head motion and other non-neural sources of signal variation (172). This procedure decomposes the data and identifies components related to head motion, applying four robust and standardized features. Additionally, correlations between framewise head displacement and overall signal variation after regressing the ICA-AROMA components (established as the voxel-wise root mean square intensity difference between subsequent time points) were obtained as quality control indicators (173). Significant correlations would imply that the signal change could be explained by head motion.



### **3. Statistical analyses**

This section covers the general method used for the different analyzed outcomes.

#### **3.1. Demographic, clinical and neuropsychological measures**

In all the studies, t-test, analysis of variance (ANOVA), and analysis of covariance (ANCOVA) followed by post-hoc tests corrected by Bonferroni or Games–Howell Kruskal–Wallis H and Mann–Whitney U were used as appropriate for quantitative variables. Pearson's chi-squared test was used for categorical variables.

#### **3.2. Structural MRI measures**

##### **Cortical thickness**

Intergroup CTh comparisons using vertex-by-vertex general linear models with *FreeSurfer version 6.0*. were performed. These models included cortical thickness as a dependent variable and group as an independent variable. Covariates were used when required. A pre-cached cluster-wise Monte Carlo simulation with 10,000 iterations was used for correction for multiple comparisons. The reported cortical regions reached a two-tailed corrected significance level of  $P\text{-value} \leq 0.05$ . Analyses using the mean CTh measure followed the procedures explained in the next point.

## **Volumetry**

Group differences and interactions in MRI volumetry measures were analyzed using ANOVA and ANCOVA approaches, followed by post-hoc tests corrected by Bonferroni.

## **Correlation and regression analyses**

Correlations between MRI measures and neuropsychological performance were conducted in *study 1*, using Pearson or Spearman correlation coefficient, as appropriate. Furthermore, multiple linear regression analyses were tested in the PD-pRBD group using R 4.0.2 (2020; R Core Team) on RStudio 1.1.1093 (2020; Boston, MA: RStudio PBC). The models included as response variables neuropsychological tasks in which the PD-pRBD group had lower scores than one or both of the other groups. As predictors, the models included global (model type 1) or partial (model type 2) volumetry measures with significant reductions in the PD-pRBD group. A stepwise model selection by Akaike information criterion (AIC) was applied to determine the best-fitted models (174). The models which reached the statistical significance threshold of  $P$ -value  $\leq 0.05$  were reported.

### 3.3. Characterization of brain functional connectivity

#### Threshold-free network-based statistics

The between-group comparisons of interregional brain functional connectivity were performed using threshold-free network-based statistics (TFNBS), which allows statistical inference on brain graphs (175). This technique combines network-based statistics (176) and threshold-free cluster enhancement (177). The first method is commonly used for statistical analysis of brain connectivity graphs; the second one is frequently applied in voxel-wise statistical inference.

The main characteristic of TFNBS is the generation of edge-wise significance values. These values can be used for the selection of relevant connectivity features. In this study, the *Human Brainnetome Atlas* (available at: <https://atlas.brainnetome.org/>) was used to characterize global brain functional connectivity, using 246 regions (178).

#### Graph-theory connectivity implementation

Complementary to the characterization of brain functional connectivity using TFNBS, the global and local properties of the network were analyzed (179,180). In the study of brain connectivity, these measures correspond to the whole brain and the nodal level. The parameters extraction was performed using the *Brain Connectivity Toolbox* (BCT, available at: <https://sites.google.com/site/bctnet/>). The analyzed measures were: clustering coefficient, global degree, node degree, “small-world-ness,” path length, local efficiency, and betweenness centrality (See Figure 9, Rubinov et al., 2010 (180) and Sporns et al., 2011 (181) for detailed definitions and calculations). Nine different density thresholds were used (maintaining the 5% to 25% strongest

edges, at intervals of 2.5%), with a reporting criterion of statistical significance in more than 75% of the density thresholds.

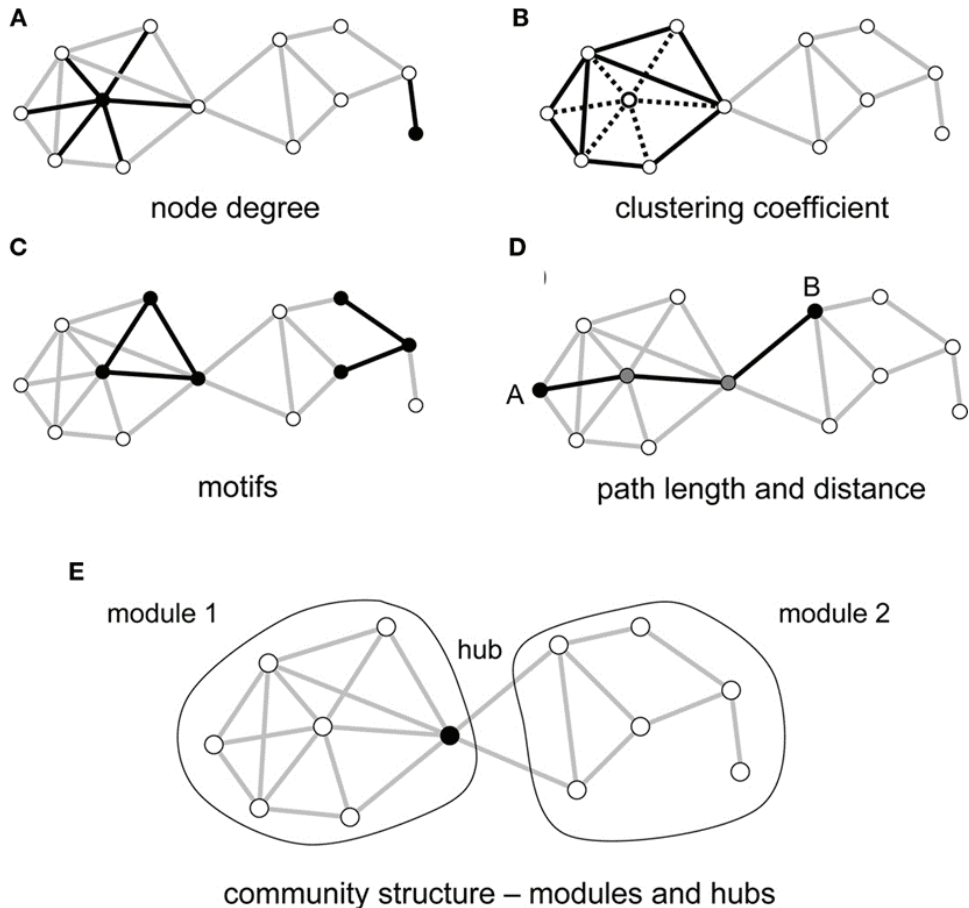


**Figure 9.** Key graph measures and their definitions. The measures are illustrated in a rendering of a simple undirected graph with 12 nodes and 23 edges. (A) Node degree corresponds to the number of edges attached to a given node, shown here for a highly connected node (left) and a peripheral node (right). (B) The clustering coefficient is shown here for a central node and its six neighbors. These neighbors maintain 8 out of 15 possible edges, for a clustering coefficient of 0.53. (C) Each network can be decomposed into subgraphs of motifs. The plot shows two examples of two different classes of three-node motifs. (D) The distance between two nodes is the length of the shortest path. Nodes A and B connect in three steps, through two intermediate nodes (shown in gray). The average of the finite distances for all node pairs is the graph’s path length. (E) The network forms two modules interconnected by a single hub node. Adapted from “Key graph measures and their definitions” by Sporns (181) licensed under CC BY-ND 4.0.

## **Correlation analyses using functional connectivity measures**

Correlations of functional connectivity measures with neuropsychological performance were conducted using Pearson or Spearman correlation coefficient, as appropriate.



# Chapter 4

---

## Results





## Study 1

---

**Oltra J**, Uribe C, Segura B, Campabadal A, Inguanzo A, Monté-Rubio GC, Pardo J, Martí MJ, Compta Y, Valldeoriola F, Junque C, Iranzo, A. Brain atrophy pattern in *de novo* Parkinson's disease with probable RBD associated with cognitive impairment. *npj Parkinson's Disease*. 2022; 8: 2 doi:10.1038/s41531-022-00326-7.

## ARTICLE OPEN



# Brain atrophy pattern in de novo Parkinson's disease with probable RBD associated with cognitive impairment

Javier Oltra<sup>1,2</sup>, Carme Uribe<sup>1,2,3</sup>, Barbara Segura<sup>1,2,4</sup>✉, Anna Campabadal<sup>1,2</sup>, Anna Inguanzo<sup>1,2</sup>, Gemma C. Monté-Rubio<sup>1,2</sup>, Jèssica Pardo<sup>1,2</sup>, Maria J. Marti<sup>2,4,5</sup>, Yaroslau Compta<sup>2,4,5</sup>, Francesc Valldeoriola<sup>1,2,4,5</sup>, Carme Junque<sup>1,2,4</sup> and Alex Iranzo<sup>2,4,6</sup>

Rapid eye movement sleep behavior disorder (RBD) is associated with high likelihood of prodromal Parkinson's disease (PD) and is common in de novo PD. It is associated with greater cognitive impairment and brain atrophy. However, the relation between structural brain characteristics and cognition remains poorly understood. We aimed to investigate subcortical and cortical atrophy in de novo PD with probable RBD (PD-pRBD) and to relate it with cognitive impairment. We analyzed volumetry, cortical thickness, and cognitive measures from 79 PD-pRBD patients, 126 PD without probable RBD patients (PD-non pRBD), and 69 controls from the Parkinson's Progression Markers Initiative (PPMI). Regression models of cognition were tested using magnetic resonance imaging measures as predictors. We found lower left thalamus volume in PD-pRBD compared with PD-non pRBD. Compared with controls, PD-pRBD group showed atrophy in the bilateral putamen, left hippocampus, left amygdala, and thinning in the right superior temporal gyrus. Specific deep gray matter nuclei volumes were associated with impairment in global cognition, phonemic fluency, processing speed, and visuospatial function in PD-pRBD. In conclusion, cognitive impairment and gray matter atrophy are already present in de novo PD-pRBD. Thalamus, hippocampus, and putamen volumes were mainly associated with these cognitive deficits.

*npj Parkinson's Disease* (2022)8:60; <https://doi.org/10.1038/s41531-022-00326-7>

## INTRODUCTION

Rapid eye movement (REM) sleep behavior disorder (RBD) is a parasomnia characterized by vivid dreams, increased electromyographic activity during REM sleep associated with complex movements and loss of atonia<sup>1</sup>. RBD is a common symptom in Parkinson's disease (PD) patients, with a prevalence of about 40%<sup>2</sup>. Also, isolated RBD (iRBD) is a prodromal symptom of PD and other synucleinopathies, with a rate of conversion to a clinically defined synucleinopathy up to 90% after 15 years of follow-up<sup>3</sup>. Results from postmortem studies in PD revealed pathological changes, with more diffuse and severe deposition of synuclein in patients with RBD symptoms<sup>4</sup>.

The diagnosis of RBD is performed by clinical history and videopolysomnography (vPSG) showing REM sleep with loss of atonia. When vPSG is not available the term probable RBD (pRBD) refers to individuals with clinical symptoms suggestive of RBD or fulfilling validated RBD validated questionnaires. A recent meta-analysis reported that in PD, the occurrence of RBD is associated with male sex, advance age, longer disease duration, increased Hoehn and Yahr (H&Y) stage, and with a higher Movement Disorder Society Unified Parkinson's Disease Rating Scale (MDS-UPDRS) Part III score. The frequency of PD-pRBD increases with disease duration, H&Y stage, and MDS-UPDRS Part III score as well<sup>5</sup>. Furthermore, PD-pRBD has been associated with worse cognitive performance<sup>6,7</sup> and more rapid cognitive decline<sup>7</sup>. Also, PD-RBD has been associated with a higher prevalence of mild cognitive impairment (MCI)<sup>8</sup>. Altogether, these results suggest that PD-RBD patients have different clinical and neuropsychological characteristic features and prognosis, being proposed as a specific PD subtype<sup>9</sup>.

Magnetic resonance imaging (MRI) studies may allow investigating the differences between PD with and without RBD. To the best of our knowledge, there are only three studies with de novo PD-pRBD patients in which quantified MRI was examined. They were performed with the Parkinson's Progression Markers Initiative (PPMI) database, in which participants were classified according the RBD Screening Questionnaire (RBDSQ). One study performed with deformed-based morphometry (DBM), reported reduced volumes of pontomesencephalic tegmentum, medullary reticular formation, hypothalamus, thalamus, putamen, amygdala, and anterior cingulate in PD-pRBD compared with PD without probable RBD (PD-non pRBD) patients<sup>10</sup>. A second study showed that PD-pRBD had volume reduction in the putamen compared with PD-non pRBD patients by means of voxel-based morphometry (VBM)<sup>11</sup>. Lastly, the most recent study performed longitudinal analyses with a reduced sample and without control group. The results reported that in the baseline (de novo PD stage) the PD-pRBD group had thinning in the bilateral inferior temporal cortex compared with the PD-non pRBD group through cortical thickness analysis<sup>12</sup>.

Previous studies in advanced PD with small samples, comparing PD-RBD patients with PD-non RBD patients, have found volume decreases in the thalamus using volumetry and VBM<sup>13</sup>; decreased gray matter volume of the left posterior cingulate and hippocampus thought MRI volumetry<sup>14</sup>; and cortical thinning in the right perisylvian and inferior temporal cortices; as well as volume shape contraction in the putamen using cortical thickness and DBM approaches<sup>15</sup>.

In this context, the association between cognitive impairment and brain atrophy in de novo PD with RBD symptomatology has

<sup>1</sup>Medical Psychology Unit, Department of Medicine, Institute of Neurosciences, University of Barcelona, Barcelona, Catalonia, Spain. <sup>2</sup>Institute of Biomedical Research August Pi i Sunyer (IDIBAPS), Barcelona, Catalonia, Spain. <sup>3</sup>Research Imaging Centre, Campbell Family Mental Health Research Institute, Centre for Addiction and Mental Health (CAMH), University of Toronto, Toronto, Ontario, Canada. <sup>4</sup>Centro de Investigación Biomédica en Red Enfermedades Neurodegenerativas (CIBERNED: CB06/05/0018-ISCIII), Barcelona, Catalonia, Spain. <sup>5</sup>Parkinson's Disease & Movement Disorders Unit, Neurology Service, Hospital Clínic de Barcelona, Institute of Neurosciences, University of Barcelona, Barcelona, Catalonia, Spain. <sup>6</sup>Multidisciplinary Sleep Disorders Unit, Neurology Service, Hospital Clínic de Barcelona, Barcelona, Catalonia, Spain. ✉email: bsegura@ub.edu

been poorly investigated. Furthermore, cortical thickness between-groups differences have never been explored in a large sample of de novo PD patients, including PD groups with and without pRBD and a healthy control group. The current work aims to examine subcortical and cortical measures of atrophy, concerning pRBD status, in a large sample of newly diagnosed drug naïve PD patients through MRI volumetry from global to deep gray matter (GM) nuclei segmentation, and cortical thickness analysis. Then, we aimed to find associations between structural abnormalities and cognitive impairments in PD-pRBD patients.

## RESULTS

### Demographic and clinical characteristics

The final sample comprised of 79 PD-pRBD and 126 PD-non pRBD patients.

There were no differences between groups in sex, age, years of education, age of onset, disease duration, MDS-UPDRS Part III scores, and H&Y stage. PD-pRBD had higher RBDSQ, 15-item Geriatric Depression Scale (GDS-15) frequency of depression, Epworth Sleepiness Scale (ESS) total and frequency of sleepiness, Scales for Outcomes in Parkinson Disease (SCOPA-AUT) item 6 total and frequency of constipation, and MDS-UPDRS scores compared with PD-non pRBD; and higher RBDSQ, GDS-15 total, ESS total and frequency of sleepiness, SCOPA-AUT item 6 total and frequency of constipation, and lower University of Pennsylvania Smell Identification Test (UPSIT-40) scores compared with controls. Higher RBDSQ, higher SCOPA-AUT item 6 total and frequency of constipation, and lower UPSIT-40 scores were found in PD-non pRBD compared with controls (Table 1). Around 31% of the available MRI scans of PD patients were discarded after quality control (Supplementary Fig. 1).

### Neuropsychological performance

PD-pRBD scored lower in semantic fluency and Benton Judgment of Line Orientation (JLO) than PD-non pRBD; when comparing them with controls, had lower Montreal Cognitive Assessment (MoCA), semantic fluency, phonetic fluency, Symbol Digit Modalities Test (SDMT), Letter-Number Sequencing (LNS), JLO, Hopkins Verbal Learning Test-Revised (HVLN-R) immediate and delayed recall scores. When comparing the PD-non pRBD group with the control group, MoCA and SDMT scores were lower in the former (Fig. 1, Supplementary Table 1). As supplementary, we performed analyses with the MDS-UPDRS score as a covariate, the PD-pRBD group had lower scores than the PD-non pRBD group in semantic fluency, LNS, and JLO (see Supplementary Table 2).

### Global and partial volume ratios

PD-pRBD had less left thalamus volume than PD-non pRBD. Atrophy of the left and right putamen, left hippocampus, and left amygdala was observed in PD-pRBD patients with respect to the control group. Finally, PD-non pRBD showed a decreased partial volume ratio in the right amygdala compared with the control group (Table 2). Additional analyses with the MDS-UPDRS score as a covariate were also performed. The PD-pRBD group showed decreased left thalamus and right pallidum volumes with respect to the PD-non pRBD group (see Supplementary Table 3).

PD-pRBD compared with controls showed decreases in total cortical and subcortical GM volume ratios, as well as an increment in the ventricular system volume ratio. PD-non pRBD showed a decrease in total cortical GM volume ratio with respect to controls (Table 2).

Descriptive statistics of global and partial volumes in mm<sup>3</sup> are shown in Supplementary Table 4.

**Table 1.** Demographic and clinical characteristics of PD-non pRBD, PD-pRBD, and HC.

	PD-non pRBD (n = 126)	PD-pRBD (n = 79)	HC (n = 69)	Test stats	P-value
Sex, male, n (%)	73 (57.9)	54 (68.4)	40 (58.0)	2.558 <sup>1</sup>	0.278
Age, y, mean (SD)	62.2 (7.5)	64.3 (7.1)	62.6 (6.8)	2.126 <sup>2</sup>	0.121
Education, y, mean (SD)	15.6 (2.9)	15.8 (3.0)	16.7 (2.6)	3.008 <sup>2</sup>	0.051
Age of onset, y, mean (SD)	61.3 (7.4)	63.3 (7.1)	NA	1.908 <sup>3</sup>	0.058
Disease duration, m, mean (SD)	10.5 (7.2)	11.0 (7.1)	NA	0.560 <sup>3</sup>	0.576
RBDSQ, mean (SD)	2.6 (1.1)	6.8 (1.8)	1.7 (1.3)	300.998 <sup>4</sup>	<0.001 <sup>5,6,7</sup>
GDS-15, mean (SD)	2.0 (2.1)	2.7 (2.5)	1.5 (3.0)	4.335 <sup>2</sup>	0.014 <sup>7</sup>
Depressed, n (%)	13 (10.3)	16 (20.3)	7 (10.1)	4.924 <sup>1</sup>	0.085 <sup>5</sup>
ESS, mean (SD)	5.3 (3.1)	6.5 (3.6)	5.0 (3.2)	4.692 <sup>2</sup>	0.010 <sup>5, 7</sup>
Sleepy, n (%)	16 (12.8)	19 (24.1)	6 (8.8)	7.553 <sup>1</sup>	0.023 <sup>5,6,7</sup>
SCOPA-AUT item 6, mean (SD)	0.5 (0.6)	0.8 (0.7)	0.2 (0.4)	19.148 <sup>4</sup>	<0.001 <sup>5,6,7</sup>
Constipated, n (%)	60 (47.6)	51 (64.6)	10 (14.7)	37.832 <sup>1</sup>	<0.001 <sup>5,6,7</sup>
MDS-UPDRS, mean (SD)	29.4 (10.8)	35.7 (13.6)	NA	3.676 <sup>3</sup>	<0.001
MDS-UPDRS Part III, mean (SD)	19.8 (8.0)	21.6 (9.1)	NA	1.478 <sup>4</sup>	0.141
H&Y stage, n, 1/2/3	55/69/2	33/46/0	NA	1.398 <sup>1</sup>	0.497
UPSIT, mean (SD)	22.2 (8.0)	19.6 (8.3)	34.1 (3.8)	84.620 <sup>4</sup>	<0.001 <sup>6,7</sup>

RBDSQ REM Sleep Behavior Disorder Screening Questionnaire, GDS-15 15-item Geriatric Depression Scale, ESS Epworth Sleepiness Scale, MDS-UPDRS Movement Disorder Society Unified Parkinson's Disease Rating Scale, H&Y Hoehn & Yahr scale, UPSIT University of Pennsylvania Smell Identification Test, PD-non pRBD PD without probable RBD, PD-pRBD PD with probable RBD, HC healthy controls.

<sup>1</sup>The  $\chi^2$  test was used.

<sup>2</sup>Analysis of variance (ANOVA) followed by post hoc test corrected by Bonferroni was used.

<sup>3</sup>t-test was used.

<sup>4</sup>Analysis of variance (ANOVA) followed by post hoc test corrected by Games-Howell was used.

<sup>5</sup>Significant differences ( $p < 0.05$ ) were found between PD-non pRBD and PD-pRBD.

<sup>6</sup>Significant differences ( $p < 0.05$ ) were found between PD-non pRBD and HC.

<sup>7</sup>Significant differences ( $p < 0.05$ ) were found between PD-pRBD and HC.

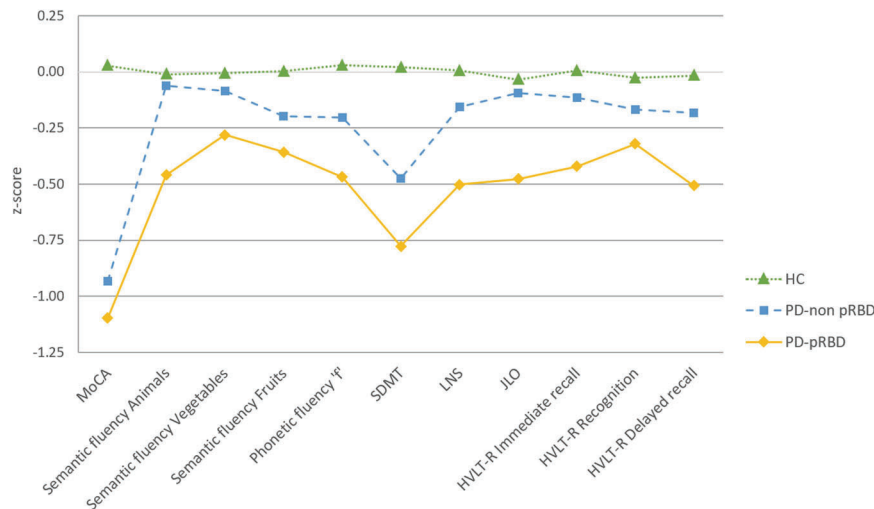


**Fig. 1 Neuropsychological performance.** Tasks are indicated in the x axis. Group means in each task are presented as z-scores, as indicate in y axis. Data are presented as z-scores adjusted by age, sex and education. Lower z-scores indicate worse performance. Descriptive statistics of raw scores, as mean (SD), are available in Supplementary Table 1. Healthy controls in green, PD-non pRBD in blue, PD-pRBD in yellow. Healthy controls represented by filled triangles and a dotted line, PD-non pRBD by filled squares and a dashed line and PD-pRBD by filled rhombuses and a continuous line. MoCA Montreal Cognitive Assessment, SDMT Symbol Digit Modalities Test, LNS Letter-Number Sequencing, JLO Benton Judgment of Line Orientation, HVLt-R Hopkins Verbal Learning Test-Revised, HC healthy controls, PD-non pRBD PD without probable RBD, PD-pRBD PD with probable RBD.

**Table 2.** Global and partial volume ratios of PD-non pRBD, PD-pRBD, and HC.

	PD-non pRBD	PD-pRBD	HC	Test stats	P-value
<b>Global atrophy volumes</b>					
Cortical GM	28.6704 (2.16624)	28.7482 (2.51696)	29.6923 (2.09360)	5.020	0.007 <sup>1,2</sup>
Subcortical GM	3.5597 (0.25621)	3.4926 (0.29242)	3.6037 (0.28252)	3.140	0.045 <sup>1</sup>
Ventricular system	1.9743 (0.99272)	2.2429 (1.04248)	1.7940 (0.82571)	4.082	0.018 <sup>1</sup>
<b>Deep GM nuclei</b>					
Left thalamus	0.4559 (0.04486)	0.4407 (0.04097)	0.4556 (0.04221)	3.464	0.033 <sup>3</sup>
Right thalamus	0.4460 (0.04276)	0.4348 (0.04267)	0.4451 (0.04165)	1.841	0.161
Left caudate	0.2124 (0.02607)	0.2108 (0.02504)	0.2155 (0.02593)	0.636	0.530
Right caudate	0.2190 (0.02797)	0.2167 (0.02808)	0.2201 (0.02643)	0.311	0.733
Left putamen	0.2902 (0.03366)	0.2811 (0.03785)	0.2955 (0.03683)	3.124	0.046 <sup>1</sup>
Right putamen	0.2883 (0.03211)	0.2816 (0.03791)	0.2955 (0.03659)	2.934	0.055 <sup>1</sup>
Left pallidum	0.1280 (0.01427)	0.1259 (0.01687)	0.1267 (0.01498)	0.509	0.602
Right pallidum	0.1256 (0.01355)	0.1212 (0.01663)	0.1236 (0.01422)	2.159	0.117
Left hippocampus	0.2548 (0.02980)	0.2494 (0.02969)	0.2623 (0.02942)	3.507	0.031 <sup>1</sup>
Right hippocampus	0.2619 (0.03127)	0.2606 (0.03106)	0.2699 (0.02957)	2.028	0.134
Left amygdala	0.1000 (0.01482)	0.0984 (0.01815)	0.1052 (0.01435)	3.710	0.026 <sup>1</sup>
Right amygdala	0.1089 (0.01427)	0.1088 (0.01671)	0.1146 (0.01425)	3.813	0.023 <sup>2</sup>
Left accumbens	0.0294 (0.00680)	0.0300 (0.00732)	0.0299 (0.00597)	0.233	0.792
Right accumbens	0.0317 (0.00662)	0.0317 (0.00700)	0.0322 (0.00583)	0.156	0.856
Brainstem	1.3904 (0.12004)	1.3618 (0.12659)	1.3870 (0.12034)	1.435	0.240

GM gray matter, PD-non pRBD PD without probable RBD, PD-pRBD PD with probable RBD, HC healthy controls.

Data are presented by groups as mean (SD). Analysis of variance (ANOVA) followed by post hoc test corrected by Bonferroni was used.

<sup>1</sup>Significant differences ( $p < 0.05$ ) were found between PD-pRBD and HC.

<sup>2</sup>Significant differences ( $p < 0.05$ ) were found between PD-non pRBD and HC.

<sup>3</sup>Significant differences ( $p < 0.05$ ) were found between PD-non pRBD and PD-pRBD.

**Regression models predicting cognition in PD-pRBD**

Exploratory results of correlations are shown in Supplementary Tables 5 and 6. We performed two regression analyses in the PD-pRBD group, one using global measures of atrophy and the other using the volumes of deep GM nuclei (Table 3). Complementary,

the regression analyses were also performed in the whole PD sample (Supplementary Tables 7 and 8).

When using global volume ratios to predict cognition in PD-pRBD, cortical GM explained a proportion of the phonetic fluency variance ( $R^2 = 0.121$ ; adjusted  $R^2 = 0.110$ ;  $F = 10.600$ ;  $p = 0.002$ );

**Table 3.** Multiple regression results of global and partial volume ratios as predictors of performance in neuropsychological tasks in the PD-pRBD group.

	Model 1 Global MRI measures		Model 2 Partial MRI measures	
	Variables	t-stat ( <i>P</i> -value)	Variables	t-stat ( <i>P</i> -value)
MoCA	Subcortical GM	3.277 (0.002)	Right putamen	2.124 (0.037)
			Left hippocampus	2.021 (0.047)
Semantic fluency Animals	No prediction model		No prediction model	
Semantic fluency Fruits	Non-significant model		Non-significant model	
Phonetic fluency 'f'	Cortical GM	3.256 (0.002)	Left putamen	2.476 (0.015)
SDMT	Subcortical GM	2.465 (0.016)	Left hippocampus	2.765 (0.007)
LNS	Non-significant model		No prediction model	
JLO	Non-significant model		Left thalamus	2.261 (0.011)
HVLT-R immediate recall	No prediction model		Non-significant model	
HVLT-R delayed recall	No prediction model		Non-significant model	

GM gray matter, MoCA Montreal Cognitive Assessment, SDMT Symbol Digit Modalities Test, LNS Letter-Number Sequencing, JLO Benton Judgment of Line Orientation, HVLT-R Hopkins Verbal Learning Test-Revised.

subcortical GM significantly explained a proportion of the MoCA variance ( $R^2 = 0.122$ ; adjusted  $R^2 = 0.111$ ;  $F = 10.740$ ;  $p = 0.002$ ), and the SDMT variance ( $R^2 = 0.0740$ ; adjusted  $R^2 = 0.062$ ;  $F = 6.075$ ;  $p = 0.016$ ).

When using partial volume ratios to predict cognition in PD-pRBD, right putamen and left hippocampus explained a proportion of the MoCA variance ( $R^2 = 0.180$ ; adjusted  $R^2 = 0.158$ ;  $F = 8.317$ ;  $p < 0.001$ ); left putamen explained a proportion of the phonetic fluency variance ( $R^2 = 0.074$ ; adjusted  $R^2 = 0.062$ ;  $F = 6.133$ ;  $p = 0.015$ ); left hippocampus explained a proportion of the SDMT variance ( $R^2 = 0.091$ ; adjusted  $R^2 = 0.079$ ;  $F = 7.647$ ;  $p = 0.007$ ); and left thalamus explained a proportion of the JLO variance ( $R^2 = 0.082$ ; adjusted  $R^2 = 0.070$ ;  $F = 6.819$ ;  $p = 0.011$ ).

### Cortical thickness

PD-pRBD had cortical thinning in the right superior temporal gyrus compared with controls (MNI coordinates:  $x, y, z = 44, 17, -28$ ; cluster size =  $2461.25 \text{ mm}^2$ ;  $t\text{-stat} = 2.836$ ,  $p = 0.010$ ) (Supplementary Fig. 2). None significant correlation was found between the cortical thickness of the significant cluster and cognition in the group PD-pRBD (see Supplementary Table 6 for significant results in the whole PD group).

### DISCUSSION

In this study, we described the neuropsychological and brain structural characteristics in a large sample of PD-pRBD patients as well as the relation between cognitive impairment and measures of brain atrophy. PD-pRBD showed significant differences from controls and PD-non pRBD in neuropsychological tests and deep GM structures. Cognitive impairment of this subgroup of PD patients is related to diffuse global brain atrophy and reduced volumes of basal ganglia, thalamus, and hippocampus. Regarding clinical measures, remarkably, the PD-pRBD group had more presence of depression, sleepiness, constipation, and higher MDS-UPDRS total score than the PD-non pRBD group. Altogether, these findings suggest that the presence of RBD symptomatology is related to a more severe PD phenotype.

Patients with PD-pRBD had cognitive impairment in global cognition as well as in several domains involving memory, visuospatial and executive functions. The PD-pRBD subgroup showed worse performance in all neuropsychological tests with respect to controls of similar age and education. Compared with the control group, PD-pRBD showed statistically significant

differences in MoCA, semantic and phonemic fluency, SDMT, JLO, HVLT-R immediate and delayed recall. In contrast, PD-non pRBD patients differed from controls only in MoCA and SDMT, although they were similar to PD-pRBD in age, education, and clinical characteristics. The results between PD-pRBD and PD-non pRBD group remain when controlling for MDS-UPDRS score. The PD subgroups comparison showed statistical differences in semantic fluency and JLO. More severe cognitive impairment in de novo PD patients with RBD symptoms has been previously reported<sup>16,7</sup>. This severe cognitive impairment in PD-pRBD is in accordance with the significant differences compared with healthy controls that we obtained in the three measures of global atrophy showing reduced cortical and subcortical GM, and ventricular volumes enlargement. PD-non pRBD only differed from controls in reduced cortical GM.

Cortical thickness analyses did not show significant differences between PD patients with and without pRBD. Regarding the analyses of cortical thickness maps, we found thinning in the right superior temporal gyrus extended to middle and inferior temporal gyri in PD-pRBD compared with controls. Similarly, recent studies found significant thinning in the right inferior temporal gyrus in PD-RBD compared with PD-non RBD<sup>15</sup>, as well as in PD-pRBD in the bilateral inferior temporal gyrus compared with PD-non pRBD<sup>12</sup>, both using smaller samples and the second in absence of a healthy control group to perform comparisons.

In addition to the greater global atrophy measures, we also found that PD-pRBD had a reduction of several subcortical GM structures. Comparably to previous reports using different data analysis approaches<sup>10,11</sup> we found atrophy in the putamen and amygdala, but we also identified reductions in the hippocampus. The hippocampal atrophy is also coherent with the memory impairment identified in our study, even if we did not find significant correlations or regression models in this regard. iRBD is considered a prodromal symptom of alpha-synucleinopathies, thus in part comparable with PD-pRBD. In this context, it has been reported reductions in bilateral and right putamen<sup>16,17</sup> and hippocampus<sup>18</sup>.

The contrast between both PD samples showed that PD-pRBD had lower left thalamus volume compared with PD-non pRBD. Similar findings regarding thalamic reductions associated with RBD in PD were reported with other MRI methodological approaches<sup>10,13</sup>. In the same line, correlation analyses also reinforce the role of the thalamus in subjects with RBD symptomatology. It has been found a negative correlation between the severity of RBD symptoms and bilateral thalamic

volume<sup>11</sup>. PET studies also pointed to the relevance of thalamic structures linked to this symptomatology. Concretely, a recent PET study in iRBD found an increased cholinergic innervation in some nuclei of the brainstem and the ventromedial area of the thalamus<sup>19</sup>. This finding raises the possibility of an initial compensatory cholinergic activity in the prodromal phase of PD that would be behind the volume reduction too, even more, considering our sample is formed by newly diagnosed drug naïve PD cases. Thalamic volume decrease in our study might be explained in this way.

The differences in subcortical GM measures reflected a left-lateralized pattern in the PD-pRBD group. Previous neuroimaging research has reported structural and functional left asymmetries in PD and iRBD patients. For example, predominant left-hemispheric findings in cortical thinning in early PD<sup>20</sup>, in reductions of structural connectivity in PD-MCI<sup>21</sup>, and reductions of functional connectivity in iRBD<sup>22</sup>. The origin of this pattern of degeneration is unknown. However, the absence or minority of significant results in the right hemisphere does not necessarily imply that the right hemisphere is unaffected. Thus, the specific threshold established for statistical significance could contribute to explain this fact.

We observed significant correlations between neuropsychological and brain atrophy measures. To minimize the effects of multiple comparisons we performed two regression analyses, one focused on global measures of brain atrophy and the other only including the subcortical GM volumes. In the whole de novo PD group, we found that subcortical gray matter and ventricular system volumes, as well as of the left amygdala, bilateral putamen, left thalamus, and left hippocampus volumes were related with cognition. Regarding the PD-pRBD group, the worst performance in MoCA was predicted by reductions of global subcortical gray matter volume and specifically by reductions of the right putamen and left hippocampus. The impairment of speed of mental processing assessed by SDMT was related with subcortical gray matter and left hippocampus reductions. Visuospatial function impairment measured by JLO was related with the left thalamus reduction and phonetic fluency by cortical gray matter and left putamen volume. These data reinforce the value of aforesaid tests to identify early brain degeneration in de novo PD patients, in special those with more brain atrophy and cognitive impairment such as patients with RBD symptomatology. Supporting the relevance of these tests, a longitudinal study in de novo PD patients found that baseline RBD was associated with a greater annual rate of decline in MoCA and SDMT scores<sup>7</sup>. To our knowledge, no previous study relate MRI and neuropsychological findings in de novo PD with probable RBD. We report that cognitive impairment was mainly related with subcortical gray matter reductions.

The main strength of our study was the large sample of de novo PD patients that precludes pharmacological effects on cognitive performance as well as the effects of progressive brain atrophy involving widespread cortical atrophy. Moreover, we studied subcortical and cortical brain atrophy and cognition in a large sample of PD-pRBD, as well as studying cortical thickness differences in a large sample of de novo PD including PD-pRBD as a group. However, our study has two main limitations. First, and important, is that the diagnosis of RBD was carried out by means of a validated questionnaire but was not confirmed through vPSG. Second, PPMI is a multicenter cohort study thus there are evident differences in MRI acquisition, some of them of 1.5 Tesla. Last, even though the final sample was large, around 31% of the available MRI scans of PD patients were discarded after initial quality control, mainly due to motion artifacts and associated problems of registration, skull stripping, segmentation, and cortical surface reconstruction after preprocessing. This fact could affect the representativeness of the results.

From the whole data analyses, we can conclude that de novo PD patients with probable RBD show worse cognitive performance

than those PD patients without probable RBD. The greater neuropsychological impairment is coherent with signs of global brain atrophy. Moreover, this subgroup of early PD with probable RBD shows decreased volumes in specific deep gray matter nuclei involving the amygdala, hippocampus, thalamus, and basal ganglia. The main difference between both PD subgroups is seen in the thalamus. Lastly, cognitive impairment is essentially related with subcortical gray matter reductions.

## METHODS

### Participants

Data were obtained from the PPMI database (<http://www.ppmi-info.org>)<sup>23</sup>. T1-weighted images, clinical and neuropsychological data obtained from 205 newly diagnosed drug naïve PD patients, and 69 healthy controls were included. We divided PD patients into two groups, 79 PD-pRBD and 126 PD-non pRBD patients, based on available data from RBDSQ, with a 5-points cutoff<sup>24</sup>. All imaging and clinical data were acquired before any L-DOPA intake. All participating PPMI sites received approval from an ethical standards committee prior to study initiation, for a list of participant sites see <https://www.ppmi-info.org/about-ppmi/ppmi-clinical-sites>. Central IRB approval provided by CWG IRB (tracking number: 20200597; current clinical trial identifier of PPMI study in [clinicaltrials.gov](https://clinicaltrials.gov): NCT04477785). All participants provided written informed consent. Inclusion criteria were: (1) recent diagnosis of PD with asymmetric resting tremor or asymmetric bradykinesia, or two of: bradykinesia, resting tremor, and rigidity; (2) absence of treatment for PD; (3) neuroimaging evidence of significant dopamine transporter deficit consistent with the clinical diagnosis of PD and ruling out PD lookalike conditions such as drug-induced and vascular parkinsonism or essential tremor; (4) available T1-weighted images (for both PD patients and controls); and (5) age between 50 and 85 years old (for both PD patients and controls). Exclusion criteria for all participants were: (1) diagnosis of dementia; (2) significant psychiatric, neurologic, or systemic comorbidity; (3) first-degree family member with PD; and (4) presence of MRI motion artifacts, field distortions, intensity inhomogeneities, or detectable structural brain lesions. We include a detailed flow diagram of sample selection, in which we reflect the process after consulting the PPMI clinical databases and preprocessing MRI images, beyond the inclusion criteria applied by the research centers (Supplementary Fig. 1).

### Clinical and neuropsychological assessments

PD symptoms were assessed with the MDS-UPDRS, motor symptoms with the MDS-UPDRS Part III, and disease severity with H&Y. Global cognition was assessed with the MoCA, depressive symptoms using the GDS-15 (with a 5-points cutoff for depression), olfactory function using the UPSIT-40, and presence of constipation with the item 6 of the Scales for SCOPA-AUT (with a 1-point cutoff for constipation). The presence of pRBD status was assessed using the RBDSQ<sup>24</sup>, and the occurrence of excessive daytime sleepiness using the ESS (with a 10-points cutoff for sleepiness)<sup>23</sup>.

All subjects underwent a neuropsychological battery including HVLT-R, JLO short form (15-item version), SDMT, LNS, phonemic (letter 'f'), and semantic (animals, fruits, and vegetables) verbal fluency<sup>23</sup>. All neuropsychological tasks were z-scored adjusted by age, sex, and education taking the control group as reference, as previously described in Segura et al.<sup>25</sup>.

### MRI acquisition and preprocessing

T1-weighted MRI scans were acquired using 1.5 or 3 Tesla scanners at different centers using MPRAGE sequences. Typical MRI parameters were repetition time 5–11 ms; echo time 2–6 ms; slice thickness 11.5 mm; inter-slice gap 0 mm; voxel size 1 × 1 × 1.2 mm; matrix 256 × minimum 160. There were no differences in the distribution of 1.5 and 3 Tesla MRI acquisitions between-groups ( $\chi^2 = 1.933$ ,  $p = 0.380$ ; Supplementary Table 9).

Global atrophy measures including total cortical GM, total subcortical GM and estimated total intracranial volume (eTIV); ventricular system volume; as well as deep GM structures<sup>26</sup>. Volume ratios using eTIV were calculated to perform global and partial volumetric analyses ((volume/eTIV) \* 100). Cortical thickness was estimated using FreeSurfer version 6.0 (<https://surfer.nmr.mgh.harvard.edu>) specific tools and the automated stream. Detailed information about the processing FreeSurfer stream is described in Uribe et al.<sup>27</sup>. After preprocessing, results for each subject were visually inspected to ensure accuracy of registration, skull stripping,

segmentation, and cortical surface reconstruction. Possible errors were fixed by manual intervention following standard procedures (applied corrections are specified in Supplementary Fig. 1).

### Statistical analyses

Group differences in demographic, neuropsychological, clinical, and volumetric variables were conducted using IBM SPSS Statistics 25.0.0 (2017; Armonk, NY: IBM Corp) using analysis of variance (ANOVA) followed by post hoc test corrected by Bonferroni or Games-Howell. Pearson's  $\chi^2$  tests were used for categorical measures. Correlation analyses between structural and neuropsychological variables were also conducted. Statistical significance threshold was set at  $p < 0.05$ .

Multiple linear regression analyses were performed using RStudio 1.1.1093 (2020; Boston, MA: RStudio PBC). As a response variable, each model included a neuropsychological variable showing significant differences in the intergroup comparisons between PD-pRBD and one of the other two groups, PD-non pRBD or controls. We tested, in the PD-pRBD group, models including global (model 1) or partial volume ratios (model 2) with a significant reduction in PD-pRBD group as predictors separately. Additionally, we tested these models in the de novo PD group, as a whole. A stepwise model selection by Akaike information criterion (AIC) was applied to the multiple linear regression models to pick the best-fitted model<sup>28</sup>. Only models with statistical significance threshold set at  $p < 0.05$  were reported.

Intergroup cortical thickness comparisons were performed using a vertex-by-vertex general linear model with FreeSurfer version 6.0. The model included cortical thickness as a dependent factor and group as an independent factor. All results were corrected for multiple comparisons using a pre-cached cluster-wise Monte Carlo simulation with 10,000 iterations. Reported cortical regions reached a two-tailed corrected significance level of  $p < 0.05$ .

### Reporting summary

Further information on research design is available in the Nature Research Reporting Summary linked to this article.

### DATA AVAILABILITY

Data used in the preparation of this article were obtained from the Parkinson's Progression Markers Initiative (PPMI) database (<https://www.ppmi-info.org/access-data-specimens/download-data>). For up-to-date information on the study, visit <http://www.ppmi-info.org>.

Received: 18 October 2021; Accepted: 27 April 2022;

Published online: 24 May 2022

### REFERENCES

- Iranzo, A. The REM sleep circuit and how its impairment leads to REM sleep behavior disorder. *Cell Tissue Res.* **373**, 245–266 (2018).
- Zhang, X., Sun, X., Wang, J., Tang, L. & Xie, A. Prevalence of rapid eye movement sleep behavior disorder (RBD) in Parkinson's disease: a meta and meta-regression analysis. *J. Neurol. Sci.* **38**, 163–170 (2017).
- Galbiati, A., Verga, L., Giora, E., Zucconi, M. & Ferini-Strambi, L. The risk of neurodegeneration in REM sleep behavior disorder: a systematic review and meta-analysis of longitudinal studies. *Sleep Med. Rev.* **43**, 37–46 (2019).
- Postuma, R. B. et al. REM sleep behavior disorder and neuropathology in Parkinson's disease. *Mov. Disord.* **30**, 1413–1417 (2015).
- Zhu, R., Xie, C., Hu, P. & Wang, K., Clinical variations in Parkinson's disease patients with or without REM sleep behaviour disorder: a meta-analysis. *Sci. Rep.* <https://doi.org/10.1038/srep40779> (2017).
- Trout, J. et al. Cognitive impairments and self-reported sleep in early-stage Parkinson's disease with versus without probable REM sleep behavior disorder. *Brain Sci.* <https://doi.org/10.3390/brainsci10010009> (2019).
- Chahine, L. M. et al. Longitudinal changes in cognition in early Parkinson's disease patients with REM sleep behavior disorder. *Park. Relat. Disord.* **27**, 102–106 (2016).
- Jozwiak, N. et al. REM Sleep behavior disorder and cognitive impairment in Parkinson's disease. *Sleep* <https://doi.org/10.1093/sleep/zsx101> (2017).
- Fereshtehnejad, S. M. et al. New clinical subtypes of Parkinson disease and their longitudinal disease progression: a prospective cohort comparison with other phenotypes. *JAMA Neurol.* **72**, 863–873 (2015).

- Boucetta, S. et al. Structural brain alterations associated with rapid eye movement sleep behavior disorder in Parkinson's disease. *Sci. Rep.* <https://doi.org/10.1038/srep26782> (2016).
- Kamps, S. et al. Smaller subcortical volume in Parkinson patients with rapid eye movement sleep behavior disorder. *Brain Imaging Behav.* **13**, 1352–1360 (2019).
- Yoon, E. J. & Monchi, O. Probable REM sleep behavior disorder is associated with longitudinal cortical thinning in Parkinson's disease. *npj Parkinson's Dis.* <https://doi.org/10.1038/s41531-021-00164-z> (2021).
- Salsone, M. et al. Reduced thalamic volume in Parkinson disease with REM sleep behavior disorder: volumetric study. *Parkinsonism Relat. Disord.* **20**, 1004–1008 (2014).
- Lim, J. S. et al. Neural substrates of rapid eye movement sleep behavior disorder in Parkinson's disease. *Parkinsonism Relat. Disord.* **23**, 31–36 (2016).
- Rahayel, S. et al. Brain atrophy in Parkinson's disease with polysomnography-confirmed REM sleep behavior disorder. *Sleep* <https://doi.org/10.1093/sleep/zsz062> (2019).
- Ellmore, T. M. et al. Reduced volume of the putamen in REM sleep behavior disorder patients. *Parkinsonism Relat. Disord.* **16**, 645–649 (2010).
- Rahayel, S. et al. Abnormal gray matter shape, thickness, and volume in the motor cortico-subcortical loop in idiopathic rapid eye movement sleep behavior disorder: association with clinical and motor features. *Cereb. Cortex* **28**, 658–671 (2018).
- Campabadal, A. et al. Cortical gray matter and hippocampal atrophy in idiopathic rapid eye movement sleep behavior disorder. *Front. Neurol.* <https://doi.org/10.3389/fneur.2019.00312> (2019).
- Bedard, M. A. et al. Brain cholinergic alterations in idiopathic REM sleep behaviour disorder: a PET imaging study with 18F-FE0BV. *Sleep. Med.* **58**, 35–41 (2019).
- Claassen, D. O. et al. Cortical asymmetry in Parkinson's disease: early susceptibility of the left hemisphere. *Brain Behav.* <https://doi.org/10.1002/brb3.573> (2016).
- Inguanzo, A. et al. Impaired structural connectivity in Parkinson's disease patients with mild cognitive impairment: a study based on probabilistic tractography. *Brain Connect.* **11**, 380–392 (2021).
- Campabadal, A. et al. Disruption of posterior brain functional connectivity and its relation to cognitive impairment in idiopathic REM sleep behavior disorder. *Neuroimage Clin.* <https://doi.org/10.1016/j.nicl.2019.102138> (2020).
- Marek, K. et al. The Parkinson progression marker initiative (PPMI). *Prog. Neurobiol.* <https://doi.org/10.1016/j.pneurobio.2011.09.005> (2011).
- Stiasny-Kolster, K. et al. The REM sleep behavior disorder screening questionnaire — a new diagnostic instrument. *Mov. Disord.* **22**, 2386–2393 (2007).
- Segura, B. et al. Cortical thinning associated with mild cognitive impairment in Parkinson's disease. *Mov. Disord.* **29**, 1495–1503 (2014).
- Fischl, B. et al. Whole brain segmentation: automated labeling of neuroanatomical structures in the human brain. *Neuron* **33**, 341–355 (2002).
- Uribe, C. et al. Neuroanatomical and functional correlates of cognitive and affective empathy in young healthy adults. *Front. Behav. Neurosci.* <https://doi.org/10.3389/fnbeh.2019.00085> (2019).
- Zhang, Z. Variable selection with stepwise and best subset approaches. *Ann. Transl. Med.* <https://doi.org/10.21037/atm.2016.03.35> (2016).

### ACKNOWLEDGEMENTS

This study was sponsored by the Spanish Ministry of Economy, Industry and Competitiveness (PSI2017- 86930-P), cofinanced by Agencia Estatal de Investigación (AEI) and the European Regional Development Fund (ERDF) and PID2020-114640GB-I00/MCIN/AEI/10.13039/501100011033, by Generalitat de Catalunya (2017SGR748), and supported by Maria de Maeztu Unit of Excellence (Institute of Neurosciences, University of Barcelona) MDM-2017-0729, Ministry of Science, Innovation and Universities. J.O. was supported by a 2018 fellowship from the Spanish Ministry of Science, Innovation and Universities; and co-financed by the European Social Fund (PRE2018-086675). CU was supported by the European Union's Horizon 2020 research and innovation program under the Marie Skłodowska-Curie fellowship (grant agreement 888692). A.C. and A.I. were supported by APIF predoctoral fellowship from the University of Barcelona (2017–2018). M.J.M. received grants from Michael J. Fox Foundation for Parkinson Disease (MJFF): MJF\_PPMI\_10\_001, PI044024. Y.C. has received funding in the past 5 years from FIS/FEDER, H2020 program. We acknowledge the CERCA Programme/Generalitat de Catalunya, the Institute of Neurosciences, and the Institute of Biomedical Research August Pi i Sunyer (IDIBAPS). Parkinson's Progression Marker Initiative (PPMI) - a public-private partnership - is funded by the Michael J. Fox Foundation for Parkinson's Research and funding partners, including Abbvie, Acurex Therapeutics, Allergan, Amathus Therapeutics, Aligning Science Across Parkinson's, Avid Radiopharmaceuticals, Bial Biotech, Biogen, BioLegend, Bristol Myers Squibb, Calico, Celgene, Dacapo Brainscience, Denali, 4D Pharma Plc, F. Dmond J. Safra Philanthropic Foundation, GE Healthcare, Genentech, GlaxoSmithKline, Golub Capital, Handl Therapeutics, Insitro, Janssen Neuroscience, Lilly, Lundbeck, Merck, Meso Scale Discovery, Neurocrine Biosciences, Pfizer, Piramal, Prevalet Therapeutics, Roche, Sanofi Genzyme, Servier, Takeda, Teva, Ucb, Verily, Voyager Therapeutics.

## AUTHOR CONTRIBUTIONS

Research project conception and acquisition of data are explained in Marek et al. as cited in the text. B.S. and C.J. contributed in the design of the study. J.O. and C.U. contributed to the analysis of the data and J.O., C.U., B.S., A.C., A.I., G.C.M.R., J.P., M.J.M., Y.C., F.V., C.J. and A.Iranzo contributed to the interpretation of the data. J.O., C.U., B.S., and C.J. contributed to the draft of the article. J.O., C.U., B.S., M.J.M., Y.C., F.V., C.J. and A.Iranzo revised the manuscript critically for important intellectual content and approved the final version of the manuscript.

## COMPETING INTERESTS

M.J.M. received honoraria for advice and lecture from Abbvie, Bial, and Merz Pharma. Y.C. has received funding in the past 5 years from Union Chimique Belge (Ucb pharma), Teva, Medtronic, Abbvie, Novartis, Merz, Piramal Imaging, and Esteve, Bial, and Zambon; and is currently an Associate Editor for Parkinsonism & Related Disorders. J.O., C.U., B.S., A.C., A.I., G.C.M.R., J.P., F.V., C.J., and A.Iranzo declare no competing interests.

## ADDITIONAL INFORMATION

**Supplementary information** The online version contains supplementary material available at <https://doi.org/10.1038/s41531-022-00326-7>.

**Correspondence** and requests for materials should be addressed to Barbara Segura.

**Reprints and permission information** is available at <http://www.nature.com/reprints>

**Publisher's note** Springer Nature remains neutral with regard to jurisdictional claims in published maps and institutional affiliations.



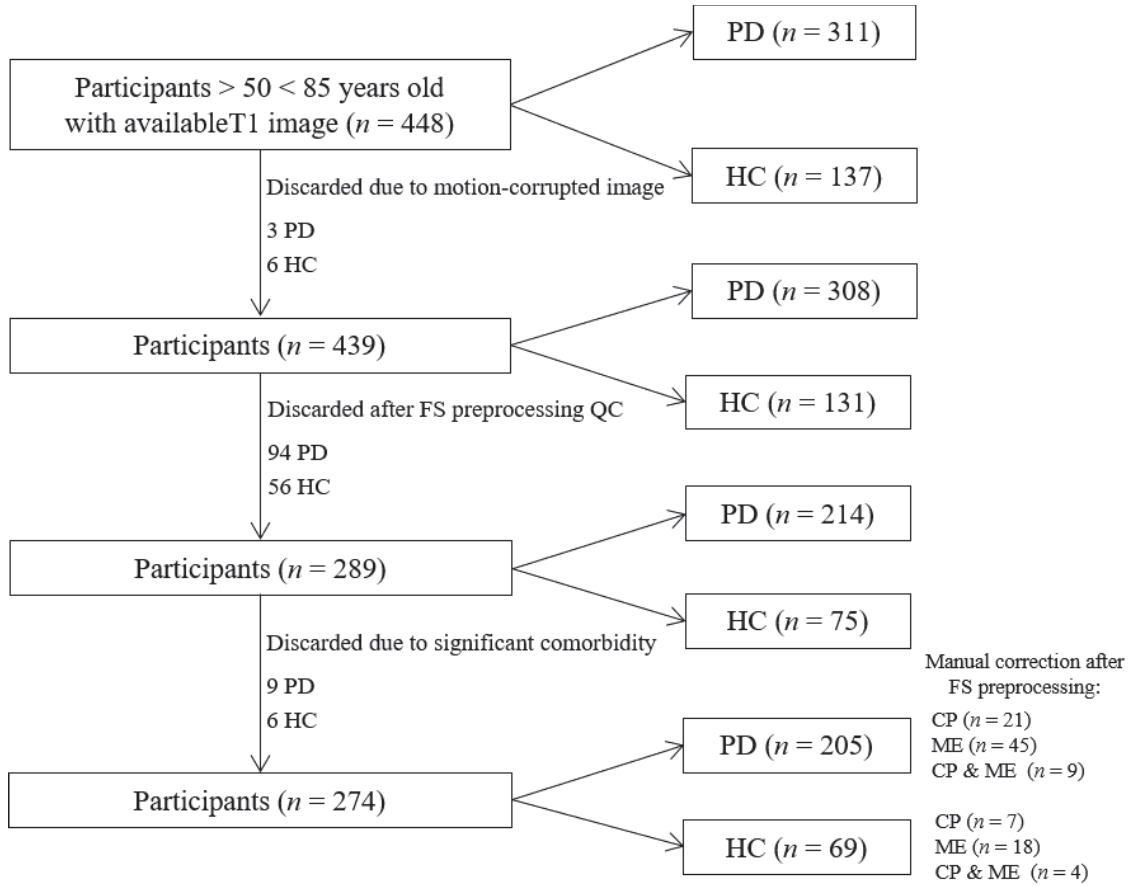
**Open Access** This article is licensed under a Creative Commons Attribution 4.0 International License, which permits use, sharing, adaptation, distribution and reproduction in any medium or format, as long as you give appropriate credit to the original author(s) and the source, provide a link to the Creative Commons license, and indicate if changes were made. The images or other third party material in this article are included in the article's Creative Commons license, unless indicated otherwise in a credit line to the material. If material is not included in the article's Creative Commons license and your intended use is not permitted by statutory regulation or exceeds the permitted use, you will need to obtain permission directly from the copyright holder. To view a copy of this license, visit <http://creativecommons.org/licenses/by/4.0/>.

© The Author(s) 2022

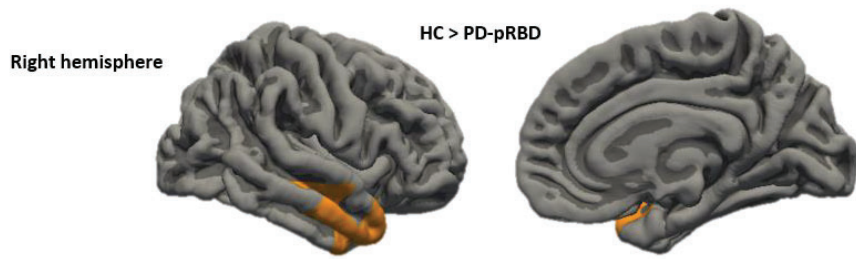


**SUPPLEMENTARY FIGURES**

**Supplementary Figure 1.** Flow diagram of sample selection. Abbreviations: CP = control points; FS = FreeSurfer; HC = healthy controls; ME = manual erase; PD = Parkinson’s disease; QC = quality control.



**Supplementary Figure 2.** Cortical thickness differences between HC and PD-pRBD. Color maps indicate significant differences (corrected  $p < 0.05$ ). Results were corrected by Monte Carlo simulation. Abbreviations: HC = healthy controls; PD-pRBD = PD with probable RBD.



Right superior temporal (MNI coordinates  $x, y, z = 44, 17, -28$ ; cluster size = 2461.25 mm<sup>2</sup>; t-stat = 2.836;  $p = 0.010$ )

**P-value** 0.05  0.001

## SUPPLEMENTARY TABLES

### Supplementary Table 1

Neuropsychological tasks scores of PD-non pRBD, PD-pRBD and HC

	PD-non pRBD	PD-pRBD	HC	Test stats	P-value
MoCA	27.0 (2.2)	26.8 (2.1)	28.1 (1.1)	9.105 <sup>1</sup>	<0.001 <sup>3,4</sup>
Semantic fluency					
Animals	21.8 (5.2)	19.5 (4.4)	22.7 (5.4)	5.623 <sup>2</sup>	0.004 <sup>4,5</sup>
Vegetables	14.7 (4.4)	13.6 (4.0)	15.4 (3.7)	1.498 <sup>2</sup>	0.226
Fruits	14.3 (4.1)	13.1 (4.0)	15.5 (4.2)	2.924 <sup>2</sup>	0.055 <sup>4</sup>
Phonetic fluency 'f'	12.9 (4.7)	12.1 (4.2)	14.3 (4.5)	4.439 <sup>2</sup>	0.013 <sup>4</sup>
SDMT	42.0 (8.3)	38.9 (9.7)	46.6 (8.9)	12.939 <sup>2</sup>	<0.001 <sup>3,4</sup>
LNS	10.8 (2.6)	9.9 (2.4)	11.3 (2.6)	5.422 <sup>2</sup>	0.005 <sup>4</sup>
JLO	13.1 (1.9)	12.5 (2.2)	13.3 (1.7)	4.019 <sup>2</sup>	0.019 <sup>4,5</sup>
HVLT-R Immediate recall	25.0 (5.0)	23.3 (4.7)	25.9 (4.4)	3.465 <sup>2</sup>	0.033 <sup>4</sup>
HVLT-R Recognition	9.6 (2.9)	9.2 (3.0)	9.9 (3.2)	1.708 <sup>2</sup>	0.183
HVLT-R Delayed recall	8.5 (2.4)	7.7 (2.6)	9.2 (2.4)	4.528 <sup>2</sup>	0.012 <sup>4</sup>

Abbreviations: MoCA = Montreal Cognitive Assessment; SDMT = Symbol Digit Modalities Test; LNS = Letter-Number Sequencing; JLO = Benton Judgment of Line Orientation; HVLT-R = Hopkins Verbal Learning Test-Revised; PD-non pRBD = PD without probable RBD; PD-pRBD = PD with probable RBD; HC = healthy controls.

Data are presented by groups as mean (SD). Analyses were conducted on z-scores adjusted by age, sex and education.

<sup>1</sup> Analysis of variance (ANOVA) followed post hoc test corrected by Games-Howell was used.

<sup>2</sup> Analysis of variance (ANOVA) followed by post hoc test corrected by Bonferroni was used.

<sup>3</sup> Significant differences ( $p < 0.05$ ) were found between PD-non pRBD and HC.

<sup>4</sup> Significant differences ( $p < 0.05$ ) were found between PD-pRBD and HC.

<sup>5</sup> Significant differences ( $p < 0.05$ ) were found between PD-non pRBD and PD-pRBD.

## Supplementary Table 2

Neuropsychological tasks scores of PD-non pRBD and PD-pRBD analyzed with MDS-UPDRS score as a covariate

	<b>PD-non pRBD</b>	<b>PD-pRBD</b>	<b>Test stats</b>	<b>P-value</b>
MoCA	27.0 (2.2)	26.8 (2.1)	0.135	0.713
Semantic fluency				
Animals	21.8 (5.2)	19.5 (4.4)	7.737	0.006 <sup>1</sup>
Vegetables	14.7 (4.4)	13.6 (4.0)	1.215	0.272
Fruits	14.3 (4.1)	13.1 (4.0)	1.415	0.236
Phonetic fluency 'f'	12.9 (4.7)	12.1 (4.2)	2.872	0.092
SDMT	42.0 (8.3)	38.9 (9.7)	1.756	0.187
LNS	10.8 (2.6)	9.9 (2.4)	4.553	0.034 <sup>1</sup>
JLO	13.1 (1.9)	12.5 (2.2)	4.434	0.036 <sup>1</sup>
HVLT-R Immediate recall	25.0 (5.0)	23.3 (4.7)	2.423	0.121
HVLT-R Recognition	9.6 (2.9)	9.2 (3.0)	0.515	0.474
HVLT-R Delayed recall	8.5 (2.4)	7.7 (2.6)	3.529	0.062

Abbreviations: MoCA = Montreal Cognitive Assessment; SDMT = Symbol Digit Modalities Test; LNS = Letter-Number Sequencing; JLO = Benton Judgment of Line Orientation; HVLT-R = Hopkins Verbal Learning Test-Revised; PD-non pRBD = PD without probable RBD; PD-pRBD = PD with probable RBD.

Data are presented by groups as mean (SD). Analyses were conducted on z-scores adjusted by age, sex and education.

Analysis of covariance (ANCOVA) with MDS-UPDRS as a covariate followed post hoc test corrected by Bonferroni was used.

<sup>1</sup> Significant differences ( $p < 0.05$ ) were found between PD-non pRBD and PD-pRBD.

### Supplementary Table 3

Global and partial volume ratios of PD-non pRBD and PD-pRBD analyzed with MDS-UPDRS score as a covariate

	PD-non pRBD	PD-pRBD	Test stats	P-value
<b>Global volumes</b>				
Cortical GM	28.6704 (2.16624)	28.7482 (2.51696)	0.280	0.598
Subcortical GM	3.5597 (0.25621)	3.4926 (0.29242)	2.187	0.141
Ventricular system	1.9743 (0.99272)	2.2429 (1.04248)	2.604	0.108
<b>Deep GM nuclei volumes</b>				
Left Thalamus	0.4559 (0.04486)	0.4407 (0.04097)	4.780	0.030 <sup>1</sup>
Right Thalamus	0.4460 (0.04276)	0.4348 (0.04267)	2.183	0.141
Left Caudate	0.2124 (0.02607)	0.2108 (0.02504)	0.035	0.851
Right Caudate	0.2190 (0.02797)	0.2167 (0.02808)	0.116	0.734
Left Putamen	0.2902 (0.03366)	0.2811 (0.03785)	2.081	0.151
Right Putamen	0.2883 (0.03211)	0.2816 (0.03791)	1.159	0.283
Left Pallidum	0.1280 (0.01427)	0.1259 (0.01687)	1.105	0.294
Right Pallidum	0.1256 (0.01355)	0.1212 (0.01663)	6.095	0.014 <sup>1</sup>
Left Hippocampus	0.2548 (0.02980)	0.2494 (0.02969)	1.487	0.224
Right Hippocampus	0.2619 (0.03127)	0.2606 (0.03106)	0.027	0.870
Left Amygdala	0.1000 (0.01482)	0.0984 (0.01815)	0.327	0.568
Right Amygdala	0.1089 (0.01427)	0.1088 (0.01671)	0.000	0.991
Left Accumbens	0.0294 (0.00680)	0.0300 (0.00732)	0.969	0.326
Right Accumbens	0.0317 (0.00662)	0.0317 (0.00700)	0.037	0.848
Brainstem	1.3904 (0.12004)	1.3618 (0.12659)	3.096	0.080

Abbreviations: GM = gray matter; PD-non pRBD = PD without probable RBD; PD-pRBD = PD with probable RBD.

Data are presented by groups as mean (SD). Analysis of covariance (ANCOVA) with MDS-UPDRS score as covariate followed by post hoc test corrected by Bonferroni was used.

<sup>1</sup> Significant differences ( $p < 0.05$ ) were found between PD-non pRBD and PD-pRBD.

#### Supplementary Table 4

Global and partial volumes of PD-non pRBD, PD-pRBD and HC

	<b>PD-non pRBD</b>	<b>PD-pRBD</b>	<b>HC</b>
<b>eTIV</b>	1597513.1 (168028.4)	1585321.3 (182638.3)	1517584.7 (161845.2)
<b>Global volumes</b>			
Cortical GM	456759.5 (49193.7)	453153.9 (44220.5)	449381.8 (46580.6)
Subcortical GM	56683.9 (5676.9)	55031.7 (4772.8)	54383.8 (4176.4)
Ventricular system	32091.7 (18125.7)	36245.6 (21389.0)	27705.2 (14698.7)
<b>Deep GM nuclei volumes</b>			
Left Thalamus	7267.1 (944.1)	6964.1 (869.3)	6880.9 (696.7)
Right Thalamus	7107.0 (891.9)	6873.6 (891.5)	6729.9 (771.9)
Left Caudate	3381.5 (483.9)	3321.9 (413.4)	3255.8 (411.9)
Right Caudate	3488.5 (527.4)	3418.6 (510.0)	3326.6 (433.9)
Left Putamen	4626.5 (644.9)	4423.5 (558.2)	4453.8 (502.9)
Right Putamen	4588.9 (585.8)	4423.6 (514.2)	4450.6 (447.5)
Left Pallidum	2039.9 (271.4)	1978.6 (227.1)	1912.8 (227.7)
Right Pallidum	2002.1 (271.9)	1904.7 (217.1)	1866.1 (212.2)
Left Hippocampus	4050.0 (498.6)	3919.0 (377.0)	3950.5 (355.4)
Right Hippocampus	4159.7 (504.9)	4095.1 (397.8)	4067.7 (377.8)
Left Amygdala	1593.3 (266.9)	1543.5 (228.1)	1585.4 (198.0)
Right Amygdala	1733.7 (263.5)	1709.1 (220.2)	1728.0 (187.7)
Left Accumbens	468.1 (110.9)	471.2 (108.4)	452.1 (91.0)
Right Accumbens	504.4 (106.2)	498.3 (103.5)	486.2 (84.6)
Brainstem	22154.5 (2587.9)	21523.3 (2708.2)	20963.2 (2149.7)

Abbreviations: eTIV = estimated total intracranial volume; GM = gray matter; PD-non pRBD = PD without probable RBD; PD-pRBD = PD with probable RBD; HC = healthy controls.

Data are presented by groups as mean (SD) in mm<sup>3</sup>.

### Supplementary Table 5

Bivariate significant correlations between MRI measures and performance in neuropsychological tasks in the PD-pRBD group

	<i>Global MRI measures</i>	<i>r (P-value)</i>	<i>Partial MRI measures</i>	<i>r (P-value)</i>
MoCA	Cortical GM	0.229 (0.042)	Left Putamen	0.334 (0.003)
	Subcortical GM	0.350 (0.002)	Right Putamen	0.368 (<0.001)
			Left Hippocampus	0.362 (0.001)
			Left Amygdala	0.284 (0.011)
Phonetic fluency 'f'	Cortical GM	0.348 (0.002)	Left Putamen	0.272 (0.015)
	Subcortical GM	0.269 (0.017)	Right Putamen	0.266 (0.018)
SDMT	Cortical GM	0.247 (0.030)	Right Putamen	0.236 (0.038)
	Subcortical GM	0.272 (0.016)	Left Hippocampus	0.302 (0.007)
	Ventricular system	-0.267 (0.018)	Left Amygdala	0.241 (0.034)
JLO			Left Thalamus	0.296 (0.009)

Abbreviations: GM = gray matter; MoCA = Montreal Cognitive Assessment; SDMT = Symbol Digit Modalities Test; JLO = Benton Judgment of Line Orientation.

### Supplementary Table 6

Bivariate significant correlations between MRI measures and performance in neuropsychological tasks in the whole PD group

	<i>Global MRI measures</i>	<i>r (P-value)</i>	<i>Partial MRI measures</i>	<i>r (P-value)</i>
MoCA	Cortical GM	0.209 (0.003)	Left Putamen	0.225 (0.001)
	Subcortical GM	0.221 (0.001)	Right Putamen	0.240 (<0.001)
			Left Hippocampus	0.178 (0.011)
			Left Amygdala	0.215 (0.002)
Semantic fluency Animals	Subcortical GM	0.163 (0.020)	Left Amygdala	0.184 (0.009)
			Right superior temporal	0.171 (0.015)
Semantic fluency Fruits	Ventricular system	-0.167 (0.017)	Left Amygdala	0.142 (0.044)
			Right superior temporal	0.169 (0.016)
Phonetic fluency 'f'	Cortical GM	0.141 (0.043)	Left Thalamus	0.176 (0.012)
	Subcortical GM	0.175 (0.012)	Right Putamen	0.179 (0.010)
			Left Hippocampus	0.139 (0.048)
			Left Amygdala	0.198 (0.004)
SDMT	Cortical GM	0.166 (0.018)	Left Thalamus	0.192 (0.006)
	Subcortical GM	0.246 (<0.001)	Left Putamen	0.166 (0.018)
			Right Putamen	0.186 (0.008)
	Ventricular system	-0.237 (<0.001)	Left Hippocampus	0.192 (0.004)
			Left Amygdala	0.181 (0.010)
LNS			Left Thalamus	0.189 (0.007)
JLO	Ventricular system	-0.156 (0.026)		
HVLТ-R Immediate recall	Subcortical GM	0.141 (0.045)	Left Hippocampus	0.171 (0.015)
	Ventricular system	-0.179 (0.011)	Left Amygdala	0.156 (0.026)
			Right superior temporal	0.196 (0.005)
HVLТ-R Delayed recall	Subcortical GM	0.186 (0.008)	Left Thalamus	0.219 (0.002)
	Ventricular system	-0.211 (0.003)	Left Hippocampus	0.160 (0.022)
			Left Amygdala	0.148 (0.035)
			Right superior temporal	0.150 (0.032)

Abbreviations: GM = gray matter; MoCA = Montreal Cognitive Assessment; SDMT = Symbol Digit Modalities Test; LNS = Letter-Number Sequencing; JLO = Benton Judgment of Line Orientation; HVLТ-R = Hopkins Verbal Learning Test-Revised.



### Supplementary Table 7

Multiple regression results of partial and global volume ratios as predictors of performance in neuropsychological tasks in the whole PD group

	<i>Model 1 Global MRI measures</i>		<i>Model 2 Partial MRI measures</i>	
	<b>variables</b>	<b>t-stat (P-value)</b>	<b>variables</b>	<b>t-stat (P-value)</b>
MoCA	Subcortical GM	3.113 (0.002)	Right Putamen	2.539 (0.012)
			Left Amygdala	2.107 (0.036)
Semantic fluency Animals	Subcortical GM	2.338 (0.020)	Left Amygdala	2.647 (0.009)
Semantic fluency Fruits	Ventricular system	-2.484 (0.014)	Right Putamen	-2.250 (0.025)
			Left Amygdala	2.453 (0.015)
Phonetic fluency 'f'	Subcortical GM	3.335 (0.001)	Left Thalamus	2.383 (0.018)
			Left Amygdala	2.304 (0.022)
SDMT	Subcortical GM	2.277 (0.024)	Left Thalamus	2.190 (0.030)
			Left Amygdala	1.981 (0.049)
LNS	Non-significant model		Left Thalamus	3.202 (0.002)
JLO	Non-significant model		Non-significant model	
HVLT-R Immediate recall	Ventricular system	-2.585 (0.010)	Left Hippocampus	2.922 (0.004)
HVLT-R Delayed recall	Ventricular system	-3.445 (<0.001)	Left Thalamus	1.980 (0.049)

Abbreviations: GM = gray matter; MoCA = Montreal Cognitive Assessment; SDMT = Symbol Digit Modalities Test; LNS = Letter-Number Sequencing; JLO = Benton Judgment of Line Orientation; HVLT-R = Hopkins Verbal Learning Test-Revised.

### Supplementary Table 8

Adjustment of multiple regression results of partial and global volume ratios as predictors of performance in neuropsychological tasks in the whole PD group

	<i>Model 1 Global MRI measures</i>				<i>Model 2 Partial MRI measures</i>			
	<i>R</i> <sup>2</sup>	Adjusted <i>R</i> <sup>2</sup>	<i>F</i>	<i>P</i> -value	<i>R</i> <sup>2</sup>	Adjusted <i>R</i> <sup>2</sup>	<i>F</i>	<i>P</i> -value
MoCA	0.046	0.041	9.691	0.002	0.089	0.080	9.869	<0.001
Semantic fluency Animals	0.026	0.022	5.465	0.020	0.034	0.029	7.007	0.009
Semantic fluency Fruits	0.030	0.025	6.172	0.014	0.050	0.036	3.495	0.017
Phonetic fluency 'f'	0.052	0.047	11.120	0.001	0.069	0.060	7.465	<0.001
SDMT	0.074	0.064	7.958	<0.001	0.055	0.046	5.870	0.003
LNS					0.049	0.039	5.131	0.007
JLO								
HVLT-R Immediate recall	0.032	0.027	6.680	0.010	0.041	0.036	8.539	0.004
HVLT-R Delayed recall	0.056	0.051	11.870	<0.001	0.055	0.046	5.860	0.003

Abbreviations: GM = gray matter; MoCA = Montreal Cognitive Assessment; SDMT = Symbol Digit Modalities Test; JLO = Benton Judgment of Line Orientation; LNS = Letter-Number Sequencing; HVLT-R = Hopkins Verbal Learning Test-Revised.

**Supplementary Table 9**

MRI field strength distribution of the groups

	<b>1.5 T</b>	<b>3 T</b>	<b>Test stat (<i>P</i>-value)</b>
PD-non pRBD	37 (29.4%)	89 (70.6%)	1.933 (0.380)
PD-pRBD	20 (25.3%)	59 (74.7%)	
HC	14 (20.3%)	55 (79.7%)	

Abbreviations: T = Tesla; PD-non pRBD = PD without probable RBD; PD-pRBD = PD with probable RBD; HC = healthy controls.

Data are presented by groups as *n* (%). Pearson's chi-squared was used.



## Study 2

---

**Oltra J**, Campabadal A, Segura B, Uribe C, Martí MJ, Compta Y, Valdeoriola F, Bargallo N, Iranzo A, Junque C. Disrupted functional connectivity in PD with probable RBD and its cognitive correlates. *Scientific Reports*. 2021; 11: 24351. doi:10.1038/s41598-021-



OPEN

## Disrupted functional connectivity in PD with probable RBD and its cognitive correlates

Javier Oltra<sup>1,2</sup>, Anna Campabadal<sup>1,2</sup>, Barbara Segura<sup>1,2,3✉</sup>, Carme Uribe<sup>1,2,4</sup>, Maria Jose Marti<sup>2,3,5</sup>, Yaroslau Compta<sup>2,3,5</sup>, Francesc Valldeoriola<sup>2,3,5</sup>, Nuria Bargallo<sup>2,6</sup>, Alex Iranzo<sup>2,3,7</sup> & Carme Junque<sup>1,2,3</sup>

Recent studies associated rapid eye movement sleep behavior disorder (RBD) in Parkinson's disease (PD) with severe cognitive impairment and brain atrophy. However, whole-brain functional connectivity has never been explored in this group of PD patients. In this study, whole-brain network-based statistics and graph-theoretical approaches were used to characterize resting-state interregional functional connectivity in PD with probable RBD (PD-pRBD) and its relationship with cognition. Our sample consisted of 30 healthy controls, 32 PD without probable RBD (PD-non pRBD), and 27 PD-pRBD. The PD-pRBD group showed reduced functional connectivity compared with controls mainly involving cingulate areas with temporal, frontal, insular, and thalamic regions ( $p < 0.001$ ). Also, the PD-pRBD group showed reduced functional connectivity between right ventral posterior cingulate and left medial precuneus compared with PD-non pRBD ( $p < 0.05$ ). We found increased normalized characteristic path length in PD-pRBD compared with PD-non pRBD. In the PD-pRBD group, mean connectivity strength from reduced connections correlated with visuoperceptual task and normalized characteristic path length correlated with processing speed and verbal memory tasks. This work demonstrates the existence of disrupted functional connectivity in PD-pRBD, together with abnormal network integrity, that supports its consideration as a severe PD subtype.

Rapid eye movement (REM) sleep behavior disorder (RBD) is a parasomnia characterized by vivid dreams associated with complex movements and dream-enacting behaviors, increased electromyographic activity, and loss of normal muscle atonia during REM sleep<sup>1,2</sup>. Evidence suggests that isolated RBD is a prodromal symptom of Parkinson's disease (PD) and other synucleinopathies, with an up to 90% 15-year rate of progression to a defined condition<sup>3</sup>. Furthermore, the prevalence of RBD in PD patients is around 40%<sup>4</sup>. Postmortem studies reveal more diffuse and severe deposition of synuclein in PD patients with RBD<sup>5</sup>.

Structural neuroimaging studies show that the presence of RBD in PD is associated with greater gray matter atrophy by means of voxel-based morphometry<sup>6,7</sup> and cortical thickness analysis<sup>7</sup> in PD patients with video-polysomnographic (vPSG) confirmed RBD diagnosis; as well as by means of deformation-based morphometry<sup>8</sup>, and voxel-based morphometry<sup>9</sup> in PD patients with questionnaire-based probable RBD status (PD-pRBD). Note that in the case of using questionnaires PD patients can be classified as PD-pRBD or PD without probable RBD (PD-non pRBD). Clinically, a recent meta-analysis shows that PD with vPSG confirmed RBD diagnosis and PD-pRBD are related to disease duration, increased Hoehn and Yahr stage, and higher Movement Disorder Society Unified Parkinson's Disease Rating Scale (MDS-UPDRS) Part III score<sup>10</sup>. Moreover, PD-pRBD is associated with lower cognitive performance<sup>11,12</sup>, a higher prevalence of mild cognitive impairment<sup>13</sup>, and faster cognitive decline<sup>11</sup>.

<sup>1</sup>Medical Psychology Unit, Department of Medicine, Institute of Neurosciences, University of Barcelona, Barcelona, Catalonia, Spain. <sup>2</sup>Institute of Biomedical Research August Pi i Sunyer (IDIBAPS), Barcelona, Catalonia, Spain. <sup>3</sup>Centro de Investigación Biomédica en Red Enfermedades Neurodegenerativas (CIBERNED), Hospital Clínic de Barcelona, Barcelona, Catalonia, Spain. <sup>4</sup>Research Imaging Centre, Campbell Family Mental Health Research Institute, Centre for Addiction and Mental Health (CAMH), University of Toronto, Toronto, ON, Canada. <sup>5</sup>Parkinson's Disease and Movement Disorders Unit, Neurology Service, Hospital Clínic de Barcelona, Institute of Neurosciences, University of Barcelona, Barcelona, Catalonia, Spain. <sup>6</sup>Centre de Diagnòstic per la Imatge (CDI), Hospital Clínic de Barcelona, Barcelona, Catalonia, Spain. <sup>7</sup>Multidisciplinary Sleep Unit, Neurology Service, Hospital Clínic de Barcelona, University of Barcelona, Barcelona, Catalonia, Spain. ✉email: bsegura@ub.edu

Concerning resting-state functional MRI (rs-fMRI) prior works in PD with vPSG confirmed RBD diagnosis found decreased functional connectivity between the pedunculopontine nucleus and the anterior cingulate cortex<sup>14</sup>, decreased amplitude of low-frequency fluctuations in the primary motor and premotor cortices<sup>15</sup>, as well as reduced posterior functional connectivity based on right superior occipital gyrus<sup>16</sup>. Contrary to region-centered approaches, a network-based perspective conceptualizes the brain as a complex network and allows characterizing dynamic interactions between regions through Network-Based Statistics (NBS) and graph-derived metrics<sup>17</sup>. In this context, Li et al.<sup>18</sup>, by graph-derived metrics, found extensive changes of nodal properties in PD-pRBD than PD-non pRBD in comparison with healthy controls in the neocortex and limbic system; as well as enhanced nodal efficiency in the bilateral thalamus and betweenness centrality in the left insula, and reduced betweenness centrality in the right dorsolateral superior frontal gyrus in PD-pRBD compared with PD-non pRBD. The development of the threshold-free network-based statistics (TFNBS) method<sup>19</sup>, which, unlike NBS, does not require the a priori definition of a component-defining threshold and generates edge-wise significant values, has been proposed as a step forward. Recently, this approach revealed in isolated RBD a disruption of posterior functional connectivity<sup>20</sup>. Nevertheless, as far as we know, there is no previous literature in PD-pRBD studying rs-fMRI interregional functional connectivity through network-based statistics. Our main aim is to characterize dysfunction of brain connectivity in PD-pRBD using TFNBS whole-brain and graph theory analyses and to investigate its possible relation with cognitive dysfunctions. We hypothesize that PD patients with probable RBD will show a reduction in brain functional connectivity compared with healthy controls and PD patients without probable RBD and the reduction will be associated with cognitive impairment.

## Methods

**Participants.** Seventy-one PD patients were recruited from the Parkinson's Disease and Movement Disorders Unit (Hospital Clínic de Barcelona, Barcelona, Spain); and 69 voluntary healthy controls recruited from the Institut Català de l'Envel·liment (Universitat Autònoma de Barcelona, Barcelona, Catalonia, Spain) and patients' relatives. The patient's inclusion criteria were: (a) attaining UK PD Society Brain Bank diagnostic criteria for PD and (b) no treatment with deep-brain stimulation. Exclusion criteria were: (a) mild cognitive impairment (MCI) for healthy controls, (b) PD age of onset less than 40 years; (c) age less than 50 years; (d) severe comorbidity due to psychiatric or neurological conditions; (e) score below 25 obtained in Mini-Mental State Examination (MMSE) for healthy controls; (f) claustrophobia; (g) pathological MRI findings apart from mild white matter hyperintensities in the fluid-attenuated inversion recovery (FLAIR) acquisition; (h) MRI artifacts; (i) absence of fMRI resting-state acquisition; (j) fMRI head motion parameter of mean interframe head motion at  $\geq 0.3$  mm translation or  $0.3^\circ$  rotation; (k) fMRI head motion parameter of maximum interframe head motion at  $\geq 1$  mm translation or  $1^\circ$  rotation; (l) no response to Innsbruck RBD Inventory; (m) probable RBD (pRBD) condition based on Innsbruck RBD Inventory for healthy controls. Inclusion criteria and exclusion criteria (b) to (g) were also used in Uribe et al. 2016<sup>21</sup>.

After applying the criteria, we selected 59 PD patients and 30 healthy controls. The excluded PD participants were: 1 because of young-onset, 1 for age  $< 50$  years, 1 for young-onset and age  $< 50$  years, 1 for vascular parkinsonism lookalike condition, 1 for claustrophobia, 2 for absence of fMRI, 5 for no Innsbruck RBD Inventory response. From healthy controls participants, were excluded: 4 for age  $< 50$  years, 3 for psychiatric comorbidity, 8 for MCI condition, 1 for MMSE score below 25, 1 for MRI artifact, 1 for MCI condition and MRI artifact, 3 for fMRI head motion parameters, 5 for no Innsbruck RBD Inventory response, 13 for pRBD condition.

PD patients were classified in PD-pRBD ( $n = 27$ ) and PD-non pRBD ( $n = 32$ ) following the 5-item test Innsbruck REM Sleep Behavior Disorder Inventory, with a 0.25 cutoff (number of positive symptoms/number of answered questions)<sup>22</sup>.

The study had the approval of the Ethics Committee of the University of Barcelona (IRB00003099) and Hospital Clínic (HCB/2014/0224). All participants provided written informed consent after a full explanation of the procedures involved. It was performed in accordance with relevant regulations and guidelines.

**Neuropsychological and clinical assessment.** All subjects underwent a neuropsychological battery including Digit Span Forward and Backward (WAIS), phonemic fluency (letter 'p'), semantic fluency (animals), Stroop Color and Word Test, Trail Making Test (TMT), Symbol Digits Modalities Test-Oral version (SDMT), Rey Auditory Verbal Learning Test (RAVLT), Benton Judgment of Line Orientation (JLO), Benton Visual Form Discrimination (BVF), Benton Facial Recognition Test short form (27-item, BFRT), Boston Naming Test (BNT). The presence of mild cognitive impairment (MCI) was established as in a previous study based on z scores adjusted for age, sex, and education extracted by a multiple regression analysis<sup>23</sup> performed in a healthy control reference group<sup>24</sup>.

Clinical evaluation included motor symptoms assessed with the MDS-UPDRS Part III, disease severity with Hoehn and Yahr scale, global cognition with the MMSE, and olfactory function using the University of Pennsylvania Smell Identification Test (UPSIT-40)<sup>25</sup>.

L-dopa equivalent daily dose (LEDD)<sup>26</sup> was calculated for standardization purposes by the different doses of antiparkinsonian drugs that the PD patients took.

**MRI acquisition.** MRI acquisition with a 3 T scanner (MAGNETOM Trio, Siemens, Germany). The scanning protocol included: (a) high-resolution 3-dimensional T1-weighted images acquired in the sagittal plane repetition time = 2300 ms, echo time = 2.98 ms, inversion time = 900 ms, 240 slices, field-of-view = 256 mm; 1 mm isotropic voxel); (b) axial FLAIR sequence (repetition time = 9000 ms, echo time = 96 ms); and (c) resting-state 10-min-long functional gradient-echo echo-planar imaging sequence (240 T2\* weighted images, repetition time = 2.5 s, echo time = 28 ms, flip angle =  $80^\circ$ , slice thickness = 3 mm, field-of-view = 240 mm). Subjects were

instructed to keep their eyes closed, not to fall asleep, and not to think anything in particular. The same acquisition protocol was used in Campabadal et al. 2020<sup>20</sup>.

**MRI preprocessing.** Main functional image preprocessing, using AFNI tools, described in Campabadal et al. 2020<sup>20</sup> included “discarding the first five volumes to allow magnetization stabilization, despiking, motion correction, grand-mean scaling, linear detrending, and temporal filtering (maintaining frequencies above 0.01 Hz)”. Moreover, the preprocessing included an Independent Component Analysis (ICA-AROMA)<sup>27</sup> based strategy for Automatic Removal of Motion Artifacts<sup>20</sup>, along with a quality control based on correlations between framewise head displacement and overall signal variation<sup>28</sup>.

**Characterization of brain functional connectivity and network properties.** To test for inter-group differences in interregional connectivity, we applied threshold-free network-based statistics (TFNBS)<sup>19</sup>. This approach allows performing statistical inference on brain graphs through network-based statistics<sup>29</sup> and threshold-free cluster enhancement<sup>30</sup>. One of the main characteristics of TFNBS is the estimation of edge-wise significance values, which is useful for the selection of relevant connectivity features. The 246 regions defined in the Brainnetome Atlas (<https://atlas.brainnetome.org/bnatlas.html>) were used for the characterization of global functional connectivity (for a detailed list of the used nodes see Supplementary Methods 1)<sup>31</sup>.

Complementary, a graph theory implementation was applied to describe the network topology through its global (whole-brain) and local (nodal) properties<sup>32,33</sup>. The extraction of the global and local parameters, using Brain Connectivity Toolbox (BCT), included: clustering coefficient, node degree, small-worldness, path length, efficiency, and betweenness centrality. For detailed definitions and calculations of these graph metrics, see Rubinov and Sporns<sup>33</sup>. Computation used nine different density thresholds (maintaining the 5% to 25% strongest edges, at intervals of 2.5%), followed by a reporting results criterion of significance in more than 75% of the thresholds.

**Statistical analyses.** Group differences were conducted in demographic, neuropsychological and clinical variables using IBM SPSS Statistics 27.0.0 (2020; Armonk, NY: IBM Corp) by analysis of variance (ANOVA) or analysis of covariance (ANCOVA) followed by Bonferroni or Games-Howell post hoc tests, or Kruskal–Wallis H and Mann–Whitney U tests as appropriate. Differences in categorical measures were analyzed by Pearson’s chi-squared. To perform correlation analyses between neuroimaging and neuropsychological variables, the Pearson and Spearman correlation coefficients were applied. The statistical significance threshold was set at  $p < 0.05$ .

Between groups differences in connectivity measures were tested with the general linear model using in-house MATLAB scripts. Statistical significance was established using Monte Carlo simulations with 5,000 permutations. Two-tailed  $p$ -values were calculated as the proportion of values in the null distribution more extreme than those observed in the actual model.

## Results

**Sociodemographic, clinical, and neuropsychological data.** Table 1 shows the sociodemographic and clinical characteristics of participants. There were no significant differences between groups in age and education. However, differences between healthy control and PD groups were observed for sex, subsequent analyses that included both groups were controlled by this variable. The PD groups were similar on age of onset, LEDD, and disease severity. PD-pRBD showed slightly longer disease duration (not reaching statistical significance  $p = 0.055$ ), even so, this variable was controlled in subsequent comparison between PD groups. Both PD groups differed from controls in olfactory function.

Table 2 describes neuropsychological results by group. Inter-group comparisons showed PD-pRBD patients had lower performance than PD-non pRBD and healthy controls in Stroop Word and Word-Color and TMT-A. PD-pRBD patients also had significantly lower scores than healthy controls in Stroop Color, semantic fluency, RAVLT Total, JLO, SDMT, TMT B and B minus A, as well as BFRT-short. PD-pRBD differed from PD-non pRBD in Stroop Word, Color and Word-Color when controlling by disease duration (Supplementary Table 1). There were no between PD groups differences in MCI distribution (Supplementary Table 2). To facilitate the interpretation of neuropsychological data we include the descriptive statistics in  $z$ -scores calculated based on a healthy control reference group means and standard deviations<sup>24</sup> in Supplementary Table 3.

**Functional connectivity and network graph metrics.** Significant difference between healthy controls and PD-non pRBD group was found for maximum translation (Table 1), hence it was introduced as a covariate in all subsequent analyses that included these two groups.

Whole-brain functional connectivity analysis showed that PD-pRBD had 16 connections with significantly reduced functional connectivity strength when compared with healthy controls ( $p < 0.001$ , FWE corrected; Fig. 1a,b and Supplementary Table 4 for a detailed list of the altered connections). From the 16 connections, 10 (62.5%) were found to be cortico-cortical edges and 6 (37.5%) were cortico-deep gray matter edges (Supplementary Table 5). When comparing PD groups controlling by disease duration, the PD-pRBD group had significantly reduced functional connectivity strength between the right ventral posterior cingulate (Brodmann area 23) and the left medial precuneus (pEM, Brodmann area 5) that correspond to CG\_R\_7\_4 and Pkun\_L\_4\_2 labels of the Brainnetome Atlas respectively ( $p < 0.05$ , FWE corrected).

Intergroup difference in global graph parameters showed increased normalized characteristic path length in PD-pRBD patients compared with PD-non pRBD in 7 out of 9 thresholds controlling by disease duration (Fig. 1c).



	PD-non pRBD (n = 32)	PD-pRBD (n = 27)	HC (n = 30)	Test stat	p-value
<b>Sociodemographic and clinical data</b>					
Sex, male, n (%)	21 (65.6)	23 (85.2)	13 (43.3)	10.863 <sup>a</sup>	0.004 <sup>f,g</sup>
Age, y, mean (SD)	64.5 (9.9)	68.8 (9.2)	67.5 (7.7)	1.827 <sup>b</sup>	0.167
Education, y, mean (SD)	12.8 (5.3)	11.4 (5.4)	11.4 (4.0)	1.255 <sup>c</sup>	0.534
Age of onset, y, mean (SD)	58.2 (10.5)	59.2 (9.6)	NA	0.378 <sup>d</sup>	0.707
Disease duration, y, mean (SD)	6.3 (3.6)	8.6 (5.0)	NA	1.977 <sup>d</sup>	0.055
LEDD, mean (SD)	516.6 (277.4)	707.8 (469.2)	NA	336.5 <sup>c</sup>	0.146
MDS-UPDRS-Part III, mean (SD)	15.4 (10.2)	17.1 (8.1)	NA	314.5 <sup>c</sup>	0.228
H&Y stage, n, 1/2/2.5/3/4	6/17/1/6/0	2/11/0/10/1	NA	5.689 <sup>a</sup>	0.224
UPSIT, mean (SD)	18.9 (6.8)	16.8 (6.8)	29.2 (4.3)	39.319 <sup>c</sup>	< 0.001 <sup>f,g</sup>
RBD-I, symptoms/answers, mean (SD)	0.08 (0.09)	0.56 (0.14)	0.05 (0.07)	59.453	< 0.001 <sup>g,h</sup>
<b>Mean interframe head motion</b>					
Rotation, degrees, mean (SD)	0.051 (0.033)	0.051 (0.030)	0.039 (0.020)	2.215 <sup>c</sup>	0.330
Translation, mm, mean (SD)	0.100 (0.057)	0.095 (0.043)	0.124 (0.058)	2.523 <sup>b</sup>	0.086
<b>Maximum interframe head motion</b>					
Rotation, degrees, mean (SD)	0.308 (0.215)	0.327 (0.200)	0.267 (0.165)	0.840 <sup>c</sup>	0.657
Translation, mm, mean (SD)	0.377 (0.190)	0.481 (0.211)	0.502 (0.170)	7.164 <sup>c</sup>	0.028 <sup>f</sup>

**Table 1.** Sociodemographic, clinical, and head motion comparisons among PD-non pRBD, PD-pRBD and HC. *PD-non pRBD* Parkinson's disease patients without probable REM sleep behavior disorder, *PD-pRBD* Parkinson's disease patients with probable REM sleep behavior disorder, *HC* healthy controls, *y* years, *LEDD* levodopa equivalent daily doses, *MDS-UPDRS* Movement Disorder Society Unified Parkinson's Disease Rating Scale, *H&Y* Hoehn and Yahr scale, *UPSIT* University of Pennsylvania Smell Identification Test, *RBD-I* Innsbruck REM Sleep Behavior Disorder Inventory. <sup>a</sup>Chi-squared test. <sup>b</sup>Analysis of variance (ANOVA) test followed by Bonferroni post-hoc test. <sup>c</sup>Kruskal–Wallis H test followed by Mann–Whitney U test. <sup>d</sup>t-test. <sup>e</sup>Mann–Whitney U test. <sup>f</sup>Post-hoc differences between PD-non pRBD and HC ( $p < 0.05$ ). <sup>g</sup>Post-hoc differences between PD-pRBD and HC ( $p < 0.05$ ). <sup>h</sup>Post-hoc differences between PD-non pRBD and PD-pRBD ( $p < 0.05$ ).

Additionally, we explored the potential influence of cognitive impairment in functional connectivity and network graph metrics. We performed a whole-brain functional connectivity analysis with the four resulting groups (PD-non pRBD-non MCI = 19, PD-non pRBD-MCI = 13, PD-pRBD-non MCI = 13, PD-pRBD-MCI = 14) and did not find statistical significant differences ( $p < 0.05$ , FWE corrected). Further, we found increased normalized characteristic path length in PD-pRBD-MCI patients compared with PD-non pRBD-MCI in 9 out of 9 thresholds after applying network graph metrics analyses with those four groups (Supplementary Fig. 1).

**Correlation of cognitive measures with functional connectivity and network graph metrics.** The global mean strength of the 16 edges was correlated with the neuropsychological measures with significantly lower performance in PD-pRBD compared with the other two groups. Positive correlations were found with BFRT-short (Fig. 2a).

In the PD-pRBD group the normalized characteristic path length correlated with scores in the Stroop Word and Color, SDMT and RAVLT Total (Fig. 2b).

No significant correlations between cognitive measures and functional connectivity measures were found in the PD-non pRBD and healthy control groups.

## Discussion

This is the first work investigating resting-state interregional functional connectivity through whole-brain network-based statistics in PD-pRBD patients. Our results suggest that PD-pRBD patients had reduced resting-state functional connectivity and increased normalized characteristic path length in comparison with healthy controls. PD-pRBD patients showed posterior connectivity disruption compared with PD-non pRBD patients. Moreover, functional abnormalities were associated with cognitive impairment only in the PD-pRBD group.

The whole-brain analyses revealed an extended reduced functional connectivity in PD-pRBD patients compared with healthy controls, mainly involving posterior cingulate areas, and their connections with temporal, frontal, insular and thalamic regions. Besides, we found reduced connectivity between the left superior temporal and the right parietal cortex. Concerning cortico-deep gray matter connection, we also identified a significant decrease in fronto-striatal, parietal-striatal, parietal-thalamic regions, as well as between amygdala and posterior middle temporal cortex. Overall, our results supported the existence of an abnormal connectivity pattern in PD-pRBD patients that mainly included cortical paralimbic connections.

Our findings evidenced a relevant cingulate cortex implication in the pattern shown by PD-pRBD. Previous work also found cingulate cortex abnormalities in a resting-state study with reduced connectivity between the anterior cingulate cortex and the pedunculopontine nucleus, as regions from the arousal network. The authors of that work suggested that decreased connectivity in the arousal network would be related to alertness regulation in

Test	PD-non pRBD	PD-pRBD	HC	Test stat (p-value)
MMSE	29.06 (1.24)	28.07 (2.93)	29.13 (0.94)	3.265 (0.043)
<b>Digit span</b>				
Forward	5.38 (1.21)	5.44 (1.28)	5.57 (1.33)	0.675 (0.512)
Backward	3.97 (1.00)	4.11 (1.34)	4.10 (0.92)	0.298 (0.743)
Forward minus backward	1.41 (1.41)	1.33 (1.21)	1.47 (0.90)	0.210 (0.811)
Phonetic fluency "p"	15.47 (6.04)	6.04 (5.29)	15.77 (5.96)	1.368 (0.260)
Semantic fluency "animals"	16.94 (6.51)	15.07 (7.73)	20.57 (4.08)	6.136 (0.003) <sup>a</sup>
<b>Stroop</b>				
Word	89.74 (17.42)	78.26 (23.32)	97.07 (15.39)	8.309 (0.001) <sup>a,b</sup>
Color	56.32 (13.83)	47.92 (16.25)	64.30 (9.90)	7.431 (0.001) <sup>a</sup>
Word-Color	34.55 (11.80)	26.96 (13.42)	37.03 (9.09)	5.918 (0.004) <sup>a,b</sup>
<b>TMT</b>				
A	51.63 (35.24)	85.11 (98.20)	38.93 (10.85)	6.022 (0.004) <sup>a,b</sup>
B	146.43 (143.93)	189.50 (215.69)	95.87 (46.23)	3.394 (0.039) <sup>a</sup>
B minus A	96.07 (115.84)	138.73 (196.38)	56.93 (39.83)	3.038 (0.054) <sup>a</sup>
SDMT	41.91 (14.79)	37.37 (18.38)	47.50 (8.47)	3.792 (0.026) <sup>a</sup>
<b>RAVLT</b>				
Total	44.06 (10.38)	38.96 (11.38)	46.00 (6.21)	3.246 (0.044) <sup>a</sup>
Recall	8.22 (3.66)	7.56 (3.46)	9.43 (2.06)	2.088 (0.130)
True recognition	13.22 (2.76)	13.44 (1.72)	14.13 (1.31)	1.591 (0.210)
JLO	23.81 (5.72)	22.00 (6.87)	25.20 (3.40)	5.537 (0.005) <sup>a</sup>
BVFD	29.44 (2.61)	27.93 (4.11)	29.17 (2.35)	2.534 (0.085)
BFRT-short	21.66 (2.62)	20.96 (2.89)	23.17 (1.97)	5.631 (0.005) <sup>a</sup>
BNT	13.56 (1.22)	13.48 (1.01)	13.67 (0.88)	0.970 (0.383)

**Table 2.** Neuropsychological performance of PD-non pRBD, PD-pRBD and HC. Data are presented as mean (SD) of raw scores. Analyses of covariance (ANCOVA) with sex as covariate, followed by Bonferroni post-hoc tests. *PD-non pRBD* Parkinson's disease patients without probable REM sleep behavior disorder, *PD-pRBD* Parkinson's disease patients with probable REM sleep behavior disorder, *HC* healthy controls, *MMSE* Mini-Mental State Examination, *TMT* Trail Making Test, *SDMT* Symbol Digit Modalities Test, *RAVLT* Rey Auditory Verbal Learning Test, *JLO* Benton Judgment of Line Orientation, *BVFD* Benton Visual Form Discrimination, *BFRT* Benton Facial Recognition Test, *BNT* Boston Naming Test. <sup>a</sup>Post-hoc differences between PD-pRBD and HC ( $p < 0.05$ ). <sup>b</sup>Post-hoc differences between PD-pRBD and PD-non pRBD ( $p < 0.05$ ).

PD patients with vPSG RBD confirmed diagnosis<sup>14</sup>. Additionally, we found reduced connectivity between motor and premotor regions and basal ganglia in PD-pRBD compared with healthy controls. In this line, functional abnormalities have been reported previously in motor fronto-striatal circuitry in PD with RBD diagnosed by vPSG using Amplitude of Low-Frequency Fluctuations (ALFF). These results suggested that RBD pathophysiology involves not only midbrain dysfunction but also cortico-subcortical altered connectivity<sup>15</sup>. Of interest, previous evidence pointed to increased REM sleep without atonia in PD with freezing of gait<sup>34</sup> and subliminal gait initiation deficits in isolated RBD<sup>35</sup>. Future research could explore the relation between both symptoms, freezing of gait and RBD, using functional connectivity approaches.

Our study used a complex approach that allows characterizing the whole brain functional connectivity. Regarding between PD groups comparison, we evidenced disrupted posterior functional connectivity in PD-pRBD between the right ventral area of the cingulate and the left medial area of the precuneus. In this context, a recent work identified reduced posterior functional connectivity in PD with RBD confirmed by vPSG compared with PD without RBD. However, this study used a seed-to-whole brain approach based on a priori region of interest located at the right superior occipital gyrus<sup>16</sup>. It is noteworthy that our group identified disrupted posterior connectivity in isolated RBD applying the same whole-brain methodological approach used in the current study<sup>20</sup>. Altogether might reflect that this regional pattern would be associated with RBD condition in the synucleinopathies spectrum.

On the other hand, our graph analyses reported increased normalized characteristic path length in the PD-pRBD group compared with PD-non pRBD. This finding might reflect global integration and efficiency abnormalities in the network<sup>33</sup>. The unique previous research performed in PD-pRBD reported enhanced nodal efficiency in the thalami and betweenness centrality in the right dorsolateral superior frontal gyrus in PD-pRBD compared with healthy controls. Nevertheless, they did not find differences in global graph metrics between groups<sup>18</sup>. Although an early work reported an incremented normalized characteristic path length in PD patients compared with healthy controls<sup>36</sup>. Further studies showed that global integration seems preserved in early-stage drug-naïve PD patients<sup>37</sup>, but altered in severe disease phenotypes with early-stage PD-MCI<sup>38</sup>. These findings are of great interest considering that pRBD condition is associated with worse cognitive prognosis<sup>11</sup>. In our study, the MCI condition by itself did not explain the obtained between PD groups results from TFNBS and graph

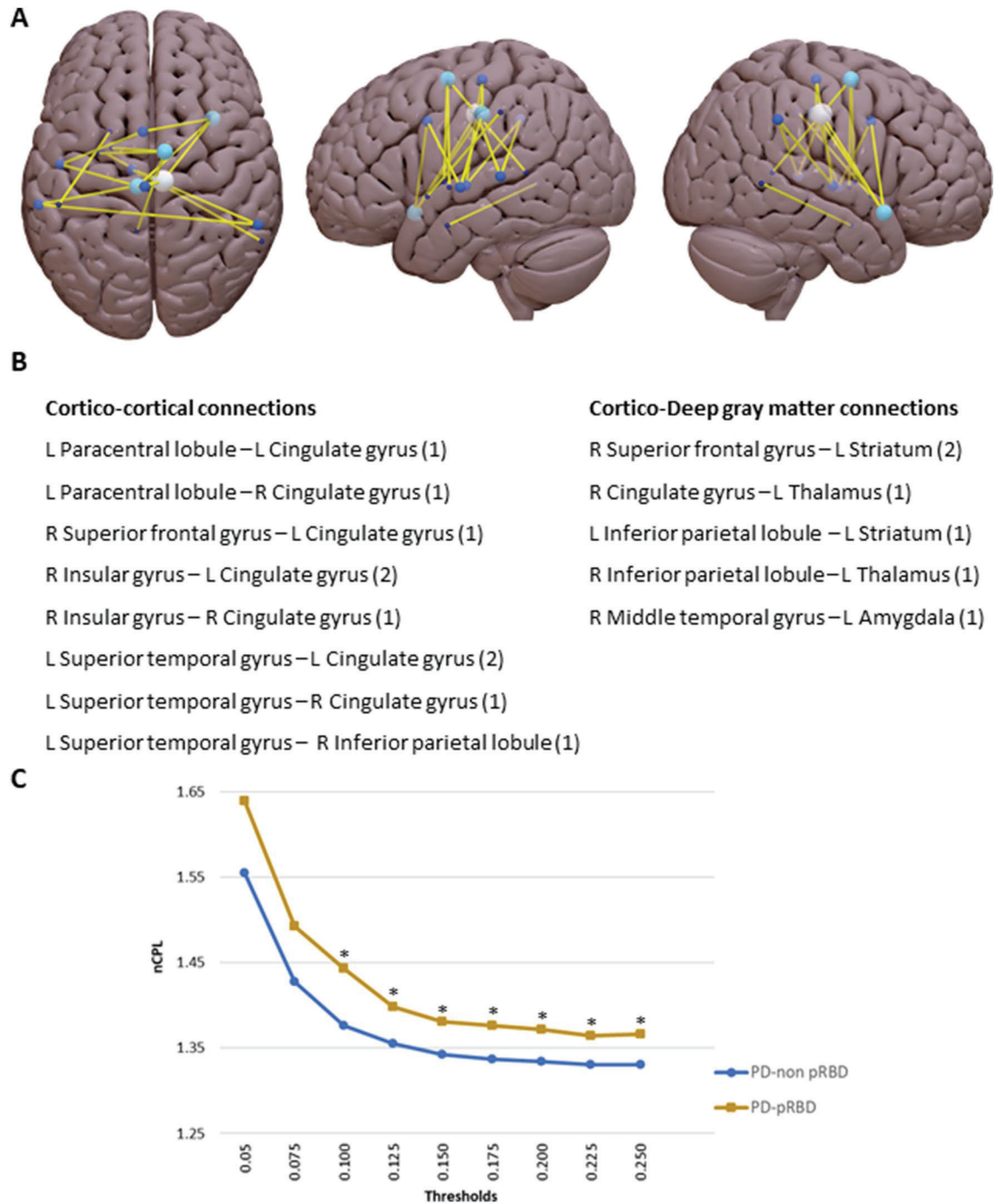


**Figure 1.** (A) Schematic representation of the reduced functional connectivity strength in Parkinson's disease patients with probable REM sleep behavior disorder (PD-pRBD) compared with healthy controls (HC) in the whole-brain analysis consisting of sixteen edges found to be significantly different between groups. Lighter colors represent nodes connected to a greater number of altered connections. Comparison using threshold-free network-based statistics ( $p < 0.001$ , FWE corrected) with sex and maximum translation as covariate. (B) Summary of the altered edges in PD-pRBD represented in panel A classified in cortico-cortical and cortico-deep gray matter connections. The altered edges are classified in types according to the structures of the nodes involved. To see a more detailed list with the specific edges and their corresponding node pairs see Supplementary Table 4. In parentheses the number of connections of corresponding to each type, e.g. in "R Insular gyrus–L Cingulate gyrus (2)" indicates two altered connections of this type. Regions were defined based on the Brainnetome Atlas (see Supplementary Methods 1). (C) Shows the normalized characteristic path length (nCPL) increment in PD-pRBD patients compared with Parkinson's disease patients without probable REM sleep behavior disorder (PD-non pRBD). Normalized characteristic path length (vertical axis) as a function of sparsity thresholds (horizontal axis) for PD-pRBD and PD-non pRBD. (\*) indicate significant differences between PD-non pRBD and PD-pRBD. Brain plots were created with Surf Ice (<https://www.nitrc.org/projects/surface/>). L left, R right.

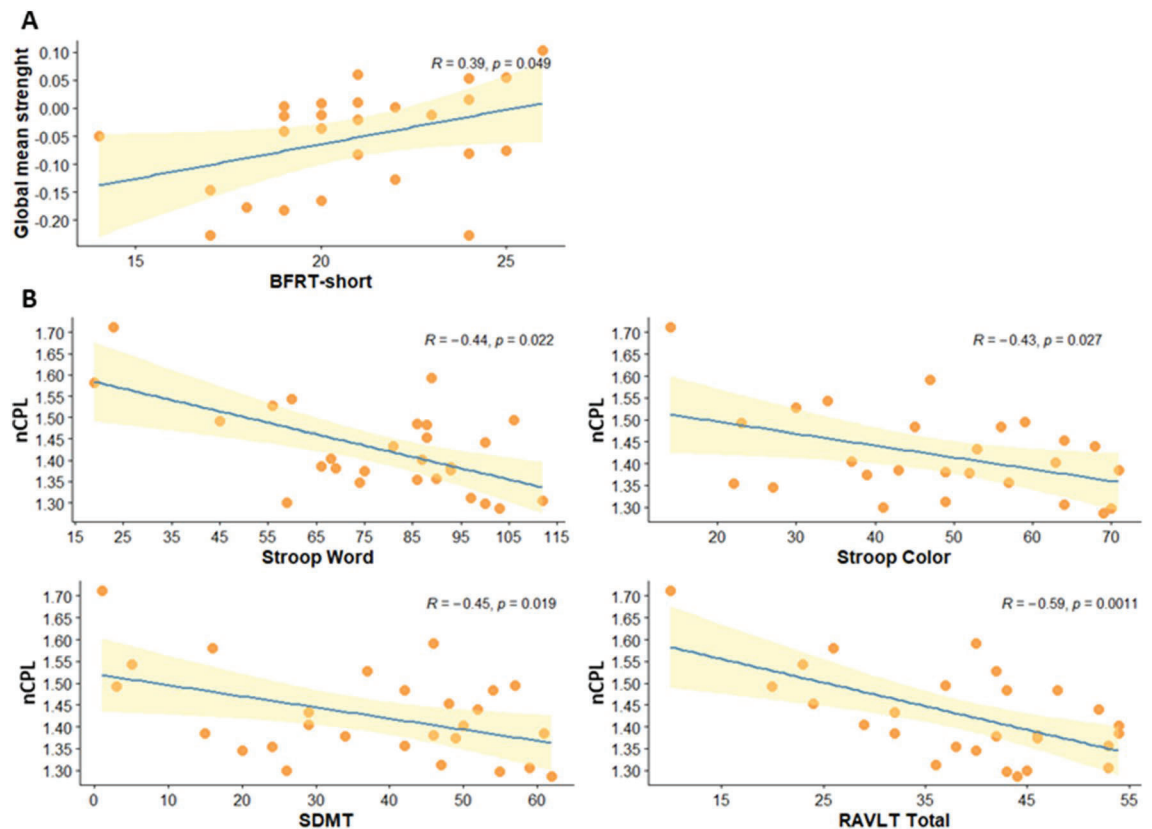


**Figure 2.** (A) Significant correlation between the global mean strength and the BFRT-short (Benton Facial Recognition Test short form) in PD-pRBD group. (B) Significant correlations between normalized characteristic path length (nCPL) and Stroop Word, Stroop Color, Symbol Digits Modalities Test-Oral version (SDMT) and Rey Auditory Verbal Learning Test (RAVLT) total in PD-pRBD group. Left to right, top to bottom. Shaded area represents 95% confidence interval.

metrics. In additional analyses, the found difference in normalized characteristic path length appeared between PD-pRBD-MCI and PD-non pRBD-MCI groups replicated the main result and may indicated that differences could be aggravated between PD-MCI subgroups.

In this context, despite we did not find differences in MCI diagnosis between groups, the PD-pRBD group showed a widespread impairment in the neuropsychological battery with lower performance in mental processing speed, verbal fluency, verbal memory, visuospatial (VS) and visuoperceptual (VP) tasks. This result is in line with previous works in PD-pRBD<sup>11,12</sup>. Furthermore, we found a significant correlation between the mean functional connectivity strength and a visuoperceptual task in PD-pRBD, as well as significant correlations between the normalized characteristic path length and measures of mental processing speed and verbal learning in PD-pRBD. The role of altered brain functional connectivity in cognitive impairment in PD-pRBD is congruent since an incremented path length implies a less efficient transfer of information due to the altered integrity of the network<sup>39,40</sup>. Our result concurs well with a previous work of our group with isolated RBD patients, finding a correlation between mental processing speed domain and temporoparietal connectivity disruption<sup>20</sup>. It is interesting to note that the mental processing speed domain is assessed with the SDMT and Stroop Color in both studies. It may be assumed that SDMT and Stroop Color test require not only mental processing speed, but also the integration of attention, VS, and VP functions. So, this may be the reason why they are more sensitive when it comes to reflecting brain dysfunctions in patients with RBD. In summary, PD-pRBD patients showed worse cognitive profile and functional connectivity abnormalities suggesting an association between pRBD and severe phenotype.

The main limitation of the present study is the absence of polysomnography-based RBD diagnosis, which is the gold standard for diagnosing RBD. However, the Innsbruck REM sleep behavior disorder inventory had good psychometric properties in PD population, a sensitivity of 0.91, and a specificity of 0.86 (AUC = 0.89)<sup>22</sup> and has been frequently used to characterize probable RBD in PD in previous studies<sup>41,42</sup>.

In summary, in this study, we demonstrate the existence of abnormal network integrity and disrupted functional connectivity in PD-pRBD. Furthermore, we found evidence that reduced connectivity was associated with impaired visuoperceptual functions; as well as abnormal functional integrity was associated with lower performance in verbal learning and mental processing speed. Our results underpin the presence of pRBD as a condition related to severe phenotype in PD.

## Data availability

The data that support the findings of this study are available from the corresponding author upon reasonable request.

Received: 1 June 2021; Accepted: 9 December 2021

Published online: 21 December 2021

## References

- Schenck, C. H. & Mahowald, M. W. REM sleep behavior disorder: Clinical, developmental, and neuroscience perspectives 16 years after its formal identification in SLEEP. *Sleep* **25**, 120–138 (2002).
- Iranzo, A. The REM sleep circuit and how its impairment leads to REM sleep behavior disorder. *Cell Tissue Res.* **373**, 245–266 (2018).
- Galbiati, A., Verga, L., Giora, E., Zucconi, M. & Ferini-Strambi, L. The risk of neurodegeneration in REM sleep behavior disorder: A systematic review and meta-analysis of longitudinal studies. *Sleep Med. Rev.* **43**, 13 (2019).
- Zhang, J., Xu, C. Y. & Liu, J. Meta-analysis on the prevalence of REM sleep behavior disorder symptoms in Parkinson's disease. *BMC Neurol.* **17**, 4–9 (2017).
- Postuma, R. B. *et al.* REM sleep behavior disorder and neuropathology in Parkinson's disease. *Mov. Disord.* **30**, 1413–1417 (2015).
- Salzone, M. *et al.* Reduced thalamic volume in Parkinson disease with REM sleep behavior disorder: Volumetric study. *Parkinsonism Relat. Disord.* **20**, 1004–1008 (2014).
- Rahayel, S. *et al.* Brain atrophy in Parkinson's disease with polysomnography-confirmed REM sleep behavior disorder. *Sleep* **42**, 1–12 (2019).
- Boucetta, S. *et al.* Structural brain alterations associated with rapid eye movement sleep behavior disorder in Parkinson's disease. *Sci. Rep.* **6**, 26782 (2016).
- Kamps, S. *et al.* Smaller subcortical volume in Parkinson patients with rapid eye movement sleep behavior disorder. *Brain Imaging Behav.* **13**, 1352–1360 (2019).
- Zhu, R., Xie, C., Hu, P. & Wang, K. Clinical variations in Parkinson's disease patients with or without REM sleep behaviour disorder: A meta-analysis. *Sci. Rep.* **7**, 40779 (2017).
- Chahine, L. M. *et al.* Longitudinal changes in cognition in early Parkinson's disease patients with REM sleep behavior disorder. *Parkinsonism Relat. Disord.* **27**, 102–106 (2016).
- Trout, J. *et al.* Cognitive impairments and self-reported sleep in early-stage Parkinson's disease with versus without probable REM sleep behavior disorder. *Brain Sci.* **10**, 9 (2020).
- Jozwiak, N. *et al.* Rem sleep behavior disorder and cognitive impairment in Parkinson's disease. *Sleep* **40**, 8 (2017).
- Gallea, C. *et al.* Pedunculopontine network dysfunction in Parkinson's disease with postural control and sleep disorders. *Mov. Disord.* **32**, 693–704 (2017).
- Li, D. *et al.* Abnormal baseline brain activity in Parkinson's disease with and without REM sleep behavior disorder: A resting-state functional MRI study. *J. Magn. Reson. Imaging* **46**, 697–703 (2017).
- Jiang, X. *et al.* Abnormal gray matter volume and functional connectivity in Parkinson's disease with rapid eye movement sleep behavior disorder. *Parkinsons Dis.* **8851027** (2021).
- Telesford, Q. K., Simpson, S. L., Burdette, J. H., Hayasaka, S. & Laurienti, P. J. The brain as a complex system: Using network science as a tool for understanding the brain. *Brain Connect.* **1**, 295–308 (2011).
- Li, J. *et al.* Altered brain functional network in Parkinson disease with rapid eye movement sleep behavior disorder. *Front. Neurol.* **11**, 563624 (2020).
- Baggio, H. C. *et al.* Statistical inference in brain graphs using threshold-free network-based statistics. *Hum. Brain Mapp.* **39**, 2289–2302 (2018).
- Campabadal, A. *et al.* Disruption of posterior brain functional connectivity and its relation to cognitive impairment in idiopathic REM sleep behavior disorder. *NeuroImage Clin.* **25**, 102138 (2020).
- Uribe, C. *et al.* Patterns of cortical thinning in nondemented Parkinson's disease patients. *Mov. Disord.* **31**, 699–708 (2016).
- Frauscher, B. *et al.* Validation of the Innsbruck REM sleep behavior disorder inventory. *Mov. Disord.* **27**, 1673–1678 (2012).
- Aarsland, D., Brønnick, K., Larsen, J. P., Tysnes, O. B. & Alves, G. Cognitive impairment in incident, untreated Parkinson disease: The Norwegian ParkWest study. *Neurology* **72**, 1121–1126 (2009).
- Segura, B. *et al.* Cortical thinning associated with mild cognitive impairment in Parkinson's disease. *Mov. Disord.* **29**, 1495–1503 (2014).
- Doty, R. L. *The Smell Identification Test. Administration Manual.* (Sensonics, 1995).
- Tomlinson, C. L. *et al.* Systematic review of levodopa dose equivalency reporting in Parkinson's disease. *Mov. Disord.* **25**, 2649–2653 (2010).
- Pruim, R. H. R. *et al.* ICA-AROMA: A robust ICA-based strategy for removing motion artifacts from fMRI data. *Neuroimage* **112**, 267–277 (2015).
- Power, J. D., Barnes, K. A., Snyder, A. Z., Schlaggar, B. L. & Petersen, S. E. Spurious but systematic correlations in functional connectivity MRI networks arise from subject motion. *Neuroimage* **59**, 2142–2154 (2012).
- Zalesky, A., Fornito, A. & Bullmore, E. T. Network-based statistic: Identifying differences in brain networks. *Neuroimage* **53**, 1197–1207 (2010).
- Smith, S. M. & Nichols, T. E. Threshold-free cluster enhancement: Addressing problems of smoothing, threshold dependence and localisation in cluster inference. *Neuroimage* **44**, 83–98 (2009).
- Fan, L. *et al.* The human brainnetome Atlas: A new brain atlas based on connective architecture. *Cereb. Cortex* **26**, 3508–3526 (2016).
- Bullmore, E. & Sporns, O. Complex brain networks: Graph theoretical analysis of structural and functional systems. *Nat. Rev. Neurosci.* **10**, 186–198 (2009).
- Rubinov, M. & Sporns, O. Complex network measures of brain connectivity: Uses and interpretations. *Neuroimage* **52**, 1059–1069 (2010).
- Videnovic, A. *et al.* Increased REM sleep without atonia in Parkinson disease with freezing of gait. *Neurology* **81**, 1030–1035 (2013).
- Alibiglou, L., Videnovic, A., Planetta, P. J., Vaillancourt, D. E. & MacKinnon, C. D. Subliminal gait initiation deficits in rapid eye movement sleep behavior disorder: A harbinger of freezing of gait? *Mov. Disord.* **31**, 1711–1719 (2016).
- Göttlich, M. *et al.* Altered resting state brain networks in Parkinson's disease. *PLoS ONE* **8**, e77336 (2013).
- Luo, C. Y. *et al.* Functional connectome assessed using graph theory in drug-naive Parkinson's disease. *J. Neurol.* **262**, 1557–1567 (2015).
- Pereira, J. B. *et al.* Aberrant cerebral network topology and mild cognitive impairment in early Parkinson's disease. *Hum. Brain Mapp.* **36**, 2980–2995 (2015).
- Watts, D. J. & Strogatz, S. H. Collective dynamics of 'small-world' networks. *Nature* **393**, 440–442 (1998).
- Bassett, D. S. & Bullmore, E. T. Small-world brain networks revisited. *Neuroscientist* **23**, 499–516 (2017).

41. Stefani, A. *et al.* Long-term follow-up investigation of isolated rapid eye movement sleep without atonia without rapid eye movement sleep behavior disorder: A pilot study. *J. Clin. Sleep Med.* **11**, 1273–1279 (2015).
42. Kaufmann, H. *et al.* The natural history of pure autonomic failure: A U.S. prospective cohort. *Ann. Neurol.* **81**, 287–297 (2017).

## Acknowledgements

We thank the cooperation of the patients, their families and control subjects. We are also indebted to the Magnetic Resonance Imaging core facility of the IDIBAPS for the technical support, especially to C. Garrido, G. Lasso, V. Sanchez and A. Albaladejo; and we would also like to acknowledge the Centres de Recerca de Catalunya (CERCA) Programme/Generalitat de Catalunya, the Institute of Neurosciences, and the Institute of Biomedical Research August Pi i Sunyer (IDIBAPS). This study was sponsored by the Spanish Ministry of Economy and Competitiveness (PSI2017-86930-P) cofinanced by Agencia Estatal de Investigación (AEI) and the European Regional Development Fund (ERDF), and PID2020-114640GB-I00/MCIN/AEI/10.13039/501100011033, by Generalitat de Catalunya (2017SGR748), and supported by María de Maeztu Unit of Excellence (Institute of Neurosciences, University of Barcelona) MDM-2017-0729, Ministry of Science, Innovation and Universities. JO was supported by a 2018 fellowship from the Spanish Ministry of Science, Innovation and Universities Research and co-financed by the European Social Fund (PRE2018-086675). CU was supported by the European Union's Horizon 2020 research and innovation programme under the Marie Skłodowska-Curie fellowship (grant agreement 888692). YC has received funding in the past 5 years from FIS/FEDER, H2020 programme.

## Author contributions

C.J. and B.S. contributed to the design of the study. J.O., A.C. and B.S. contributed to the analysis of the data and J.O., A.C., B.S., C.U. and C.J. contributed to the interpretation of the data. J.O., A.C., B.S., and C.J. contributed to the draft of the article. J.O., A.C., B.S., C.U., M.J.M., Y.C., F.V., N.B., A.I. and C.J. revised the manuscript critically for important intellectual content and approved the final version of the manuscript.

## Competing interests

MJM received honoraria for advice and lecture from Abbvie, Bial and Merzt Pharma and grants from Michael J. Fox Foundation for Parkinson Disease (MJFF): MJF\_PPMI\_10\_001, PI044024. YC has received funding in the past five years from Union Chimique Belge (UCB pharma), Teva, Medtronic, Abbvie, Novartis, Merz, Piramal Imaging, and Esteve, Bial, and Zambon. YC is currently an associate editor for Parkinsonism and Related Disorders. JO, AC, BS, CU, FV, NB, AI and CJ declare no potential conflict of interest.

## Additional information

**Supplementary Information** The online version contains supplementary material available at <https://doi.org/10.1038/s41598-021-03751-5>.

**Correspondence** and requests for materials should be addressed to B.S.

**Reprints and permissions information** is available at [www.nature.com/reprints](http://www.nature.com/reprints).

**Publisher's note** Springer Nature remains neutral with regard to jurisdictional claims in published maps and institutional affiliations.



**Open Access** This article is licensed under a Creative Commons Attribution 4.0 International License, which permits use, sharing, adaptation, distribution and reproduction in any medium or format, as long as you give appropriate credit to the original author(s) and the source, provide a link to the Creative Commons licence, and indicate if changes were made. The images or other third party material in this article are included in the article's Creative Commons licence, unless indicated otherwise in a credit line to the material. If material is not included in the article's Creative Commons licence and your intended use is not permitted by statutory regulation or exceeds the permitted use, you will need to obtain permission directly from the copyright holder. To view a copy of this licence, visit <http://creativecommons.org/licenses/by/4.0/>.

© The Author(s) 2021

# Disrupted functional connectivity in PD with probable RBD and its cognitive correlates

Javier Oltra<sup>1,2</sup>, Anna Campabadal<sup>1,2</sup>, Barbara Segura<sup>1,2,3\*</sup>, Carme Uribe<sup>1,2,4</sup>, Maria Jose Marti<sup>2,3,5</sup>, Yaroslau Compta<sup>2,3,5</sup>, Francesc Valldeoriola<sup>2,3,5</sup>, Nuria Bargallo<sup>2,6</sup>, Alex Iranzo<sup>2,3,7</sup>, Carme Junque<sup>1,2,3</sup>

<sup>1</sup> Medical Psychology Unit, Department of Medicine, Institute of Neurosciences, University of Barcelona, Barcelona, Catalonia, Spain

<sup>2</sup> Institute of Biomedical Research August Pi i Sunyer (IDIBAPS), Barcelona, Catalonia, Spain

<sup>3</sup> Centro de Investigación Biomédica en Red Enfermedades Neurodegenerativas (CIBERNED), Hospital Clínic de Barcelona, Barcelona, Catalonia, Spain

<sup>4</sup> Research Imaging Centre, Campbell Family Mental Health Research Institute, Centre for Addiction and Mental Health (CAMH), University of Toronto, Toronto, Ontario, Canada

<sup>5</sup> Parkinson's Disease and Movement Disorders Unit, Neurology Service, Hospital Clínic de Barcelona, Institute of Neurosciences, University of Barcelona, Barcelona, Catalonia, Spain

<sup>6</sup> Centre de Diagnòstic per la Imatge, Hospital Clínic, Barcelona, Catalonia, Spain

<sup>7</sup> Multidisciplinary Sleep Unit, Neurology Service, Hospital Clínic de Barcelona, University of Barcelona, Barcelona, Catalonia, Spain

\*Corresponding author. Dr Barbara Segura. Medical Psychology Unit, Department of Medicine, University of Barcelona, Casanova 143, 08036, Barcelona, Catalonia, Spain. phone [+34] 934039297 // 93 4034446 Fax: [+34] 93 4035294. E-mail addres: bsegura@ub.edu (B.Segura).

E-mail addresses: joltra@ub.edu (J.Oltra), anna.campabadal@ub.edu (A. Campabadal), bsegura@ub.edu (B. Segura), carme.uribe@ub.edu (C.Uribe), mjmarti@clinic.cat (M.J. Marti), ycompta@clinic.cat (Y. Compta), fvalde@clinic.cat (F. Valldeoriola), bargallo@clinic.cat (N. Bargallo), airanzo@clinic.cat (A.Iranzo), cjunque@ub.edu (C. Junque).

## Supplementary Material

### Supplementary Table 1

Neuropsychological performance of PD-non pRBD and PD-pRBD.

<i>Test</i>	PD-non pRBD	PD-pRBD	Test stat (p-value)
MMSE	29.06 (1.24)	28.07 (2.93)	3.065 (0.086)
Digit Span			
Forward	5.38 (1.21)	5.44 (1.28)	0.212 (0.647)
Backward	3.97 (1.00)	4.11 (1.34)	0.149 (0.701)
Forward minus Backward	1.41 (1.41)	1.33 (1.21)	0.008 (0.928)
Phonetic fluency "p"	15.47 (6.04)	6.04 (5.29)	2.815 (0.099)
Semantic fluency "Animals"	16.94 (6.51)	15.07 (7.73)	1.010 (0.319)
Stroop			
Word	89.74 (17.42)	78.26 (23.32)	5.170 (0.027)
Color	56.32 (13.83)	47.92 (16.25)	4.463 (0.039)
Word-Color	34.55 (11.80)	26.96 (13.42)	4.711 (0.035)
TMT			
A	51.63 (35.24)	85.11 (98.20)	3.380 (0.071)
B	146.43 (143.93)	189.50 (215.69)	0.172 (0.680)
B minus A	96.07 (115.84)	138.73 (196.38)	0.236 (0.629)
SDMT	41.91 (14.79)	37.37 (18.38)	0.633 (0.430)
RAVLT			
Total	44.06 (10.38)	38.96 (11.38)	3.459 (0.068)
Recall	8.22 (3.66)	7.56 (3.46)	0.698 (0.407)
True recognition	13.22 (2.76)	13.44 (1.72)	0.034 (0.853)
JLO	23.81 (5.72)	22.00 (6.87)	1.064 (0.307)
BVFD	29.44 (2.61)	27.93 (4.11)	1.382 (0.245)
BFRT-short	21.66 (2.62)	20.96 (2.89)	0.088 (0.768)
BNT	13.56 (1.22)	13.48 (1.01)	0.128 (0.722)

Data are presented as mean (SD) of raw scores. Analyses of covariance (ANCOVA) with disease duration as covariate, followed by Bonferroni post-hoc tests.

Abbreviations: PD-non pRBD = Parkinson's disease patients without probable REM sleep behavior disorder; PD-pRBD = Parkinson's disease patients with probable REM sleep behavior disorder; MMSE = Mini-Mental State Examination; TMT = Trail Making Test; SDMT = Symbol Digit Modalities Test; RAVLT = Rey Auditory Verbal Learning Test; JLO = Benton Judgment of Line Orientation; BVFD = Benton Visual Form Discrimination; BFRT = Benton Facial Recognition Test; BNT = Boston Naming Test.



## Supplementary Table 2

Mild cognitive impairment distribution of the PD groups

	PD-non pRBD	PD-pRBD	Test stat (p-value)
MCI, n (%)	13 (40.6%)	14 (51.9%)	0.733 (0.388)

Pearson's chi-squared was used.

Abbreviations: MCI = mild cognitive impairment; PD-non pRBD = Parkinson's disease patients without probable REM sleep behavior disorder; PD-pRBD = Parkinson's disease patients with probable REM sleep behavior disorder.

### Supplementary Table 3

Neuropsychological performance descriptive statistics of PD-non pRBD and PD-pRBD on z-scores based on HC healthy control reference group<sup>24</sup>

<i>Test</i>	PD-non pRBD	PD-pRBD	HC
MMSE	-0.46 (1.34)	-1.53 (3.17)	-0.39 (1.01)
Digit Span			
Forward	-0.24 (0.84)	-0.20 (0.88)	-0.11 (0.92)
Backward	-0.10 (0.78)	0.01 (1.05)	0.00 (0.72)
Forward minus Backward	-0.24 (1.29)	-0.31 (1.10)	-0.19 (0.82)
Phonetic fluency "p"	-0.17 (1.24)	-0.62 (1.09)	-0.11 (1.22)
Semantic fluency "Animals"	-0.78 (1.21)	-1.12 (1.43)	-0.10 (0.76)
Stroop			
Word	-0.48 (1.05)	-1.17 (1.40)	-0.04 (0.92)
Color	-0.30 (0.93)	-0.87 (1.09)	0.24 (0.67)
Word-Color	0.03 (0.94)	-0.57 (1.07)	0.23 (0.72)
TMT			
A	-0.71 (2.09)	-2.70 (5.83)	0.04 (0.64)
B	-1.29 (3.62)	-2.37 (5.42)	-0.02 (1.16)
B minus A	-3.52 (2.79)	- 4.54 (4.73)	-2.57 (0.96)
SDMT	-0.46 (1.22)	-0.83 (1.51)	0.00 (0.70)
RAVLT			
Total	0.01 (1.51)	-0.73 (1.65)	0.29 (0.90)
Recall	-0.36 (1.63)	-0.65 (1.54)	0.18 (0.92)
True recognition	-0.26 (1.71)	-0.12 (1.07)	0.31 (0.81)
JLO	0.17 (1.18)	-0.20 (1.42)	0.46 (0.70)
BVFD	0.11 (0.86)	-0.39 (1.35)	0.02 (0.77)
BFRT-short	-0.19 (1.10)	-0.48 (1.21)	0.45 (0.82)
BNT	0.10 (0.98)	0.03 (0.81)	0.18 (0.71)

Data are presented as mean (SD) of z-scores.

Abbreviations: PD-non pRBD = Parkinson's disease patients without probable REM sleep behavior disorder; PD-pRBD = Parkinson's disease patients with probable REM sleep behavior disorder; HC = healthy controls; MMSE = Mini-Mental State Examination; TMT = Trail Making Test; SDMT = Symbol Digit Modalities Test; RAVLT = Rey Auditory Verbal Learning Test; JLO = Benton Judgment of Line Orientation; BVFD = Benton Visual Form Discrimination; BFRT = Benton Facial Recognition Test; BNT = Boston Naming Test.

<sup>24</sup> Cortical thinning associated with mild cognitive impairment in Parkinson's disease. *Mov. Disord.* **29**, 1495-1503 (2014).

### Supplementary Table 4

Connections with reduced functional connectivity in PD-pRBD patients compared with HC found by TFNBS

Cortico-cortical connections				
Node 1			Node 2	
Label	Cytoarchitectonic correspondence*		Label	Cytoarchitectonic correspondence
PCL_L_2_2	A4ll, area 4, (lower limb region)	—	CG_L_7_6	A23c, caudal area 24
PCL_L_2_2	A4ll, area 4, (lower limb region)	—	CG_R_7_6	A23c, caudal area 24
SFG_R_7_5	A6m, medial area 6	—	CG_L_7_4	A23v, ventral area 23
INS_R_6_2	vla, ventral agranular insula	—	CG_L_7_5	A24cd, caudodorsal area 24
INS_R_6_2	vla, ventral agranular insula	—	CG_L_7_6	A23c, caudal area 24
INS_R_6_2	vla, ventral agranular insula	—	CG_R_7_6	A23c, caudal area 24
STG_L_6_3	Te1.0 and Te1.2	—	CG_L_7_5	A24cd, caudodorsal area 24
STG_L_6_3	Te1.0 and Te1.2	—	CG_L_7_6	A23c, caudal area 24
STG_L_6_4	A22c, caudal area 22	—	CG_R_7_6	A23c, caudal area 24
STG_L_6_4	A22c, caudal area 22	—	IPL_R_6_4	A40c, caudal area 40 (PFm)
Cortico-DGM connections				
Node 1			Node 2	
Label	Cytoarchitectonic correspondence		Label	Cytoarchitectonic correspondence
SFG_R_7_5	A6m, medial area 6	—	Str_L_6_2	GP, globus pallidus
SFG_R_7_5	A6m, medial area 6	—	Str_L_6_6	dIPu, dorsolateral putamen
CG_R_7_6	A23c, caudal area 24	—	Tha_L_8_8	IPFtha, lateral pre-frontal thalamus
IPL_L_6_3	A40rd, rostradorsal area 40(PFt)	—	Str_L_6_4	vmPu, ventromedial putamen
IPL_R_6_4	A40c, caudal area 40(PFm)	—	Tha_L_8_8	IPFtha, lateral pre-frontal thalamus
MTG_R_4_3	A37dl, dorsolateral area 37	—	Amyg_L_2_2	lAmyg, lateral amygdala

Significant reduced connections in Parkinson's disease patients with probable REM sleep behavior disorder (PD-pRBD) compared with healthy controls (HC) found by threshold-free network-based statistics (TFNBS) with sex and maximum translation as covariates ( $p < 0.001$ , FWE corrected). Labels correspond with Brainnetome Atlas (see Supplementary Material 1 for more detail).

Abbreviations: CG = cingulate gyrus; INS = insular gyrus; IPL = inferior parietal lobule; L = left; MTG = middle temporal gyrus; PCL = paracentral lobule; R = right; SFG = superior frontal gyrus; STG = superior temporal gyrus; Str = striatum; Tha = thalamus.

\*Based on Fan, L. *et al.* The Human Brainnetome Atlas: A New Brain Atlas Based on Connectional Architecture. *Cereb. Cortex* **26**, 3508–3526 (2016).

### Supplementary Table 5

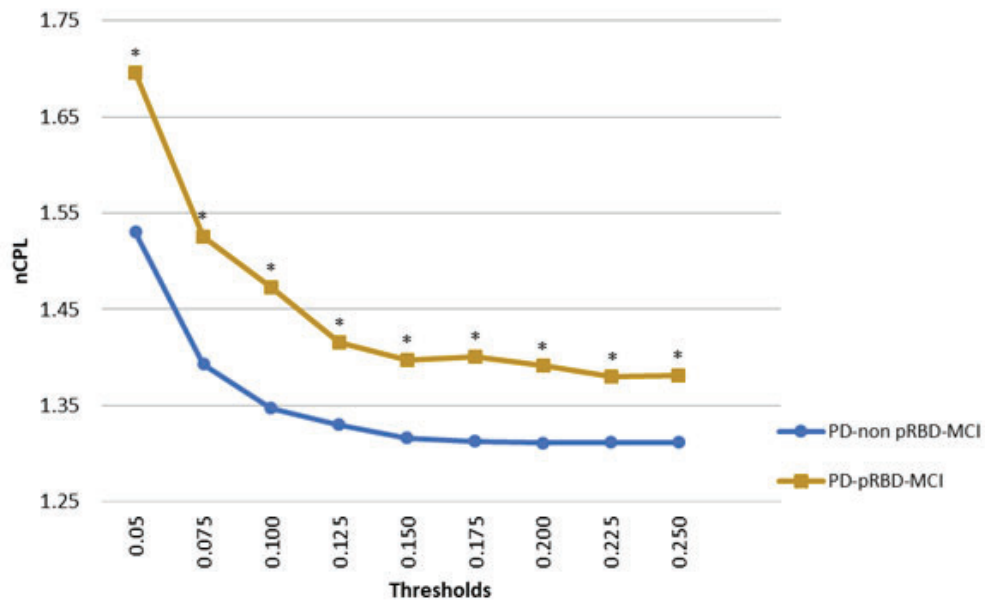
Summary of the sixteen significant reduced connections in PD-pRBD patients compared with HC found by TFNBS

<b>Cortico-cortical connections</b>				
	<b>Frontal-Limbic</b>	<b>Temporal-Parietal</b>	<b>Temporal-Limbic</b>	<b>Insular-Limbic</b>
	3	1	3	3
<b>Cortico-Deep gray matter connections</b>				
	<b>Frontal-DGM</b>	<b>Temporal-DGM</b>	<b>Parietal-DGM</b>	<b>Limbic-DGM</b>
	2	1	2	1
	<b>LH-LH</b>	<b>RH-RH</b>	<b>LH-RH/RH-LH</b>	
	4	1	11	

Summary of the significant reduced connections in Parkinson's disease patients with probable REM sleep behavior disorder (PD-pRBD) compared with healthy controls (HC) found by threshold-free network-based statistics (TFNBS) with sex and maximum translation as covariates ( $p < 0.001$ , FWE corrected).

Abbreviations: DGM = deep gray matter; LH = Left hemisphere; RH = Right hemisphere.

**Supplementary Figure 1.** Shows the normalized characteristic path length (nCPL) increment in PD-pRBD-MCI patients compared with PD-non pRBD-MCI. Normalized characteristic path length (vertical axis) as a function of sparsity thresholds (horizontal axis) for PD-pRBD-MCI and PD-non pRBD-MCI. (\*) indicate significant differences between PD-non pRBD-MCI and PD-pRBD-MCI.



## Supplementary Methods 1

Brainnetome atlas nodes and corresponding anatomical regions

<b>Cingulate</b>
CG_L(R)_7_1, CG_L(R)_7_2, CG_L(R)_7_3, CG_L(R)_7_4, CG_L(R)_7_5, CG_L(R)_7_6, CG_L(R)_7_7
<b>Frontal</b>
SFG_L(R)_7_1, SFG_L(R)_7_2, SFG_L(R)_7_3, SFG_L(R)_7_4, SFG_L(R)_7_5, SFG_L(R)_7_6, SFG_L(R)_7_7, MFG_L(R)_7_1, MFG_L(R)_7_2, MFG_L(R)_7_3, MFG_L(R)_7_4, MFG_L(R)_7_5, MFG_L(R)_7_6, MFG_L(R)_7_7, IFG_L(R)_6_1, IFG_L(R)_6_2, IFG_L(R)_6_3, IFG_L(R)_6_4, IFG_L(R)_6_5, IFG_L(R)_6_6, OrG_L(R)_6_1, OrG_L(R)_6_2, OrG_L(R)_6_3, OrG_L(R)_6_4, OrG_L(R)_6_5, OrG_L(R)_6_6, PrG_L(R)_6_1, PrG_L(R)_6_2, PrG_L(R)_6_3, PrG_L(R)_6_4, PrG_L(R)_6_5, PrG_L(R)_6_6, PCL_L(R)_2_1, PCL_L(R)_2_2
<b>Insula</b>
INS_L(R)_6_1, INS_L(R)_6_2, INS_L(R)_6_3, INS_L(R)_6_4, INS_L(R)_6_5, INS_L(R)_6_6
<b>Medial temporal</b>
FuG_L(R)_3_1, FuG_L(R)_3_2, FuG_L(R)_3_3, PhG_L(R)_6_1, PhG_L(R)_6_2, PhG_L(R)_6_3, PhG_L(R)_6_4, PhG_L(R)_6_5, PhG_L(R)_6_6, Amyg_L(R)_2_1, Amyg_L(R)_2_2, Hipp_L(R)_2_1, Hipp_L(R)_2_2
<b>Occipital</b>
MVOcC_L(R)_5_1, MVOcC_L(R)_5_2, MVOcC_L(R)_5_3, MVOcC_L(R)_5_4, MVOcC_L(R)_5_5, LOcC_L(R)_4_1, LOcC_L(R)_4_2, LOcC_L(R)_4_3, LOcC_L(R)_4_4, LOcC_L(R)_2_1, LOcC_L(R)_2_2
<b>Parietal</b>
SPL_L(R)_5_1, SPL_L(R)_5_2, SPL_L(R)_5_3, SPL_L(R)_5_4, SPL_L(R)_5_5, IPL_L(R)_6_1, IPL_L(R)_6_2, IPL_L(R)_6_3, IPL_L(R)_6_4, IPL_L(R)_6_5, IPL_L(R)_6_6, Pcun_L(R)_4_1, Pcun_L(R)_4_2, Pcun_L(R)_4_3, Pcun_L(R)_4_4, PoG_L(R)_4_1, PoG_L(R)_4_2, PoG_L(R)_4_3, PoG_L(R)_4_4
<b>Striatum</b>
STR_L(R)_6_1, STR_L(R)_6_2, STR_L(R)_6_3, STR_L(R)_6_4, STR_L(R)_6_5, STR_L(R)_6_6
<b>Temporal</b>
STG_L(R)_6_1, STG_L(R)_6_2, STG_L(R)_6_3, STG_L(R)_6_4, STG_L(R)_6_5, STG_L(R)_6_6, MTG_L(R)_4_1, MTG_L(R)_4_2, MTG_L(R)_4_3, MTG_L(R)_4_4, ITG_L(R)_7_1, ITG_L(R)_7_2, ITG_L(R)_7_3, ITG_L(R)_7_4, ITG_L(R)_7_5, ITG_L(R)_7_6, ITG_L(R)_7_7, pSTS(R)_2_1, pSTS_L(R)_2_2
<b>Thalamus</b>
Tha_L(R)_8_1, Tha_L(R)_8_2, Tha_L(R)_8_3, Tha_L(R)_8_4, Tha_L(R)_8_5, Tha_L(R)_8_6, Tha_L(R)_8_7, Tha_L(R)_8_8

This table collects all the nodes used in the functional connectivity and graph analyses and facilitates results interpretation. Further, the correspondence between label names with specific areas into the brain regions and corresponding MNI coordinates can be consulted on <http://cercor.oxfordjournals.org/content/26/8/3508.full.pdf>.

Abbreviations: CG = cingulate gyrus; SFG = superior frontal gyrus; MFG = middle frontal gyrus; IFG = inferior frontal gyrus; OrG = orbital gyrus; PrG = precentral gyrus; PCL = paracentral

lobule; INS= insula; FuG = fusiform gyrus; PhG = parahippocampal gyrus; Amyg = amygdala; Hipp = hippocampus; MVOcC = medioventral occipital cortex; LOcC = lateral occipital cortex; SPL = superior parietal lobule; IPL = inferior parietal lobule; Pcun = precuneus; PoG = postcentral gyrus; Str = striatum; STG = superior temporal gyrus; MTG = middle temporal gyrus; ITG = inferior temporal gyrus; pSTS = posterior superior temporal sulcus; Tha = thalamus.





## Study 3

---

**Oltra J, Uribe C, Campabadal A, Inguanzo A, Monté-Rubio GC, Martí MJ, Compta Y, Valldeoriola F, Iranzo, A, Junque C, Segura B.** Sex differences in brain and cognition in *de novo* Parkinson's disease. *Frontiers in Aging Neuroscience*. 2022; 13: 791532. doi: 10.3389/fnagi.2021.791532.



# Sex Differences in Brain and Cognition in *de novo* Parkinson's Disease

Javier Oltra<sup>1,2</sup>, Carme Uribe<sup>1,2,3</sup>, Anna Campabadal<sup>1,2</sup>, Anna Inguanzo<sup>1,2</sup>, Gemma C. Monté-Rubio<sup>1</sup>, Maria J. Martí<sup>2,4,5</sup>, Yaroslau Compta<sup>2,4,5</sup>, Francesc Valdeoriola<sup>2,4,5</sup>, Carme Junque<sup>1,2,4</sup> and Barbara Segura<sup>1,2,4\*</sup>

<sup>1</sup> Medical Psychology Unit, Department of Medicine, Institute of Neurosciences, University of Barcelona, Barcelona, Spain, <sup>2</sup> Institute of Biomedical Research August Pi i Sunyer (IDIBAPS), Barcelona, Spain, <sup>3</sup> Research Imaging Centre, Centre for Addiction and Mental Health, Campbell Family Mental Health Research Institute, University of Toronto, Toronto, ON, Canada, <sup>4</sup> Centro de Investigación Biomédica en Red sobre Enfermedades Neurodegenerativas, Hospital Clínic de Barcelona, Barcelona, Spain, <sup>5</sup> Parkinson's Disease and Movement Disorders Unit, Neurology Service, Hospital Clínic de Barcelona, Institute of Neurosciences, University of Barcelona, Barcelona, Spain

## OPEN ACCESS

### Edited by:

Ana I. Duarte,  
University of Coimbra, Portugal

### Reviewed by:

Saul Martínez-Horta,  
Hospital de la Santa Creu i Sant Pau,  
Spain

Gabriel Gonzalez-Escamilla,  
Johannes Gutenberg University  
Mainz, Germany  
Richard Camicioli,  
University of Alberta, Canada

### \*Correspondence:

Barbara Segura  
bsegura@ub.edu

### Specialty section:

This article was submitted to  
Parkinson's Disease and Aging-related  
Movement Disorders,  
a section of the journal  
Frontiers in Aging Neuroscience

Received: 08 October 2021

Accepted: 13 December 2021

Published: 06 January 2022

### Citation:

Oltra J, Uribe C, Campabadal A, Inguanzo A, Monté-Rubio GC, Martí MJ, Compta Y, Valdeoriola F, Junque C and Segura B (2022) Sex Differences in Brain and Cognition in *de novo* Parkinson's Disease. *Front. Aging Neurosci.* 13:791532. doi: 10.3389/fnagi.2021.791532

**Background and Objective:** Brain atrophy and cognitive impairment in neurodegenerative diseases are influenced by sex. We aimed to investigate sex differences in brain atrophy and cognition in *de novo* Parkinson's disease (PD) patients.

**Methods:** Clinical, neuropsychological and T1-weighted MRI data from 205 PD patients (127 males: 78 females) and 69 healthy controls (40 males: 29 females) were obtained from the PPMI dataset.

**Results:** PD males had a greater motor and rapid eye movement sleep behavior disorder symptomatology than PD females. They also showed cortical thinning in postcentral and precentral regions, greater global cortical and subcortical atrophy and smaller volumes in thalamus, caudate, putamen, pallidum, hippocampus, and brainstem, compared with PD females. Healthy controls only showed reduced hippocampal volume in males compared to females. PD males performed worse than PD females in global cognition, immediate verbal recall, and mental processing speed. In both groups males performed worse than females in semantic verbal fluency and delayed verbal recall; as well as females performed worse than males in visuospatial function.

**Conclusions:** Sex effect in brain and cognition is already evident in *de novo* PD not explained by age *per se*, being a relevant factor to consider in clinical and translational research in PD.

**Keywords:** Parkinson's disease, sex differences, magnetic resonance imaging, gray matter atrophy, cognitive impairment

## INTRODUCTION

Parkinson's disease (PD) has a 2-fold higher incidence in males reported in early population-based studies (Baldereschi et al., 2000). Consistent with previous meta-analytic studies (Wooten et al., 2004; Taylor et al., 2007), the most recent data revealed that the male-female ratio is around 1.50 for prevalence and incidence (Moisan et al., 2016). Moreover, the male sex in PD is associated with earlier disease onset, more severe motor symptoms and progression, and more frequent cognitive

decline compared with the female sex (Meoni et al., 2020). Previous literature suggested that the neuroprotective effect of estrogens could be one of the key factors to explain such differences (Meoni et al., 2020).

Neuropsychological studies show that PD males had worse performance than PD females in global cognition (Szewczyk-Krolikowski et al., 2014; Liu et al., 2015; Lin et al., 2018; Bakeberg et al., 2021), memory (Liu et al., 2015; Lin et al., 2018; Bakeberg et al., 2021), verbal fluency (Szewczyk-Krolikowski et al., 2014; Lin et al., 2018; Reekes et al., 2020; Bakeberg et al., 2021), processing speed (Lin et al., 2018; Reekes et al., 2020), and inhibition (Reekes et al., 2020) tasks. By contrast, females have increased impairment in visuospatial functions (Liu et al., 2015; Lin et al., 2018; Bakeberg et al., 2021). A recent meta-analysis highlights that twenty-two studies reported segregated results for males and females regarding executive functions, ten for visuospatial skills, and nine for memory. In this context, significant effect sizes showed more impairment in males for executive functions (Curtis et al., 2019). Moreover, a longitudinal study involving a large sample of PD concluded that females had a lower risk of developing cognitive impairment (Iwaki et al., 2021). Cognitive decline is more pronounced in males (Liu et al., 2017; Bakeberg et al., 2021), and there is an increased rate of progression to mild cognitive impairment (Cholerton et al., 2018; Bakeberg et al., 2021) and dementia in males (Cholerton et al., 2018).

A recent review highlighted the lack of neuroimaging studies centered on sex differences in PD, despite the clinical and epidemiological evidence (Salminen et al., 2021). To our knowledge, there are only two structural magnetic resonance imaging (MRI) studies testing sex differences in gray matter brain atrophy. Yadav et al. reported significant thinning in several cortical regions in males compared to females in treated PD using cortical thickness (CTh) (Yadav et al., 2016). In *de novo* PD patients, Tremblay et al. did not find sex differences in CTh (Tremblay et al., 2020). However, deformed-based morphometry (DBM) analyses showed sex differences in cortical regions in both directions. Males had more atrophy than females in eleven regions whereas females had more atrophy than males in only six regions. Regarding subcortical gray matter atrophy by DBM, they found more atrophy in males than females in the left thalamus. Thus, the authors concluded that males with *de novo* PD overall had more regional atrophy than females, mainly in cortical regions. In addition, both mentioned works found male-specific structural connectivity disruptions in PD (Yadav et al., 2016; Tremblay et al., 2020).

In this study, our main objective is to analyze sex differences in brain atrophy in a large sample of newly diagnosed drug-naïve PD patients, *de novo* PD patients. We used, for the first time, with that purpose global and subcortical volumetry, as well as cortical thickness analyses. We also analyzed sex differences in neuropsychological performance.

## METHODS

### Participants

Two hundred and five *de novo* PD patients and 69 healthy controls from the Parkinson's Progression Markers Initiative

database (PPMI, for up-to-date information of the study visit <http://www.ppmi-info.org>) (Marek et al., 2011), classified by sex: 127 *de novo* PD males, 78 *de novo* PD females, 40 control males, and 29 control females. All participating PPMI sites received approval from an ethical standards committee and obtained written informed consent from all participants in the study.

Inclusion criteria for PD were: (a) recent PD diagnosis with asymmetric resting tremor or asymmetric bradykinesia, or two from among bradykinesia, resting tremor, and rigidity; (b) absence of levodopa intake; (c) DaTSCAN evidence of significant dopamine transporter deficit consistent with PD diagnosis. Inclusion criteria for both groups were: (d) T1-weighted images available; and (e) age older than 50 and younger than 85 years old. Exclusion criteria were: (a) diagnosis of dementia; (b) significant psychiatric, neurologic, or systemic comorbidity; (c) a first-degree family member with PD; and (d) presence of MRI motion artifacts, field distortions, intensity inhomogeneities, or detectable structural brain lesions. The flow diagram of sample selection is shown in **Supplementary Figure 1**, see **Supplementary Methods 1** to comorbidity exclusion reasons after MRI preprocessing.

### Clinical and Neuropsychological Assessments

Clinical assessment included disease severity measured by the Movement Disorders Society Unified PD Rating Scale (MDS-UPDRS) and motor severity by the MDS-UPDRS motor section (MDS-UPDRS Part III), disease stage by Hoehn and Yahr scale (H&Y), general cognition by Montreal Cognitive Assessment (MoCA), and rapid eye movement sleep behavior disorder (RBD) symptomatology by the REM Sleep Behavior Disorder Screening Questionnaire (RBDSQ) (Marek et al., 2011). Neuropsychological battery included: phonemic (letter "f") and semantic (animals, fruits and vegetables) verbal fluency; Symbol Digit Modalities Test (SDMT); Letter-Number Sequencing (LNS); Benton Judgment of Line Orientation 15-item short form (JLO); and Hopkins Verbal Learning Test-Revised (HVLT-R) (Marek et al., 2011). Neuropsychological measures were z-scored calculated based on the control group's means and standard deviations.

### MRI Images

T1-weighted scans were acquired using 1.5 or 3-Tesla scanners using magnetization prepared rapid gradient-echo imaging (MPRAGE) sequences. Typical parameters were repetition time = 5–11 ms; echo time = 2–6 ms; slice thickness 1–1.5 mm; inter-slice gap 0 mm; voxel size 1 × 1 × 1.2 mm; matrix 256 × 160 minimum. There were no differences in the distribution of 1.5 and 3-Tesla images across groups (**Supplementary Table 1**).

CTh, subcortical and cortical volumes were estimated using the automated processing stream and specific segmentation tools of FreeSurfer (version 6.0, <https://surfer.nmr.mgh.harvard.edu>). The main preprocessing procedures are removal of non-brain data, intensity normalization (Fischl et al., 2001), tessellation of the gray matter (GM)/white matter (WM) boundary, automated topology correction (Dale et al., 1999; Ségonne et al., 2007), accurate surface deformation to identify tissue borders (Dale and Sereno, 1993; Fischl and Dale, 2000; Fischl et al., 2002), cortical

thickness calculation as the distance between the WM and GM surfaces at each vertex of the reconstructed cortical mantle (Fischl et al., 2002). After preprocessing and quality control (check the accuracy of registration, skull stripping, segmentation, and cortical surface reconstruction), errors were fixed by automated and manual interventions following standard procedures and were discarded when correction was not possible. The smoothing of the maps of CTh was fixed at full width half maximum (FWHM) of 15 mm of a circularly symmetric Gaussian kernel across the surface. Global average thickness for both hemispheres was calculated  $([lh\ thickness * lh\ surface\ area] + [rh\ thickness * rh\ surface\ area]) / [lh\ surface\ area + rh\ surface\ area]$ .

The used atlas for volumetry corresponds to the Automatic Subcortical Segmentation Atlas (Aseg Atlas) (Fischl et al., 2002). Deep gray GM mean volumes, estimated total intracranial volume (eTIV), total cortical and subcortical GM were also estimated (Fischl et al., 2002). GM volumes were bilateralized  $[(left\ volume + right\ volume) / 2]$  and transformed to ratios in percentages  $[(volume / eTIV) * 100]$ .

## Statistical Analyses

The main effects of group and sex were computed for sociodemographic variables by two-way analysis of variance (ANOVA) applying Bonferroni correction for quantitative measures to *post-hoc* tests. The main effect of sex, the within-group effect of sex and the group-by-sex interaction were computed for clinical, neuropsychological, and MRI volumetry measures by two-way analyses of covariance (ANCOVA), Bonferroni correction was applied to *post-hoc* tests and partial eta squared was computed. Pearson's chi-squared tests were used to compute differences in categorical measures. Differences in age of onset and disease duration were computed by *t*-test. Analyses were performed with IBM SPSS Statistics 27.0.0 (2020; IBM Corp., Armonk, NY).

Inter-group whole-brain CTh comparisons were performed in FreeSurfer v6.0 using a vertex-by-vertex general linear model; including CTh as a dependent factor, group as an independent factor, and demeaned age and years of education as covariates. All results were corrected for multiple comparisons using a pre-cached cluster-wise Monte Carlo simulation with 10,000 iterations.

For all analyses, the statistical significance threshold was set at  $p < 0.05$ .

## RESULTS

### Clinical Characteristics

Males were significantly older than females in the PD and healthy control groups, as well that the control group had more years of education than the PD group (Table 1). Subsequent analyses included age and years of education as covariates as required.

A significant sex effect was found in motor severity (MDS-UPDRS Part III) in the PD group. Despite similar disease duration, males had more severe motor symptoms than females. Moreover, *post-hoc* tests showed that in the PD group, males had more RBD symptoms (RBDSQ) than females (Table 1).

## Neuropsychological Performance

There was a significant sex effect in semantic fluency, JLO, and HVLT-R delayed recall. A significant group-by-sex interaction was found in MoCA ( $F = 4.215$ ,  $p = 0.041$ ,  $\eta^2 = 0.015$ ). In the PD group, *post-hoc* tests revealed that males performed worse than females in MoCA, semantic fluency, SDMT, and HVLT-R immediate and delayed recall. As well, in the healthy control group, males performed lower than females in semantic fluency and HVLT-R immediate recall. In both groups, females had lower scores than males in the JLO (Figure 1; Table 2; Supplementary Table 2).

## MRI-Derived Measures

There was a significant effect of sex in global GM volumes, *post-hoc* tests revealed that in the PD group males had smaller total cortical and subcortical GM volumes than females. Regarding subcortical volumetry, a significant main effect of sex was found in the bilateral thalamus, caudate, putamen, and hippocampus. *Post-hoc* tests showed that in the PD group, males had smaller volumes than females in the bilateral thalamus, caudate, putamen, pallidum, hippocampus, and brainstem. Within the healthy control group, males had smaller bilateral volume than females in the hippocampus (Table 3; Supplementary Table 3).

Vertex-wise analyses revealed sex effects in cortical thickness in the PD group, males had thinning in left postcentral (MNI coordinates:  $x, y, z = -43, -30, 62$ ; cluster size = 3,485.90 mm<sup>2</sup>;  $t$ -stat = 5.007,  $p < 0.001$ ) and right precentral (MNI coordinates:  $x, y, z = 12, -26, 68$ ; cluster size = 2,499.75 mm<sup>2</sup>;  $t$ -stat = 4.0728,  $p = 0.006$ ) compared with females (Figure 2).

## DISCUSSION

Our results point to a more severe clinical, cognitive, and neurodegenerative profile in *de novo* PD males compared with *de novo* PD females, despite similar disease duration and adjusting the results by age and education. Clinically, PD males had increased motor severity (MDS-UPSRS Part III) than PD females. This result is in keeping with increased cortical thinning in cortical motor region, as well as increased volume reductions in the bilateral thalamus and basal ganglia structures such as putamen, pallidum, and caudate after controlling by eTIV.

There is only one similar study performed with a *de novo* PD sample investigating the brain differences between sexes (Tremblay et al., 2020). In that study, the authors did not find sex-related differences in CTh and found larger volume in PD females than PD males in the left thalamus by DBM means. In the PD group, our results showed larger subcortical gray matter volume in females than in males in the bilateral thalamus. This result partially agrees with the mentioned result that showed reduced left thalamus volume in males compared with females. Remarkably, different atlases were used to define subcortical structures. Furthermore, the differences in the CTh results between both studies could be explained by differences in the estimation pipelines (Masouleh et al., 2020), and the statistical analysis software employed, as well as the MRI analytical approaches based on CTh atlas-based parcellations or whole-brain vertex-wise CTh maps.

**TABLE 1** | Demographic and clinical characteristics of PD and HC females and males.

		PD	HC	Sex main effect test stat (P-value)	Group main effect F stat (P-value)
Age, y	F	61.76 (7.50)	60.55 (5.86)	7.471 (0.007) <sup>a,b</sup>	0.223 (0.637)
	M	63.80 (7.24)	64.05 (7.11)		
Education, y	F	15.36 (2.96)	16.24 (2.86)	2.588 (0.109)	5.820 (0.017)
	M	15.91 (2.96)	17.00 (2.48)		
Age of onset, y	F	60.81 (7.52)		1.947 (0.053)	
	M	62.84 (7.10)			
Disease duration, m	F	10.50 (7.93)		0.310 (0.757)	
	M	10.82 (6.64)			
MDS-UPDRS	F	29.58 (10.69)		3.369 (0.068)	
	M	33.17 (13.04)			
Part III	F	18.62 (7.56)		5.510 (0.020)	
	M	21.62 (8.86)			
H&Y, n, 1/2/3	F	32/45/1		0.284 (0.867)	
	M	56/70/1			
RBDSQ	F	3.73 (1.99)	1.52 (1.21)	2.557 (0.111) <sup>a</sup>	58.211 (<0.001)
	M	4.53 (2.73)	1.88 (1.40)		

Data are presented by groups as mean (SD), except for H&Y. Two-way analyses of variance (ANOVA) with post-hoc tests corrected by Bonferroni were used for all demographic variables. Two-way analyses of covariance (ANCOVA) with age as a covariate with post-hoc tests corrected by Bonferroni were used for all clinical variables. Except for age of onset and PD duration, by two-sample t-test and H&Y, by Pearson's chi-squared.

<sup>a</sup>Sex differences in PD group ( $p < 0.05$ ).

<sup>b</sup>Sex differences in HC group ( $p < 0.05$ ).

F, female; H&Y, Hoehn and Yahr scale; HC, healthy control; m, months; M, male; MDS-UPDRS, Movement Disorder Society Unified Parkinson's Disease Rating Scale; PD, Parkinson's disease; RBDSQ, REM Sleep Behavior Disorder Screening Questionnaire; y, years.

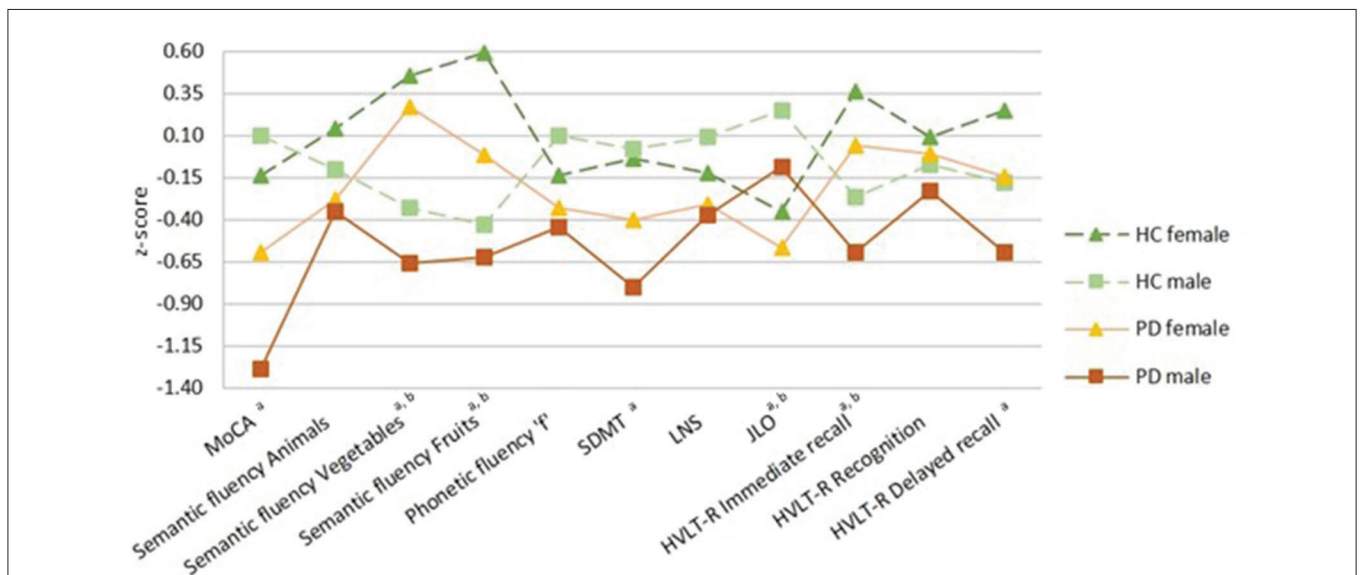


**FIGURE 1** | Neuropsychological performance. Healthy controls (HC) groups in green, Parkinson's disease (PD) groups in warm colors; darker for females and lighter for males. Females represented by filled triangles and males by filled squares. PD by a discontinuous line and HC by a continuous line. Data are presented as z-scores. Lower z-scores indicate worse performance. Two-way analyses of covariance (ANCOVA) with age and education as covariates with *post-hoc* tests corrected by Bonferroni were used for all variables. MoCA, Montreal Cognitive Assessment; SDMT, Symbol Digit Modalities Test; LNS, Letter-Number Sequencing; JLO, Benton Judgment of Line Orientation; HVLT-R, Hopkins Verbal Learning Test-Revised. <sup>a</sup>Sex differences in PD group, <sup>b</sup>sex differences in HC group ( $p < 0.05$ ).

We found cortical thinning in *de novo* PD males compared with *de novo* PD females in the left postcentral and right precentral areas. A previous study including treated PD patients

with larger disease duration (between 2.13 and 3.69 years) reported cortical thinning in PD males in the left precentral and right postcentral areas compared with PD females. As well,

**TABLE 2** | Neuropsychological performance of PD and HC females and males.

		PD		HC		Sex main effect F stat (P-value)	Partial eta squared
		Mean (SD)	Median (IQR)	Mean (SD)	Median (IQR)		
MoCA	F	-0.559 (1.742)	-0.078 (2.62)	-0.139 (0.900)	-0.078 (1.74)	1.047 (0.307) <sup>a</sup>	0.004
	M	-1.287 (1.884)	-0.950 (2.62)	0.096 (1.067)	-0.078 (1.74)		
Semantic fluency							
Animals	F	-0.278 (0.885)	-0.490 (1.11)	0.141 (0.970)	0.065 (1.11)	1.022 (0.313)	0.004
	M	-0.351 (0.951)	-0.490 (1.29)	-0.102 (1.021)	-0.305 (1.11)		
Vegetables	F	0.271 (1.098)	0.157 (1.36)	0.457 (1.031)	0.700 (1.36)	32.796 (<0.001) <sup>a,b</sup>	0.110
	M	-0.658 (1.052)	-0.927 (1.63)	-0.331 (0.845)	-0.385 (1.29)		
Fruits	F	-0.018 (0.901)	-0.123 (1.20)	0.592 (0.806)	0.600 (0.96)	37.032 (<0.001) <sup>a,b</sup>	0.122
	M	-0.624 (0.962)	-0.846 (1.45)	-0.430 (0.910)	-0.605 (1.20)		
Phonetic fluency "f"	F	-0.308 (0.975)	-0.404 (1.10)	-0.134 (0.916)	-0.294 (1.44)	0.002 (0.963)	0.000
	M	-0.440 (1.009)	-0.515 (1.33)	0.098 (1.057)	-0.073 (1.05)		
SDMT	F	-0.403 (0.934)	-0.348 (1.23)	-0.034 (0.857)	-0.292 (1.12)	0.543 (0.462) <sup>a</sup>	0.002
	M	-0.799 (1.020)	-0.623 (1.34)	0.024 (1.102)	0.100 (1.37)		
LNS	F	-0.307 (0.922)	-0.124 (1.16)	-0.124 (0.907)	-0.124 (1.55)	0.898 (0.344)	0.003
	M	-0.370 (1.042)	-0.510 (1.16)	0.089 (1.065)	-0.124 (1.45)		
JLO	F	-0.564 (1.176)	-0.187 (1.75)	-0.348 (1.125)	-0.187 (1.17)	12.665 (<0.001) <sup>a,b</sup>	0.045
	M	-0.086 (1.164)	0.397 (1.75)	0.251 (0.824)	0.397 (1.17)		
HVLTR							
Immediate recall	F	0.046 (0.986)	0.027 (1.14)	0.366 (0.897)	0.485 (1.26)	2.916 (0.089) <sup>a,b</sup>	0.059
	M	-0.594 (1.148)	-0.430 (1.60)	-0.264 (0.997)	-0.423 (1.54)		
Recognition	F	-0.010 (0.854)	0.340 (0.93)	0.095 (0.879)	0.340 (0.62)	1.632 (0.203)	0.006
	M	-0.230 (0.940)	0.031 (0.62)	-0.070 (1.085)	0.031 (0.85)		
Delayed recall	F	-0.144 (0.935)	-0.078 (1.55)	0.249 (0.768)	0.335 (0.83)	10.240 (0.002) <sup>a</sup>	0.037
	M	-0.596 (1.078)	-0.492 (1.65)	-0.182 (1.114)	-0.078 (1.65)		

Data are presented in z-scores. Two-way analyses of covariance (ANCOVA) with age and education as covariates with post-hoc tests corrected by Bonferroni were used for all variables.

<sup>a</sup>Sex differences in PD group ( $p < 0.05$ ).

<sup>b</sup>Sex differences in HC group ( $p < 0.05$ ).

F, female; HC, healthy control; HVLTR, Hopkins Verbal Learning Test-Revised; JLO, Benton Judgment of Line Orientation; LNS, Letter-Number Sequencing; M, male; MoCA, Montreal Cognitive Assessment; PD, Parkinson's disease; SDMT, Symbol Digit Modalities Test.

significant thinning in temporal and occipital regions in PD males compared with PD females (Yadav et al., 2016). These results might suggest sex differences in brain atrophy associate with the illness progression. However, longitudinal MRI studies are required.

Adult males have larger volumes than females in some subcortical gray matter structures, such as the nuclei accumbens, according to a study performed in a sample of 5,216 participants with an age range between 44 and 77 years (Ritchie et al., 2018); as well as, the amygdala, hippocampus, and putamen, according to other study performed in a sample of 2,838 participants with and age range between 21 and 90 years (Lotze et al., 2019), both controlling for age and total brain volume. In our study, sex differences in PD could be attributed to the neurodegenerative process rather than normal aging because, in healthy controls, we only found sex differences in the hippocampus. Nevertheless, it is noteworthy that the sample used in our study is modest in comparison to previous population-based studies reporting subcortical volumetric differences in healthy subjects. The pattern of atrophy in PD that we have found showed that males have reduced volumes of subcortical

nuclei compared with females, thus is the reversed pattern seen in general adult population suggesting a more marked degeneration in males or protective effect of female sex. In this regard, dysregulated gene expression and sex hormones might explain sex differences in PD. Vulnerability in the dopaminergic system, neuroinflammatory cells, and oxidative stress has been suggested as mechanisms that influence sex differences in PD (Cerri et al., 2019).

The neuropsychological results are also in agreement with greater global atrophy in males. Cognitive results showed that PD males had worse performance than PD females in general cognition (MoCA), processing speed (SDMT), and verbal memory (HVLTR delayed recall). These results agree with previous findings in *de novo* PD showing more impairment in males than females in general cognition (Szewczyk-Krolkowski et al., 2014; Liu et al., 2015; Lin et al., 2018), verbal memory (Liu et al., 2015; Lin et al., 2018), and processing speed (Lin et al., 2018). We obtained sex differences in visuospatial function, in which females performed worse than males in PD and control groups. This result is consistent with previous findings in *de novo* PD (Liu et al., 2015; Lin et al., 2018), and it would reflect

**TABLE 3** | MRI-derived measures of between sex comparisons of PD and HC females and males.

		PD		HC		Sex main effect F stat (P-value)	Partial eta squared
		Mean (SD)	Median (IQR)	Mean (SD)	Median (IQR)		
<b>Global atrophy</b>							
Cortical	F	29.598 (2.266)	29.360 (2.07)	30.114 (1.800)	30.091 (2.46)	8.721 (0.003) <sup>a</sup>	0.032
	M	28.149 (2.153)	28.309 (2.29)	29.387 (2.256)	29.246 (2.42)		
Subcortical	F	3.642 (0.282)	3.603 (0.39)	3.686 (0.270)	3.640 (0.38)	12.188 (< 0.001) <sup>a</sup>	0.043
	M	3.467 (0.244)	3.452 (0.33)	3.544 (0.280)	3.496 (0.25)		
Mean CTh	F	2.415 (0.095)	2.426 (0.11)	2.436 (0.102)	2.416 (0.10)	1.051 (0.306)	0.004
	M	2.389 (0.119)	2.415 (0.14)	2.411 (0.124)	2.412 (0.14)		
<b>Deep GM nuclei</b>							
Thalamus	F	0.462 (0.043)	0.468 (0.06)	0.460 (0.030)	0.457 (0.04)	7.874 (0.005) <sup>a</sup>	0.029
	M	0.436 (0.039)	0.434 (0.05)	0.443 (0.046)	0.443 (0.07)		
Caudate	F	0.224 (0.026)	0.219 (0.03)	0.222 (0.028)	0.219 (0.03)	7.948 (0.005) <sup>a</sup>	0.029
	M	0.210 (0.025)	0.208 (0.03)	0.215 (0.024)	0.211 (0.03)		
Putamen	F	0.295 (0.036)	0.291 (0.05)	0.303 (0.038)	0.300 (0.06)	5.690 (0.018) <sup>a</sup>	0.021
	M	0.281 (0.032)	0.282 (0.04)	0.290 (0.034)	0.284 (0.04)		
Pallidum	F	0.128 (0.015)	0.127 (0.02)	0.126 (0.013)	0.126 (0.02)	2.275 (0.133) <sup>a</sup>	0.008
	M	0.124 (0.014)	0.123 (0.02)	0.124 (0.015)	0.121 (0.02)		
Hippocampus	F	0.269 (0.030)	0.268 (0.04)	0.279 (0.028)	0.283 (0.04)	18.927 (<0.001) <sup>a,b</sup>	0.066
	M	0.250 (0.027)	0.247 (0.04)	0.257 (0.026)	0.252 (0.03)		
Accumbens	F	0.032 (0.007)	0.031 (0.01)	0.032 (0.006)	0.032 (0.01)	1.601 (0.207)	0.006
	M	0.030 (0.006)	0.029 (0.01)	0.031 (0.004)	0.030 (0.01)		
Amygdala	F	0.105 (0.017)	0.104 (0.02)	0.110 (0.013)	0.111 (0.02)	0.028 (0.868)	0.000
	M	0.104 (0.013)	0.103 (0.02)	0.110 (0.014)	0.108 (0.01)		
Brainstem	F	1.412 (0.122)	1.391 (0.16)	1.382 (0.100)	1.384 (0.13)	0.662 (0.417) <sup>a</sup>	0.002
	M	1.359 (0.120)	1.365 (0.18)	1.390 (0.134)	1.392 (0.20)		

Volumetric variables are presented in ratios as percentages estimated by  $[(\text{volume}/\text{eTIV}) * 100]$ . Two-way analyses of covariance (ANCOVA) with age and education as covariates with post-hoc tests corrected by Bonferroni were used for all variables.

<sup>a</sup>Sex differences in PD group.

<sup>b</sup>Sex differences in HC group ( $p < 0.05$ ).

CTh, cortical thickness; F, female; GM, gray matter; HC, healthy control; M, male; PD, Parkinson's disease.

premorbid abilities. Greater abilities in line orientation in males were observed in a study performed with 201,000 participants, involving 53 nations (Lippa et al., 2010). This sex differences in visuospatial function also remained in normal aging (Munro et al., 2012; McCarrey et al., 2016).

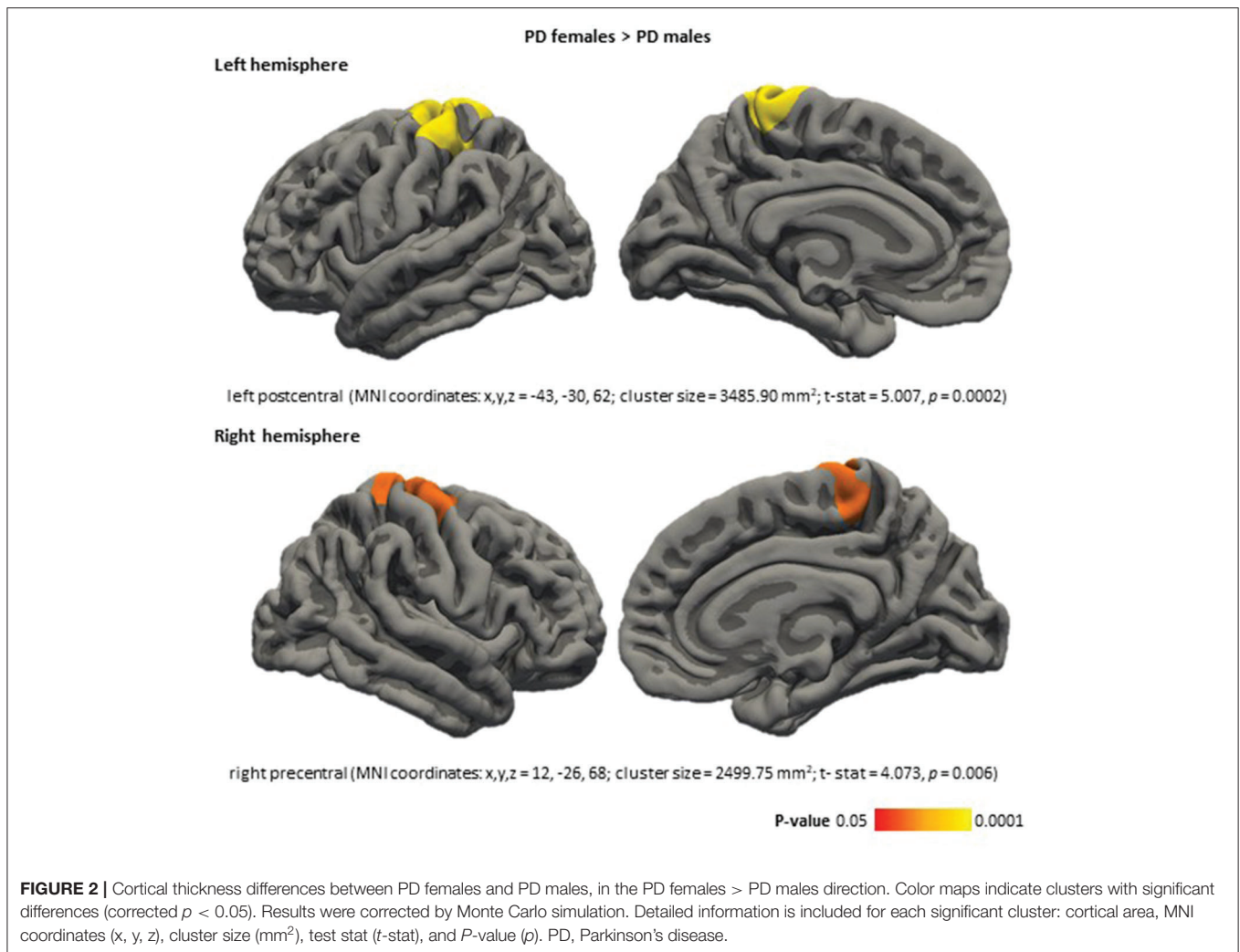
Our results show modest effect sizes of the main effect of sex in MRI-derived and cognitive measures in the PD group. The interpretation of the data should be made cautiously. Future research needs to consider the role of other co-factors such as environmental and lifestyle variables that could influence brain atrophy and functional outcomes in PD together with biological sex. In this context, diet quality and physical activity have shown a protective effect against the development of PD (Yang et al., 2015; Liu et al., 2021), and MIND and Mediterranean diets has been related to later PD onset, mainly in females (Metcalf-Roach et al., 2021). Moreover, physical activity interventions have shown improvement in functional outcomes in PD patients (Sharp and Hewitt, 2014). Another relevant factor to consider in further studies is sex differences in modifiable vascular risk factors highly related to lifestyle variables. In this regard,

hypertension has been related longitudinally to the development of MCI in PD (Nicoletti et al., 2021).

PPMI study includes multisite data including 1.5 and 3-Tesla MRI acquisitions, therefore field strength differences could be considered a potential confounder in our analyses. In this regard, we checked 1.5 and 3-Tesla acquisitions were equally distributed between our study groups.

Finally, regarding clinical variables, it must be considered that the PD diagnosis in women can be delayed, and age of onset would be biased. However, more evidence is needed concerning the expected time from disease onset to visit with a movement disorder specialist (Saunders-Pullman et al., 2011).

Of interest, other neurodegenerative diseases show relevant differential characteristics between sexes in cognition and brain atrophy. Alzheimer's disease is the most studied among all. Remarkably, females with Alzheimer's disease have higher brain atrophy rates than males (Hua et al., 2010; Ardekani et al., 2016) and have a worse performance in verbal memory tasks compared with males (Chapman et al., 2011; Benke et al., 2013). Thus, consider the effect of sex in neurodegenerative diseases in



translational research and clinical trials is a key point in the era of precision medicine.

In conclusion, PD might aggravate the sex differences in cognition and brain atrophy associated with normal aging. The characterization of phenotypic sex differences in Parkinson's disease could be crucial to develop personalized medicine approaches from the early stages of the disease.

## DATA AVAILABILITY STATEMENT

Publicly available datasets were analyzed in this study. This data can be found at: <http://www.ppmi-info.org>.

## ETHICS STATEMENT

All participating PPMI sites received approval from an ethical standards committee and obtained written informed consent from all participants in the study. The patients/participants provided their written informed consent to participate in this study.

## AUTHOR CONTRIBUTIONS

Research project conception and acquisition of data are explained in Marek et al. (2011). BS and CJ contributed to the design of the study. JO and BS contributed to the analysis of the data. JO, CU, AC, AI, GM-R, CJ, and BS contributed to the interpretation of the data. JO, CU, CJ, and BS contributed to the draft of the article. JO, CU, MJM, YC, FV, CJ, and BS revised the manuscript critically for important intellectual content and approved the final version of the manuscript. All authors contributed to the article and approved the submitted version.

## FUNDING

This study was sponsored by the Spanish Ministry of Economy and Competitiveness (PSI2017-86930-P), cofinanced by Agencia Estatal de Investigación (AEI), European Regional Development Fund (ERDF) and PID2020-114640GB-I00/MCIN/AEI/10.13039/501100011033, by Generalitat de Catalunya (2017SGR748), and supported by María de Maeztu



Unit of Excellence (Institute of Neurosciences, University of Barcelona) MDM-2017-0729, Ministry of Science, Innovation and Universities. JO was supported by a 2018 fellowship from the Spanish Ministry of Science, Universities and Research and co-financed by the European Social Fund (PRE2018-086675). CU was supported by the European Union's Horizon 2020 research and innovation programme under the Marie Skłodowska-Curie fellowship (Grant Agreement 888692). AI was supported by APIF predoctoral fellowship from the University of Barcelona (2017–2018). MJM received grants from Michael J. Fox Foundation for Parkinson's Disease (MJFF): MJF\_PPMI\_10\_001, PI044024.

## REFERENCES

- Ardekani, B. A., Convit, A., and Bachman, A. H. (2016). Analysis of the MIRIAD data shows sex differences in hippocampal atrophy progression. *J. Alzheimer's Dis.* 50, 847–857. doi: 10.3233/JAD-150780
- Bakeberg, M. C., Gorecki, A. M., Kenna, J. E., Jefferson, A., Byrnes, M., Ghosh, S., et al. (2021). Differential effects of sex on longitudinal patterns of cognitive decline in Parkinson's disease. *J. Neurol.* 268, 1903–1912. doi: 10.1007/s00415-020-10367-8
- Baldereschi, M., Di Carlo, A., Rocca, W. A., Vanni, P., Maggi, S., Perissinotto, E., et al. (2000). Parkinson's disease and parkinsonism in a longitudinal study: two-fold higher incidence in men. *Neurology* 55, 1358–1363. doi: 10.1212/WNL.55.9.1358
- Benke, T., Delazer, M., Sanin, G., Schmidt, H., Seiler, S., Ransmayr, G., et al. (2013). Cognition, gender, and functional abilities in Alzheimer's disease: how are they related? *J. Alzheimer's Dis.* 35, 247–252. doi: 10.3233/JAD-122383
- Cerri, S., Mus, L., and Blandini, F. (2019). Parkinson's disease in women and men: what's the difference? *J. Parkinsons Dis.* 9, 501–515. doi: 10.3233/JPD-191683
- Chapman, R. M., Mapstone, M., Gardner, M. N., Sandoval, T. C., McCrary, J. W., Guillily, M. D., et al. (2011). Women have farther to fall: gender differences between normal elderly and Alzheimer's disease in verbal memory engender better detection of Alzheimer's disease in women. *J. Int. Neuropsychol. Soc.* 17, 654–662. doi: 10.1017/S1355617711000452
- Cholerton, B., Johnson, C. O., Fish, B., Quinn, J. F., Chung, K. A., Peterson-Hiller, A. L., et al. (2018). Sex differences in progression to mild cognitive impairment and dementia in Parkinson's disease. *Park. Relat. Disord.* 50, 29–36. doi: 10.1016/j.parkreldis.2018.02.007
- Curtis, A. F., Masellis, M., Camicioli, R., Davidson, H., and Tierney, M. C. (2019). Cognitive profile of non-demented Parkinson's disease: meta-analysis of domain and sex-specific deficits. *Park. Relat. Disord.* 60, 32–42. doi: 10.1016/j.parkreldis.2018.10.014
- Dale, A. M., Fischl, B., and Sereno, M. I. (1999). Cortical surface-based analysis. I. Segmentation and surface reconstruction. *Neuroimage* 9, 179–194. doi: 10.1006/nimg.1998.0395
- Dale, A. M., and Sereno, M. I. (1993). Improved localization of cortical activity by combining EEG and MEG with MRI cortical surface reconstruction: a linear approach. *J. Cogn. Neurosci.* 5, 162–176. doi: 10.1162/jocn.1993.5.2.162
- Fischl, B., and Dale, A. M. (2000). Measuring the thickness of the human cerebral cortex from magnetic resonance images. *Proc. Natl. Acad. Sci. U. S. A.* 97, 11050–11055. doi: 10.1073/pnas.200033797
- Fischl, B., Liu, A., and Dale, A. M. (2001). Automated manifold surgery: constructing geometrically accurate and topologically correct models of the human cerebral cortex. *IEEE Trans. Med. Imaging* 20, 70–80. doi: 10.1109/42.906426
- Fischl, B., Salat, D. H., Busa, E., Albert, M., Dieterich, M., Haselgrove, C., et al. (2002). Whole brain segmentation: automated labeling of neuroanatomical structures in the human brain. *Neuron* 33, 341–355. doi: 10.1016/S0896-6273(02)00569-X
- Hua, X., Hibar, D. P., Lee, S., Toga, A. W., Jack, C. R., Weiner, M. W., et al. (2010). Sex and age differences in atrophic rates: an ADNI

## ACKNOWLEDGMENTS

We acknowledge the Centres de Recerca de Catalunya (CERCA) Programme/Generalitat de Catalunya, the Institute of Neurosciences, and the Institute of Biomedical Research August Pi i Sunyer (IDIBAPS).

## SUPPLEMENTARY MATERIAL

The Supplementary Material for this article can be found online at: <https://www.frontiersin.org/articles/10.3389/fnagi.2021.791532/full#supplementary-material>

- study with n=1368 MRI scans. *Neurobiol. Aging* 31, 1463–1480. doi: 10.1016/j.neurobiolaging.2010.04.033
- Iwaki, H., Blauwendraat, C., Leonard, H. L., Makarious, M. B., Kim, J. J., Liu, G., et al. (2021). Differences in the presentation and progression of Parkinson's disease by sex. *Mov. Disord.* 36, 106–117. doi: 10.1002/mds.28312
- Lin, S. J., Baumeister, T. R., Garg, S., and McKeown, M. J. (2018). Cognitive profiles and hub vulnerability in Parkinson's disease. *Front. Neurol.* 9, 1–13. doi: 10.3389/fneur.2018.00482
- Lippa, R. A., Collaer, M. L., and Peters, M. (2010). Sex differences in mental rotation and line angle judgments are positively associated with gender equality and economic development across 53 nations. *Arch. Sex. Behav.* 39, 990–997. doi: 10.1007/s10508-008-9460-8
- Liu, G., Locascio, J. J., Corvol, J. C., Boot, B., Liao, Z., Page, K., et al. (2017). Prediction of cognition in Parkinson's disease with a clinical-genetic score: a longitudinal analysis of nine cohorts. *Lancet Neurol.* 16, 620–629. doi: 10.1016/S1474-4422(17)30122-9
- Liu, R., Umbach, D. M., Peddada, S. D., Xu, Z., Tröster, A. I., Huang, X., et al. (2015). Potential sex differences in nonmotor symptoms in early drug-naive Parkinson disease. *Neurology* 84, 2107–2115. doi: 10.1212/WNL.0000000000001609
- Liu, Y. H., Jensen, G. L., Na, M., Mitchell, D. C., Craig Wood, G., Still, C. D., et al. (2021). Diet quality and risk of Parkinson's disease: a prospective study and meta-analysis. *J. Parkinsons Dis.* 11, 337–347. doi: 10.3233/JPD-202290
- Lotze, M., Domin, M., Gerlach, F. H., Gaser, C., Lueders, E., Schmidt, C. O., et al. (2019). Novel findings from 2,838 adult brains on sex differences in gray matter brain volume. *Sci. Rep.* 9, 1–7. doi: 10.1038/s41598-018-38239-2
- Marek, K., Jennings, D., Lasch, S., Siderowf, A., Tanner, C., Simuni, T., et al. (2011). The parkinson progression marker initiative (PPMI). *Prog. Neurobiol.* 95, 629–635. doi: 10.1016/j.pneurobio.2011.09.005
- Masouleh, S. K., Eickhoff, S. B., Zeigami, Y., Lewis, L. B., Dahnke, R., Gaser, C., et al. (2020). Influence of processing pipeline on cortical thickness measurement. *Cereb. Cortex* 30, 5014–5027. doi: 10.1093/cercor/bhaa097
- McCarrey, A. C., An, Y., Kitner-Triolo, M. H., Ferrucci, L., and Resnick, S. M. (2016). Sex differences in cognitive trajectories in clinically normal older adults. *Psychol. Aging* 31, 166–175. doi: 10.1037/pag0000070
- Meoni, S., Macerollo, A., and Moro, E. (2020). Sex differences in movement disorders. *Nat. Rev. Neurol.* 16, 84–96. doi: 10.1038/s41582-019-0294-x
- Metcalfe-Roach, A., Yu, A. C., Golz, E., Cirstea, M., Sundvick, K., Kliger, D., et al. (2021). MIND and mediterranean diets associated with later onset of Parkinson's disease. *Mov. Disord.* 36, 977–984. doi: 10.1002/mds.28464
- Moisan, F., Kab, S., Mohamed, F., Canonico, M., Le Guern, M., Quintin, C., et al. (2016). Parkinson disease male-to-female ratios increase with age: French nationwide study and meta-analysis. *J. Neurol. Neurosurg. Psychiatry* 87, 952–957. doi: 10.1136/jnnp-2015-312283
- Munro, C. A., Winicki, J. M., Schretlen, D. J., Gower, E. W., Turano, K. A., Muñoz, B., et al. (2012). Sex differences in cognition in healthy elderly individuals. *Aging Neuropsychol. Cogn.* 19, 759–768. doi: 10.1080/13825585.2012.690366
- Nicoletti, A., Luca, A., Baschi, R., Cicero, C. E., Mostile, G., Davi, M., et al. (2021). Vascular risk factors, white matter lesions and cognitive impairment

- in Parkinson's disease: the PACOS longitudinal study. *J. Neurol.* 268, 549–558. doi: 10.1007/s00415-020-10189-8
- Reekes, T. H., Higginson, C. L., Ledbetter, C. R., Sathivadivel, N., Zweig, R. M., and Disbrow, E. A. (2020). Sex specific cognitive differences in Parkinson disease. *npj Park. Dis.* 6, 1–6. doi: 10.1038/s41531-020-0109-1
- Ritchie, S. J., Cox, S. R., Shen, X., Lombardo, M. V., Reus, L. M., Alloza, C., et al. (2018). Sex differences in the adult human brain: evidence from 5216 UK biobank participants. *Cereb. Cortex* 28, 2959–2975. doi: 10.1093/cercor/bhy109
- Salminen, L. E., Tubi, M. A., Bright, J., Thomopoulos, S. I., Wieand, A., and Thompson, P. M. (2021). Sex is a defining feature of neuroimaging phenotypes in major brain disorders. *Hum. Brain Mapp.* 43, 500–542. doi: 10.1002/hbm.25438
- Saunders-Pullman, R., Wang, C., Stanley, K., and Bressman, S. B. (2011). Diagnosis and referral delay in women with Parkinson's disease. *Genet. Med.* 8, 209–217. doi: 10.1016/j.genm.2011.05.002
- Ségonne, F., Pacheco, J., and Fischl, B. (2007). Geometrically accurate topology-correction of cortical surfaces using nonseparating loops. *IEEE Trans. Med. Imaging* 26, 518–529. doi: 10.1109/TMI.2006.887364
- Sharp, K., and Hewitt, J. (2014). Dance as an intervention for people with Parkinson's disease: a systematic review and meta-analysis. *Neurosci. Biobehav. Rev.* 47, 445–456. doi: 10.1016/j.neubiorev.2014.09.009
- Szewczyk-Krolkowski, K., Tomlinson, P., Nithi, K., Wade-Martins, R., Talbot, K., Ben-Shlomo, Y., et al. (2014). The influence of age and gender on motor and non-motor features of early Parkinson's disease: initial findings from the Oxford Parkinson Disease Center (OPDC) discovery cohort. *Park. Relat. Disord.* 20, 99–105. doi: 10.1016/j.parkreldis.2013.09.025
- Taylor, K. S. M., Cook, J. A., and Counsell, C. E. (2007). Heterogeneity in male to female risk for Parkinson's disease [1]. *J. Neurol. Neurosurg. Psychiatry* 78, 905–906. doi: 10.1136/jnnp.2006.104695
- Tremblay, C., Abbasi, N., Zeighami, Y., Yau, Y., Dadar, M., Rahayel, S., et al. (2020). Sex effects on brain structure in *de novo* Parkinson's disease: a multimodal neuroimaging study. *Brain* 143, 3052–3066. doi: 10.1093/brain/awaa234
- Wooten, G. F., Currie, L. J., Bovbjerg, V. E., Lee, J. K., and Patrie, J. (2004). Are men at greater risk for Parkinson's disease than women? *J. Neurol. Neurosurg. Psychiatry* 75, 637–639. doi: 10.1136/jnnp.2003.020982
- Yadav, S. K., Kathiresan, N., Mohan, S., Vasileiou, G., Singh, A., Kaura, D., et al. (2016). Gender-based analysis of cortical thickness and structural connectivity in Parkinson's disease. *J. Neurol.* 263, 2308–2318. doi: 10.1007/s00415-016-8265-2
- Yang, F., Lagerros, Y. T., Bellocco, R., Adami, H. O., Fang, F., Pedersen, N. L., et al. (2015). Physical activity and risk of Parkinson's disease in the Swedish National March Cohort. *Brain* 138, 269–275. doi: 10.1093/brain/awu323

**Conflict of Interest:** MJM received honoraria for advice and lecture from Abbvie, Bial, and Merzt Pharma and grants from Michael J. Fox Foundation for Parkinson's Research (MJFF): MJF\_PPML\_10\_001, PI044024. YC has received funding in the past 5 years from Union Chimique Belge (UCB pharma), Teva, Medtronic, Abbvie, Novartis, Merz, Piramal Imaging, Esteve, Bial, and Zambon and currently an associate editor for Parkinsonism & Related Disorders.

The remaining authors declare that the research was conducted in the absence of any commercial or financial relationships that could be construed as a potential conflict of interest.

**Publisher's Note:** All claims expressed in this article are solely those of the authors and do not necessarily represent those of their affiliated organizations, or those of the publisher, the editors and the reviewers. Any product that may be evaluated in this article, or claim that may be made by its manufacturer, is not guaranteed or endorsed by the publisher.

Copyright © 2022 Oltra, Uribe, Campabadal, Inguanzo, Monté-Rubio, Martí, Compta, Valdeoriola, Junque and Segura. This is an open-access article distributed under the terms of the Creative Commons Attribution License (CC BY). The use, distribution or reproduction in other forums is permitted, provided the original author(s) and the copyright owner(s) are credited and that the original publication in this journal is cited, in accordance with accepted academic practice. No use, distribution or reproduction is permitted which does not comply with these terms.

## *Supplementary Material*

### **Supplementary Table 1**

MRI field strength distribution of the groups

	<b>1.5 T</b>	<b>3 T</b>	<b>Test stat (<i>P</i>-value)</b>
HC female	8 (27.6%)	21 (72.4%)	3.213 (0.360)
HC male	6 (15%)	34 (85%)	
PD female	20 (25.6%)	58 (74.5%)	
PD male	37 (29.1%)	90 (70.9%)	

Data are presented by groups as *n* (%). Pearson's chi-squared was used.

Abbreviations: HC = healthy control; PD = Parkinson's disease; T = Tesla.

**Supplementary Table 2**

Post hoc tests corresponding to the within-group sex main effect in neuropsychological tasks

		<b>Sex main effect F stat (<i>P</i>-value)</b>	<b>Partial eta squared</b>
MoCA	PD	9.104 (0.003)	0.033
	HC	0.341 (0.560)	0.001
<b>Semantic fluency</b>			
Animals	PD	0.215 (0.644)	0.001
	HC	0.829 (0.363)	0.003
Vegetables	PD	38.546 (<0.001)	0.127
	HC	9.142 (0.003)	0.033
Fruits	PD	20.412 (<0.001)	0.071
	HC	19.817 (<0.001)	0.069
Phonetic fluency 'f'	PD	1.372 (0.242)	0.005
	HC	0.556 (0.457)	0.001
SDMT	PD	6.467 (0.012)	0.024
	HC	0.422 (0.516)	0.002
LNS	PD	0.025 (0.874)	0.000
	HC	1.456 (0.229)	0.005
JLO	PD	9.246 (0.003)	0.034
	HC	5.598 (0.019)	0.021
<b>HVLT-R</b>			
Immediate recall	PD	17.101 (<0.001)	0.060
	HC	5.465 (0.020)	0.020
Recognition	PD	2.212 (0.138)	0.008
	HC	0.376 (0.540)	0.001
Delayed recall	PD	10.674 (0.001)	0.039
	HC	3.276 (0.071)	0.012

Two-way analyses of covariance (ANCOVA) with age and education as covariates with post-hoc tests corrected by Bonferroni were used for all variables.

Abbreviations: HC = healthy control; HVLT-R = Hopkins Verbal Learning Test-Revised; JLO = Benton Judgment of Line Orientation; LNS = Letter-Number Sequencing; MoCA = Montreal Cognitive Assessment; PD= Parkinson's disease; SDMT = Symbol Digit Modalities Test.

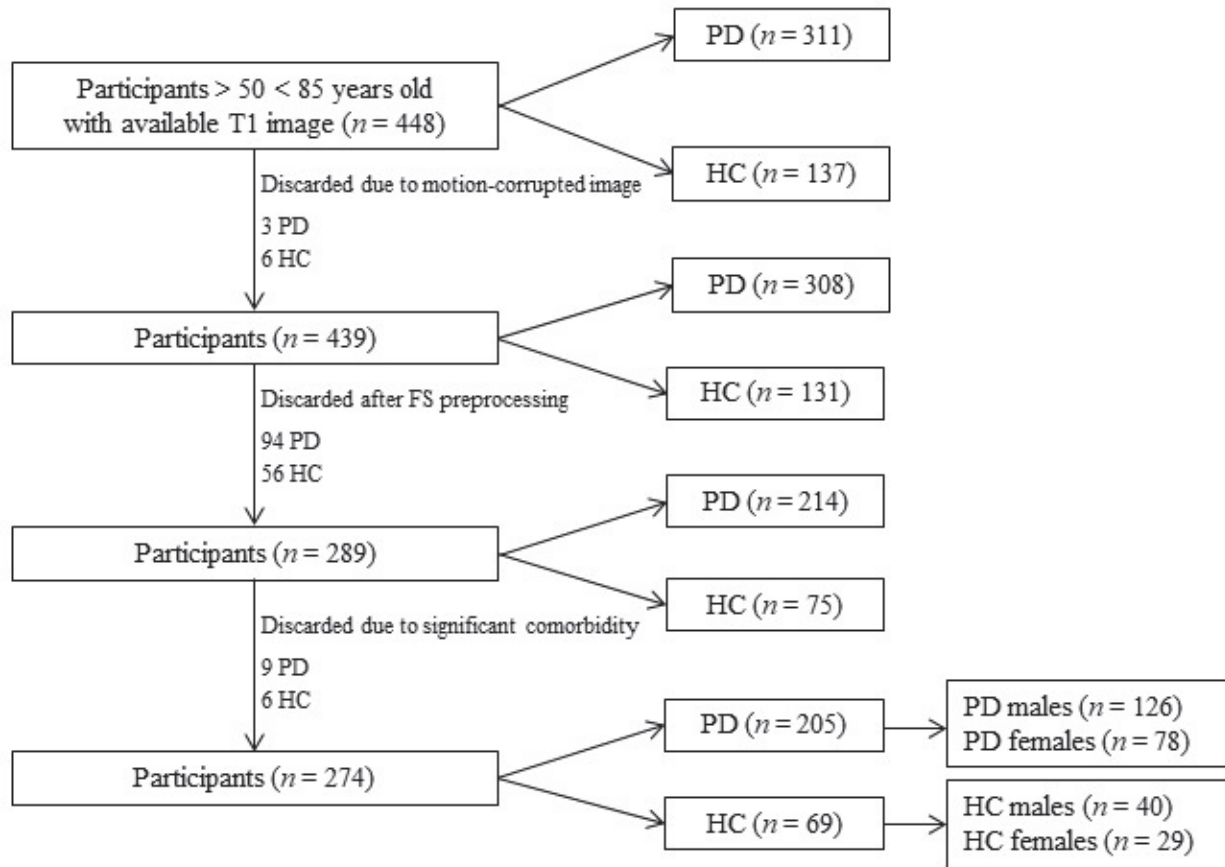
**Supplementary Table 3**

Post hoc tests corresponding to the within-group sex main effect in MRI derived measures

		<b>Sex main effect Test stat (<i>P</i>-value)</b>	<b>Partial eta squared</b>
<b>Global atrophy</b>			
Cortical	PD	17.997 (<0.001)	0.063
	HC	0.907 (0.342)	0.003
Subcortical	PD	16.926 (<0.001)	0.059
	HC	2.748 (0.099)	0.010
Mean CTh	PD	0.242 (0.624)	0.001
	HC	1.441 (0.231)	0.005
<b>Deep GM nuclei</b>			
Thalamus	PD	15.498 (<0.001)	0.055
	HC	0.923 (0.338)	0.003
Caudate	PD	14.422 (<0.001)	0.051
	HC	1.120 (0.291)	0.004
Putamen	PD	6.112 (0.014)	0.022
	HC	1.777 (0.184)	0.007
Pallidum	PD	4.702 (0.031)	0.017
	HC	0.236 (0.628)	0.001
Hippocampus	PD	17.472 (<0.001)	0.061
	HC	6.891 (0.009)	0.025
Accumbens	PD	2.802 (0.095)	0.010
	HC	0.243 (0.622)	0.001
Amygdala	PD	0.005 (0.941)	0.000
	HC	0.057 (0.812)	0.000
Brainstem	PD	7.312 (0.007)	0.027
	HC	0.415 (0.520)	0.002

Two-way analyses of covariance (ANCOVA) with age and education as covariates with post-hoc tests corrected by Bonferroni were used for all variables. Abbreviations: CTh = cortical thickness; GM = gray matter; HC = healthy control; PD = Parkinson's disease.

**Supplementary Figure 1.** Flow diagram of sample selection. Abbreviations: FS = FreeSurfer; HC = healthy control; PD = Parkinson’s disease



## **Supplementary Methods 1**

Clinical and medication databases were checked after MRI preprocessing to make sure that any PD or control participant with relevant comorbidities did not enter in posterior analyses. We excluded 9 PD participants (1 due to seizure and obsessive-compulsive disorder; 1 to depression and attention hyperactivity deficit disorder; 1 to mood disorders; 1 to mood disorders, sleep apnea, thymus removal and thalamus removal; 1 to alcoholism and anxiety; 1 to atrial fibrillation and cardiovascular accident; 1 to alcoholism: 1 to post-traumatic stress disorder and hallucinations; and 1 to attention deficit hyperactivity disorder, anxiety and depression) and 6 HC participants (4 to relevant RBD symptomatology according to RBDSQ, 1 to seizure, 1 to cardiac arrhythmia and cardiac problems).





## Study 4

---

**Oltra J**, Segura B, Uribe C, Monté-Rubio GC, Campabadal A, Inguanzo A, Pardo J, Martí MJ, Compta Y, Valdeoriola F, Iranzo, A, Junque C. Sex differences in brain atrophy and cognitive impairment in Parkinson's disease patients with and without probable rapid eye movement sleep behavior disorder. *Journal of Neurology*. 2022; 269: 1591–1599. doi:10.1007/s00415-021-10728-x.



# Sex differences in brain atrophy and cognitive impairment in Parkinson's disease patients with and without probable rapid eye movement sleep behavior disorder

Javier Oltra<sup>1,2</sup> · Barbara Segura<sup>1,2,3</sup> · Carme Uribe<sup>1,2,4</sup> · Gemma C. Monté-Rubio<sup>1</sup> · Anna Campabadal<sup>1,2</sup> · Anna Inguanzo<sup>1,2</sup> · Jèssica Pardo<sup>1</sup> · Maria J. Martí<sup>2,3,5</sup> · Yaroslau Compta<sup>2,3,5</sup> · Francesc Valldeoriola<sup>2,3,5</sup> · Alex Iranzo<sup>2,3,6</sup> · Carme Junque<sup>1,2,3</sup>

Received: 1 April 2021 / Revised: 20 July 2021 / Accepted: 25 July 2021 / Published online: 3 August 2021  
© The Author(s) 2021, corrected publication 2021

## Abstract

**Background** The presence of rapid eye movement sleep behavior disorder (RBD) contributes to increase cognitive impairment and brain atrophy in Parkinson's disease (PD), but the impact of sex is unclear. We aimed to investigate sex differences in cognition and brain atrophy in PD patients with and without probable RBD (pRBD).

**Methods** Magnetic resonance imaging and cognition data were obtained for 274 participants from the Parkinson's Progression Marker Initiative database: 79 PD with pRBD (PD-pRBD; male/female, 54/25), 126 PD without pRBD (PD-non pRBD; male/female, 73/53), and 69 healthy controls (male/female, 40/29). FreeSurfer was used to obtain volumetric and cortical thickness data.

**Results** Males showed greater global cortical and subcortical gray matter atrophy than females in the PD-pRBD group. Significant group-by-sex interactions were found in the pallidum. Structures showing a within-group sex effect in the deep gray matter differed, with significant volume reductions for males in one structure in PD-non pRBD (brainstem), and three in PD-pRBD (caudate, pallidum and brainstem). Significant group-by-sex interactions were found in Montreal Cognitive Assessment (MoCA) and Symbol Digits Modalities Test (SDMT). Males performed worse than females in MoCA, phonemic fluency and SDMT in the PD-pRBD group.

**Conclusion** Male sex is related to increased cognitive impairment and subcortical atrophy in de novo PD-pRBD. Accordingly, we suggest that sex differences are relevant and should be considered in future clinical and translational research.

**Keywords** Parkinson's disease · Sex differences · REM sleep behavior disorder · Magnetic resonance imaging · Gray matter atrophy · Cognitive impairment

## Introduction

There is significant cumulative evidence for Alzheimer's disease [1] and Parkinson's disease (PD) [2, 3] that susceptibility to regional brain atrophy and cognitive impairment differs by sex. These between-sex differences on brain degeneration have implications for implementing prevention, diagnosis, and treatment strategies in the context of precision medicine.

Early population-based studies report that males have a two-fold increased risk of developing PD [4]. Males with PD, in comparison to females, also have decreased performance in global cognition [5–8], memory [6–8], verbal fluency [5, 7–9], processing speed [7, 9], and inhibition [9]. In contrast, females with PD have greater impairment in visuospatial function than males [6–8]. A recent meta-analysis revealed greater frontal executive deficit in males than females [10]. In addition, male sex is associated with cognitive impairment [11] and with progression to mild cognitive impairment (MCI) [8, 12] as well as dementia [12]. Male sex is an established predictor of progressive cognitive decline [13].

Structural magnetic resonance imaging (MRI) studies have also evidenced sex-based differences in PD. Males have

✉ Barbara Segura  
bsegura@ub.edu

Extended author information available on the last page of the article

pronounced cortical thinning in frontal, parietal, temporal, and occipital regions compared with females [14]. Greater tissue loss in males with de novo PD has also been described in some cortical regions and in the left thalamus by deformation-based morphometry [15]. Studies have also identified disrupted structural connectivity in PD males compared to PD females [14, 15].

Isolated rapid eye movement behavior disorder (RBD) is a well-known prodrome of the synucleinopathies, with a rate of conversion of 90% after 15-year follow-up [16]. For unknown reasons, about 80% of the patients diagnosed in sleep centers with isolated RBD are of male sex [17]. PD patients have a prevalence of RBD symptomatology of around 40% [18]. The presence of probable RBD (pRBD) in PD has also been associated with more severe cognitive impairment in patients with de novo PD [19, 20], with a greater degree of cognitive decline over time [19]. Moreover a higher prevalence of MCI has been reported in PD patients with polysomnographic diagnosis of RBD [21]. Structural MRI studies in patients with de novo PD indicate that cortical [22] and subcortical volumes [22, 23] are reduced in groups with pRBD compared to groups without pRBD. To the best of our knowledge, no previous studies have investigated the impact of sex differences on brain atrophy and cognitive deficits in patients with PD and pRBD.

In the current work, we aimed to explore sex differences in brain and cognition in a large sample of newly diagnosed drug-naïve patients with PD, with and without probable RBD (PD-pRBD and PD-non pRBD groups, respectively). We hypothesized that the between-sex differences would be more marked in the PD-pRBD group than in the PD-non pRBD due to a greater degree of neurodegeneration.

## Methods

### Participants

Data were obtained from the Parkinson's Progression Markers Initiative database (PPMI, <http://www.ppmi-info.org>) [24], including T1-weighted images, clinical information, and neuropsychological data from 205 patients with PD and 69 healthy controls. The PD cohort was then divided into four groups by their sex and pRBD status, the latter of which was established based on a five-point cutoff on the RBD Screening Questionnaire (RBDSQ) [25]. The final sample comprised 6 groups: 73 PD-non pRBD males, 53 PD-non pRBD females, 54 PD-pRBD males, 25 PD-pRBD females, 40 control males, and 29 control females.

The inclusion criteria were as follows: (i) recent diagnosis of PD with asymmetric resting tremor or asymmetric bradykinesia, or two from among bradykinesia, resting tremor, and rigidity; (ii) absence of PD treatment; (iii) neuroimaging

evidence of significant dopamine transporter deficit consistent with a clinical diagnosis of PD, and excluding conditions that can mimic PD, such as drug-induced and vascular parkinsonism or essential tremor; (iv) T1-weighted images available (PD and control groups); and (v) age older than 50 and younger than 85 years old (PD and control groups). The exclusion criteria for all participants were as follows: (i) diagnosis of dementia; (ii) significant psychiatric, neurologic, or systemic comorbidity; (iii) a first-degree family member with PD; and (iv) presence of MRI motion artifacts, field distortions, intensity inhomogeneities, or detectable structural brain lesions. The sample selection process is shown in Supplementary Fig. 1.

### Clinical and neuropsychological assessments

A detailed clinical assessment was performed. This included measurements of PD symptoms by the Movement Disorders Society Unified PD Rating Scale (MDS-UPDRS), PD motor symptoms by the MDS-UPDRS motor section (Part III), disease severity by the Hoehn and Yahr scale (H&Y), global cognition by the Montreal Cognitive Assessment (MoCA), depressive symptoms by the 15-item Geriatric Depression Scale (GDS-15), olfactory function by the University of Pennsylvania Smell Identification Test (UPSIT-40), probable RBD status and symptomatology by the RBDSQ, and excessive daytime sleepiness by the Epworth Sleepiness Scale (ESS) [24]. All subjects also underwent a neuropsychological battery that included the following: phonemic (letter 'f') and semantic (animals, fruits and vegetables) verbal fluency tests; the Symbol Digit Modalities Test (SDMT); Letter-Number Sequencing (LNS); the Benton Judgment of Line Orientation short form (JLO), 15-item version; and the Hopkins Verbal Learning Test-Revised (HVLT-R) [24]. All neuropsychological data were reported using z scores calculated based on the control group's means and standard deviations.

### MRI images

T1-weighted MRI scans were acquired using 1.5 or 3-Tesla scanners at different centers using magnetization prepared rapid gradient echo imaging (MPRAGE) sequences. Typical MRI parameters were as follows: repetition time = 5–11 ms; echo time = 2–6 ms; slice thickness 1–1.5 mm; inter-slice gap 0 mm; voxel size 1 × 1 × 1.2 mm; matrix 256 × 160 minimum. Details can be found at <http://www.ppmi-info.org/wp-content/uploads/2010/07/Imaging-Manual.pdf>. There were no differences in the distribution of 1.5 and 3-Tesla images across groups (Supplementary Table 1).

Cortical thickness was estimated using the automated processing stream and specific segmentation tools of FreeSurfer (version 6.0, <http://surfer.nmr.mgh.harvard.edu>). Uribe et al. provide a detailed description about processing

with the FreeSurfer stream [26]. After preprocessing, results for each subject were inspected visually to ensure the accuracy of registration, skull stripping, segmentation, and cortical surface reconstruction. Errors were fixed by manual intervention following standard procedures (see applied manual interventions in Supplementary Fig. 1). Deep gray matter (GM) mean volumes (i.e., in the thalamus, putamen, pallidum, caudate, hippocampus, amygdala, accumbens, and brainstem) and total cortical and subcortical GM were extracted [27]. First, volumes were made bilateral by averaging those of the left and right hemisphere as [(left volume + right volume)/2]. Second, volume ratios were calculated using the estimated total intracranial volume (eTIV) to perform global and partial volumetric analyses [(volume/eTIV) × 100]. Thus, significant eTIV between-sex differences in the three groups were already controlled in the subsequent analyses (Supplementary Table 2).

## Statistical analyses

The main effects of group and sex were computed for the demographic variables by two-way analysis of variance (ANOVA) followed by Bonferroni post hoc tests to analyze sex differences in group conditions. These analyses revealed that males were significantly older than females in the control group; consequently, subsequent analyses that involved this group included age as a covariate (Table 1). No significant main effect of group was found by age ( $F = 1.892$ ,  $p = 0.153$ ), education ( $F = 2.959$ ,  $p = 0.054$ ), age of disease onset ( $F = 3.264$ ,  $p = 0.072$ ), or PD duration ( $F = 0.045$ ,  $p = 0.832$ ). There were no differences in the sex distribution across the PD groups and healthy controls (Chi-squared = 2.558,  $p = 0.278$ ).

The group-by-sex interaction for clinical, neuropsychological, volumetric, and mean cortical thickness variables was assessed by two-way ANOVA or covariance (ANCOVA), followed by Bonferroni post hoc tests, as appropriate. Pearson's Chi-squared test was used to analyze differences in categorical measures.

Additionally, we explored the within-group sex effect of neuropsychological, mean cortical thickness and volumetric variables. First, we regressed out the effect of normal aging and sex. Expected z scores adjusted for age and sex were calculated based on a multiple regression analysis performed in the HC group and subtracted from the observed variables [28]. Second, within-group sex effects and group-by-sex interactions were explored by two-way ANOVA followed by Bonferroni post hoc tests. Lastly, the between-group differences regarding the within-group sex effects were estimated to explore the significant group-by-sex interactions. The statistical significance threshold was set at  $p < 0.05$  and all

**Table 1** Demographic and clinical characteristics of HC, PD-non pRBD, and PD-pRBD females and males

	HC	PD-non pRBD	PD-pRBD	Sex main effect test stat ( $P$ value)
Age, years				
F	60.6 (5.9)	60.9 (7.4)	63.5 (7.5)	6.215 (0.013)*
M	64.1 (7.1)	63.2 (7.4)	64.7 (7.0)	
Education, years				
F	16.2 (2.9)	15.4 (2.9)	15.2 (3.1)	3.141 (0.077)
M	17.0 (2.5)	15.8 (3.0)	16.1 (2.9)	
Age of onset, years				
F	NA	60.0 (7.4)	62.6 (7.6)	2.348 (0.127)
M	NA	62.3 (7.2)	63.6 (6.9)	
PD duration, months				
F	NA	10.8 (8.5)	9.9 (6.8)	0.278 (0.599)
M	NA	10.3 (6.2)	11.6 (7.2)	
MDS-UPDRS				
F	NA	28.4 (10.0)	32.0 (11.9)	3.774 (0.053)
M	NA	30.1 (11.3)	37.4 (14.1)	
MDS-UPDRS Part III				
F	NA	19.0 (7.6)	17.9 (7.6)	7.371 (0.007)**
M	NA	20.4 (8.3)	23.3 (9.4)	
H&Y stage, $n$ , 1/2/3				
F	NA	1.7 (2.1)	2.6 (2.5)	0.002 (0.967)
M	NA	35/37/1	21/33/0	
GDS-15				
F	1.9 (3.2)	1.7 (2.1)	2.6 (2.5)	0.002 (0.967)
M	1.2 (2.8)	2.3 (2.2)	2.7 (2.4)	
ESS				
F	4.6 (2.9)	4.9 (3.4)	6.8 (3.6)	0.822 (0.365)
M	5.3 (3.5)	5.7 (2.9)	6.4 (3.7)	
RBDSQ				
F	1.5 (1.2)	2.7 (1.1)	6.0 (1.4)	7.405 (0.007)**
M	1.9 (1.4)	2.6 (1.1)	7.2 (1.9)	
UPSIT				
F	34.9 (3.4)	23.8 (8.6)	21.4 (8.7)	3.401 (0.066)
M	33.6 (4.1)	21.0 (7.4)	18.7 (8.0)	

Data are presented by groups as mean (SD), except for H&Y. Two-way analyses of variance (ANOVA) followed by Bonferroni post hoc tests were used for all demographic variables. Two-way analyses of covariance (ANCOVA) with age as covariable, followed by Bonferroni post hoc tests were used for all clinical variables. Except for MDS-UPDRS, that was analyzed by two-way analysis of variance (ANOVA); and H&Y, by Pearson's Chi-squared

ESS Epworth Sleepiness Scale; F female; GDS-15 the 15-item Geriatric Depression Scale; HC healthy controls; H&Y Hoehn and Yahr scale; M male; MDS-UPDRS Movement Disorder Society Unified Parkinson's Disease Rating Scale; PD-non pRBD PD without probable RBD; PD-pRBD PD with probable RBD; RBDSQ REM Sleep Behavior Disorder Screening Questionnaire; UPSIT University of Pennsylvania Smell Identification Test

\*Sex differences in HC group ( $P < 0.05$ )

\*\*Sex differences in PD-pRBD group ( $P < 0.05$ )

analyses were performed with IBM SPSS Statistics 27.0.0 (2020; IBM Corp., Armonk, NY).

Intergroup comparisons of cortical thickness were performed using a vertex-by-vertex general linear model in FreeSurfer v6.0. The model included cortical thickness as a dependent factor, group as an independent factor, and demeaned age as covariable. All results were corrected for multiple comparisons using a pre-cached cluster-wise Monte Carlo simulation with 10,000 iterations. Reported cortical regions reached a two-tailed corrected significance level of  $p < 0.05$ .

## Results

### Clinical characteristics

A significant sex effect was found with motor severity (MDS-UPDRS Part III) and RBD (RBDSQ). There was a significant group-by-sex interaction in the RBDSQ score ( $F = 4.749$ ,  $p = 0.009$ ), with post hoc analyses also showing that males in the PD-pRBD group had more severe motor and RBD symptoms than females in this group. No significant main effect of sex was found in the global

MDS-UPDRS score, the H&Y stage, GDS-15, ESS, and UPSIT scores (Table 1).

### Neuropsychological performance

A significant group-by-sex interaction was found in the MoCA ( $F = 4.758$ ,  $p = 0.009$ ) and SDMT ( $F = 4.196$ ,  $p = 0.016$ ). Both groups of PD males performed worse than HC males in MoCA and SDMT, PD-pRBD males performed worse than PD-non pRBD males in SDMT (Fig. 1 and Supplementary Table 3).

Complementary, significant within-group sex effects were found in the MoCA, phonemic fluency and SDMT in the PD-pRBD group after regressing out age and sex, in which males performed lower than females (Supplementary Table 4). A significant within-group sex effect in semantic fluency (fruits) was observed in the PD-non pRBD group, with lower performance in females than males. No within-group sex effect was observed in the control group. Significant group-by-sex interactions remained after controlling the effect of normal aging and sex (Supplementary Tables 4 and 5). Between-groups differences regarding the within-group sex effects in MoCA

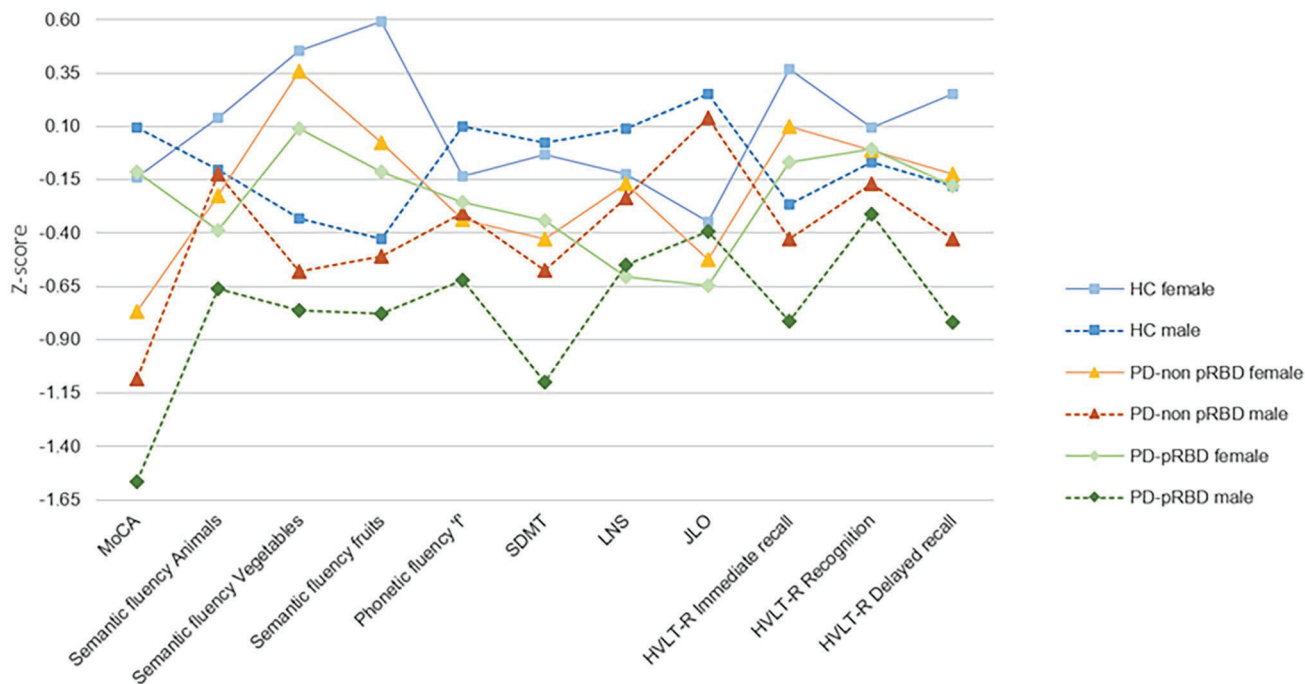


**Fig. 1** Neuropsychological performance. Tasks are indicated in the x axis. Group means in each task are presented as z scores, as indicate in y axis. Lower z scores indicate worse performance. Descriptive statistics, as mean (SD), are available in Supplementary Table 3. Healthy controls in blue, PD-non pRBD in warm colors, PD-pRBD in green; lighter for females and darker for males. HC represented by filled squares, PD-non pRBD by filled triangles and PD-pRBD by

filled rhombuses. Females by a continuous line and males by a dashed line. Data are presented as z scores. Abbreviations: *MoCA* Montreal Cognitive Assessment; *SDMT* Symbol Digit Modalities Test; *LNS* Letter-Number Sequencing; *JLO* Benton Judgment of Line Orientation; *HVLTR* Hopkins Verbal Learning Test-Revised, *HC* healthy controls; *PD-non pRBD* PD without probable RBD; *PD-pRBD* PD with probable RBD

and SDMT showed significant differences between PD-pRBD and the other two groups (Supplementary Table 5).

## MRI volumetry

We did not find any vertex-wise sex effects in cortical thickness. Regarding subcortical volumetry, there was a significant group-by-sex interaction in the bilateral pallidum ( $F = 3.084$ ,  $p = 0.047$ ). Post hoc analyses showed that PD-pRBD males had smaller pallidum volume than PD-non pRBD males (Table 2).

Supplementary analysis, after regressing out age and sex, showed that in the PD-pRBD group males had smaller global cortical and subcortical GM volumes than females. Furthermore, males had significantly smaller volume than females in three subcortical structures in the PD-pRBD group (caudate, pallidum and brainstem) versus in one in the PD-non pRBD group (brainstem), and in none in the control group (Supplementary Table 6). Significant group-by-sex interaction remained after controlling the effect of normal aging and sex (Supplementary Tables 5 and 6). Between-groups differences regarding the within-group sex effects showed a significant difference between PD groups and a trend to significance between PD-pRBD and HC in the pallidum. As expected, there were no differences between PD-non pRBD and HC (Supplementary Table 5).

Significant group-by-sex interactions in neuropsychological (MoCA) and MRI (pallidum) measures remain significant after controlling by motor disease severity (Supplementary Tables 7 and 8).

In summary, we showed a significant interaction in pallidum, showing smaller pallidum volume in PD-pRBD males than in PD-non pRBD males. Additionally, PD-pRBD males showed smaller global cortical and subcortical GM volumes than females, as well as, a different number of structures showing within-group sex differences. This applied to no structure in the control group, one in the PD-non pRBD group, and three in the PD-pRBD group. In all cases, males showed decreased volumes compared with females.

## Discussion

Among drug-naïve patients, in the PD-pRBD group males had more severe motor and RBD symptomatology, worse cognitive performance, and greater subcortical volume atrophy than females. Such sex differences were also observed in subcortical volumes in PD-non pRBD group, but to a greater extent in the former.

**Table 2** Magnetic resonance imaging derived measures of HC, PD-non pRBD, and PD-pRBD females and males

	HC	PD-non pRBD	PD-pRBD	Group-by-sex test stat ( $P$ value)
Global atrophy				
Cortical GM				
F	30.11 (1.80)	29.39 (2.23)	30.03 (2.34)	1.577 (0.209)
M	29.39 (2.26)	28.15 (1.98)	28.15 (2.39)	
Subcortical GM				
F	3.69 (0.27)	3.63 (0.26)	3.66 (0.32)	1.773 (0.172)
M	3.54 (0.28)	3.51 (0.24)	3.41 (0.24)	
Mean CTh, mm				
F	2.44 (0.10)	2.42 (0.10)	2.41 (0.09)	0.017 (0.984)
M	2.41 (0.12)	2.39 (0.12)	2.38 (0.12)	
Deep GM nuclei				
Thalamus				
F	0.460 (0.030)	0.465 (0.042)	0.456 (0.044)	0.741 (0.478)
M	0.443 (0.046)	0.441 (0.040)	0.429 (0.037)	
Caudate				
F	0.222 (0.028)	0.221 (0.027)	0.229 (0.022)	2.047 (0.131)
M	0.215 (0.024)	0.212 (0.025)	0.207 (0.024)	
Putamen				
F	0.303 (0.038)	0.294 (0.035)	0.296 (0.039)	0.995 (0.371)
M	0.290 (0.034)	0.286 (0.029)	0.275 (0.035)	
Pallidum				
F	0.126 (0.013)	0.127 (0.014)	0.131 (0.015)	3.084 (0.047)*
M	0.124 (0.015)	0.127 (0.013)	0.120 (0.015)	
Hippocampus				
F	0.279 (0.028)	0.267 (0.030)	0.272 (0.031)	0.802 (0.449)
M	0.257 (0.026)	0.252 (0.028)	0.247 (0.025)	
Amygdala				
F	0.110 (0.013)	0.103 (0.015)	0.108 (0.022)	2.397 (0.093)
M	0.110 (0.014)	0.105 (0.013)	0.101 (0.013)	
Accumbens				
F	0.032 (0.006)	0.031 (0.007)	0.034 (0.007)	1.618 (0.200)
M	0.031 (0.004)	0.030 (0.006)	0.030 (0.006)	
Brainstem				
F	1.382 (0.100)	1.412 (0.128)	1.412 (0.110)	2.393 (0.093)
M	1.390 (0.134)	1.375 (0.113)	1.338 (0.128)	

Data are presented by groups as mean (SD). Volumetric variables are presented in ratios estimated by  $((\text{volume}/\text{eTIV}) \times 100)$ . Two-way analyses of covariance (ANCOVA) with age as covariable, followed by Bonferroni post hoc tests, were used for all variables

CTh cortical thickness; F female; GM gray matter; HC healthy controls; M male; PD-non pRBD PD without probable RBD; PD-pRBD PD with probable RBD

\*Differences between PD-non pRBD males and PD-pRBD males ( $P < 0.05$ )

Clinically, despite a similar age at the time of the study, age of disease onset and PD duration, males in the PD-pRBD group had greater motor impairment and more RBD symptoms. Cognitive impairment was also greater in males in the PD-pRBD group. We found a significant group-by-sex interaction in MoCA and SDMT. Notably, the sex effects in MoCA and SDMT were greater in the PD-pRBD group compared with the other two groups. Specifically, we found that males performed significantly worse than females in MoCA, phonemic fluency and SDMT in the PD-pRBD group. By contrast, females in the PD-non pRBD showed greater impairment only in one semantic fluency test than males. These results suggest that, if PD patients with RBD symptomatology, showed sex differences consistent with those of previous studies in drug-naïve patients with PD as a whole group, showing that males have greater global cognitive impairment [6, 7], verbal fluency, and processing speed [7] impairments. In contrast, those differences mostly disappear, in the PD-non pRBD group.

Global MRI measures revealed smaller total cortical and subcortical GM volumes in males of the PD-pRBD group, but not in the PD-non pRBD and control groups. This finding suggesting that, just like the atrophy patterns are more severe in PD with RBD symptomatology [22, 23], the sex differences are more marked in this PD subtype.

It has been reported that males, even adjusting for brain size, have larger volumes in several structures than females [29, 30]. Nonetheless, more accelerated aging effects have been described in males in regional volumes [31, 32]. In summary, aging seems to reverse sex-related structural differences in the brain, probably due to hormonal effects, resulting in a greater vulnerability of males to brain atrophy, especially in degenerative conditions.

In addition to the greater global atrophy among males compared with females, we also found vulnerability to differential volumetric atrophy by sex among various subcortical structures. There was increased subcortical atrophy in males compared with females in both PD groups, and we observed that sex differences in subcortical regions were more evident in the PD-pRBD group, with a significant group-by-sex interaction in the pallidum. The sex effect in the pallidum was greater in the PD-pRBD group compared with the PD-non pRBD group. Specifically, we found significant differences in three structures in the PD-pRBD group compared with only one structures in the PD-non pRBD group and none structure in the control group. In de novo PD as a whole group, using voxel-based morphometry, males have been shown to have increased atrophy in the left thalamus compared to females [15]. However, following the applied classification, the PD-pRBD group showed sex differences in the bilateral pallidum, caudate, and brainstem; but the PD-non pRBD group showed only one sex difference, in the brainstem.

Together, our results provide evidence for the presence of sex differences in cognition and brain structure following a continuum from normal aging to patients with PD and pRBD. In both PD groups, males show more severe atrophy, suggesting that female sex confers protective benefits against neurodegeneration. Several pathophysiological mechanisms have been suggested as being responsible for sex differences in neurodegenerative processes. Dysregulated gene expression and sex hormones have been related to these sex differences in the pathophysiology of PD, including vulnerability of the dopaminergic system, neuroinflammation, and oxidative stress [2]. Another implicated mechanism is the alpha-synuclein, that has been observed in more decreased plasma concentrations in males than females in advanced stages of PD; and its concentration has been associated with cognitive impairment and sleep disorders in PD males [33]. By analyzing the subcortical structural volumes of 38,851 subjects, several genes involved in the regulation of neuronal apoptosis, inflammation/immunity, and susceptibility to neurological disorders have been identified [34]. Nevertheless, in the future, other functional biomarkers and imaging techniques are needed to investigate the specific mechanisms underlying sex-related brain differences in PD.

The main strength of the paper is a very large sample that allows testing sex effects on brain and cognition in PD and the main limitation of our study is using a validated RBD questionnaire instead of a confirmed polysomnography diagnosis. In this sense, the RBDSQ showed a sensitivity of 0.47 and a specificity of 0.78 in a cohort of PD de novo patients [35]. The use of a questionnaire could increment the false positive discovery rate by overestimating the incidence of clinically significant RBD symptomatology and limit the generalisability of the obtained results. Another limitation is that PPMI data were acquired from a multicenter cohort having differences in MRI acquisition. Finally, we could not have a group of healthy controls with probable RBD to take into account the influence of this condition isolated.

In summary, our results underpin the role of sex as being important to understanding the phenotypic expression of PD. Our findings also indicate that sex male is related to increased functional alterations in motor, RBD, and cognitive domains among drug-naïve PD patients with pRBD. Also, PD-pRBD male patients show more atrophy in subcortical structures than PD-pRBD females and these sex differences are in more structures than in patients without pRBD. Accordingly, we suggest that sex differences are relevant factors to be considered in clinical trials.

**Supplementary Information** The online version contains supplementary material available at <https://doi.org/10.1007/s00415-021-10728-x>.

**Acknowledgements** Parkinson's Progression Marker Initiative (PPMI)—a public–private partnership—is funded by the Michael J. Fox Foundation for Parkinson's Research and funding partners,

including Abbvie, Acurex Therapeutics, Allergan, Amathus Therapeutics, Aligning Science Across Parkinson's, Avid Radiopharmaceuticals, Bial Biotech, Biogen, BioLegend, Bristol Myers Squibb, Calico, Celgene, Dacapo Brainscience, Denali, 4D Pharma Plc, F. Dmond J. Safra Philanthropic Foundation, GE Healthcare, Genentech, GlaxoSmithKline, Golub Capital, Handl Therapeutics, Insitro, Janssen Neuroscience, Lilly, Lundbeck, Merck. Meso Scale Discovery, Neurocrine Biosciences, Pfizer, Piramal, Prevail Therapeutics, Roche, Sanofi Genzyme, Servier, Takeda, Teva, Ucb, Verily and Voyager Therapeutics. We acknowledge the Centres de Recerca de Catalunya (CERCA) Programme/Generalitat de Catalunya, the Institute of Neurosciences, and the Institute of Biomedical Research August Pi i Sunyer (IDIBAPS).

**Author contributions** Research project conception and acquisition of data are explained in Marek et al. 2011 as cited in the text. CJ and BS contributed to the design of the study. JO, BS, CU and GM contributed to the analysis of the data and JO, BS, CU, GM, AC, AInguanzo, JP and CJ contributed to the interpretation of the data. JO, BS, CU, and CJ contributed to the draft of the article. JO, BS, CU, MJM, YC, FV, AIranzo and CJ revised the manuscript critically for important intellectual content and approved the final version of the manuscript.

**Funding** This study was sponsored by the Spanish Ministry of Economy and Competitiveness (PSI2017-86930-P) cofinanced by Agencia Estatal de Investigación (AEI) and the European Regional Development Fund (ERDF), by Generalitat de Catalunya (2017SGR748), and supported by María de Maeztu Unit of Excellence (Institute of Neurosciences, University of Barcelona) MDM-2017-0729, Ministry of Science, Innovation and Universities. JO was supported by a 2018 fellowship from the Spanish Ministry of Science, Universities and Research and cofinanced by the European Social Fund (PRE2018-086675). CU was supported by the European Union's Horizon 2020 research and innovation programme under the Marie Skłodowska-Curie fellowship (Grant Agreement 888692). AInguanzo was supported by APIF predoctoral fellowship from the University of Barcelona (2017–2018). YC has received funding in the past 5 years from FIS/FEDER, H2020 programme. Open Access funding provided thanks to the CRUE-CSIC agreement with Springer Nature.

**Data availability** Data used in the preparation of this article were obtained from the Parkinson's Progression Markers Initiative (PPMI) database ([www.ppmi-info.org/data](http://www.ppmi-info.org/data)). For up-to-date information on the study, visit [www.ppmi-info.org](http://www.ppmi-info.org).

**Code availability** Not applicable.

## Declarations

**Conflicts of interest** MJM received honoraria for advice and lecture from Abbvie, Bial and Merzt Pharma and grants from Michael J. Fox Foundation for Parkinson's Research (MJFF): MJF\_PPMI\_10\_001, PI044024. YC has received funding in the past 5 years from Union Chimique Belge (UCB pharma), Teva, Medtronic, Abbvie, Novartis, Merz, Piramal Imaging, and Esteve, Bial, and Zambon. YC is currently an associate editor for Parkinsonism & Related Disorders.

**Ethical approval** All participating PPMI sites received approval from an ethical standards committee prior to study initiation.

**Consent to participate and consent to publication** All participating PPMI sites obtained written informed consent for research from all participants in the study as described in the PPMI study protocol, available in <https://www.ppmi-info.org/study-design/research-documents-and-sops/>.

**Open Access** This article is licensed under a Creative Commons Attribution 4.0 International License, which permits use, sharing, adaptation, distribution and reproduction in any medium or format, as long as you give appropriate credit to the original author(s) and the source, provide a link to the Creative Commons licence, and indicate if changes were made. The images or other third party material in this article are included in the article's Creative Commons licence, unless indicated otherwise in a credit line to the material. If material is not included in the article's Creative Commons licence and your intended use is not permitted by statutory regulation or exceeds the permitted use, you will need to obtain permission directly from the copyright holder. To view a copy of this licence, visit <http://creativecommons.org/licenses/by/4.0/>.













## References

1. Ferretti MT, Iulita MF, Cavedo E et al (2018) Sex differences in Alzheimer disease—the gateway to precision medicine. *Nat Rev Neurol* 14:457–469. <https://doi.org/10.1038/s41582-018-0032-9>
2. Cerri S, Mus L, Blandini F (2019) Parkinson's disease in women and men: what's the difference? *J Parkinsons Dis* 9:501–515. <https://doi.org/10.3233/JPD-191683>
3. Turcano P, Savica R (2020) Sex differences in movement disorders, 1st edn. Elsevier B.V
4. Baldereschi M, Di Carlo A, Rocca WA et al (2000) Parkinson's disease and parkinsonism in a longitudinal study: two-fold higher incidence in men. *Neurology* 55:1358–1363. <https://doi.org/10.1212/WNL.55.9.1358>
5. Szweczyk-Krolikowski K, Tomlinson P, Nithi K et al (2014) The influence of age and gender on motor and non-motor features of early Parkinson's disease: initial findings from the Oxford Parkinson Disease Center (OPDC) discovery cohort. *Parkinsonism Relat Disord* 20:99–105. <https://doi.org/10.1016/j.parkreldis.2013.09.025>
6. Liu R, Umbach DM, Peddada SD et al (2015) Potential sex differences in nonmotor symptoms in early drug-naive Parkinson disease. *Neurology* 84:2107–2115. <https://doi.org/10.1212/WNL.0000000000001609>
7. Lin SJ, Baumeister TR, Garg S, McKeown MJ (2018) Cognitive profiles and hub vulnerability in Parkinson's disease. *Front Neurol* 9:1–13. <https://doi.org/10.3389/fneur.2018.00482>
8. Bakeberg MC, Gorecki AM, Kenna JE et al (2021) Differential effects of sex on longitudinal patterns of cognitive decline in Parkinson's disease. *J Neurol*. <https://doi.org/10.1007/s00415-020-10367-8>
9. Reekes TH, Higginson CI, Ledbetter CR et al (2020) Sex specific cognitive differences in Parkinson disease. *NPJ Parkinsons Dis* 6:1–6. <https://doi.org/10.1038/s41531-020-0109-1>
10. Curtis AF, Masellis M, Camicioli R et al (2019) Cognitive profile of non-demented Parkinson's disease: meta-analysis of domain and sex-specific deficits. *Parkinsonism Relat Disord* 60:32–42. <https://doi.org/10.1016/j.parkreldis.2018.10.014>
11. Iwaki H, Blauwendraat C, Leonard HL et al (2021) Differences in the presentation and progression of Parkinson's disease by sex. *Mov Disord* 36:106–117. <https://doi.org/10.1002/mds.28312>
12. Cholerton B, Johnson CO, Fish B et al (2018) Sex differences in progression to mild cognitive impairment and dementia in Parkinson's disease. *Parkinsonism Relat Disord* 50:29–36. <https://doi.org/10.1016/j.parkreldis.2018.02.007>
13. Liu G, Locascio JJ, Corvol JC et al (2017) Prediction of cognition in Parkinson's disease with a clinical-genetic score: a longitudinal analysis of nine cohorts. *Lancet Neurol* 16:620–629. [https://doi.org/10.1016/S1474-4422\(17\)30122-9](https://doi.org/10.1016/S1474-4422(17)30122-9)
14. Yadav SK, Kathiresan N, Mohan S et al (2016) Gender-based analysis of cortical thickness and structural connectivity in



- Parkinson's disease. *J Neurol* 263:2308–2318. <https://doi.org/10.1007/s00415-016-8265-2>
15. Tremblay C, Abbasi N, Zeighami Y et al (2020) Sex effects on brain structure in de novo Parkinson's disease: a multimodal neuroimaging study. *Brain* 143:3052–3066. <https://doi.org/10.1093/brain/awaa234>
  16. Galbiati A, Verga L, Giora E et al (2019) The risk of neurodegeneration in REM sleep behavior disorder: a systematic review and meta-analysis of longitudinal studies. *Sleep Med Rev* 43:37–46. <https://doi.org/10.1016/j.smr.2018.09.008>
  17. Fernández-Arcos A, Iranzo A, Serradell M et al (2016) The clinical phenotype of idiopathic rapid eye movement sleep behavior disorder at presentation: a study in 203 consecutive patients. *Sleep* 39:121–132. <https://doi.org/10.5665/sleep.5332>
  18. Zhang J, Xu CY, Liu J (2017) Meta-analysis on the prevalence of REM sleep behavior disorder symptoms in Parkinson's disease. *BMC Neurol* 17:23. <https://doi.org/10.1186/s12883-017-0795-4>
  19. Chahine LM, Xie SX, Simuni T et al (2016) Longitudinal changes in cognition in early Parkinson's disease patients with REM sleep behavior disorder. *Parkinsonism Relat Disord* 27:102–106. <https://doi.org/10.1016/j.parkreldis.2016.03.006>
  20. Trout J, Christiansen T, Bulkley MB et al (2020) Cognitive impairments and self-reported sleep in early-stage Parkinson's disease with versus without probable REM sleep behavior disorder. *Brain Sci*. <https://doi.org/10.3390/brainsci10010009>
  21. Jozwiak N, Postuma RB, Montplaisir J et al (2017) Rem sleep behavior disorder and cognitive impairment in Parkinson's disease. *Sleep*. <https://doi.org/10.1093/sleep/zsx101>
  22. Boucetta S, Salimi A, Dadar M et al (2016) Structural brain alterations associated with rapid eye movement sleep behavior disorder in Parkinson's disease. *Sci Rep* 6:26782. <https://doi.org/10.1038/srep26782>
  23. Kamps S, van den Heuvel OA, van der Werf YD et al (2019) Smaller subcortical volume in Parkinson patients with rapid eye movement sleep behavior disorder. *Brain Imaging Behav* 13:1352–1360. <https://doi.org/10.1007/s11682-018-9939-4>
  24. Marek K, Jennings D, Lasch S et al (2011) The Parkinson progression marker initiative (PPMI). *Prog Neurobiol* 95:629–635. <https://doi.org/10.1016/j.pneurobio.2011.09.005>
  25. Stiasny-Kolster K, Mayer G, Schäfer S et al (2007) The REM sleep behavior disorder screening questionnaire—a new diagnostic instrument. *Mov Disord* 22:2386–2393. <https://doi.org/10.1002/mds.21740>
  26. Uribe C, Puig-Davi A, Abos A et al (2019) Neuroanatomical and functional correlates of cognitive and affective empathy in young healthy adults. *Front Behav Neurosci* 13:85
  27. Fischl B, Salat DH, Busa E et al (2002) Whole brain segmentation: automated labeling of neuroanatomical structures in the human brain. *Neuron* 33:341–355. [https://doi.org/10.1016/S0896-6273\(02\)00569-X](https://doi.org/10.1016/S0896-6273(02)00569-X)
  28. Aarsland D, Bronnick K, Larsen JP et al (2009) Cognitive impairment in incident, untreated Parkinson disease: the Norwegian ParkWest Study. *Neurology* 72:1121–1126. <https://doi.org/10.1212/01.wnl.0000338632.00552.cb>
  29. Ritchie SJ, Cox SR, Shen X et al (2018) Sex differences in the adult human brain: evidence from 5216 UK biobank participants. *Cereb Cortex* 28:2959–2975. <https://doi.org/10.1093/cercor/bhy109>
  30. Lotze M, Domin M, Gerlach FH et al (2019) Novel findings from 2838 adult brains on sex differences in gray matter brain volume. *Sci Rep* 9:1–7. <https://doi.org/10.1038/s41598-018-38239-2>
  31. Király A, Szabó N, Tóth E et al (2016) Male brain ages faster: the age and gender dependence of subcortical volumes. *Brain Imaging Behav* 10:901–910. <https://doi.org/10.1007/s11682-015-9468-3>
  32. Wang Y, Xu Q, Luo J et al (2019) Effects of age and sex on subcortical volumes. *Front Aging Neurosci* 11:1–12. <https://doi.org/10.3389/fnagi.2019.00259>
  33. Caranci G, Piscopo P, Rivabene R et al (2013) Gender differences in Parkinson's disease: focus on plasma alpha-synuclein. *J Neural Transm* 120:1209–1215. <https://doi.org/10.1007/s00702-013-0972-6>
  34. Satizabal CL, Adams HHH, Hibar DP et al (2019) Genetic architecture of subcortical brain structures in 38,851 individuals. *Nat Genet* 51:1624–1636. <https://doi.org/10.1038/s41588-019-0511-y>
  35. Halsband C, Zapf A, Sixel-Döring F et al (2018) The REM sleep behavior disorder screening questionnaire is not valid in de novo Parkinson's disease. *Mov Disord Clin Pract* 5:171–176. <https://doi.org/10.1002/mdc3.12591>

## Authors and Affiliations

Javier Oltra<sup>1,2</sup>  · Barbara Segura<sup>1,2,3</sup>  · Carme Uribe<sup>1,2,4</sup>  · Gemma C. Monté-Rubio<sup>1</sup>  · Anna Campabadal<sup>1,2</sup>  · Anna Inguanzo<sup>1,2</sup>  · Jèssica Pardo<sup>1</sup>  · Maria J. Martí<sup>2,3,5</sup>  · Yaroslau Compta<sup>2,3,5</sup>  · Francesc Valldeoriola<sup>2,3,5</sup>  · Alex Iranzo<sup>2,3,6</sup>  · Carme Junque<sup>1,2,3</sup> 

Javier Oltra  
joltra@ub.edu

Carme Uribe  
carme.uribe@ub.edu

Gemma C. Monté-Rubio  
gmonte@ub.edu

Anna Campabadal  
anna.campabadal@ub.edu

Anna Inguanzo  
annainguanzo@ub.edu

Jèssica Pardo  
jpardoru@ub.edu

Maria J. Martí  
mjmarti@clinic.cat

Yaroslau Compta  
ycompta@clinic.cat

Francesc Valldeoriola  
fvallde@clinic.cat

Alex Iranzo  
airanzo@clinic.cat

Carme Junque  
cjunque@ub.edu

<sup>1</sup> Medical Psychology Unit, Department of Medicine, Institute of Neurosciences, University of Barcelona, Barcelona, Spain

<sup>2</sup> Institute of Biomedical Research August Pi i Sunyer (IDIBAPS), Barcelona, Catalonia, Spain

- <sup>3</sup> Centro de Investigación Biomédica en Red Enfermedades Neurodegenerativas (CIBERNED: CB06/05/0018-ISCI), Barcelona, Catalonia, Spain
- <sup>4</sup> Research Imaging Centre, Campbell Family Mental Health Research Institute, Centre for Addiction and Mental Health (CAMH), University of Toronto, Toronto, Canada
- <sup>5</sup> Parkinson's Disease and Movement Disorders Unit, Neurology Service, Hospital Clínic de Barcelona, Institute of Neurosciences, University of Barcelona, Barcelona, Catalonia, Spain
- <sup>6</sup> Sleep Disorders Center, Neurology Service, Hospital Clínic, Barcelona, Catalonia, Spain

**Sex differences in brain atrophy and cognitive impairment in Parkinson's disease patients with and without probable rapid eye movement sleep behavior disorder**

**Journal of Neurology**

Javier Oltra<sup>a, b</sup>, Barbara Segura<sup>a, b, c\*</sup>, Carme Uribe<sup>a, b, d</sup>, Gemma C. Monté-Rubio<sup>a</sup>, Anna Campabadal<sup>a, b</sup>, Anna Inguanzo<sup>a, b</sup>, Jèssica Pardo<sup>a</sup>, Maria J. Martí<sup>b, c, e</sup>, Yaroslau Compta<sup>b, c, e</sup>, Francesc Valldeoriola<sup>b, c, e</sup>, Alex Iranzo<sup>b, c, f</sup>, Carme Junque<sup>a, b, c</sup>

<sup>a</sup> Medical Psychology Unit, Department of Medicine, Institute of Neurosciences, University of Barcelona, Barcelona, Catalonia, Spain

<sup>b</sup> Institute of Biomedical Research August Pi i Sunyer (IDIBAPS), Barcelona, Catalonia, Spain

<sup>c</sup> Centro de Investigación Biomédica en Red Enfermedades Neurodegenerativas (CIBERNED: CB06/05/0018-ISCI), Barcelona, Catalonia, Spain

<sup>d</sup> Research Imaging Centre, Campbell Family Mental Health Research Institute, Centre for Addiction and Mental Health (CAMH), University of Toronto, Toronto, Canada

<sup>e</sup> Parkinson's Disease & Movement Disorders Unit, Neurology Service, Hospital Clínic de Barcelona, Institute of Neurosciences, University of Barcelona, Barcelona, Catalonia, Spain

<sup>f</sup> Sleep Disorders Center, Neurology Service, Hospital Clínic, Barcelona, Catalonia, Spain

\*Corresponding author. Dr Barbara Segura. Medical Psychology Unit, Department of Medicine, University of Barcelona, Casanova 143, 08036, Barcelona, Spain. phone [+34] 934039297 // 93 4034446 Fax: [+34] 93 4035294. E-mail address: bsegura@ub.edu (B.Segura).

**Supplementary Table 1**

MRI field strength distribution of the groups

	<b>1.5 T</b>	<b>3 T</b>	<b>Test stat (P value)</b>
HC female	8 (27.6%)	21 (72.4%)	3.913 (0.562)
HC male	6 (15.0%)	34 (85.0%)	
PD-non pRBD female	15 (28.3%)	38 (71.7%)	
PD-non pRBD male	22 (30.1%)	51 (69.9%)	
PD-pRBD female	5 (20.0%)	20 (80.0%)	
PD-pRBD male	15 (27.8%)	39 (72.2%)	

Data are presented by groups as n (%). Pearson's chi-squared was used.

Abbreviations: HC = healthy controls; PD-non pRBD = PD without probable RBD; PD-pRBD = PD with probable RBD; T = Tesla.

**Supplementary Table 2**

Estimated total intracranial volume of HC, PD-non pRBD, and PD-pRBD females and males

		<b>HC</b>	<b>PD-non pRBD</b>	<b>PD-pRBD</b>	<b>Sex main effect test stat (P value)</b>
eTIV, cm <sup>3</sup>	F	1418.4 (112.5)	1480.9 (138.1)	1442.2 (132.9)	111.003 (<0.001) <sup>a, b, c</sup>
	M	1589.5 (154.8)	1682.2 (134.0)	1651.6 (164.2)	

Data are presented by groups as mean (SD). Two-way analyses of variance (ANOVA), followed by Bonferroni post-hoc tests, were used.

<sup>a</sup> Sex differences in HC group; <sup>b</sup> Sex differences in PD-non pRBD group; <sup>c</sup> Sex differences in PD-pRBD group (P < 0.05)

Abbreviations: F= female; eTIV = estimated total intracranial volume; HC = healthy controls; M = male; PD-non pRBD = PD without probable RBD; PD-pRBD = PD with probable RBD.

**Supplementary Table 3**

Neuropsychological tasks scores of HC, PD-non pRBD, and PD-pRBD females and males

		HC	PD-non pRBD	PD-pRBD	Group-by-sex test stat (P value)
MoCA	F	-0.14 (0.90)	-0.77 (1.81)	-0.11 (1.52)	4.758 (0.009) <sup>a, b</sup>
	M	0.10 (1.07)	-1.08 (1.93)	-1.56 (1.81)	
Semantic fluency					
Animals	F	0.14 (0.97)	-0.23 (0.94)	-0.39 (0.75)	1.270 (0.283)
	M	-0.10 (1.02)	-0.12 (0.97)	-0.66 (0.84)	
Vegetables	F	0.46 (1.03)	0.36 (1.19)	0.09 (0.88)	0.156 (0.856)
	M	-0.33 (0.84)	-0.58 (1.05)	-0.76 (1.06)	
Fruits	F	0.59 (0.81)	0.03 (0.95)	-0.11 (0.80)	1.379 (0.254)
	M	-0.43 (0.91)	-0.51 (0.96)	-0.78 (0.95)	
Phonetic fluency 'f'	F	-0.13 (0.92)	-0.34 (1.04)	-0.25 (0.84)	1.577 (0.209)
	M	0.10 (1.06)	-0.31 (1.03)	-0.62 (0.95)	
SDMT	F	-0.03 (0.86)	-0.43 (0.98)	-0.34 (0.86)	4.196 (0.016) <sup>a, b, c</sup>
	M	0.02 (1.10)	-0.58 (0.89)	-1.10 (1.11)	
LNS	F	-0.12 (0.91)	-0.17 (0.92)	-0.61 (0.88)	0.548 (0.579)
	M	0.09 (1.06)	-0.23 (1.09)	-0.55 (0.95)	
JLO	F	-0.35 (1.13)	-0.52 (1.08)	-0.65 (1.39)	0.917 (0.401)
	M	0.25 (0.82)	0.14 (1.03)	-0.39 (1.27)	
HLVT-R					
Immediate recall	F	0.37 (0.90)	0.10 (1.03)	-0.07 (0.89)	0.293 (0.746)
	M	-0.26 (1.00)	-0.43 (1.18)	-0.82 (1.07)	
Recognition	F	0.09 (0.88)	-0.01 (0.90)	-0.01 (0.76)	0.162 (0.851)
	M	-0.07 (1.09)	-0.17 (0.91)	-0.31 (0.98)	
Delayed recall	F	0.25 (0.77)	-0.13 (0.94)	-0.18 (0.94)	0.655 (0.520)
	M	-0.18 (1.11)	-0.43 (1.04)	-0.82 (1.09)	

Data are presented in z-scores by groups as mean (SD). Two-way analyses of covariance (ANCOVA) with age as covariable, followed by Bonferroni post-hoc tests, were used for all variables.

<sup>a</sup> Differences between HC males and PD-non pRBD males, <sup>b</sup> Differences between HC males and PD-pRBD males, <sup>c</sup> Differences between PD-non pRBD males and PD-pRBD males (P < 0.05).

Abbreviations: F= female; HC = healthy controls; HVLTV-R = Hopkins Verbal Learning Test-Revised; JLO = Benton Judgment of Line Orientation; LNS = Letter-Number Sequencing; M = male; MoCA = Montreal Cognitive Assessment; PD-non pRBD = PD without probable RBD; PD-pRBD = PD with probable RBD; SDMT = Symbol Digit Modalities Test.

**Supplementary Table 4**

Neuropsychological tasks in z-scores adjusted by age and sex of HC, PD-non pRBD, and PD-pRBD females and males

		HC	PD-non pRBD	PD-pRBD	Group-by-sex test stat (P value)
MoCA	F	-0.01 (0.91)	-0.64 (1.82)	0.05 (1.53)	4.828 (0.009) <sup>a, b</sup>
	M	-0.01 (1.06)	-1.20 (1.93)	-1.66 (1.79)	
	<b>Within-group sex effect, test stat (P value)</b>	<b>0.000 (0.998)</b>	<b>3.584 (0.059)</b>	<b>18.419 (&lt;0.001)</b>	
Semantic fluency					
Animals	F	-0.01 (0.96)	-0.38 (0.97)	-0.57 (0.79)	0.963 (0.383)
	M	-0.01 (1.02)	-0.05 (0.94)	-0.57 (0.85)	
	<b>Within-group sex effect, test stat (P value)</b>	<b>0.000 (0.997)</b>	<b>3.607 (0.059)</b>	<b>0.000 (0.985)</b>	
Vegetables	F	0.02 (1.02)	-0.08 (1.17)	-0.32 (0.87)	0.137 (0.872)
	M	0.02 (0.85)	-0.24 (1.04)	-0.41 (1.05)	
	<b>Within-group sex effect, test stat (P value)</b>	<b>0.000 (0.996)</b>	<b>0.751 (0.387)</b>	<b>0.751 (0.387)</b>	
Fruits	F	-0.01 (0.80)	-0.57 (0.93)	-0.70 (0.78)	1.514 (0.222)
	M	-0.01 (0.86)	-0.09 (0.96)	-0.36 (.94)	
	<b>Within-group sex effect, test stat (P value)</b>	<b>0.000 (0.999)</b>	<b>8.441 (0.004)</b>	<b>2.348 (0.127)</b>	
Phonetic fluency 'f'	F	-0.00 (0.92)	-0.22 (1.04)	-0.22 (0.86)	1.196 (0.304)
	M	-0.00 (1.01)	-0.37 (1.10)	-0.74 (1.00)	
	<b>Within-group sex effect, test stat (P value)</b>	<b>0.000 (0.999)</b>	<b>0.719 (0.397)</b>	<b>4.466 (0.036)</b>	
SDMT	F	0.01 (0.88)	-0.38 (0.88)	-0.21 (0.80)	4.040 (0.019) <sup>a, b, c</sup>
	M	0.01 (1.07)	-0.62 (0.85)	-1.10 (1.12)	
	<b>Within-group sex effect, test stat (P value)</b>	<b>0.000 (1.000)</b>	<b>1.906 (0.169)</b>	<b>14.596 (&lt;0.001)</b>	
LNS	F	0.01 (0.89)	-0.03 (0.90)	-0.42 (0.85)	0.522 (0.594)
	M	0.01 (1.06)	-0.34 (1.07)	-0.62 (0.94)	
	<b>Within-group sex effect, test stat (P value)</b>	<b>0.000 (0.998)</b>	<b>2.911 (0.089)</b>	<b>0.756 (0.385)</b>	
JLO	F	0.00 (1.12)	-0.17 (1.07)	-0.28 (1.36)	0.811 (0.446)
	M	0.00 (0.82)	-0.12 (1.03)	-0.64 (1.27)	
	<b>Within-group sex effect, test stat (P value)</b>	<b>0.000 (1.000)</b>	<b>0.083 (0.773)</b>	<b>1.768 (0.185)</b>	
HVLVT-R					
Immediate recall	F	-0.00 (0.90)	-0.27 (1.04)	-0.45 (0.89)	0.226 (0.798)
	M	-0.00 (1.00)	-0.17 (1.19)	-0.56 (1.07)	
	<b>Within-group sex effect, test stat (P value)</b>	<b>0.000 (0.999)</b>	<b>0.311 (0.577)</b>	<b>0.171 (0.679)</b>	
Recognition	F	-0.02 (0.85)	-0.13 (0.97)	-0.21 (0.84)	0.070 (0.932)
	M	-0.02 (1.08)	-0.09 (0.96)	-0.28 (0.97)	
	<b>Within-group sex effect, test stat (P value)</b>	<b>0.000 (0.996)</b>	<b>0.047 (0.828)</b>	<b>0.094 (0.760)</b>	
Delayed recall	F	0.02 (0.79)	-0.36 (1.03)	-0.50 (1.03)	0.438 (0.646)
	M	0.02 (1.07)	-0.19 (1.13)	-0.063 (1.10)	
	<b>Within-group sex effect, test stat (P value)</b>	<b>0.250 (0.618)</b>	<b>0.745 (0.389)</b>	<b>0.250 (0.618)</b>	

Data are presented by groups as mean (SD). Neuropsychological variables are presented in z-scores adjusted by age and sex. Two-way analyses of variance (ANOVA), followed by Bonferroni post-hoc tests, were used for all variables.

<sup>a</sup> Differences between HC males and PD-non pRBD males, <sup>b</sup> Differences between HC males and PD-pRBD males, <sup>c</sup> Differences between PD-non pRBD males and PD-pRBD males (P < 0.05).

Abbreviations: F= female; HC = healthy controls; HVLVT-R = Hopkins Verbal Learning Test-Revised; JLO = Benton Judgment of Line Orientation; LNS = Letter-Number Sequencing; M = male; MoCA = Montreal Cognitive Assessment; PD-non pRBD = PD without probable RBD; PD-pRBD = PD with probable RBD; SDMT = Symbol Digit Modalities Test.

**Supplementary Table 5**

Between-group differences regarding the within-group sex effects in those z-scored variables adjusted by age and sex that showed group-by-sex interaction

	<b>Group-by sex interaction test stat (P value)</b>	<b>Contrast 1 HC vs. PD-non pRBD (P value)</b>	<b>Contrast 2 HC vs. PD-pRBD (P value)</b>	<b>Contrast 3 PD-non pRBD vs. PD-pRBD (P value)</b>
<b>Neuropsychological tasks</b>				
MoCA	4.828 (0.009)	0.501	0.003	0.022
SDMT	4.040 (0.019)	0.411	0.007	0.025
<b>Deep GM nuclei</b>				
Pallidum	3.159 (0.044)	0.796	0.058	0.016

Post-hoc contrasts were applied after two-way analysis of variance (ANOVA) of z-scored variables adjusted by age and sex.

Contrast 1 compare the sex effects between HC (HC males – HC females) and PD-non pRBD (PD-non pRBD males – PD-non pRBD females) groups.

Contrast 2 compare the sex effects between HC (HC males – HC females) and PD-pRBD (PD-pRBD males – pRBD females) groups.

Contrast 3 compare the sex effects between PD-non pRBD (PD-non pRBD males – PD-non pRBD females) and PD-pRBD (PD-pRBD males – PD-pRBD females) groups.

Abbreviations: GM = gray matter; HC = healthy controls; MoCA = Montreal Cognitive Assessment; PD-non pRBD = PD without probable RBD; PD-pRBD = PD with probable RBD; SDMT = Symbol Digit Modalities Test.



**Supplementary Table 6**

Magnetic resonance imaging derived measures in z-scores adjusted by age and sex of HC, PD-non pRBD, and PD-pRBD females and males

		HC	PD-non pRBD	PD-pRBD	Group-by-sex test stat (P value)
<b>Global atrophy</b>					
Cortical GM	F	0.01 (0.85)	-0.32 (1.03)	0.01 (1.09)	1.363 (0.258)
	M	0.01 (1.08)	-0.59 (0.92)	-0.57 (1.14)	
<i>Within-group sex effect, test stat (P value)</i>		<b>0.000 (0.997)</b>	<b>2.037 (0.155)</b>	<b>5.457 (0.020)</b>	
Subcortical GM	F	0.00 (0.97)	-0.18 (0.88)	0.02 (1.12)	1.771 (0.172)
	M	0.00 (0.93)	-0.16 (0.79)	-0.44 (0.84)	
<i>Within-group sex effect, test stat (P value)</i>		<b>0.000 (1.000)</b>	<b>0.012 (0.914)</b>	<b>4.587 (0.033)</b>	
Mean CTh, mm	F	0.02 (0.85)	-0.12 (0.84)	-0.19 (0.73)	0.011 (0.989)
	M	0.02 (1.08)	-0.16 (0.98)	-0.21 (1.06)	
<i>Within-group sex effect, test stat (P value)</i>		<b>0.000 (0.996)</b>	<b>0.058 (0.809)</b>	<b>0.007 (0.936)</b>	
<b>Deep GM nuclei</b>					
Thalamus	F	0.01 (0.78)	0.15 (1.00)	0.08 (1.00)	0.751 (0.473)
	M	0.01 (1.00)	-0.09 (0.87)	-0.29 (0.78)	
<i>Within-group sex effect, test stat (P value)</i>		<b>0.000 (0.996)</b>	<b>2.179 (0.141)</b>	<b>2.900 (0.090)</b>	
Caudate	F	0.00 (1.09)	-0.02 (1.05)	0.30 (0.86)	2.080 (0.127)
	M	0.00 (0.93)	-0.12 (0.98)	-0.32 (0.93)	
<i>Within-group sex effect, test stat (P value)</i>		<b>0.000 (1.000)</b>	<b>0.317 (0.574)</b>	<b>6.850 (0.009)</b>	
Putamen	F	-0.03 (1.05)	-0.28 (0.97)	-0.12 (1.15)	1.085 (0.339)
	M	-0.03 (0.90)	-0.17 (0.82)	-0.43 (0.94)	
<i>Within-group sex effect, test stat (P value)</i>		<b>0.000 (0.995)</b>	<b>0.375 (0.541)</b>	<b>1.877 (0.172)</b>	
Pallidum	F	-0.01 (0.95)	0.05 (1.04)	0.35 (1.01)	3.159 (0.044) <sup>a</sup>
	M	-0.02 (1.04)	0.05 (1.04)	-0.31 (1.10)	
<i>Within-group sex effect, test stat (P value)</i>		<b>0.000 (0.997)</b>	<b>0.185 (0.667)</b>	<b>7.341 (0.007)</b>	
Hippocampus	F	0.03 (0.97)	-0.36 (0.99)	-0.14 (1.05)	0.759 (0.469)
	M	0.03 (0.88)	-0.17 (0.90)	-0.30 (0.91)	
<i>Within-group sex effect, test stat (P value)</i>		<b>0.000 (0.995)</b>	<b>1.184 (0.278)</b>	<b>0.489 (0.485)</b>	
Amygdala	F	-0.01 (0.95)	-0.54 (1.06)	-0.12 (1.64)	2.253 (0.107)
	M	-0.01 (1.03)	-0.34 (0.94)	-0.60 (1.00)	
<i>Within-group sex effect, test stat (P value)</i>		<b>0.000 (0.998)</b>	<b>1.076 (0.301)</b>	<b>3.492 (0.063)</b>	
Accumbens	F	0.02 (1.19)	-0.13 (1.25)	0.36 (1.29)	1.507 (0.223)
	M	0.02 (0.82)	-0.045 (1.12)	-0.14 (1.18)	
<i>Within-group sex effect, test stat (P value)</i>		<b>0.000 (0.997)</b>	<b>0.156 (0.693)</b>	<b>3.291 (0.071)</b>	
Brainstem	F	-0.03 (0.84)	0.22 (1.05)	0.25 (0.91)	2.113 (0.123)
	M	-0.03 (1.11)	-0.17 (0.92)	-0.46 (1.05)	
<i>Within-group sex effect, test stat (P value)</i>		<b>0.000 (0.995)</b>	<b>4.752 (0.030)</b>	<b>8.518 (0.004)</b>	

Data are presented by groups as mean (SD). Volumetric variables are presented in z-scores adjusted by age and sex. Two-way analyses of variance (ANOVA), followed by Bonferroni post-hoc tests, were used for all variables.

<sup>a</sup>Differences between PD-non pRBD males and PD-pRBD males (P < 0.05).

Abbreviations: CTh = cortical thickness; F= female; GM = gray matter; HC = healthy controls; M = male; PD-non pRBD = PD without probable RBD; PD-pRBD = PD with probable RBD.

**Supplementary Table 7**

Neuropsychological tasks scores of PD-non pRBD and PD-pRBD females and males

		PD-non pRBD	PD-pRBD	Group-by-sex test stat (P value)
MoCA	F	-0.77 (1.81)	-0.11 (1.52)	4.175 (0.042)
	M	-1.08 (1.93)	-1.56 (1.81)	
Semantic fluency				
Animals	F	-0.23 (0.94)	-0.39 (0.75)	1.837 (0.177)
	M	-0.12 (0.97)	-0.66 (0.84)	
Vegetables	F	0.36 (1.19)	0.09 (0.88)	0.080 (0.778)
	M	-0.58 (1.05)	-0.76 (1.06)	
Fruits	F	0.03 (0.95)	-0.11 (0.80)	0.292 (0.590)
	M	-0.51 (0.96)	-0.78 (0.95)	
Phonetic fluency 'f'	F	-0.34 (1.04)	-0.25 (0.84)	2.158 (0.143)
	M	-0.31 (1.03)	-0.62 (0.95)	
SDMT	F	-0.43 (0.98)	-0.34 (0.86)	3.061 (0.082)
	M	-0.58 (0.89)	-1.10 (1.11)	
LNS	F	-0.17 (0.92)	-0.61 (0.88)	0.294 (0.588)
	M	-0.23 (1.09)	-0.55 (0.95)	
JLO	F	-0.52 (1.08)	-0.65 (1.39)	1.062 (0.304)
	M	0.14 (1.03)	-0.39 (1.27)	
HLVT-R				
Immediate recall	F	0.10 (1.03)	-0.07 (0.89)	0.276 (0.600)
	M	-0.43 (1.18)	-0.82 (1.07)	
Recognition	F	-0.01 (0.90)	-0.01 (0.76)	0.187 (0.666)
	M	-0.17 (0.91)	-0.31 (0.98)	
Delayed recall	F	-0.13 (0.94)	-0.18 (0.94)	0.918 (0.339)
	M	-0.43 (1.04)	-0.82 (1.09)	

Data are presented in z-scores by groups as mean (SD). Two-way analyses of covariance (ANCOVA) with MDS-UPDRS part III as covariable were used for all variables.

Abbreviations: F= female; HC = healthy controls; HVLTV-R = Hopkins Verbal Learning Test-Revised; JLO = Benton Judgment of Line Orientation; LNS = Letter-Number Sequencing; M = male; MoCA = Montreal Cognitive Assessment; PD-non pRBD = PD without probable RBD; PD-pRBD = PD with probable RBD; SDMT = Symbol Digit Modalities Test.

**Supplementary Table 8**

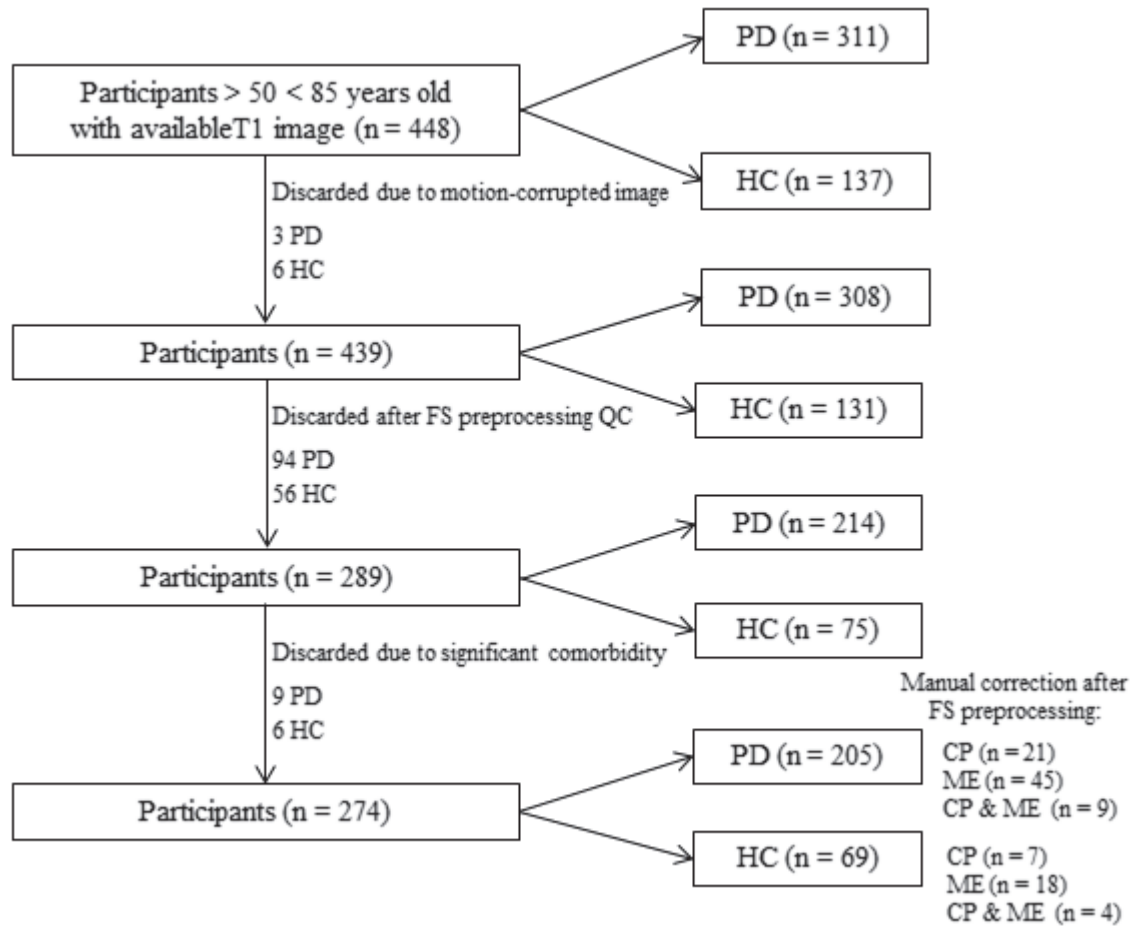
Magnetic resonance imaging derived measures of PD-non pRBD and PD-pRBD females and males

		PD-non pRBD	PD-pRBD	Group-by-sex test stat (P value)
<b>Global atrophy</b>				
Cortical GM	F	29.39 (2.23)	30.03 (2.34)	0.856 (0.356)
	M	28.15 (1.98)	28.15 (2.39)	
Subcortical GM	F	3.63 (0.26)	3.66 (0.32)	2.429 (0.121)
	M	3.51 (0.24)	3.41 (0.24)	
Mean CTh, mm	F	2.42 (0.10)	2.41 (0.09)	0.028 (0.866)
	M	2.39 (0.12)	2.38 (0.12)	
<b>Deep GM nuclei</b>				
Thalamus	F	0.465 (0.042)	0.456 (0.044)	0.209 (0.865)
	M	0.441 (0.040)	0.429 (0.037)	
Caudate	F	0.221 (0.027)	0.229 (0.022)	2.875 (0.092)
	M	0.212 (0.025)	0.207 (0.024)	
Putamen	F	0.294 (0.035)	0.296 (0.039)	1.473 (0.226)
	M	0.286 (0.029)	0.275 (0.035)	
Pallidum	F	0.127 (0.014)	0.131 (0.015)	6.267 (0.013) <sup>a</sup>
	M	0.127 (0.013)	0.120 (0.015)	
Hippocampus	F	0.267 (0.030)	0.272 (0.031)	1.122 (0.291)
	M	0.252 (0.028)	0.247 (0.025)	
Amygdala	F	0.103 (0.015)	0.108 (0.022)	2.397 (0.046)
	M	0.105 (0.013)	0.101 (0.013)	
Accumbens	F	0.031 (0.007)	0.034 (0.007)	2.180 (0.141)
	M	0.030 (0.006)	0.030 (0.006)	
Brainstem	F	1.412 (0.128)	1.412 (0.110)	1.066 (0.303)
	M	1.375 (0.113)	1.338 (0.128)	

Data are presented by groups as mean (SD). Volumetric variables are presented in ratios estimated by ((volume / eTIV) \* 100). Two-way analyses of covariance (ANCOVA) with MDS-UPDRS part III as covariable were used for all variables.

<sup>a</sup>Differences between PD-non pRBD males and PD-pRBD males (P < 0.05).

Abbreviations: CTh = cortical thickness; F= female; GM = gray matter; HC = healthy controls; M = male; PD-non pRBD = PD without probable RBD; PD-pRBD = PD with probable RBD.



**Supplementary Figure 1.** Flow diagram of sample selection. Abbreviations: CP = control points; FS = FreeSurfer; HC = healthy controls; ME = manual erase; PD = Parkinson's disease; QC = quality control.

# Chapter 5

---

## General discussion

In the present doctoral thesis, we aimed to describe cognitive impairment and functional and structural MRI characteristics of PD with RBD and establish the correlates between cognition and MRI measures.

We also tried to elucidate if there are sex differences in clinical variables, cognition, and MRI measures in PD with RBD. For these purposes, we performed four studies. The main results of the four studies will be discussed and integrated into this section.

### **Clinical differences of Parkinson's disease with and without RBD**

In the *de novo* stage of the disease (*study 1*), the PD-pRBD compared with the PD-non pRBD group had a more severe impairment (*MDS-UPDRS* total score), presence of constipation, and symptoms and frequency of depression and sleepiness. In a more advanced stage of the disease (*study 2*), we did not find significant differences in the explored clinical variables between groups. However, we cannot conclude that, in more advanced stages, there are no clinical differences between these PD groups. The absence of statistically significant differences in *study 2* could be biased because of the sample size and the heterogeneity of the sample. Furthermore, we need to consider that we included different clinical variables in *studies 1 and 2*.

In this context, *study 1* findings disagree with previous literature that associated RBD in PD with male sex, older age, and longer disease duration (35). Therefore, in *de novo* PD, PD with RBD could reflect a particular point of the disease progression from prodromal phases of PD as iRBD; then, the differences in age and disease duration could be diluted at this time point of the disease evolution. In addition, *de novo* PD without RBD patients could develop RBD later along the disease course and influence the relation between this symptom,

age, and disease progression. Concerning male sex predominance in *study 1*, there were no significant differences between PD-pRBD and PD-non pRBD. The balanced male predominance between groups could be influenced by the PPMI study design because of the recruitment process and the generalized screening of RBD symptomatology with questionnaires. These possible explanations for the absence of significant differences in sex distributions between PD groups are extensible to *study 2*. Besides, the use of questionnaires could increase the rate of false negatives in PD-pRBD female cases. As a note, as we highlighted in the Introduction, the female cases of iRBD and PD with RBD are potentially underdiagnosed (23,24,III). As regards PD symptoms, in *study 1*, we did not find a significant difference in motor symptoms (*MDS-UPDRS Part III*) as reported in the literature (35). But, the PD-pRBD group had more disease severity (*MDS-UPDRS* total score). Additionally, the presence of constipation in the PD-pRBD group agrees with previous studies that reported their association; for example, both symptoms jointly are associated with worse cognitive prognosis in male PD patients (182). The relation between constipation and RBD could reflect the dual-hit hypothesis proposed by Braak et al. (40), extensible to the body-first PD subtype of the alpha-Synuclein Origin and Connectome (SOC) Model (46), highlighting the potential role of the gut-brain axis in PD pathogenesis (183). Moreover, the prevalence of depression in the PD-pRBD group links with previous results that showed an association between RBD symptomatology and depression mediated by autonomic dysfunction in general and specific by gastrointestinal dysfunction (184). The presence of depression in the PD-pRBD group could be associated with a more extensive alpha-synuclein pathology and related neurodegeneration in the *de novo* stage of the disease. Of interest, white matter alterations have been reported in *de novo* PD patients with RBD and depression symptoms compared with those without both symptoms in

concomitance (185,186). Last, increased sleepiness in PD-pRBD agrees with the presence of somnolence in iRBD patients (187).

### **Cognitive impairment in Parkinson's disease with RBD**

Regarding the characterization of the cognitive profile of PD-pRBD patients, we found that this subtype of patients had the worst cognitive profile in the *de novo* stage of the disease (*study 1*) and also in more advanced disease (*study 2*).

In *study 1*, the PD-pRBD group had verbal fluency and visuospatial impairment compared with the PD-non pRBD. Furthermore, the PD-pRBD compared with the control group had impairment in verbal fluency, working memory, short-term and long-term verbal recall, and visuospatial function. Both PD groups showed impairment in global cognitive function and processing speed. In *study 2*, the PD-pRBD compared with PD-non pRBD patients had inhibition and processing speed impairment. Moreover, the PD-pRBD group had impairment in verbal fluency, inhibition, shifting, processing speed, short-term verbal recall, and visuospatial function compared with the control group. On the other hand, the PD-non pRBD group did not show impairment compared with the control group.

The cognitive profile found in *study 1* is in line with previously reported verbal fluency and visuospatial impairment in PD-RBD compared with PD-non RBD (48) and the one found in *study 2* with inhibition impairment (48). Despite the absence of widespread differences between PD groups, the PD-pRBD groups had distinctive impairment compared with controls in verbal fluency, inhibition, working memory, long-term verbal recall, and visuospatial function that are in coherence with previous literature (48). Overall, our findings



support the entity of PD with RBD as a clinical subtype with worse cognitive impairment.

### **Structural and functional brain characteristics of Parkinson's disease with RBD**

We explored the brain characteristics of PD-pRBD in *studies 1 and 2*, using structural MRI and resting-state fMRI approaches, respectively.

In *study 1*, we found that PD-pRBD patients had decremented volume in the left thalamus compared with the PD-non pRBD patients. These results agree with those previously obtained, which reported thalamic reductions in PD with RBD *de novo* PD (68) and in more advanced PD patients (66) compared with PD without RBD. Similarly, another study reinforces the thalamic involvement in such patients showing a negative correlation between the severity of RBD symptoms and the thalamic volume in a *de novo* PD sample (70). Two different factors may be influencing GM loss in the thalamus. The first factor is the pathological accumulation of alpha-synuclein in thalamic regions, which was described in early studies in PD (188,189) and later specifically in those PD patients with sleep disturbances, including RBD (190). The second one is the altered neurotransmission in PD with RBD. In this context, PET studies have found cholinergic and noradrenergic denervation in thalamic regions in PD with RBD compared with PD without RBD (76,93). In contrast, Bedard et al. found increased cholinergic innervation in the ventromedial area of the thalamus in iRBD patients compared with controls (191). Moreover, compensation processes could concur, such as the incremented resting-state nodal efficiency in the thalamus in PD-pRBD compared with PD-non pRBD found in a previous study (86).

Regarding other structural MRI measures in *study I*, we found that the pattern of atrophy of PD-pRBD patients was more widespread than the PD-non pRBD one, especially in subcortical structures. In global measures, the PD-pRBD patients had decreased volume in subcortical and cortical GM compared with controls and increased ventricular volume. On the other hand, the PD-non pRBD group had only decreased total cortical GM volume compared with controls. Concerning regional measures, the PD-pRBD group had volume decrements compared with the control group in bilateral putamen, left hippocampus, and left amygdala and cortical thinning in the right superior temporal gyrus. Meanwhile, the PD-non pRBD group had only volume reduction in the right amygdala compared with the control group. Concurrently, other studies have informed putamen reductions in PD with RBD compared with PD without RBD patients in the *de novo* stage of the disease (68,70) and more advanced PD, together with shape changes (71). Besides, reduced volume in the putamen has been reported in iRBD patients compared with controls (192,193). A possible mechanism involved in putamen neurodegeneration is the impairment of the nigrostriatal pathway. In this regard, some PET and SPECT studies in *de novo* PD have shown reduced DAT binding in PD with RBD compared with PD without RBD (90,95,100,102). Concerning hippocampal reduction, previous studies reported significant volume decrements in PD-RBD compared with PD-non RBD (67). Of interest, Campabadal et al. reported reduced hippocampal volumes in iRBD patients compared with controls (194). The interpretation of the medial temporal degeneration in PD with RBD should be cautious because insomnia is present in most iRBD patients (187), and sleep deprivation is strongly associated with hippocampal dysfunction and volume reduction (195). Therefore, possibly the atrophy of the hippocampus is not explained only by the neurodegenerative process *per se*, as Campabadal et al. highlighted elsewhere (194). As regards the

amygdala, we found volume decrements in the left amygdala in PD-pRBD compared with controls. Previous studies have found similar reductions in the amygdala cross-sectionally and longitudinally (68,73). Previous neuropathological studies reported an increased synuclein deposition in PD with RBD (38), and this mechanism could be implicated in the reduction of the amygdala. Of interest, the PD-non pRBD group had a decrement in the right amygdala compared with controls in our study. The sole structure that appeared altered in the PD-non pRBD group coincides with the main suggested initial point of the atrophy in the brain-first subtype in the SOC model (46). The unilaterality of the results in the PD-non pRBD group could reflect a unilateral focus that propagates to the ipsilateral hemisphere dependent on connection strength (46). Conversely, a widespread and bilateral atrophy pattern, as well as the presence of RBD symptomatology in the PD-pRBD, suggest that this group resembles the body-first subtype. Last, we found thinning in the right superior temporal gyrus in PD-pRBD compared with controls. In this line, other studies have reported volume reductions and thinning in temporal regions in PD with RBD compared with PD without RBD patients in the *de novo* stage of the disease (68,73) and more advanced disease (71). Possible factors associated with temporal neurodegeneration are decreased cortical metabolism (90) and the presence of neocortical alpha-synuclein depositions (38). Altogether these findings suggest that the PD with RBD patients have extended neurodegeneration to the neocortex.

In *study 2*, we characterized for the first time resting-state interregional functional connectivity through whole-brain network-based statistics in PD-pRBD patients using TFNBS. We found a reduced posterior functional connectivity between the right ventral area of the cingulate and the left medial area of the precuneus. The results agree with previous data of reduced posterior

resting-state functional connectivity in PD-RBD compared with PD-non RBD using a seed-to-whole brain approach (72) and a more widespread posterior pattern of reduced connectivity in iRBD compared with controls through TFNBS (196). Therefore, a posterior pattern of disrupted resting-state functional connectivity could be associated with RBD along the spectrum of PD. The comparisons between PD groups and controls showed significant differences in the PD-pRBD group with an extended reduced functional connectivity, mainly between cortical and paralimbic regions. The reduced connections in the PD-pRBD group mostly involved posterior cingulate regions with temporal, frontal, insular, and thalamic regions. These results link with a previous finding in PD-RBD compared with PD-non RBD of reduced functional connectivity between the anterior cingulate cortex and the pedunculopontine nucleus as regions of the arousal network (85). In addition, we found reduced functional connectivity between the left superior temporal and the right parietal cortex and in cortico-deep gray matter connections (fronto-striatal, parietal-striatal, parietal-thalamic, and amygdala-posterior middle temporal cortex connections). The fronto-striatal implication was previously described in PD-pRBD compared with PD-non pRBD, showing functional abnormalities in the fronto-striatal pathway using an ALFF approach (83). As regards global graph measures, the PD-pRBD had an increased normalized characteristic path length compared with the PD-non pRBD group. Indeed, a reduced path length implies a low efficiency (179,180) in the network and has been reported before in PD patients compared with controls (197), also altered in severe PD phenotypes, namely PD-MCI compared with PD with normal cognition (198). Although, it remains preserved in *de novo* PD patients (199). Therefore, the global network efficiency alteration could correspond to advanced stages of PD and severe disease phenotypes, the PD with RBD among them.

## **Brain correlates of cognitive impairment in Parkinson's disease with RBD**

We analyzed the association between cognitive impairment and the brain characteristics of PD-pRBD in *studies 1 and 2*.

In *study 1*, we explored the associations between altered structural brain measures and cognitive impairment in PD-pRBD using regression analyses. We found that the right putamen and left hippocampus volumes were positively associated with general cognition, left putamen with phonemic verbal fluency, left hippocampus with processing speed, and left thalamus with visuospatial function. Besides, total cortical GM was positively associated with phonemic verbal fluency and subcortical GM with general cognition and processing speed. The conception of the brain as a distributed network could help us to interpret the pattern of associations of cognitive impairment with subcortical structures that we found in *de novo* PD-pRBD patients. This functional understanding of the brain and its application to pathologic populations are inferred from the research field of the relation of subcortical structures with cognition; Crosson briefly revised the research field context and its upcoming research elsewhere (200). This concept of the brain as a complex system could allow us to reinterpret the classical consideration of PD as subcortical dementia (201,202). The subcortical structures could play different roles along the disease course. Thus, in the first stages of the disease, especially in PD with RBD, understood as body-first subtype: a more specific weight of subcortical neurodegeneration and altered connectivity with other brain regions. Then, in more advanced stages of the disease, cortical neurodegeneration may explain the evolution from specific cognitive impairment to MCI and dementia.

We analyzed the associations between altered functional brain measures and cognitive impairment in PD-pRBD in *study 2* through correlation analyses. First, we found a significant positive correlation between visuoperceptual function and the mean strength of the altered connections in PD-pRBD in comparison with controls. Moreover, we found significant negative correlations of normalized characteristic path length with processing speed and short-term verbal recall. These correlations of cognition with normalized characteristic path length are congruent, especially with processing speed tasks, since the increment of this measure implies a less efficient information transference within the network (203,204).

### **Sex differences in Parkinson's disease with RBD**

In *studies 3 and 4*, we analyzed sex differences in clinical features, cognition, and structural MRI measures in a *de novo* PD sample. First, with a focus on the *de novo* PD group as a whole (*study 3*) and then centered on how these variables differ or not between sexes in PD-pRBD and PD-non pRBD groups (*study 4*).

The analyses of clinical variables revealed that in the *de novo* PD group, males had more motor severity and RBD symptomatology than females (*study 3*). Indeed, when we analyzed the groups separately according to the RBD status (*study 4*), the results showed that the differences in motor and RBD symptomatology remained only in the PD-pRBD group. The more severe motor symptomatology in males agrees with a previous study (117). Regarding RBD symptomatology, the sex differences obtained through the questionnaire may reflect the female RBD presentation with less conspicuous symptoms (23,24,111).

Cognitive measures in the *de novo* PD group showed that females outperformed males in general cognition, verbal fluency, processing speed, and short-term and long-term verbal recall, while males outperformed females in visuospatial function (*study 3*). Whereas, with the divided sample (*study 4*), the PD-pRBD group females outperformed males in general cognition, verbal fluency, and processing speed, while the PD-non pRBD group solely showed sex differences in the same direction in verbal fluency. The sex differences in verbal fluency concord with the previously reported impairment in executive function in PD males compared with PD females (119).

The structural MRI analyses reported that *de novo* PD males had reduced volumes compared with *de novo* PD females in the bilateral thalamus, caudate, putamen, pallidum, hippocampus, and brainstem (*study 3*); as well as in total cortical and subcortical GM. Furthermore, cortical thickness analysis revealed thinning in the left postcentral and right precentral regions in *de novo* PD males compared with *de novo* PD females. When analyzing the PD-pRBD and PD-non pRBD groups separately (*study 4*), males had decreased volume than females in one subcortical structure in the PD-non pRBD group (brainstem). In the PD-pRBD group, males had reduced volumes compared with females in three subcortical structures (caudate, pallidum, and brainstem), total cortical, and subcortical GM. Comparably, a previous study using a VBM approach reported volume decrement in *de novo* PD males compared with *de novo* PD females in the left thalamus (126), which concurs with the sex difference in the thalamus found in *study 3*. The same study reported sex differences in cortical regions volume in both directions, with *de novo* PD males atrophy predominance. The cortical differences included reduced volume in *de novo* PD males compared with *de novo* PD females in the right postcentral, which partially agrees with thinning in the left postcentral described in *study 3*. However, they did not find

sex differences in the CTh analysis. As regards CTh, in more advanced PD, a previous study reported thinning in PD males compared with PD females in several frontal, parietal and occipital regions (125). The subcortical predominance of our results agrees with previously reported disruptions in measures of local efficiency in *de novo* PD males compared with *de novo* PD males in the basal ganglia, amygdala, and thalamus using a graph analysis approach with GM measures (126). Besides, the impairment of striatal volumes also agrees with reduced dopamine binding found in PD males compared with PD females (114).

Overall, in our studies, the PD males showed worse clinical, cognitive, and neurodegeneration characteristics than PD females, more marked in PD-pRBD. Our findings suggest that PD males have a subcortical vulnerability more pronounced in patients with RBD, congruent with the more conspicuous RBD symptomatology. Future research is needed to clarify the mechanisms behind these sex differences.

### **Future perspectives on Parkinson's disease with RBD**

One of the main questions for future research is if different trajectories of alpha-synuclein spreading are possible in PD and which is their associated neurodegeneration process. In this context, RBD could be one clinical feature with value as a marker of the disease progression. The impairment of the RBD-related circuits could happen in different stages of neurodegeneration. For example, the pathophysiology of PD may follow one trajectory in which the RBD symptomatology occurs with a high likelihood at the first PD stages, with the starting point at the vagus nerve, body-first subtype according to the SOC model (46) with its equivalent in the firsts Braak stages (40,43). However, other trajectories in which RBD appears later or even never along the disease



progression are possible. Therefore, we are making a great effort to characterize PD with RBD, but we are probably dealing with a heterogeneous group with different pathology trajectories and RBD onsets. Nowadays, we have a pretty sharp picture of PD with RBD: a group of patients with a distinctive clinical profile (35), more cognitive impairment (48), and neurodegeneration (205). Although, as a next step, future research should put RBD in the context of PD, passing from "PD with RBD as a clinical subtype" to "RBD in the context of PD trajectories." Two innovative research fields are dealing with some necessary steps for putting into practice this perspective. The first is the development of in vivo alpha-synuclein neuroimaging (206,207), which would allow tracing the alpha-synuclein depositions and following its spreading longitudinally. The second is the development of longitudinal clustering approaches (208,209), from which this hypothesis of synucleinopathy trajectory and neurodegeneration heterogeneity could benefit. Complementary, clinical and cognitive profiling, multimodal neuroimaging approaches, and other biomarkers would allow the thorough characterization of these neurodegenerative trajectories in PD.

## **Final remarks**

In summary, in the present doctoral thesis, we found evidence that supports the entity of PD with RBD as a more severe clinical subtype in terms of neurodegeneration and cognitive impairment. For the first time, we described in this group of patients the subcortical basis of cognitive impairment, the functional connectivity disruption using whole-brain network-based statistics, and its association with cognitive performance. Furthermore, as a novelty, we found sex differences in structural brain features and cognition, which indicate a more marked male vulnerability in this PD clinical subtype.



# Chapter 6

---

## Conclusions

Through the combined analysis of the studies included in this doctoral thesis, we can conclude that:

1. Structural MRI findings point towards an early GM subcortical atrophy in *de novo* PD-pRBD patients, involving thalamic, limbic, and striatal regions together with temporocortical atrophy in comparison to healthy controls. The main difference between PD subgroups is a decreased thalamic volume in PD-pRBD.
2. The distinctive cognitive profile of PD-pRBD patients in comparison to PD-non pRBD is already present in *de novo* PD stages, and it is characterized by increased verbal fluency and visuospatial impairment. The subcortical GM atrophy is associated with the cognitive impairment of these patients. In advanced stages, worse neuropsychological performance in PD-pRBD is seen in mental processing speed and inhibitory function.
3. PD-pRBD patients show decreased functional connectivity compared with healthy controls involving cortico-cortical and cortico-subcortical connections. The pattern of functional connectivity reduction in PD-PRBD compared with PD non-pRBD is characterized by posterior cortico-cortical connectivity and network efficiency alterations.
4. The results show that connectivity strength from reduced functional connections correlates with visuoperceptual impairment, and increased normalized characteristic path length correlated with mental processing speed and verbal learning impairment. Therefore, less efficient information transfer within brain networks is associated with cognitive impairment in PD-pRBD patients.
5. Sex differences in structural data show cortical thinning in *de novo* PD males compared with *de novo* PD females in the left postcentral and right

precentral areas and smaller volume in several subcortical regions, more extended in PD-pRBD. The presence of RBD is also a factor contributing to sex differences in atrophy.

6. Cognitive data highlight that *de novo* PD males have increased neuropsychological impairment than *de novo* PD females, including general cognition, verbal fluency, mental processing speed, and verbal memory impairment. Notable, female outperformance in cognitive tasks is more extended in *de novo* PD-pRBD. Sex effect on brain and cognition is already evident in *de novo* PD, not explained by age per se, being a relevant factor to consider in clinical and translational research in PD.



# References

1. United Nations, Department of Economic and Social Affairs, Population Division. World Population Prospects 2022: Summary of Results. 2022.
2. Schenck CH, Bundlie SR, Ettinger MG, Mahowald MW. Chronic behavioral disorders of human REM sleep: a new category of parasomnia. *Sleep*. 1986;9(2):293–308. doi:10.1093/sleep/9.2.293
3. Diagnostic Classification Steering Committee. International Classification of Sleep Disorders: Diagnostic and Coding Manual. First Edition. Thorpy MJ, editor. Rochester, MN: American Sleep Disorders Association; 1990.
4. Schenck CH, Mahowald MW. REM Sleep Behavior Disorder: Clinical, Developmental, and Neuroscience Perspectives 16 Years After its Formal Identification in SLEEP. *Sleep*. 2002;25(2):120–38. doi:10.1093/sleep/25.2.120
5. Fernández-Arcos A, Iranzo A, Serradell M, Gaig C, Santamaria J. The Clinical Phenotype of Idiopathic Rapid Eye Movement Sleep Behavior Disorder at Presentation: A Study in 203 Consecutive Patients. *Sleep*. 2016;39(1):121–32. doi:10.5665/sleep.5332
6. Oudiette D, de Cock VC, Lavault S, Leu S, Vidailhet M, Arnulf I. Nonviolent elaborate behaviors may also occur in REM sleep behavior disorder. *Neurology*. 2009;72(6):551–7. doi:10.1212/01.wnl.0000341936.78678.3a
7. Boeve BF. REM sleep behavior disorder: Updated review of the core features, the REM sleep behavior disorder-neurodegenerative disease association, evolving concepts, controversies, and future directions. *Ann N Y Acad Sci*. 2010;1184(1):15–54. doi:10.1111/j.1749-6632.2009.05115.x
8. Rolinski M, Szewczyk-Krolikowski K, Tomlinson PR, Nithi K, Talbot K, Ben-Shlomo Y, et al. REM sleep behaviour disorder is associated with worse quality of life and other non-motor features in early Parkinson's disease. *J Neurol Neurosurg Psychiatry*. 2014;85(5):560–6. doi:10.1136/jnnp-2013-306104

9. American Academy of Sleep Medicine. International Classification of Sleep Disorders: Diagnostic and Coding Manual. Third Edition. Darien, IL: American Academy of Sleep Medicine; 2014.
10. Berry RB, Quan SF, Abreu AR, Bibbs ML, DelRosso L, Harding SM, et al. The AASM Manual for the Scoring of Sleep and Associated Events: Rules, Terminology and Technical Specifications. Version 2.6. Darien, IL: American Academy of Sleep Medicine; 2020.
11. Stefani A, Heidbreder A, Brandauer E, Guaita M, Neier LM, Mitterling T, et al. Screening for idiopathic REM sleep behavior disorder: usefulness of actigraphy. *Sleep*. 2018;41(6):zsy053. doi:10.1093/sleep/zsy053
12. Högl B, Stefani A, Videnovic A. Idiopathic REM sleep behaviour disorder and neurodegeneration — an update. *Nat Rev Neurol*. 2018;14:40–55. doi:10.1038/nrneurol.2017.157
13. Galbiati A, Verga L, Giora E, Zucconi M, Ferini-Strambi L. The risk of neurodegeneration in REM sleep behavior disorder: A systematic review and meta-analysis of longitudinal studies. *Sleep Med Rev*. 2019;43:37–46. doi:10.1016/j.smr.v.2018.09.008
14. Postuma RB, Iranzo A, Hu M, Högl B, Boeve BF, Manni R, et al. Risk and predictors of dementia and parkinsonism in idiopathic REM sleep behaviour disorder: a multicentre study. *Brain*. 2019;142(3):744–59. doi:10.1093/brain/awz030
15. Iranzo A, Fairfoul G, Na Ayudhaya AC, Serradell M, Gelpi E, Vilaseca I, et al. Detection of  $\alpha$ -synuclein in CSF by RT-QuIC in patients with isolated rapid-eye-movement sleep behaviour disorder: a longitudinal observational study. *Lancet Neurol*. 2021;20(3):203–12. doi:10.1016/S1474-4422(20)30449-X
16. Campabadal A, Segura B, Junque C, Iranzo A. Structural and functional magnetic resonance imaging in isolated REM sleep behavior disorder: A systematic review of studies using neuroimaging software. *Sleep Med Rev*. 2021;59:101495. doi:10.1016/j.smr.v.2021.101495
17. Cicero CE, Giuliano L, Luna J, Zappia M, Preux PM, Nicoletti A. Prevalence of idiopathic REM behavior disorder: a systematic review and meta-analysis. *Sleep*. 2021;44(6):zsa294. doi:10.1093/sleep/zsa294



18. Schenck CH, Hurwitz TD, Mahowald MW. REM sleep behaviour disorder: an update on a series of 96 patients and a review of the world literature. *J Sleep Res.* 1993;2(4):224–31. doi:10.1111/j.1365-2869.1993.tb00093.x
19. Olson EJ, Boeve BF, Silber MH. Rapid eye movement sleep behaviour disorder: demographic, clinical and laboratory findings in 93 cases. *Brain.* 2000;123(2):331–9. doi:10.1093/brain/123.2.331
20. Postuma RB, Gagnon JF, Vendette M, Fantini ML, Massicotte-Marquez J, Montplaisir J. Quantifying the risk of neurodegenerative disease in idiopathic REM sleep behavior disorder. *Neurology.* 2009;72(15):1296–300. doi:10.1212/WNL.0b013e3181a52f8e
21. Li Y, Kang W, Yang Q, Zhang L, Zhang L, Dong F, et al. Predictive markers for early conversion of iRBD to neurodegenerative synucleinopathy diseases. *Neurology.* 2017;88(16):1493–500. doi:10.1212/WNL.0000000000003838
22. Haba-Rubio J, Frauscher B, Marques-Vidal P, Toriel J, Tobback N, Andries D, et al. Prevalence and determinants of rapid eye movement sleep behavior disorder in the general population. *Sleep.* 2018;41(2):zsz197. doi:10.1093/sleep/zsz197
23. Zhou J, Zhang J, Li Y, Du L, Li Z, Lei F, et al. Gender differences in REM sleep behavior disorder: a clinical and polysomnographic study in China. *Sleep Med.* 2015;16(3):414–8. doi:10.1016/j.sleep.2014.10.020
24. Bodkin CL, Schenck CH. Rapid Eye Movement Sleep Behavior Disorder in Women: Relevance to General and Specialty Medical Practice. *J Womens Health (Larchmt).* 2009;18(12):1955–63. doi:10.1089/jwh.2008.1348
25. Roguski A, Rayment D, Whone AL, Jones MW, Rolinski MA. A Neurologist’s Guide to REM Sleep Behavior Disorder. *Front Neurol.* 2020;11:610. doi:10.3389/fneur.2020.00610
26. Iranzo A. The REM sleep circuit and how its impairment leads to REM sleep behavior disorder. *Cell Tissue Res.* 2018;373:245–66. doi:10.1007/s00441-018-2852-8

27. Knudsen K, Fedorova TD, Hansen AK, Sommerauer M, Otto M, Svendsen KB, et al. In-vivo staging of pathology in REM sleep behaviour disorder: a multimodality imaging case-control study. *Lancet Neurol.* 2018;17(7):618–28. doi:10.1016/S1474-4422(18)30162-5
28. Schenck CH, Bundlie SR, Mahowald MW. Delayed emergence of a parkinsonian disorder in 38% of 29 older men initially diagnosed with idiopathic rapid eye movement sleep behavior disorder. *Neurology.* 1996;46(2):388–93. doi:10.1212/wnl.46.2.388
29. Schenck CH, Boeve BF, Mahowald MW. Delayed emergence of a parkinsonian disorder or dementia in 81% of older men initially diagnosed with idiopathic rapid eye movement sleep behavior disorder: a 16-year update on a previously reported series. *Sleep Med.* 2013;14(8):744–8. doi:10.1016/j.sleep.2012.10.009
30. de Natale ER, Wilson H, Politis M. Predictors of RBD progression and conversion to synucleinopathies. *Curr Neurol Neurosci Rep.* 2022;22:93–104. doi:10.1007/s11910-022-01171-0
31. Fereshtehnejad SM, Yao C, Pelletier A, Montplaisir JY, Gagnon JF, Postuma RB. Evolution of prodromal Parkinson’s disease and dementia with Lewy bodies: a prospective study. *Brain.* 2019;142(7):2051–67. doi:10.1093/brain/awz111
32. Zhang J, Xu CY, Liu J. Meta-analysis on the prevalence of REM sleep behavior disorder symptoms in Parkinson’s disease. *BMC Neurol.* 2017;17:23. doi:10.1186/s12883-017-0795-4
33. Zhang X, Sun X, Wang J, Tang L, Xie A. Prevalence of rapid eye movement sleep behavior disorder (RBD) in Parkinson’s disease: a meta and meta-regression analysis. *Neurol Sci.* 2017;38:163–70. doi:10.1007/s10072-016-2744-1
34. Baumann-Vogel H, Hor H, Poryazova R, Valko P, Werth E, Baumann CR. REM sleep behavior in Parkinson disease: Frequent, particularly with higher age. *PLoS One.* 2020;15(12):e0243454. doi:10.1371/journal.pone.0243454
35. Zhu RL, Xie CJ, Hu PP, Wang K. Clinical variations in Parkinson’s disease patients with or without REM sleep behaviour disorder: a meta-analysis. *Sci Rep.* 2017;7:40779. doi:10.1038/srep40779

36. Barasa A, Wang J, Dewey RB. Probable REM Sleep Behavior Disorder Is a Risk Factor for Symptom Progression in Parkinson Disease. *Front Neurol.* 2021;12:651157. doi:10.3389/fneur.2021.651157
37. Folle AD, Paul KC, Bronstein JM, Ritz B. Clinical progression in Parkinson's disease with features of REM sleep behavior disorder: A population-based longitudinal study. *Parkinsonism Relat Disord.* 2020;62:105–11. doi:10.1016/j.parkreldis.2019.01.018
38. Postuma RB, Adler CH, Dugger BN, Hentz JG, Shill HA, Driver-Dunckley E, et al. REM sleep behavior disorder and neuropathology in Parkinson's disease. *Mov Disord.* 2015;30(10):1413–7. doi:10.1002/mds.26347
39. Wang XT, Yu H, Liu FT, Zhang C, Ma YH, Wang J, et al. Associations of sleep disorders with cerebrospinal fluid  $\alpha$ -synuclein in prodromal and early Parkinson's disease. *J Neurol.* 2022;269:2469–78. doi:10.1007/s00415-021-10812-2
40. Braak H, del Tredici K, Rüb U, de Vos RAI, Jansen Steur ENH, Braak E. Staging of brain pathology related to sporadic Parkinson's disease. *Neurobiol Aging.* 2003;24(2):197–211. doi:10.1016/S0197-4580(02)00065-9
41. Hawkes CH, del Tredici K, Braak H. Parkinson's disease: a dual-hit hypothesis. *Neuropathol Appl Neurobiol.* 2007;33(6):599–614. doi:10.1111/j.1365-2990.2007.00874.x
42. Hawkes CH, del Tredici K, Braak H. Parkinson's Disease: The Dual Hit Theory Revisited. In: *International Symposium on Olfaction and Taste.* 2009. p. 615–22. doi:10.1111/j.1749-6632.2009.04365.x
43. Boeve BF. Idiopathic REM sleep behaviour disorder in the development of Parkinson's disease. *Lancet Neurol.* 2013;12(5):469–82. doi:10.1016/S1474-4422(13)70054-1
44. del Tredici K, Braak H. To stage, or not to stage. *Curr Opin Neurobiol.* 2020;61:10–22. doi:10.1016/j.conb.2019.11.008
45. Borghammer P, van den Berge N. Brain-First versus Gut-First Parkinson's Disease: A Hypothesis. *J Parkinsons Dis.* 2019;9(s2):S281–95. doi:10.3233/JPD-191721

46. Borghammer P. The  $\alpha$ -Synuclein Origin and Connectome Model (SOC Model) of Parkinson's Disease: Explaining Motor Asymmetry, Non-Motor Phenotypes, and Cognitive Decline. *J Parkinsons Dis*. 2021;11(2):455–74. doi:10.3233/JPD-202481
47. Pyatigorskaya N, Yahia-Cherif L, Valabregue R, Gaurav R, Gargouri F, Ewencyk C, et al. Parkinson Disease Propagation Using MRI Biomarkers and Partial Least Squares Path Modeling. *Neurology*. 2021;96(3):e460–71. doi:10.1212/WNL.0000000000011155
48. Mao J, Huang X, Yu J, Chen L, Huang Y, Tang B, et al. Association Between REM Sleep Behavior Disorder and Cognitive Dysfunctions in Parkinson's Disease: A Systematic Review and Meta-Analysis of Observational Studies. *Front Neurol*. 2020;11:577874. doi:10.3389/fneur.2020.577874
49. Jozwiak N, Postuma RB, Montplaisir J, Latreille V, Panisset M, Chouinard S, et al. REM Sleep Behavior Disorder and Cognitive Impairment in Parkinson's Disease. *Sleep*. 2017;40(8):zsx101. doi:10.1093/sleep/zsx101
50. Postuma RB, Bertrand JA, Montplaisir J, Desjardins C, Vendette M, Rios Romanets S, et al. Rapid eye movement sleep behavior disorder and risk of dementia in Parkinson's disease: A prospective study. *Mov Disord*. 2012;27(6):720–6. doi:10.1002/mds.24939
51. Chahine LM, Xie SX, Simuni T, Tran B, Postuma R, Amara A, et al. Longitudinal changes in cognition in early Parkinson's disease patients with REM sleep behavior disorder. *Parkinsonism Relat Disord*. 2016;27:102–6. doi:10.1016/j.parkreldis.2016.03.006
52. Forbes E, Tropea TF, Mantri S, Xie SX, Morley JF. Modifiable Comorbidities Associated with Cognitive Decline in Parkinson's Disease. *Mov Disord Clin Pract*. 2021;8(2):254–63. doi:10.1002/mdc3.13143
53. van Patten R, Mahmood Z, Pickell D, Maye JE, Roesch S, Twamley EW, et al. REM Sleep Behavior Disorder in Parkinson's Disease: Change in Cognitive, Psychiatric, and Functional Outcomes from Baseline to 16–47-Month Follow-Up. *Arch Clin Neuropsychol*. 2022;37(1):1–11. doi:10.1093/arclin/acabo37

54. Bjørnarå KA, Pihlstrøm L, Dietrichs E, Toft M. Risk variants of the  $\alpha$ -synuclein locus and REM sleep behavior disorder in Parkinson's disease: a genetic association study. *BMC Neurol.* 2018;18:20. doi:10.1186/s12883-018-1023-6
55. Krohn L, Wu RYJ, Heilbron K, Ruskey JA, Laurent SB, Blauwendraat C, et al. Fine-Mapping of SNCA in Rapid Eye Movement Sleep Behavior Disorder and Overt Synucleinopathies. *Ann Neurol.* 2020;87(4):584–98. doi:10.1002/ana.25687
56. Gan-Or Z, Mirelman A, Postuma RB, Arnulf I, Bar-Shira A, Dauvilliers Y, et al. GBA mutations are associated with Rapid Eye Movement Sleep Behavior Disorder. *Ann Clin Transl Neurol.* 2015;2(9):941–5. doi:10.1002/acn3.228
57. Ouled Amar Bencheikh B, Ruskey JA, Arnulf I, Dauvilliers Y, Monaca CC, de Cock VC, et al. LRRK2 protective haplotype and full sequencing study in REM sleep behavior disorder. *Parkinsonism Relat Disord.* 2018;52:98–101. doi:10.1016/j.parkreldis.2018.03.019
58. Krohn L, Öztürk TN, Vanderperre B, Ouled Amar Bencheikh B, Ruskey JA, Laurent SB, et al. Genetic, Structural, and Functional Evidence Link TMEM175 to Synucleinopathies. *Ann Neurol.* 2020;87(1):139–53. doi:10.1002/ana.25629
59. Fernández-Santiago R, Iranzo A, Gaig C, Serradell M, Fernández M, Tolosa E, et al. Absence of LRRK2 mutations in a cohort of patients with idiopathic REM sleep behavior disorder. *Neurology.* 2016;86(11):1072–3. doi:10.1212/WNL.0000000000002304
60. Li J, Ruskey JA, Arnulf I, Dauvilliers Y, Hu MTM, Högl B, et al. Full sequencing and haplotype analysis of MAPT in Parkinson's disease and rapid eye movement sleep behavior disorder. *Mov Disord.* 2018;33(6):1016–20. doi:10.1002/mds.27385
61. Puschmann A. Monogenic Parkinson's disease and parkinsonism: Clinical phenotypes and frequencies of known mutations. *Parkinsonism Relat Disord.* 2013;19(4):407–15. doi:10.1016/j.parkreldis.2013.01.020
62. ben Romdhan S, Farhat N, Nasri A, Lesage S, Hdiji O, ben Djebara M, et al. LRRK2 G2019S Parkinson's disease with more benign phenotype

- than idiopathic. *Acta Neurol Scand.* 2018;138(5):425–31.  
doi:10.1111/ane.12996
63. Ford AH, Duncan GW, Firbank MJ, Yarnall AJ, Khoo TK, Burn DJ, et al. Rapid eye movement sleep behavior disorder in Parkinson's disease: Magnetic resonance imaging study. *Mov Disord.* 2013;28(6):832–6.  
doi:10.1002/mds.25367
64. García-Lorenzo D, Longo-Dos Santos C, Ewenczyk C, Leu-Semenescu S, Gallea C, Quattrocchi G, et al. The coeruleus/subcoeruleus complex in rapid eye movement sleep behaviour disorders in Parkinson's disease. *Brain.* 2013;136(7):2120–9. doi:10.1093/brain/awt152
65. Boeve BF, Molano JR, Ferman TJ, Smith GE, Lin SC, Bieniek K, et al. Validation of the Mayo Sleep Questionnaire to screen for REM sleep behavior disorder in an aging and dementia cohort. *Sleep Med.* 2011;12(5):445–53. doi:10.1016/j.sleep.2010.12.009
66. Salsone M, Cerasa A, Arabia G, Morelli M, Gambardella A, Mumoli L, et al. Reduced thalamic volume in Parkinson disease with REM sleep behavior disorder: Volumetric study. *Parkinsonism Relat Disord.* 2014;20(9):1004–8. doi:10.1016/j.parkreldis.2014.06.012
67. Lim JS, Shin SA, Lee JY, Nam H, Lee JY, Kim YK. Neural substrates of rapid eye movement sleep behavior disorder in Parkinson's disease. *Parkinsonism Relat Disord.* 2016;23:31–6.  
doi:10.1016/j.parkreldis.2015.11.027
68. Boucetta S, Salimi A, Dadar M, Jones BE, Collins DL, Dang-Vu TT. Structural Brain Alterations Associated with Rapid Eye Movement Sleep Behavior Disorder in Parkinson's Disease. *Sci Rep.* 2016;6:26782.  
doi:10.1038/srep26782
69. Stiasny-Kolster K, Mayer G, Schäfer S, Möller JC, Heinzel-Gutenbrunner M, Oertel WH. The REM sleep behavior disorder screening questionnaire—A new diagnostic instrument. *Mov Disord.* 2007;22(16):2386–93. doi:10.1002/mds.21740
70. Kamps S, van den Heuvel OA, van der Werf YD, Berendse HW, Weintraub D, Vriend C. Smaller subcortical volume in Parkinson patients with rapid eye movement sleep behavior disorder. *Brain Imaging Behav.* 2019;13:1352–60. doi:10.1007/s11682-018-9939-4

71. Rahayel S, Gaubert M, Postuma RB, Montplaisir J, Carrier J, Monchi O, et al. Brain atrophy in Parkinson's disease with polysomnography-confirmed REM sleep behavior disorder. *Sleep*. 2019;42(6):zsz062. doi:10.1093/sleep/zsz062
72. Jiang X, Wu Z, Zhong M, Shen B, Zhu J, Pan Y, et al. Abnormal Gray Matter Volume and Functional Connectivity in Parkinson's Disease with Rapid Eye Movement Sleep Behavior Disorder. *Parkinsons Dis*. 2021;2021:8851027. doi:10.1155/2021/8851027
73. Yoon EJ, Monchi O. Probable REM sleep behavior disorder is associated with longitudinal cortical thinning in Parkinson's disease. *npj Parkinsons Dis*. 2021;7(19). doi:10.1038/s41531-021-00164-z
74. O'Donnell LJ, Westin CF. An Introduction to Diffusion Tensor Image Analysis. *Neurosurg Clin N Am*. 2011;22(2):185–96. doi:10.1016/j.nec.2010.12.004
75. Ansari M, Rahmani F, Dolatshahi M, Pooyan A, Aarabi MH. Brain pathway differences between Parkinson's disease patients with and without REM sleep behavior disorder. *Sleep Breath*. 2017;21:155–61. doi:10.1007/s11325-016-1435-8
76. Sommerauer M, Fedorova TD, Hansen AK, Knudsen K, Otto M, Jeppesen J, et al. Evaluation of the noradrenergic system in Parkinson's disease: an IIC-MeNER PET and neuromelanin MRI study. *Brain*. 2018;141(2):496–504. doi:10.1093/brain/awx348
77. Horsager J, Andersen KB, Knudsen K, Skjærbæk C, Fedorova TD, Okkels N, et al. Brain-first versus body-first Parkinson's disease: a multimodal imaging case-control study. *Brain*. 2020;143(10):3077–88. doi:10.1093/brain/awaa238
78. Guo T, Guan X, Zeng Q, Xuan M, Gu Q, Huang P, et al. Alterations of Brain Structural Network in Parkinson's Disease With and Without Rapid Eye Movement Sleep Behavior Disorder. *Front Neurol*. 2018;9:334. doi:10.3389/fneur.2018.00334
79. Chen A, Li Y, Wang Z, Huang J, Ruan X, Cheng X, et al. Disrupted Brain Structural Network Connection in de novo Parkinson's Disease With Rapid Eye Movement Sleep Behavior Disorder. *Front Hum Neurosci*. 2022;16:902614. doi:10.3389/fnhum.2022.902614

80. Inguanzo A, Segura B, Sala-Llonch R, Monte-Rubio GC, Abos A, Campabadal A, et al. Impaired Structural Connectivity in Parkinson's Disease Patients with Mild Cognitive Impairment: A Study Based on Probabilistic Tractography. *Brain Connect.* 2021;11(5):380–92. doi:10.1089/brain.2020.0939
81. Hillman EMC. Coupling Mechanism and Significance of the BOLD Signal: A Status Report. *Annu Rev Neurosci.* 2014;37:161–81. doi:10.1146/annurev-neuro-071013-014111
82. Lv H, Wang Z, Tong E, Williams LM, Zaharchuk G, Zeineh M, et al. Resting-State Functional MRI: Everything That Nonexperts Have Always Wanted to Know. *AJNR Am J Neuroradiol.* 2018;39(8):1390–9. doi:10.3174/ajnr.A5527
83. Li D, Huang P, Zang Y, Lou Y, Cen Z, Gu Q, et al. Abnormal baseline brain activity in Parkinson's disease with and without REM sleep behavior disorder: A resting-state functional MRI study. *J Magn Reson Imaging.* 2017;46(3):697–703. doi:10.1002/jmri.25571
84. Zang YF, Yong H, Chao-Zhe Z, Qing-Jiu C, Man-Qiu S, Meng L, et al. Altered baseline brain activity in children with ADHD revealed by resting-state functional MRI. *Brain Dev.* 2007;29(2):83–91. doi:10.1016/j.braindev.2006.07.002
85. Gallea C, Ewencyk C, Degos B, Welter ML, Grabli D, Leu-Semenescu S, et al. Pedunculopontine network dysfunction in Parkinson's disease with postural control and sleep disorders. *Mov Disord.* 2017;32(5):693–704. doi:10.1002/mds.26923
86. Li J, Zeng Q, Zhou W, Zhai X, Lai C, Zhu J, et al. Altered Brain Functional Network in Parkinson Disease With Rapid Eye Movement Sleep Behavior Disorder. *Front Neurol.* 2020;563624. doi:10.3389/fneur.2020.563624
87. Gan C, Ma K, Wang L, Si Q, Wang M, Yuan Y, et al. Dynamic functional connectivity changes in Parkinson's disease patients with REM sleep behavior disorder. *Brain Res.* 2021;1764:147477. doi:10.1016/j.brainres.2021.147477
88. Fox MD, Snyder AZ, Vincent JL, Corbetta M, van Essen DC, Raichle ME. The human brain is intrinsically organized into dynamic, anticorrelated



- functional networks. *Proc Natl Acad Sci USA*. 2005;102(27):9673–8. doi:10.1073/pnas.0504136102
89. Chang C, Glover GH. Time–frequency dynamics of resting-state brain connectivity measured with fMRI. *Neuroimage*. 2010;50(1):81–98. doi:10.1016/j.neuroimage.2009.12.011
  90. Arnaldi D, Morbelli S, Brugnolo A, Girtler N, Picco A, Ferrara M, et al. Functional neuroimaging and clinical features of drug naive patients with de novo Parkinson’s disease and probable RBD. *Parkinsonism Relat Disord*. 2016;29:47–53. doi:10.1016/j.parkreldis.2016.05.031
  91. Yoon EJ, Lee JY, Nam H, Kim HJ, Jeon B, Jeong JM, et al. A New Metabolic Network Correlated with Olfactory and Executive Dysfunctions in Idiopathic Rapid Eye Movement Sleep Behavior Disorder. *J Clin Neurol*. 2019;15(2):175–83. doi:10.3988/jcn.2019.15.2.175
  92. Shin JH, Lee JY, Kim YK, Yoon EJ, Kim H, Nam H, et al. Parkinson Disease-Related Brain Metabolic Patterns and Neurodegeneration in Isolated REM Sleep Behavior Disorder. *Neurology*. 2021;97(4):e378–88. doi:10.1212/WNL.000000000012228
  93. Kotagal V, Albin RL, Müller MLTM, Koeppe RA, Chervin RD, Frey KA, et al. Symptoms of rapid eye movement sleep behavior disorder are associated with cholinergic denervation in Parkinson disease. *Ann Neurol*. 2012;71(4):560–8. doi:10.1002/ana.22691
  94. Valli M, Cho SS, Uribe C, Masellis M, Chen R, Mihaescu A, et al. VMAT2 availability in Parkinson’s disease with probable REM sleep behaviour disorder. *Mol Brain*. 2021;14:165. doi:10.1186/s13041-021-00875-7
  95. Chung SJ, Lee Y, Lee JJ, Lee PH, Sohn YH. Rapid eye movement sleep behaviour disorder and striatal dopamine depletion in patients with Parkinson’s disease. *Eur J Neurol*. 2017;24(10):1314–9. doi:10.1111/ene.13388
  96. Lee JY, Yoon EJ, Kim YK, Shin CW, Nam H, Jeong JM, et al. Nonmotor and Dopamine Transporter Change in REM Sleep Behavior Disorder by Olfactory Impairment. *J Mov Disord*. 2019;12(2). doi:10.14802/jmd.18061

97. Valli M, Cho SS, Masellis M, Chen R, Koshimori Y, Diez-Cirarda M, et al. Extra-striatal dopamine in Parkinson's disease with rapid eye movement sleep behavior disorder. *J Neurosci Res.* 2021;99(4):1177–87. doi:10.1002/jnr.24779
98. Andersen KB, Hansen AK, Sommerauer M, Fedorova TD, Knudsen K, Vang K, et al. Altered sensorimotor cortex noradrenergic function in idiopathic REM sleep behaviour disorder – A PET study. *Parkinsonism Relat Disord.* 2020;75:63–9. doi:10.1016/j.parkreldis.2020.05.013
99. Arnaldi D, de Carli F, Picco A, Ferrara M, Accardo J, Bossert I, et al. Nigro-caudate dopaminergic deafferentation: a marker of REM sleep behavior disorder? *Neurobiol Aging.* 2015;36(12):3300–5. doi:10.1016/j.neurobiolaging.2015.08.025
100. Cao R, Chen X, Xie C, Hu P, Wang K. Serial Dopamine Transporter Imaging of Nigrostriatal Function in Parkinson's Disease With Probable REM Sleep Behavior Disorder. *Front Neurosci.* 2020;14:349. doi:10.3389/fnins.2020.00349
101. Kim YE, Kim YJ, Hwang HS, Ma HI. REM sleep behavior disorder in early Parkinson's disease predicts the rapid dopaminergic denervation. *Parkinsonism Relat Disord.* 2020;80:120–6. doi:10.1016/j.parkreldis.2020.09.032
102. Mašková J, Školoudík D, Štofániková P, Ibarburu V, Kemlink D, Zogala D, et al. Comparative study of the substantia nigra echogenicity and I23I-Ioflupane SPECT in patients with synucleinopathies with and without REM sleep behavior disorder. *Sleep Med.* 2020;70:116–23. doi:10.1016/j.sleep.2020.02.012
103. Zoetmulder M, Nikolic M, Biernat H, Korbo L, Friberg L, Jennum P. Increased Motor Activity During REM Sleep Is Linked with Dopamine Function in Idiopathic REM Sleep Behavior Disorder and Parkinson Disease. *J Clin Sleep Med.* 2016;12(6):895–903. doi:10.5664/jcsm.5896
104. Pagano G, de Micco R, Yousaf T, Wilson H, Chandra A, Politis M. REM behavior disorder predicts motor progression and cognitive decline in Parkinson disease. *Neurology.* 2018;91(10):e894–905. doi:10.1212/WNL.0000000000006134

105. Dimech AS, Ferretti MT, Sandset EC, Chadha AS. The role of sex and gender differences in precision medicine: the work of the Women's Brain Project. *Eur Heart J*. 2021;42(34):3215–7. doi:10.1093/eurheartj/ehab297
106. Salminen LE, Tubi MA, Bright J, Thomopoulos SI, Wieand A, Thompson PM. Sex is a defining feature of neuroimaging phenotypes in major brain disorders. *Hum Brain Mapp*. 2022;43(1):500–42. doi:10.1002/hbm.25438
107. Baldereschi M, di Carlo A, Rocca WA, Vanni P, Maggi S, Perissinotto E, et al. Parkinson's disease and parkinsonism in a longitudinal study: Two-fold higher incidence in men. *Neurology*. 2000;55(9):1358–63. doi:10.1212/WNL.55.9.1358
108. Wooten GF, Currie LJ, Bovbjerg VE, Lee JK, Patrie J. Are men at greater risk for Parkinson's disease than women? *J Neurol Neurosurg Psychiatry*. 2004;75(4):637–9. doi:10.1136/jnnp.2003.020982
109. Taylor KSM, Cook JA, Counsell CE. Heterogeneity in male to female risk for Parkinson's disease. *J Neurol Neurosurg Psychiatry*. 2007;78(8):905–6. doi:10.1136/jnnp.2006.104695
110. Moisan F, Kab S, Mohamed F, Canonico M, le Guern M, Quintin C, et al. Parkinson disease male-to-female ratios increase with age: French nationwide study and meta-analysis. *J Neurol Neurosurg Psychiatry*. 2016;87(9):952–7. doi:10.1136/jnnp-2015-312283
111. Mahale RR, Yadav R, Pal PK. Rapid eye movement sleep behaviour disorder in women with Parkinson's disease is an underdiagnosed entity. *Journal of Clinical Neuroscience*. 2016;28:43–6. doi:10.1016/j.jocn.2015.08.046
112. Caranci G, Piscopo P, Rivabene R, Traficante A, Riozzi B, Castellano AE, et al. Gender differences in Parkinson's disease: focus on plasma alpha-synuclein. *J Neural Transm*. 2013;120:1209–15. doi:10.1007/s00702-013-0972-6
113. Cerri S, Mus L, Blandini F. Parkinson's Disease in Women and Men: What's the Difference? *J Parkinsons Dis*. 2019;9(3):501–15. doi:10.3233/JPD-191683

114. Haaxma CA, Bloem BR, Borm GF, Oyen WJG, Leenders KL, Eshuis S, et al. Gender differences in Parkinson's disease. *J Neurol Neurosurg Psychiatry*. 2007;78(8):819–24. doi:10.1136/jnnp.2006.103788
115. Solla P, Cannas A, Ibba FC, Loi F, Corona M, Orofino G, et al. Gender differences in motor and non-motor symptoms among Sardinian patients with Parkinson's disease. *J Neurol Sci*. 2012;323(1–2):33–9. doi:10.1016/j.jns.2012.07.026
116. Zappia M, Annesi G, Nicoletti G, Arabia G, Annesi F, Messina D, et al. Sex Differences in Clinical and Genetic Determinants of Levodopa Peak-Dose Dyskinesias in Parkinson Disease: An Exploratory Study. *Arch Neurol*. 2005;62(4):601–5. doi:10.1001/archneur.62.4.601
117. Kang KW, Choi SM, Kim BC. Gender differences in motor and non-motor symptoms in early Parkinson disease. *Medicine*. 2022;101(3):e28643. doi:10.1097/MD.00000000000028643
118. Picillo M, Lafontant DE, Bressman S, Caspell-Garcia C, Coffey C, Cho HR, et al. Sex-Related Longitudinal Change of Motor, Non-Motor, and Biological Features in Early Parkinson's Disease. *J Parkinsons Dis*. 2022;12(1):421–36. doi:10.3233/JPD-212892
119. Curtis AF, Masellis M, Camicioli R, Davidson H, Tierney MC. Cognitive profile of non-demented Parkinson's disease: Meta-analysis of domain and sex-specific deficits. *Parkinsonism Relat Disord*. 2019;60:32–42. doi:10.1016/j.parkreldis.2018.10.014
120. Iwaki H, Blauwendraat C, Leonard HL, Makarious MB, Kim JJ, Liu G, et al. Differences in the Presentation and Progression of Parkinson's Disease by Sex. *Mov Disord*. 2021;36(1):106–17. doi:10.1002/mds.28312
121. Liu G, Locascio JJ, Corvol JC, Boot B, Liao Z, Page K, et al. Prediction of cognition in Parkinson's disease with a clinical–genetic score: a longitudinal analysis of nine cohorts. *Lancet Neurol*. 2017;16(8):620–9. doi:10.1016/S1474-4422(17)30122-9
122. Cholerton B, Johnson CO, Fish B, Quinn JF, Chung KA, Peterson-Hiller AL, et al. Sex differences in progression to mild cognitive impairment and dementia in Parkinson's disease. *Parkinsonism Relat Disord*. 2018;50:29–36. doi:10.1016/j.parkreldis.2018.02.007

123. Bakeberg MC, Gorecki AM, Kenna JE, Jefferson A, Byrnes M, Ghosh S, et al. Differential effects of sex on longitudinal patterns of cognitive decline in Parkinson's disease. *J Neurol*. 2021;268:1903–12. doi:10.1007/s00415-020-10367-8
124. Salminen LE, Tubi MA, Bright J, Thomopoulos SI, Wieand A, Thompson PM. Sex is a defining feature of neuroimaging phenotypes in major brain disorders. *Hum Brain Mapp*. 2022;43(1):500–42. doi:10.1002/hbm.25438
125. Yadav SK, Kathiresan N, Mohan S, Vasileiou G, Singh A, Kaura D, et al. Gender-based analysis of cortical thickness and structural connectivity in Parkinson's disease. *J Neurol*. 2016;263:2308–18. doi:10.1007/s00415-016-8265-2
126. Tremblay C, Abbasi N, Zeighami Y, Yau Y, Dadar M, Rahayel S, et al. Sex effects on brain structure in de novo Parkinson's disease: a multimodal neuroimaging study. *Brain*. 2020;143(10):3052–66. doi:10.1093/brain/awaa234
127. Boccalini C, Carli G., Pilotto A, Padovani A, Perani D. Gender differences in dopaminergic system dysfunction in de novo Parkinson's disease clinical subtypes. *Neurobiol Dis*. 2022;167:105668. doi:10.1016/j.nbd.2022.105668
128. Subramanian I, Mathur S, Oosterbaan A, Flanagan Ri, Keener AM, Moro E. Unmet Needs of Women Living with Parkinson's Disease: Gaps and Controversies. *Mov Disord*. 2022;37(3):444–55. doi:10.1002/mds.28921
129. Bourque M, Dluzen DE, di Paolo T. Neuroprotective actions of sex steroids in Parkinson's disease. *Front Neuroendocrinol*. 2009;30(2):142–57. doi:10.1016/j.yfrne.2009.04.014
130. Hirohata M, Ono K, Morinaga A, Ikeda T, Yamada M. Anti-aggregation and fibril-destabilizing effects of sex hormones on  $\alpha$ -synuclein fibrils in vitro. *Exp Neurol*. 2009;217(2):434–9. doi:10.1016/j.expneurol.2009.03.003
131. Gatto NM, Deapen D, Stoyanoff S, Pinder R, Narayan S, Bordelon Y, et al. Lifetime exposure to estrogens and Parkinson's disease in California

- teachers. *Parkinsonism Relat Disord*. 2014;20(11):1149–56.  
doi:10.1016/j.parkreldis.2014.08.003
132. Yoo JE, Shin DW, Jang W, Han K, Kim D, Won HS, et al. Female reproductive factors and the risk of Parkinson's disease: a nationwide cohort study. *Eur J Epidemiol*. 2020;35:871–8. doi:10.1007/s10654-020-00672-x
133. Canonico M, Pesce G, Bonaventure A, le Noan-Lainé M, Benatru I, Ranoux D, et al. Increased Risk of Parkinson's Disease in Women after Bilateral Oophorectomy. *Mov Disord*. 2021;36(7):1696–700.  
doi:10.1002/mds.28563
134. Kusters CDJ, Paul KC, Duarte Folle A, Keener AM, Bronstein JM, Bertram L, et al. Increased Menopausal Age Reduces the Risk of Parkinson's Disease: A Mendelian Randomization Approach. *Mov Disord*. 2021;36(10):2264–72. doi:10.1002/mds.28760
135. Rugbjerg K, Christensen J, Tjønneland A, Olsen JH. Exposure to estrogen and women's risk for Parkinson's disease: A prospective cohort study in Denmark. *Parkinsonism Relat Disord*. 2013;19(4):457–60. doi:10.1016/j.parkreldis.2013.01.008
136. Casas S, Giuliani F, Cremaschi F, Yunes R, Cabrera R. Neuromodulatory effect of progesterone on the dopaminergic, glutamatergic, and GABAergic activities in a male rat model of Parkinson's disease. *Neurol Res*. 2013;35(7):719–25. doi:10.1179/1743132812Y.0000000142
137. Litim N, Morissette M, di Paolo T. Effects of progesterone administered after MPTP on dopaminergic neurons of male mice. *Neuropharmacology*. 2017;117:209–18.  
doi:10.1016/j.neuropharm.2017.02.007
138. Lv M, Zhang Y, Chen GC, Li G, Rui Y, Qin L, et al. Reproductive factors and risk of Parkinson's disease in women: A meta-analysis of observational studies. *Behav Brain Res*. 2017;335:103–10.  
doi:10.1016/j.bbr.2017.07.025
139. Jarras H, Bourque M, Poirier AA, Morissette M, Coulombe K, di Paolo T, et al. Neuroprotection and immunomodulation of progesterone in the gut of a mouse model of Parkinson's disease. *J Neuroendocrinol*. 2020;32(1):e12782. doi:10.1111/jne.12782

140. Rozani V, Gurevich T, Giladi N, El-Ad B, Tsamir J, Hemo B, et al. Higher serum cholesterol and decreased Parkinson's disease risk: A statin-free cohort study. *Mov Disord.* 2018;33(8):1298–305. doi:10.1002/mds.27413
141. Willis AW, Schootman M, Evanoff BA, Perlmutter JS, Racette BA. Neurologist care in Parkinson disease: A utilization, outcomes, and survival study. *Neurology.* 2011;77(9):851–7. doi:10.1212/WNL.0b013e31822c9123
142. Saunders-Pullman R, Wang C, Stanley K, Bressman SB. Diagnosis and Referral Delay in Women With Parkinson's Disease. *Gen Med.* 2011;8(3):209–17. doi:10.1016/j.genm.2011.05.002
143. Marek K, Jennings D, Lasch S, Siderowf A, Tanner C, Simuni T, et al. The Parkinson Progression Marker Initiative (PPMI). *Prog Neurobiol.* 2011;95(4):629–35. doi:10.1016/j.pneurobio.2011.09.005
144. Goetz CG, Tilley BC, Shaftman SR, Stebbins GT, Fahn S, Martinez-Martin P, et al. Movement Disorder Society-sponsored revision of the Unified Parkinson's Disease Rating Scale (MDS-UPDRS): Scale presentation and clinimetric testing results. *Mov Disord.* 2008;23(15):2129–70. doi:10.1002/mds.22340
145. Hoehn MM, Yahr MD. Parkinsonism: onset, progression and mortality. *Neruology.* 1967;17(5):427–42. doi:10.1212/wnl.17.5.427
146. Goetz CG, Poewe W, Rascol O, Sampaio C, Stebbins GT, Counsell C, et al. Movement Disorder Society Task Force report on the Hoehn and Yahr staging scale: Status and recommendations The Movement Disorder Society Task Force on rating scales for Parkinson's disease. *Mov Disord.* 2004;19(9):1020–8. doi:10.1002/mds.20213
147. Yesavage JA, Sheikh JI. Geriatric Depression Scale (GDS). Recent Evidence and Development of a Shorter Version. *Clin Gerontol.* 1986;5(1–2):165–73. doi:10.1300/J018v05n01\_09
148. Doty RL, Shaman P, Kimmelman CP, Dann MS. University of pennsylvania smell identification test: A rapid quantitative olfactory function test for the clinic. *Laryngoscope.* 1984;94(2):176–8. doi:10.1288/00005537-198402000-00004

149. Visser M, Marinus J, Stiggelbout AM, van Hilten JJ. Assessment of autonomic dysfunction in Parkinson's disease: The SCOPA-AUT. *Mov Disord.* 2004;19(11):1306–12. doi:10.1002/mds.20153
150. Johns MW. A New Method for Measuring Daytime Sleepiness: The Epworth Sleepiness Scale. *Sleep.* 1991;14(6):540–5. doi:10.1093/sleep/14.6.540
151. Nasreddine ZS, Phillips NA, Bédirian V, Charbonneau S, Whitehead V, Collin I, et al. The Montreal Cognitive Assessment, MoCA: A Brief Screening Tool For Mild Cognitive Impairment. *J Am Geriatr Soc.* 2005;53(4):695–9. doi:10.1111/j.1532-5415.2005.53221.x
152. Benton AL, Varney NR, Hamsher KD. Visuospatial judgment. A clinical test. *Arch Neurol.* 1978;35(6):364–7.
153. Brandt J, Benedict RHB. Verbal Learning Test-Revised. Professional manual. Lutz, FL: Psychological Assessment Resources; 2001.
154. Smith A. The Symbol-Digit Modalities Test: A Neuropsychologic Test of Learning and Other Cerebral Disorders. In: Helmuth J, editor. *Learning Disorders, Special Child Publications.* Seattle, WA; 1968. p. 83–91.
155. Smith A. Symbol Digits Modalities Test. Los Angeles, CA: Western Psychological Services; 1982.
156. Wechsler D. Wechsler Abbreviated Scale of Intelligence (WASI). San Antonio, TX: Psychological Corporation; 1999.
157. Hughes AJ, Daniel SE, Kilford L, Lees AJ. Accuracy of clinical diagnosis of idiopathic Parkinson's disease: a clinico-pathological study of 100 cases. *J Neurol Neurosurg Psychiatry.* 1992;55(3):181–4. doi:10.1136/jnnp.55.3.181
158. Folstein MF, Folstein SE, McHugh PR. "Mini-mental state": A practical method for grading the cognitive state of patients for the clinician. *J Psychiatr Res.* 1975;12(3):189–98. doi:10.1016/0022-3956(75)90026-6
159. Frauscher B, Ehrmann L, Zamarian L, Auer F, Mitterling T, Gabelia D, et al. Validation of the Innsbruck REM sleep behavior disorder inventory. *Mov Disord.* 2012;27(13):1673–8. doi:10.1002/mds.25223



160. Tomlinson CL, Stowe R, Patel S, Rick C, Gray R, Clarke CE. Systematic review of levodopa dose equivalency reporting in Parkinson's disease. *Mov Disord.* 2010;25(15):2649–53. doi:10.1002/mds.23429
161. Benton AL, Sivan AB, Hamsher KD, Varney NE, Spreen O. Visual Form Discrimination. In: *Contributions to Neuropsychological Assessment A Clinical Manual*. 2nd ed. New York, NY: Oxford University Press; 1994. p. 65–72.
162. Benton AL, Sivan AB, Hamsher KD, Varney NE, Spreen O. Facial Recognition. In: *Contributions to Neuropsychological Assessment A Clinical Manual*. 2nd ed. New York, NY: Oxford University Press; 1994. p. 35–52.
163. Lezak M, Howieson D, Bigler E, Tranel D. *Neuropsychological Assessment*. 5th ed. New York, NY: Oxford University Press; 2012.
164. Stroop JR. Studies of interference in serial verbal reactions. *J Exp Psychol.* 1935;18(6):643–62. doi:10.1037/h0054651
165. Kaplan E, Goodglass H, Weintraub S. Boston Naming Test. Kreutzer JS, DeLuca J, Caplan B, editors. Philadelphia, PA: Lea & Febiger; 1983.
166. Fischl B, Liu A, Dale AM. Automated manifold surgery: constructing geometrically accurate and topologically correct models of the human cerebral cortex. *IEEE Trans Med Imaging.* 2001;20(1):70–80. doi:10.1109/42.906426
167. Dale AM, Fischl B, Sereno MI. Cortical Surface-Based Analysis: I. Segmentation and Surface Reconstruction. *Neuroimage.* 1999;9(2):179–94. doi:10.1006/nimg.1998.0395
168. Ségonne F, Pacheco J, Fischl B. Geometrically Accurate Topology-Correction of Cortical Surfaces Using Nonseparating Loops. *IEEE Trans Med Imaging.* 2007;26(4):518–29. doi:10.1109/TMI.2006.887364
169. Dale AM, Sereno MI. Improved Localizadon of Cortical Activity by Combining EEG and MEG with MRI Cortical Surface Reconstruction: A Linear Approach. *J Cogn Neurosci.* 1993;5(2):162–76. doi:10.1162/jocn.1993.5.2.162

170. Fischl B, Dale AM. Measuring the thickness of the human cerebral cortex from magnetic resonance images. *Proc Natl Acad Sci USA*. 2000;97(20):11050–5. doi:10.1073/pnas.200033797
171. Fischl B, Salat DH, Busa E, Albert M, Dieterich M, Haselgrove C, et al. Whole Brain Segmentation: Automated Labeling of Neuroanatomical Structures in the Human Brain. *Neuron*. 2002;33(3):341–55. doi:10.1016/S0896-6273(02)00569-X
172. Pruim RHR, Mennes M, van Rooij D, Llera A, Buitelaar JK, Beckmann CF. ICA-AROMA: A robust ICA-based strategy for removing motion artifacts from fMRI data. *Neuroimage*. 2015;112:267–77. doi:10.1016/j.neuroimage.2015.02.064
173. Power JD, Barnes KA, Snyder AZ, Schlaggar BL, Petersen SE. Spurious but systematic correlations in functional connectivity MRI networks arise from subject motion. *Neuroimage*. 2012;59(3):2142–54. doi:10.1016/j.neuroimage.2011.10.018
174. Zhang Z. Variable selection with stepwise and best subset approaches. *Ann Transl Med*. 2016;4(7):1–6. doi:10.21037/atm.2016.03.35
175. Baggio HC, Abos A, Segura B, Campabadal A, Garcia-Diaz A, Uribe C, et al. Statistical inference in brain graphs using threshold-free network-based statistics. *Hum Brain Mapp*. 2018;39(6):2289–302. doi:10.1002/hbm.24007
176. Zalesky A, Fornito A, Bullmore ET. Network-based statistic: Identifying differences in brain networks. *Neuroimage*. 2010;53(4):1197–207. doi:10.1016/j.neuroimage.2010.06.041
177. Smith SM, Nichols TE. Threshold-free cluster enhancement: Addressing problems of smoothing, threshold dependence and localisation in cluster inference. *Neuroimage*. 2009;44(1):83–98. doi:10.1016/j.neuroimage.2008.03.061
178. Fan L, Li H, Zhuo J, Zhang Y, Wang J, Chen L, et al. The Human Brainnetome Atlas: A New Brain Atlas Based on Connectional Architecture. *Cereb Cortex*. 2016;26(8):3508–26. doi:10.1093/cercor/bhw157

179. Bullmore E, Sporns O. Complex brain networks: graph theoretical analysis of structural and functional systems. *Nat Rev Neurosci*. 2009;10:186–98. doi:10.1038/nrn2575
180. Rubinov M, Sporns O. Complex network measures of brain connectivity: Uses and interpretations. *Neuroimage*. 2010;52(3):1059–69. doi:10.1016/j.neuroimage.2009.10.003
181. Sporns O. The non-random brain: efficiency, economy, and complex dynamics. *Front Comput Neurosci*. 2011;5:5. doi:10.3389/fncom.2011.00005
182. Kong WL, Huang Y, Qian E, Morris MJ. Constipation and sleep behaviour disorder associate with processing speed and attention in males with Parkinson’s disease over five years follow-up. *Sci Rep*. 2020;10:19014. doi:10.1038/s41598-020-75800-4
183. Klann EM, Dissanayake U, Gurralla A, Farrer M, Shukla AW, Ramirez-Zamora A, et al. The Gut–Brain Axis and Its Relation to Parkinson’s Disease: A Review. *Front Aging Neurosci*. 2022;13:782082. doi:10.3389/fnagi.2021.782082
184. Ma J, Dou K, Liu R, Liao Y, Yuan Ze, Xie A. Associations of Sleep Disorders With Depressive Symptoms in Early and Prodromal Parkinson’s Disease. *Front Aging Neurosci*. 2022;14:898149. doi:10.3389/fnagi.2022.898149
185. Ghazi Sherbaf F, Rahmani F, Jooyandeh SM, Aarabi MH. Microstructural changes in patients with Parkinson disease and REM sleep behavior disorder: depressive symptoms versus non-depressed. *Acta Neurol Belg*. 2018;118:415–21. doi:10.1007/s13760-018-0896-x
186. Sherbaf FG, Abadi YR, Zadeh MM, Ashraf-Ganjouei A, Moghaddam HS, Aarabi MH. Microstructural Changes in Patients With Parkinson’s Disease Comorbid With REM Sleep Behaviour Disorder and Depressive Symptoms. *Front Neurol*. 2018;9:441. doi:10.3389/fneur.2018.00441
187. Postuma RB, Gagnon JF, Pelletier A, Montplaisir JY. Insomnia and somnolence in idiopathic RBD: a prospective cohort study. *npj Parkinsons Dis* . 2017;3:9. doi:10.1038/s41531-017-0011-7

188. Rüb U, del Tredici K, Schultz C, Ghebremedhin E, de Vos RAI, Jansen Steur E, et al. Parkinson's disease: the thalamic components of the limbic loop are severely impaired by  $\alpha$ -synuclein immunopositive inclusion body pathology. *Neurobiol Aging*. 2002;23(2):245–54. doi:10.1016/s0197-4580(01)00269-x
189. Brooks D, Halliday GM. Intralaminar nuclei of the thalamus in Lewy body diseases. *Brain Res Bull*. 2009;78(2–3):97–104. doi:10.1016/j.brainresbull.2008.08.014
190. Kalaitzakis ME, Gentleman SM, Pearce RKB. Disturbed sleep in Parkinson's disease: anatomical and pathological correlates. *Neuropathol Appl Neurobiol*. 2013;39(6):644–53. doi:10.1111/nan.12024
191. Bedard MA, Aghourian M, Legault-Denis C, Postuma RB, Soucy JP, Gagnon JF, et al. Brain cholinergic alterations in idiopathic REM sleep behaviour disorder: a PET imaging study with 18F-FE0BV. *Sleep Med*. 2019;58:35–41. doi:10.1016/j.sleep.2018.12.020
192. Ellmore TM, Castriotta RJ, Hendley KL, Aalbers BM, Furr-Stimming E, Hood AJ, et al. Altered Nigrostriatal and Nigrocortical Functional Connectivity in Rapid Eye Movement Sleep Behavior Disorder. *Sleep*. 2013;36(12):1885–92. doi:10.5665/sleep.3222
193. Rahayel S, Postuma RB, Montplaisir J, Bedetti C, Brambati S, Carrier J, et al. Abnormal Gray Matter Shape, Thickness, and Volume in the Motor Cortico-Subcortical Loop in Idiopathic Rapid Eye Movement Sleep Behavior Disorder: Association with Clinical and Motor Features. *Cereb Cortex*. 2018;28(2):658–71. doi:10.1093/cercor/bhx137
194. Campabadal A, Segura B, Junque C, Serradell M, Abos A, Uribe C, et al. Cortical Gray Matter and Hippocampal Atrophy in Idiopathic Rapid Eye Movement Sleep Behavior Disorder. *Front Neurol*. 2019;10:312. doi:10.3389/fneur.2019.00312
195. Kreutzmann JC, Havekes R, Abel T, Meerlo P. Sleep deprivation and hippocampal vulnerability: changes in neuronal plasticity, neurogenesis and cognitive function. *Neuroscience*. 2015;309:173–90. doi:10.1016/j.neuroscience.2015.04.053
196. Campabadal A, Abos A, Segura B, Serradell M, Uribe C, Baggio HC, et al. Disruption of posterior brain functional connectivity and its relation

- to cognitive impairment in idiopathic REM sleep behavior disorder. *Neuroimage Clin.* 2020;25:102138. doi:10.1016/j.nicl.2019.102138
197. Göttlich M, Münte TF, Heldmann M, Kasten M, Hagenah J, Krämer UM. Altered Resting State Brain Networks in Parkinson's Disease. *PLoS One.* 2013;8(10):e77336. doi:10.1371/journal.pone.0077336
  198. Pereira JB, Aarsland D, Ginestet CE, Lebedev AV, Wahlund LO, Simmons A, et al. Aberrant Cerebral Network Topology and Mild Cognitive Impairment in Early Parkinson's Disease. *Hum Brain Mapp.* 2015;36:2980–95. doi:10.1002/hbm.22822
  199. Luo CY, Guo XY, Song W, Chen Q, Cao B, Yang J, et al. Functional connectome assessed using graph theory in drug-naive Parkinson's disease. *J Neurol.* 2015;262:1557–67. doi:10.1007/s00415-015-7750-3
  200. Crosson B. Subcortical Functions in Cognition. *Neuropsychol Rev.* 2021;31:419–21. doi:10.1007/s11065-021-09511-6
  201. Cummings JL, Benson DF. Subcortical Dementia Review of an Emerging Concept. *Arch Neurol.* 1984;41(8):874–9. doi:10.1001/archneur.1984.04050190080019
  202. Huber SJ, Shuttleworth EC, Paulson GW, Bellchambers MJG, Clapp LE. Cortical vs Subcortical Dementia: Neuropsychological Differences. *Arch Neurol.* 1986;43(4):392–4. doi:10.1001/archneur.1986.00520040072023
  203. Watts DJ, Strogatz SH. Collective dynamics of 'small-world' networks. *Nature.* 1998;393:440–2. doi:10.1038/30918
  204. Bassett DS, Bullmore ET. Small-World Brain Networks Revisited. *Neuroscientist.* 2017;23(5):499–516. doi:10.1177/1073858416667720
  205. Matzaras R, Shi K, Artemiadis A, Zis P, Hadjigeorgiou G, Rominger A, et al. Brain Neuroimaging of Rapid Eye Movement Sleep Behavior Disorder in Parkinson's Disease: A Systematic Review. *J Parkinsons Dis.* 2022;12(1):69–83. doi:10.3233/JPD-212571
  206. Korat Š, Bidesi NSR, Bonanno F, di Nanni A, Hoàng ANN, Herfert K, et al. Alpha-Synuclein PET Tracer Development—An Overview about Current Efforts. *Pharmaceuticals.* 2021;14(9):847. doi:10.3390/ph14090847

207. Alzghool OM, van Dongen G, van de Giessen E, Schoonmade L, Beaino W.  $\alpha$ -Synuclein Radiotracer Development and In Vivo Imaging: Recent Advancements and New Perspectives. *Mov Disord*. 2022;37(5):936–48. doi:10.1002/mds.28984
208. Poulakis K, Ferreira D, Pereira JB, ÖSmedby Ö, Vemuri B, Westman E. Fully bayesian longitudinal unsupervised learning for the assessment and visualization of AD heterogeneity and progression. *Aging*. 2020;12(13):12622–47. doi:10.18632/aging.103623
209. Poulakis K, Pereira JB, Muehlboeck JS, Wahlund LO, Smedby Ö, Volpe G, et al. Multi-cohort and longitudinal Bayesian clustering study of stage and subtype in Alzheimer’s disease. *Nat Commun*. 2022;13:4566. doi:10.1038/s41467-022-32202-6